
Electronic Thesis and Dissertation Repository

10-28-2014 12:00 AM

Regulation of the High-Affinity Choline Transporter Activity and Trafficking in Alzheimer's Disease-Related Pathological Conditions

Leah K. Cuddy, *The University of Western Ontario*

Supervisor: Jane Rylett, *The University of Western Ontario*

A thesis submitted in partial fulfillment of the requirements for the Doctor of Philosophy degree in Pharmacology and Toxicology

© Leah K. Cuddy 2014

Follow this and additional works at: <https://ir.lib.uwo.ca/etd>

 Part of the [Medical Molecular Biology Commons](#), and the [Medical Pharmacology Commons](#)

Recommended Citation

Cuddy, Leah K., "Regulation of the High-Affinity Choline Transporter Activity and Trafficking in Alzheimer's Disease-Related Pathological Conditions" (2014). *Electronic Thesis and Dissertation Repository*. 2513.
<https://ir.lib.uwo.ca/etd/2513>

This Dissertation/Thesis is brought to you for free and open access by Scholarship@Western. It has been accepted for inclusion in Electronic Thesis and Dissertation Repository by an authorized administrator of Scholarship@Western. For more information, please contact wlsadmin@uwo.ca.

**REGULATION OF THE HIGH-AFFINITY CHOLINE TRANSPORTER
ACTIVITY AND TRAFFICKING IN ALZHEIMER'S DISEASE-RELATED
PATHOLOGICAL CONDITIONS**

(Thesis format: Integrated Article)

by

Leah Katherine Cuddy

Graduate Program in Pharmacology

A thesis submitted in partial fulfillment
of the requirements for the degree of
Doctor of Philosophy

The School of Graduate and Postdoctoral Studies
The University of Western Ontario
London, Ontario, Canada

© Leah Katherine Cuddy 2014

Abstract

Cholinergic neurons play a key role in cognitive processes through the action of the neurotransmitter acetylcholine (ACh). Dysfunction of these neurons occurs in several neurodegenerative disorders, including Alzheimer's disease (AD). The high-affinity choline transporter CHT recycles choline back into synaptic terminals, which is the rate-limiting step to ACh production. CHT proteins traffic between the cell surface and subcellular organelles in a constitutive manner, which maintains plasma membrane transporter levels, thereby regulating CHT activity and maintaining cholinergic transmission. Pathological conditions associated with AD may alter CHT function in a manner that reduces choline uptake activity and impairs cholinergic neurotransmission. Thus, my experiments focused on understanding the mechanisms regulating the subcellular distribution and activity of CHT in neural cells stably expressing the transporter exposed to AD-related pathological conditions. Important AD risk factors that can lead to pathological changes in the cholinergic nerve terminal microenvironment include increased generation of the reactive oxygen species (ROS) peroxynitrite (ONOO^-), high serum cholesterol level at midlife and mutations in genes encoding the amyloid precursor protein (APP). My investigation revealed that ONOO^- alters CHT function through changes to CHT subcellular trafficking, as opposed to nitrosative or oxidative modification to CHT itself. Moreover, CHT movement through subcellular endosomes and lysosomes was not altered by ONOO^- , but blocking proteasome function attenuated ONOO^- mediated inhibition of CHT function. Second, I evaluated how CHT activity and trafficking is regulated by plasma membrane cholesterol and its association with cholesterol-rich lipid rafts. The results of these experiments showed that membrane cholesterol and lipid rafts play an important role in regulating CHT trafficking and activity by retaining functional CHT at the cell surface. Finally, my studies revealed that CHT function is inhibited by both wild-type and Swedish mutant APP but the underlying mechanisms differ. Wild-type APP facilitates CHT endocytosis, whereas Swedish mutant APP mediated inhibition of CHT function is caused by the susceptibility of CHT to $\text{A}\beta$ released into the extracellular environment. My studies help define the molecular regulation of CHT proteins under pathological conditions. Information from studies such

as these will aid the design of therapeutic strategies to treat pathologies involving cholinergic dysfunction.

Keywords: Alzheimer's disease, cholinergic neurons, high-affinity choline transporter, oxidative stress, cholesterol, amyloid precursor protein

Co-Authorship Statement

The studies in chapters 2, 3, and 4 were performed by Leah Cuddy in the laboratory of Dr. Jane Rylett, with assistance of the co-authors named below.

Chapter 2: Alexis Gordon performed choline uptake assay and HC-3 binding assay experiments and assisted with manuscript writing. Stefanie Black assisted with manuscript writing. Ewa Jaworski provided performed confocal microscopy. Stephen Ferguson provided AP180C and DynK44A plasmids. Jane Rylett designed the project, assisted with data interpretation and analysis and revised the manuscript.

Chapter 3: Warren Winick-Ng performed confocal microscopy. Jane Rylett designed the project, assisted with data interpretation and analysis and revised the manuscript.

Chapter 4: Claudia Seah performed confocal microscopy. Shawn Albers performed the A β ₁₋₄₂ ELISA assay. Jane Rylett contributed to experimental design, data interpretation and manuscript preparation.

Acknowledgements

I would like to acknowledge my family and friends. Thank you for your support throughout graduate school. I would also like to thank all present and past members of the Rylett lab. Most importantly, I would like to acknowledge Dr. Jane Rylett, who has always been a supportive and inspirational mentor.

Table of Contents

Abstract.....	ii
Co-Authorship Statement.....	iv
Acknowledgements.....	v
Table of Contents.....	vi
List of Figures.....	xii
List of Abbreviations.....	xv
1 General introduction.....	1
1.1 Significance of this PhD thesis.....	2
1.2 The cholinergic system.....	2
1.2.1 Cholinergic projections.....	2
1.2.2 Acetylcholine signalling and metabolism.....	3
1.2.3 Molecular features of CHT.....	5
1.2.4 Regulation of high-affinity choline uptake by CHT trafficking.....	7
1.2.5 CHT subcellular trafficking.....	8
1.3 Cholinergic dysfunction in AD.....	10
1.4 Evidence of oxidative stress in AD.....	12
1.5 Sources of ROS in the AD brain.....	13
1.5.1 Overview.....	13
1.5.2 Metal ions as a source of ROS.....	14

1.5.3	A β as a source of ROS.....	15
1.6	ROS cellular targets.....	15
1.7	APP features and trafficking.....	16
1.8	APP metabolism.....	17
1.9	Intracellular sites of A β production.....	19
1.10	Assembly state of A β	21
1.11	Physiological roles of APP.....	22
1.12	Cholesterol as a risk factor for AD	23
1.13	The role of cholesterol in the brain.....	23
1.14	Cholesterol metabolism in the brain.....	24
1.15	Statins in AD.....	27
1.16	Hypotheses for my thesis research.....	29
1.16.1	Working hypothesis.....	29
1.16.2	Hypothesis for Chapter 2.....	29
1.16.3	Hypothesis for Chapter 3.....	29
1.16.4	Hypothesis for Chapter 4.....	30
1.17	References.....	31
Chapter 2	59
2	Peroxynitrite donor SIN-1 modifies high-affinity choline transporter activity by altering its intracellular trafficking.....	59

2.1	Introduction.....	60
2.2	Materials and methods.....	61
2.2.1	Materials.....	61
2.2.2	Stable transfection and selection of cell lines.....	62
2.2.3	SIN-1 treatment.....	62
2.2.4	Confocal cell imaging.....	63
2.2.5	[³ H]Choline uptake assay.....	64
2.2.6	[³ H]HC-3 binding assay.....	64
2.2.7	Cell surface protein biotinylation assay.....	65
2.2.8	Data analysis.....	66
2.3	Results.....	66
2.3.1	SIN-1 decreases activity of wild-type CHT, but not mutant L531A-CHT.....	66
2.3.2	SIN-1 decreases cell surface levels of wild-type CHT, but not mutant L531A-CHT.....	69
2.3.3	Blockade of clathrin-mediated endocytosis attenuates inhibition of CHT by SIN-1.....	71
2.3.4	CHT internalizes into Rab5a-positive organelles in control and SIN-1 treated cells.....	74
2.3.5	CHT is present in the late endosome/lysosome system under both vehicle and SIN-1 treatment.....	74

2.3.6	Inhibition of the proteasome, but not the lysosome, blocks the SIN-1 effect on choline uptake.....	81
2.3.7	Ubiquitination of CHT is enhanced in SIN-1 treated cells.....	82
2.4	Discussion.....	86
2.5	References.....	90
Chapter 3.....		94
3	Regulation of the high-affinity choline transporter activity and trafficking by its association with cholesterol-rich lipid rafts.....	94
3.1	Introduction.....	95
3.2	Materials and methods.....	96
3.2.1	Materials.....	96
3.2.2	Selection of cell line and cell culture	97
3.2.3	[³ H]Choline uptake assay.....	97
3.2.4	[³ H]HC-3 binding assay.....	98
3.2.5	Lipid raft preparation and sucrose flotation gradients.....	98
3.2.6	Synaptosome preparation.....	99
3.2.7	Cellular imaging.....	100
3.2.8	Cholesterol quantification.....	100
3.2.9	Cell surface protein biotinylation assay.....	101
3.2.10	Internalization cell surface biotinylation assay.....	102
3.2.11	Data analysis.....	102

3.3	Results.....	103
3.3.1	Membrane cholesterol manipulation modulates choline uptake activity.....	103
3.3.2	M β C decreases both the B _{max} and K _D for [3H]HC-3 binding to CHT.....	106
3.3.3	CHT proteins are associated with lipid rafts.....	108
3.3.4	CHT colocalizes with the lipid raft markers flotillin and ganglioside GM1.....	111
3.3.5	Effect of cholesterol manipulating drugs on cholesterol level in SH-SY5Y cell membranes.....	114
3.3.6	Lipid raft disruption decreases plasma membrane CHT protein levels.....	116
3.3.7	Effect of cholesterol manipulating drugs on cholesterol level in SH-SY5Y cell membranes.....	119
3.3.8	Identification of putative cholesterol-binding motifs in CHT protein	121
3.4	Discussion.....	123
3.5	References.....	128
	Chapter 4.....	133
4	Differential regulation of the high-affinity choline transporter CHT by wild-type and Swedish mutant amyloid precursor protein.....	133
4.1	Introduction.....	134
4.2	Materials and methods.....	135

4.2.1	Materials.....	135
4.2.2	Cell transfection and selection of cell lines.....	136
4.2.3	DNA constructs.....	137
4.2.4	Co-immunoprecipitation of FLAG-CHT and wild-type or Swedish mutant APP.....	137
4.2.5	Proximity ligation assay.....	138
4.2.6	Cell surface protein biotinylation assay.....	139
4.2.7	[³ H]Choline uptake assay.....	140
4.2.8	Confocal imaging.....	140
4.2.9	Aβ1-42 ELISA assay.....	141
4.2.10	Data analysis.....	141
4.3	Results.....	141
4.3.1	CHT interacts more with APP _{wt} than with APP _{Swe} in a neural cell line.....	141
4.3.2	<i>In-situ</i> proximity ligation assay (PLA) detection of the interaction of CHT with APP _{wt} and APP _{Swe}	145
4.3.3	BACE1 inhibition does not alter the preferential interaction between CHT and APP _{wt} versus APP _{Swe}	148
4.3.4	CHT cell surface levels and choline uptake activity are decreased by expression of APP _{wt} or APP _{Swe}	150
4.3.5	CHT colocalizes with EEA1-positive early endosomes to a similar extent in APP _{wt} or APP _{Swe} expressing cells.....	153

4.3.6	BACE1 inhibition reduces A β generation and increases CHT protein cell surface levels in SY5Y-CHT cells expressing APP _{Swe}	157
4.3.7	Choline uptake activity is reduced by conditioned medium from APP _{Swe} -expressing SY5Y-CHT cells.....	161
4.4	Discussion.....	161
4.5	References.....	167
Chapter 5	170
5	Summary of major findings, discussion of results and future directions.....	170
5.1	Summary of major findings.....	171
5.1.1	Summary of major findings from Chapter 2.....	171
5.1.2	Summary of major findings from Chapter 3.....	171
5.1.3	Summary of major findings from Chapter 4.....	172
5.2	Discussion of results and future studies.....	173
5.2.1	Significance.....	183
5.3	References.....	186
Curriculum Vitae	190

List of Figures

Figure 1 1 Acetylcholine metabolism.....	4
Figure 1 2 Schematic representation of transmembrane topology of rat high-affinity choline transporters.....	6
Figure 1 3 Pathways of CHT subcellular trafficking.	9
Figure 1 4 APP metabolism through the amyloidogenic and non-amyloidogenic pathway.....	18
Figure 2 1 SIN-1 inhibits choline uptake activity of wild-type CHT but not L531A-CHT in SH-SY5Y cells.....	68
Figure 2 2 SIN-1 decreases CHT activity by changing the number of transporter proteins at the cell surface, but not altering binding of solute to transporters.....	70
Figure 2 3 Inhibition of CHT activity by SIN-1 is attenuated by AP180C and Dyn-K44.....	72
Figure 2 4 Wild-type CHT but not L531A-CHT traffics to Rab5a-positive subcellular compartments in live cells.....	75
Figure 2 5 CHT colocalization with Rab7-GFP is seen in vehicle-treated and SIN-1-treated SY5Y-CHT cells.....	76
Figure 2 6 CHT colocalization with Rab9-YFP in SY5Y-CHT cells is not changed by SIN-1 treatment.....	77
Figure 2 7 CHT colocalization with Lamp-1 is seen in vehicle- and SIN-1-treated SY5Y-CHT cells.....	79
Figure 2 8 Inhibition of CHT activity by SIN-1 is attenuated by proteasome inhibitors lactacystin and MG-132, but not by lysosome inhibitors chloroquine and Baf-A.....	83

Figure 2 9 SIN-1 treatment causes CHT ubiquitination in SY5Y-CHT cells.....	85
Figure 3 1 Manipulation of membrane cholesterol modulates choline uptake in SH-SY5Y cells.....	104
Figure 3 2 M β C modifies the binding kinetics for [3 H]HC-3 to high-affinity choline transporters by decreasing B _{max} and K _D	107
Figure 3 3 CHT proteins are distributed between raft and non-raft membrane domains.....	109
Figure 3 4 CHT proteins colocalize with flotillin and cholera toxin-labeled GM1, and to a lesser extent with EEA1.....	112
Figure 3 5 The effect of treatments that manipulate membrane cholesterol on cholesterol levels in raft and non-raft fractions from SH-SY5Y cells.....	115
Figure 3 6 Filipin and M β C decrease cell surface CHT proteins in lipid rafts.....	117
Figure 3 7 Lipid raft disruption does not alter CHT internalization.....	120
Figure 3 8 Schematic representation of transmembrane topology of rat high-affinity choline transporters showing putative cholesterol-binding motifs.....	122
Figure 4 1 CHT interacts to a greater extent with APP _{wt} than with APP _{Swe} in SY5Y-CHT cells and cultured cortical neurons.....	143
Figure 4 2 In-situ proximity ligation assay demonstrating the greater interaction of CHT with APP _{wt} than with APP _{Swe}	146
Figure 4 3 The proportion of CHT protein interacting with APP _{wt} versus CHT interacting with APP _{Swe} is the same in cells treated with vehicle or BACE1 inhibitor IV.....	149
Figure 4 4 Both [3 H]-choline uptake activity and CHT plasma membrane levels are reduced in SY5Y-CHT cells transfected with either APP _{wt} or APP _{Swe}	151

Figure 4 5 Colocalization of CHT with EEA1 is increased in SY5Y-CHT cells expressing either APP _{wt} or APP _{Swe}	155
Figure 4 6 Both [³ H]-choline uptake activity and CHT plasma membrane levels are reduced in SY5Y-CHT cells transfected with either APP _{wt} or APP _{Swe}	159
Figure 4 7 Treatment of SY5Y-CHT cells with conditioned medium containing A β from cells expressing APP _{Swe} inhibits choline uptake activity.....	162
Figure 5 1 Pathways of CHT subcellular trafficking in cells treated with ONOO ⁻ donor SIN-1.....	175
Figure 5 2 CHT trafficking is regulated by its association with lipid rafts.....	179
Figure 5 3 The relationship between APP and the cholinergic system.....	185

List of Abbreviations

3-NT	3-nitrotyrosine
24OHC	24S-hydroxycholesterol
α CTF	α carboxyl-terminal fragment
A β	β -amyloid
A β 1-42	β -amyloid 42 amino acids in length
A β 1-40	β -amyloid 40 amino acids in length
ABC	ATP binding cassette
ACAT	Cholesterol acyltransferase 1
ACh	Acetylcholine
AD	Alzheimer's disease
AEBSF	4-(2-aminoethyl)benzenesulfonyl fluoride hydrochloride
AICD	APP intracellular domain
Akt	serine-threonine kinase Akt
ANOVA	Analysis of variance
AP180C	Carboxyl-terminal fragment of AP180
APLP1	Amyloid precursor-like protein 1
APLP2	Amyloid precursor-like protein 2
APOD	Apolipoprotein D

APOE	Apolipoprotein E
APOJ/CLU	Apolipoprotein J/clusterin
APP	Amyloid precursor protein
APP _{wt}	Wild-type APP
APP _{Swe}	Swedish-mutant APP
BACE1	β -site APP cleaving enzyme-1
β CTF	β carboxyl-terminal fragment
cAMP	Cyclic adenosine monophosphate
ChAT	Choline acetyltransferase
CHT	High-affinity choline transporter
CNS	Central nervous system
CRAC	Cholesterol recognition amino acid consensus sequence
CSF	Cerebrospinal fluid
CTB	Cholera toxin subunit B
Cu	Copper
CVD	Cardiovascular disease
DN	Dominant negative
DMEM	Dulbecco's modified Eagle medium
DMSO	Dimethyl sulfoxide
DNA	Deoxyribonucleic acid

Dyn K44A	Dominant negative dynamin mutant
ECL	Enhanced chemiluminescence
ER	Endoplasmic reticulum
FBS	Fetal bovine serum
FLAG tag	Amino acid sequence DYKDDDDK
Fe	Iron
G418	Geneticin
H ₂ O ₂	Hydrogen peroxide
HBSS	HEPES-buffered saline solution
HC-3	Hemicholinium-3
HEK 293	Human embryonic kidney 293 cells
HMG-CoA	3-hydroxy-3-methylglutaryl-coenzyme A
HNE	(E)-4-hydroxy-2-nonenal
HRP	Horseradish peroxidase
IB	Immunoblot
IP	Immunoprecipitation
IgG	Immunoglobulin G
kDa	kiloDalton
KRH	Krebs-Ringer HEPES solution
LDL-C	Low-density lipoprotein cholesterol

LDLR	Low-density lipoprotein receptor
LRP1	LDL-related protein 1
mAChR	Muscarinic acetylcholine receptor
MAPK	Mitogen-activated protein kinase-1
M β C	Methyl- β -cyclodextrin
M β C-chol	Cholesterol saturated methyl- β -cyclodextrin
MCI	Mild cognitive impairment
MesNa	Mercaptoethanesulfonic acid
mRNA	Messenger ribonucleic acid
nAChR	Nicotinic acetylcholine receptor
NGF	Nerve growth factor
NO	Nitric monoxide
O ₂ ⁻	Superoxide anion
OH \cdot	Reactive hydroxyl radical
ONOO ⁻	Peroxynitrite
PAR-4	Prostate apoptosis response-4
PBS	Phosphate-buffered saline
PBS-T	Phosphate-buffered saline containing 0.15% vol/vol Triton X-100
PET	Positron emission tomography
PI3K	Phosphoinositide-3-kinase

PKC	Protein kinase C
PLA	Proximity ligation assay
PS-1	Presenilin-1
PS-2	Presenilin-2
PVDF	Polyvinylidene difluoride
RA	All- <i>trans</i> -retinoic acid
RCT	Randomized control trials
RNA	Ribonucleic acid
RNS	Reactive nitrogen species
ROS	Reactive oxygen species
sAPP α	Soluble amyloid precursor protein α
sAPP β	Soluble amyloid precursor protein β
SDS-PAGE	Sulfate-polyacrylamide gel electrophoresis
SEC14L1	SEC-14 like protein 1
SIN-1	3-morpholinosyndnonimine
SLC5	Solute carrier 5
sortLA	Sorting protein-related receptor
SR-BI	Scavenger receptor class B type I
SV	Synaptic vesicles
TGN	Trans-Golgi network

TMD	Transmembrane domain
VACht	Vesicular acetylcholine transporter

Chapter 1

1 General Introduction

1.1 Significance of this PhD thesis

Cholinergic neurons play an important role in the central nervous system and are responsible for a wide array of activities, including memory and cognition, through the action of the neurotransmitter acetylcholine (ACh). Dysfunction of these neurons occurs in many neurologic and psychiatric disorders, with the best studied being Alzheimer's disease (AD). Many reports have suggested that the cognitive deficits seen in AD are related to the loss and dysfunction of cholinergic signalling. However, the specific changes that occur in the aging brain that result in cholinergic dysfunction, and the extent to which they can be prevented or reversed, is still unclear. While the cause of AD is unknown, several risk factors have been identified. These risk factors include increasing age, brain injury, high serum cholesterol level at midlife, mutations in genes encoding the amyloid precursor protein (APP) and increased generation of reactive oxygen species (ROS) and reactive nitrogen species (RNS) in the brain. Greater understanding of the molecular events occurring in the cholinergic presynaptic nerve terminal under these pathological situations is essential for developing new treatment methods, and is the focus of current research today.

1.2 The cholinergic system

1.2.1 Cholinergic projections

In the periphery, ACh is the main neurotransmitter used at pre- and post-ganglionic parasympathetic synapses, at pre-ganglionic sympathetic synapses and at the neuromuscular junction. In the central nervous system (CNS), ACh signalling is widely distributed through several major cell groups and pathways. Cholinergic neurons project to most regions of the brain as interneurons or by projection neurons. The cholinergic neurons that undergo neurodegeneration during aging associated with memory impairments are primarily found within the basal forebrain (1-3). This cholinergic complex is comprised of the medial septum, horizontal and vertical diagonal band of Broca, and nucleus basalis of Meynert, and provides the major cholinergic projections to the cerebral cortex, hippocampus, amygdala and olfactory bulb (4, 5). The medial septum

provides the main source of cholinergic projections to the hippocampus (6) and directly synapses with both neurons and interneurons (7, 8). Several cholinergic projections do not directly synapse with post-synaptic sites, indicating a role for cholinergic bulk transmission (9).

1.2.2 Acetylcholine signalling and metabolism

At the pre-synaptic cholinergic nerve terminal, ACh is produced in the cytoplasm by the combination of acetyl-CoA and choline by choline acetyltransferase (ChAT) and packaged into synaptic vesicles (SV) by the vesicular acetylcholine transporter (VACHT). It is stored intracellularly until depolarization of the neuron causes movement of SV to the plasma membrane and release of ACh into the extracellular environment. Once in the synaptic cleft, ACh can bind to pre-synaptic or post-synaptic G protein-coupled muscarinic ACh receptors (mAChR) or cation-permeable, cyst-loop ligand-gated nicotinic ACh receptors (nAChR) (10-12). The binding of ACh to nAChR can cause depolarization or alterations in intracellular calcium levels of the post-synaptic cell, which lead to changes in neurotransmitter release, signal transduction cascades, cell survival, and gene transcription (13-15). The mAChR are subdivided into five major groups according to their G-protein coupling with M1, M3 and M5 receptors selectively coupling to the Gq/G11 family and the M2 and M4 receptors couple to the Gi/Go G-proteins (16, 17). ACh stimulation of these receptors leads to several biochemical and electrophysiological responses, which depend on the location and identity of the receptor that is activated (18).

Alternatively, the ACh that does not bind to post-synaptic receptors is hydrolyzed rapidly into choline and acetate by the enzyme acetylcholinesterase (AChE). For the re-synthesis of ACh, the high-affinity choline transporter CHT is responsible for recycling choline back into the pre-synaptic nerve terminal, which is thought to be the rate-limiting step to ACh production (19, 20). The synthesis, storage, degradation and release of ACh are shown schematically in Figure 1-1. The significance of CHT in cholinergic neurotransmission is highlighted by the fact that the CHT specific antagonist

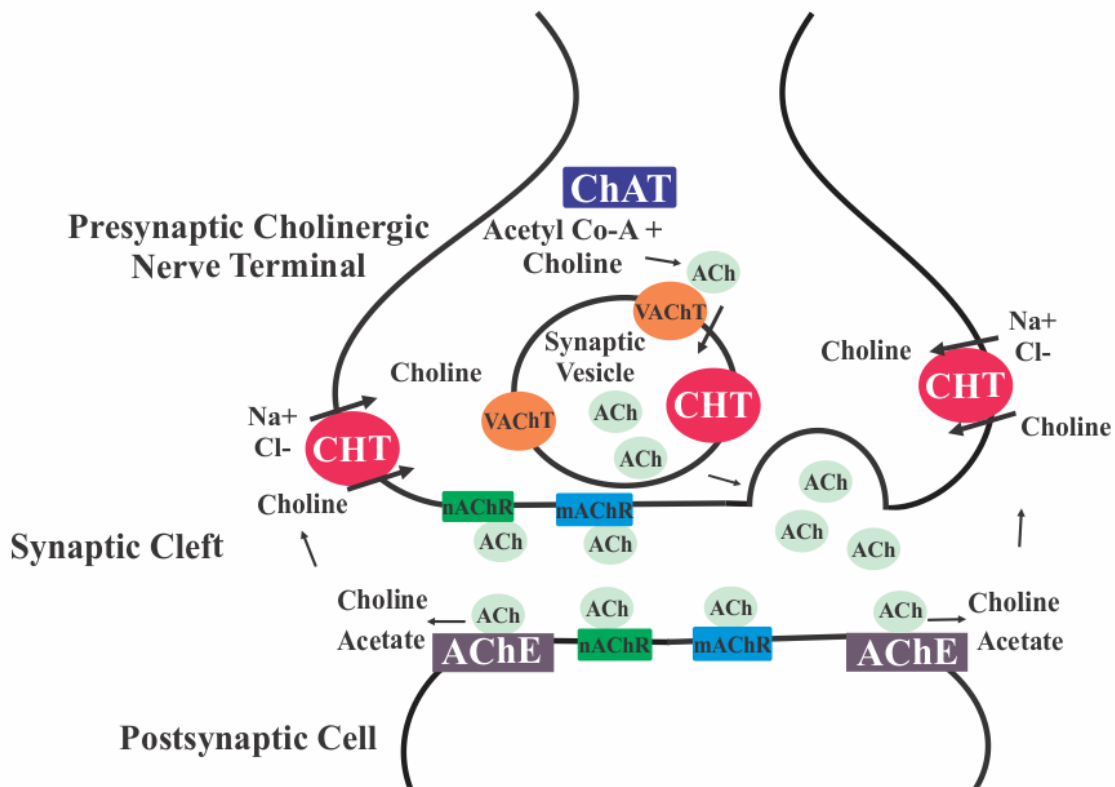


Figure 1-1 Acetylcholine metabolism.

At the pre-synaptic cholinergic nerve terminal, ACh is produced in the cytoplasm by the combination of acetyl-CoA with choline catalyzed by choline acetyltransferase (ChAT) and packaged into synaptic vesicles (SV) by the vesicular acetylcholine transporter (VACHT). Depolarization of the neuron causes movement of SV to the plasma membrane and release of ACh into the extracellular environment. Once in the synaptic cleft, ACh can bind to pre-synaptic or post-synaptic G protein-coupled muscarinic ACh receptors (mAChR) or ligand-gated nicotinic ACh receptors (nAChR). ACh that does not bind to post-synaptic receptors is hydrolyzed rapidly into choline and acetate by the enzyme acetylcholinesterase (AChE). For the re-synthesis of ACh, the high-affinity choline transporter CHT is responsible for recycling choline back into the pre-synaptic nerve terminal, which is thought to be the rate-limiting step to ACh production (19, 20).

hemicholinium-3 (HC-3) administration to animals causes lethal respiratory failure and that CHT knockout mice die at birth from hypoxia also due to respiratory failure (21).

1.2.3 Molecular features of CHT

For many years, the high-affinity choline uptake system has been well established in brain synaptosomes (22, 23, 20) and thought to be unique to cholinergic neurons (24). However, the gene for the transporter responsible, CHT, was only recently cloned in the year 2000 from *Caenorhabditis elegans* (25). The subsequent cloning of several mammalian cDNAs encoding CHT, including rat (25), mouse (26) and human (27, 28), have allowed various studies characterizing CHT distribution and regulation.

Human CHT shares 93% sequence identity with rat CHT, contains 580 amino acids and has a predicted molecular weight of approximately 63kDa. CHT provides cells with high-affinity, sodium and chloride- dependent, HC-3 - sensitive choline uptake and is a member of the solute carrier 5 (SLC5) family of solute transporters (assigned as SLC5A7) (29), sharing approximately 20-25% amino acid sequence identity with members of this family (25). CHT contains 13 predicted transmembrane domains (TMD), an extracellular amino-terminus (30) and an intracellular carboxy-terminus (Figure 1-2) (31). Cysteine scanning analysis has provided recent experimental evidence to confirm this predicted transmembrane topology of CHT (32). Primary amino acid sequence analysis predicts that human CHT has two extracellular asparagine (N) residues that may serve as putative glycosylation sites, and experimental evidence indicates that CHT is indeed glycosylated (31). CHT has several consensus phosphorylation sites for various kinases (27), a strong putative dimerization motif (GxxxGxxxG) in TMD 12 and a second GxxxG motif in TMD 2, similar to those identified recently in other neurotransmitter transporters (33). Several candidate sequences for putative cholesterol binding motifs have been identified in CHT (34). Finally, it has been identified that CHT contains a dileucine-like internalization motif [Leu-531, Val-532] in its carboxyl-terminal tail that is required for its clathrin-mediated endocytosis (30).

CHT is predominantly found within cholinergic neurons (35, 36), although there have been studies where CHT expression has been observed in non-neuronal tissues (37-

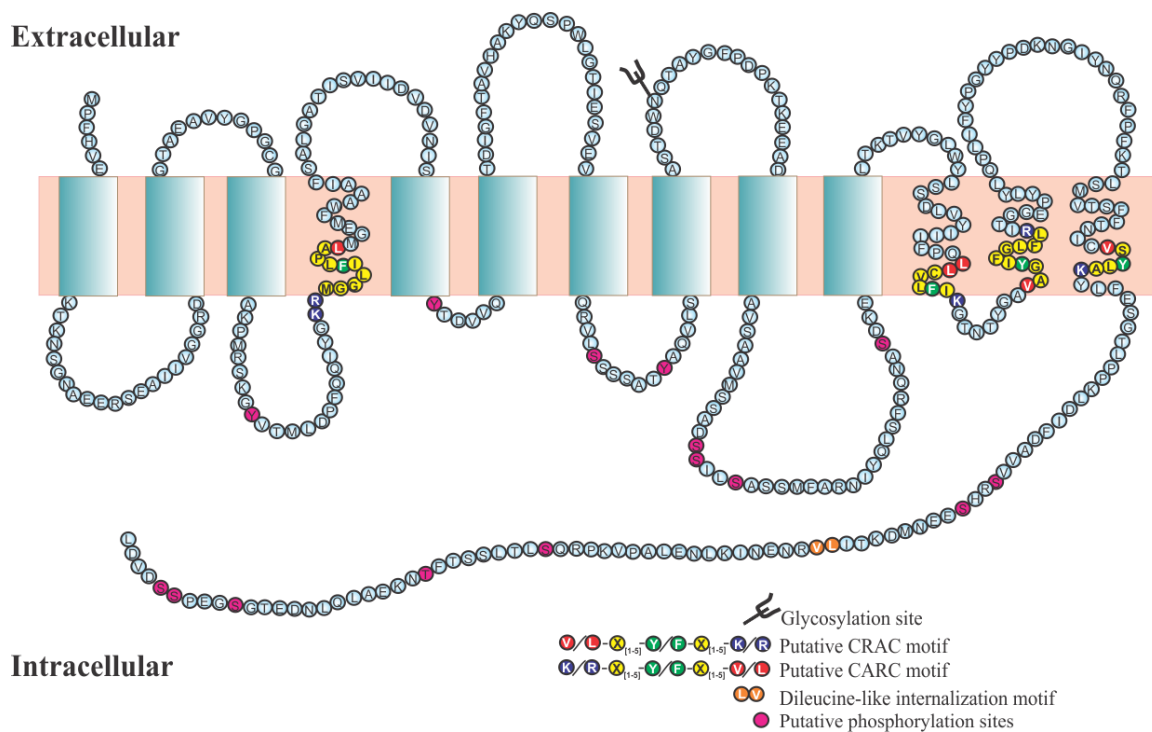


Figure 1-2 Schematic representation of transmembrane topology of rat high-affinity choline transporters.

CHT is a 13 trans-membrane domain (TMD) protein with an extracellular amino-terminus, an intracellular carboxyl-terminus that contains at least 15 putative phosphorylation sites (shown in pink) as predicted by NetPhos 2.0 software, and an extracellular asparagine residue, which serves as a consensus site for glycosylation. The dileucine-like trafficking motif is located at residues leucine-531 and valine-532 and is shown in orange. The positions of putative CRAC-like and CARC cholesterol binding sequence motifs are shown in TMDs 4, 11, 12, and 13. The positioning of transmembrane domains shown is based on data for human CHT [Q9GZV3] submitted recently to UniProtKB/Swiss-Prot at <http://www.uniprot.org/uniprot/Q9GZV3> [Last modified July 24, 2013]; rat and human CHT share 93% sequence identity.

41). The human CHT gene is approximately 25kb in length and contains 9 coding exons (25). CHT activity is regulated both post-translationally and at the transcriptional level. At the transcriptional level, CHT expression is regulated by several factors, including intraneuronal cyclic adenosine monophosphate (cAMP) concentration (42), nerve growth factor (NGF)-TrkA signalling (35, 43), post-synaptic activity dependent retrograde signalling (47). Also, mouse neurons that express the p75 neurotrophin receptor express a much higher level of CHT mRNA than do those that lack this receptor (45, 46). At the post-translational level, CHT trafficking is a critical regulatory mechanism of CHT and can be influenced by protein modifications to, or protein-protein interactions with, CHT.

1.2.4 Regulation of high-affinity choline uptake by CHT trafficking

CHT is active while present at the plasma membrane, but experimental evidence indicates that the majority of the transporter is found intracellularly within endocytic and synaptic vesicles (30, 31, 36, 47). Several observations show that an increase in neuronal activity leads to an increase in choline uptake (48-51), which is likely related to enhanced trafficking of CHT to the cell surface, as has been observed in HC-3 bindings assays and subcellular fractionation experiments (52). Because CHT is located mainly within SV, and depolarization of neurons increases the exocytosis of SV, release of ACh into the synaptic cleft enhances CHT trafficking to the cell surface, it is hypothesized that increased high-affinity choline uptake during depolarization is responsible for maintaining high levels of ACh release during neuronal stimulation (53).

Several reports support the idea that CHT trafficking is critical in regulating high-affinity choline uptake. For example, it has been observed in attentional task-performing rats that CHT plasma membrane levels and choline uptake activity are increased (54). Other studies show that despite reduced total CHT proteins in mice that are heterozygous for CHT compared to wild-type mice, HC-3 binding and high-affinity choline uptake are unchanged, suggesting a compensatory mechanism in the CHT heterozygous mice involving the recruitment of CHT to the cell surface (21). Aberrant CHT trafficking is observed in mice lacking adaptor protein-3, which is thought to be involved in the formation of synaptic vesicles from endosomes (55). These experiments showed that

while cell surface levels of CHT were reduced by 30%, choline uptake activity was unaffected and likely due to the recruitment of intracellular CHT reserve stores (56). Studies using an endosomal ablation protocol to block CHT movement into early endosomes revealed that CHT surface expression and uptake activity is reduced in a time-dependent manner (57). Taken together, the results of these studies highlight the importance of understanding the mechanisms involved in CHT trafficking since this maintains a steady-state level of transporter at the plasma membrane, thereby regulating CHT activity and ACh synthesis.

1.2.5 CHT subcellular trafficking

There is only a small amount of transporter at the plasma membrane, which constitutively traffics between the cell surface and intracellular organelles (Figure 1-3). This was shown by experiments utilizing an amino-terminal FLAG-tagged CHT and cell surface biotinylation experiments where it was observed that only 15% of CHT is located at the cell surface in HEK293 cells (30), similar to the amount found in nerve endings from rat brain (31, 36). Experiments employing the carboxyl-terminal fragment of AP180 (AP180C) and a dominant negative (DN) mutant of dynamin (Dyn K44A), which block clathrin-dependent endocytosis (58) and some forms of clathrin-independent endocytosis (59, 60), revealed that CHT is internalized through a clathrin-dependent mechanism (30). Once internalized, CHT colocalizes with GFP-tagged Rab-5 proteins (30, 47) and is recycled back to the cell surface rapidly through Rab-4 positive endosomes or through slow Rab-11 positive recycling endosomes (61). It has also been proposed that CHT recycles back to the cell surface through synaptic vesicles during depolarization-mediated exocytotic release of ACh (30, 47, 61). Alternatively, CHT can be transported through Rab-7 and Rab-9 positive late endosomes to lysosomes for degradation (62).

The mechanisms involved in the recruitment of CHT from intracellular stores to the cell surface, the internalization of CHT into early endosomes, or the recycling of CHT back to

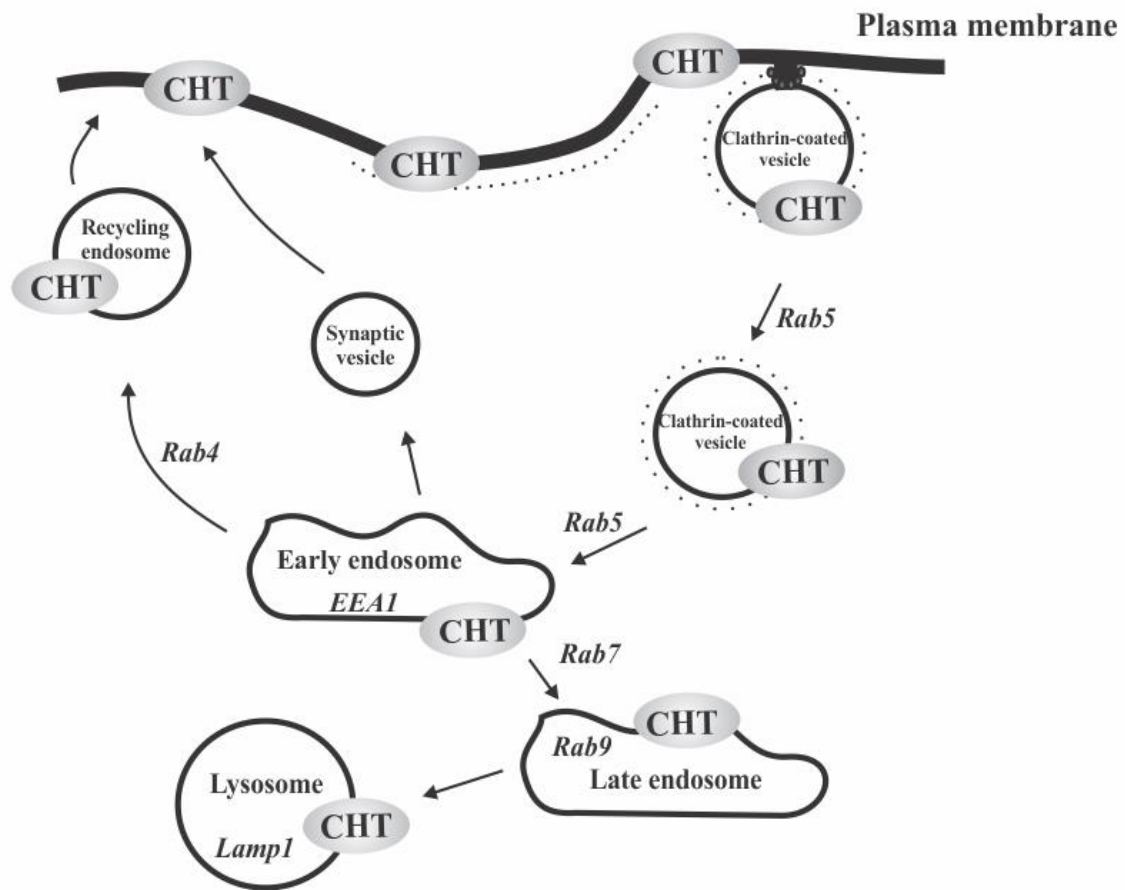


Figure 1-3 Pathways of CHT subcellular trafficking.

CHT is internalized from the plasma membrane through a clathrin-dependent mechanism. Once internalized, CHT colocalizes with GFP-tagged Rab-5 proteins and is recycled back to the cell surface rapidly through Rab-4 positive endosomes or through slow recycling endosomes. It has also been proposed that CHT recycles back to the cell surface through synaptic vesicles during depolarization-mediated exocytotic release of ACh. Alternatively, CHT can be transported through Rab-7 and Rab-9 positive late endosomes to lysosomes for degradation.

the cell surface, are not well understood. It is well known that post-translational modifications of transmembrane proteins, such as phosphorylation and ubiquitination, can alter protein trafficking and activity. Early studies showed that HC-3 binding and choline uptake in brain preparations is altered by phosphorylation (63-66), and more recently it was demonstrated that this is related to changes in CHT trafficking, as CHT internalization and choline uptake activity is reduced by protein kinase C (PKC) activators and protein phosphatase PP1/PP2A inhibitors (67,68). Other early studies identified ubiquitin as a post-translational modification that inhibits high-affinity choline uptake activity and ACh synthesis (69,70). A recent study found that CHT is ubiquitinated in HEK293 cells by the ubiquitin ligase Nedd-42 and that this negatively regulates its cell surface expression (71).

The interaction of CHT with other cellular proteins is another mechanism by which the subcellular trafficking of the transporter is regulated, but only a few proteins have been identified to date. Prostate apoptosis response-4 (Par-4), which is up-regulated during neurodegeneration and AD, has been shown to interact with CHT and inhibit high-affinity choline uptake by reducing the incorporation of CHT on the cell surface (72). The SEC-14 like protein 1 (SEC14L1), which may act as a phospholipid transfer protein, interacts with CHT and inhibits choline uptake activity, likely through alterations in CHT trafficking (73). Interestingly, wild-type APP (APP_{wt}) has been shown to interact with CHT through the carboxyl-terminal of APP. The interaction is thought to mediate CHT presynaptic localization in both the mouse neuromuscular junction and central cholinergic neurons, while over-expression of CHT and APP in HEK293 cells increases its rate of internalization from the cell surface into early endosomes (74). Finally, it has been shown that CHT co-immunoprecipitates with β -amyloid (A β) peptides in rat brain hippocampal synaptosomes, which could alter either high-affinity choline uptake activity or CHT trafficking (75).

1.3 Cholinergic dysfunction in AD

AD is characterized by specific neuronal and synaptic loss, the deposition of amyloid plaques and neurofibrillary tangles, and the loss of neurotransmitter systems. While

several neurotransmitter pathways are known to be involved in AD, the loss of cholinergic neurons is thought to be particularly important (76, 77). Basal forebrain cholinergic neurons, which play a key role in attention, learning, memory, perception, and consciousness (78, 79), are thought to undergo selective degeneration during the course of AD. This is supported by several early studies that examined post-mortem brain tissue from individuals with AD and found substantial deficits of ChAT expression (80-82), reduced ACh release and loss of cholinergic perikarya from the nucleus basalis (83, 84). In the following years, the observations that clinical dementia ratings associated with the loss of presynaptic cholinergic proteins including ChAT, mAChR, nAChR, and reduced ACh levels (85-87), led to the hypothesis that cholinergic dysfunction is related to the cognitive decline and memory loss seen in AD (77).

Support for this hypothesis was based on post-mortem analysis of brains from patients in the advanced stages of late-onset AD; however, whether loss and dysfunction of cholinergic neurons occurs in the early stages of the disease is controversial (88, 89). Positron emission tomography (PET) studies using specific AChE tracers revealed a slight loss of AChE activity in the hippocampus of patients with mild cognitive impairment (MCI) or in the early stages of AD (90, 91), while other studies observed no differences in ChAT activity measured in several brain regions between individuals with MCI or in the early stages of AD, compared to non-impaired controls (92, 93). In contrast to this, a separate study found that ChAT activity was significantly increased above controls in the hippocampus and superior frontal cortex of individuals with MCI (94). While the numbers of ChAT or VAcHT-positive basal forebrain cholinergic neurons in patients with MCI are unchanged compared to non-impaired control individuals, a decrease in the levels of high-affinity NGF receptor TrkA and the p75 low-affinity neurotrophin receptor, which are required for trophic support of basal forebrain cholinergic neurons, has been reported in individuals with early AD or MCI (95, 96). Furthermore, there is evidence from experimental lesions in animals and from post-mortem human studies to suggest that many cholinergic neurons shrink in size during AD pathology rather than die. (97-99). Taken together, these observations suggest that

cholinergic neurons may undergo dysfunction rather than die in individuals with mild AD or MCI.

While studies examining cortical and hippocampal ChAT activity have been used extensively to assay cholinergic function, there have only been a few reports on ChT in neurodegeneration and in AD patients. These studies have been contradictory, with some studies showing a significant enhancement of [^3H]HC-3 binding to the transporter in cortical regions in post-mortem AD brain (100) while others show significantly lower densities of [^3H]HC-3 binding sites in both the frontal cortex and hippocampus of AD brains compared to controls (101, 102). In terms of high-affinity choline uptake, one study showed a decrease in necropsy brain of AD subjects (103), and others indicate that while there is a general loss of cholinergic projections as measured by a decrease in ChAT activity, high-affinity choline uptake is increased significantly in the remaining nerve terminals (104).

1.4 Evidence of oxidative stress in AD

A common feature of several neurodegenerative disorders is the evidence of extensive oxidative stress, which appears to occur particularly early on in AD and contributes to the pathology of the disease by mediating the loss and dysfunction on neuronal cells (105, 106). Oxidative stress occurs when the production of ROS such as hydrogen peroxide (H_2O_2), nitric monoxide (NO), superoxide anion (O_2^-), peroxynitrite (ONOO^-) and reactive hydroxyl radical ($\text{OH}\cdot$), is unregulated and is greater than antioxidant capacity. The brain is particularly susceptible to ROS because it is low in antioxidant defense systems, has a high oxygen consumption and it is rich in polyunsaturated fatty acids, which are easily attacked by free radicals (107). Increased production of ROS in the brain can result in the oxidation of lipids, proteins, RNA and DNA, which leads to inflammation, tissue damage and subsequent cellular apoptosis of neurons or glial cells (108). The oxidative stress hypothesis of AD is formulated based on the observations that a primary risk factor for the disease is age, and during aging antioxidant capacity is reduced and ROS accumulates in the brain.

This hypothesis is supported by several lines of evidence that show that the signature markers of oxidative stress are up-regulated in AD pathology. The concentration of (E)-4-hydroxy-2-nonenal (HNE), an electrophilic breakdown product of lipid peroxidation formed by the attack of ROS on the double bond arachidonic acid (109), is significantly increased in brain tissue (110) and cerebrospinal fluid (CSF) of individuals with AD (111). Lipid peroxidation products acrolein, malondialdehyde and F2-isoprostanes are all increased in AD brains compared to controls (112), with F2-isoprostanes being elevated in the cortex and hippocampus, but not in the cerebellum, an area not typically affected by AD lesions, and in the post-mortem ventricular and lumbar CSF from patients with AD (113, 114). Increased oxidative damage occurs to all four bases of DNA in the brains of AD patients compared to cognitively intact control subjects (115) and extensive protein carbonylation (116) and nitration is observed in brains of individuals with MCI or AD (117, 118). Finally, the endogenous antioxidant defence enzymes catalase, superoxide dismutase, glutathione peroxidase and glutathione reductase are up-regulated in the hippocampus and amygdala in AD brains (119, 120).

1.5 Sources of ROS in the AD brain

1.5.1 Overview

ROS are produced in the brain by direct interactions between redox-active metals and oxygen species, or through indirect pathways involving the activation of phospholipases, nitric oxide synthases and xanthine oxidase, which occurs as a result of dysregulation of calcium homeostasis (121). It is not clear whether disruption of calcium homeostasis is a cause or result of ROS production as some studies have shown that increases in intracellular calcium induce the production of ROS, while others show low concentrations of ROS cause an increase in cytosolic calcium levels (122, 123). The most investigated potential sources of ROS within the AD brain are altered mitochondrial activity, the presence of unbound metal ions and A β peptides themselves. There is an extensive literature that supports mitochondrial dysfunction and subsequent oxidative damage during AD. Mitochondria generate O $_2^-$ and NO as physiologically important by-products of cellular respiration and contain many redox enzymes and respiratory

complexes capable of transferring single electrons to oxygen, generating O_2^- . While mitochondria contain several antioxidant defence systems, insults to the mitochondria, including ROS itself, can cause an imbalance between ROS production and removal leading to an overall net production of ROS (124).

1.5.2 Metal ions as a source of ROS

An important source of oxidative stress in the brain comes from the presence of metal ions. Metal ions are believed to play a role in the pathogenesis of AD (125). The concentrations of iron and zinc in various brain regions affected by AD are elevated in patients with AD compared to cognitively intact controls while copper levels are reduced (126, 127). Copper and iron are active redox metals that are toxic when present in excess due to their involvement in many processes related to ROS generation. The reactivity of copper and iron with molecular oxygen promotes the formation of H_2O_2 , O_2^- and the highly reactive OH^\cdot through the well-known Haber-Weiss and Fenton reactions (128, 129). It is thought that metal ions contribute to AD pathogenesis and increase cellular ROS production by binding to A β . APP has a copper binding site in its amino-terminal domain, which reduces Cu^{2+} to Cu^{1+} (130) and a zinc binding site, which is thought to play a structural role (131), and A β itself also contains specific high and low affinity Cu^{2+} and Zn^{2+} binding sites. The reduction of Cu^{2+} and Fe^{3+} by interacting with A β results in a redox-active peptide-metal ion complex which catalyzes the production of H_2O_2 , using O_2^- and biological reducing agents, such as cholesterol, vitamin E and catecholamines as substrates (132-135). The redox-active A β -metal ion complex itself can subsequently reduce H_2O_2 to OH^\cdot . The aggregation of A β is fundamental to A β -mediated toxicity; however, emphasis has shifted away from amyloid fibrils as the predominant toxic species to the soluble oligomeric forms of A β . Interestingly, the interaction with copper, zinc, or iron with A β mediates the aggregation of the peptide (136, 137) while chelation of the metal ions can reverse the aggregation of synthetic A β and dissolve amyloid in post-mortem human brain samples (138, 139). Studies examining the time course of H_2O_2 generation during A β aggregation showed that H_2O_2 generation reaches a maximum during the early stages when oligomers are the main species present and declines as fibrils are formed (140, 141). A very recent study revealed that the latter

observation is due to conversion of H_2O_2 into $\text{OH}\cdot$ through redox activity of mature fibrils in the presence of redox-active ions, challenging the idea that the end stage fibrils are non-toxic structures (142).

1.5.3 $\text{A}\beta$ as a source of oxidative stress

In addition to its ability to induce ROS formation through metal ion binding, internalized $\text{A}\beta$ can generate oxidative stress by exerting direct effects on the mitochondrial membrane resulting in damage to the electron transport chain compromising neuron viability through energy depletion (143). This has been observed in PC12 cells, where $\text{A}\beta$ causes mitochondrial dysfunction by impairing glycolysis, which results in depletion of cellular ATP levels (144). The iron-sulfur center containing enzyme complexes of the electron transport chain, α -ketoglutarate dehydrogenases and aconitase, have been shown to be vulnerable to damage by $\text{A}\beta$ in various model systems (145, 146) and $\text{A}\beta$ has been shown to potentiate induction of the mitochondrial permeability pore (147, 148), which causes depolarization of the mitochondrial membrane, calcium efflux and reduced glutathione and NADPH levels (149,150). Damage to the mitochondrial membrane and the electron transport chain increases mitochondrial ROS production (151), which can then further impair mitochondrial function. Finally, $\text{A}\beta$ activates microglia in several experimental models (153-155) which are capable of releasing of NO (155) and O_2^- (156). NO and O_2^- combine together to produce significant amounts of a much more reactive molecule, ONOO^- , which has been implicated in AD because of the levels of nitrotyrosine, a product of the reaction of ONOO^- with tyrosine, are elevated in AD (157). Consistent with this is the observation that ONOO^- can be generated by microglia activated by $\text{A}\beta$ (158).

1.6 ROS cellular targets

ROS are highly reactive molecules that can react with a number of different targets in the brain to initiate neuronal death and neurodegeneration through various different pathways. ROS impair cellular function and cause cell death through the oxidation of lipids, proteins and DNA, and through the formation of toxic molecules such as alcohols, aldehydes, peroxides, ketones and cholesterol oxide. The products of membrane lipid

peroxidation by ROS, such as HNE and acrolein, cause toxicity to cells by covalently modifying proteins on cysteine, lysine and histidine residues by a process called Michael addition. This can impair the function of membrane ion-motive ATPases, such as the Na^+/K^+ - and Ca^{2+} - ATPases, as well as glucose and glutamate transporters, which can cause membrane depolarization and a reduction in cellular ATP levels (159, 160). HNE stimulates the apoptotic cascade through disruption of cellular calcium homeostasis (161) by activating of c-Jun amino terminal kinases and mitogen-activated protein kinase-1 (MAPK) (162). The interaction of ROS with DNA can cause mutations and strand breaks, and ROS modifications to proteins can alter protein function through reversible post-translational modifications or impair protein activity. The perturbed calcium homeostasis as a result of ROS overproduction can also lead to an excitotoxic response, where excessive calcium influx results in the activation of glutamate receptors and initiates events resulting in apoptosis (163, 164).

1.7 APP features and trafficking

A major pathological hallmark feature of AD is the accumulation of insoluble aggregates of A β which is produced by the sequential proteolytic processing of its precursor, APP (165, 166). APP is a large, 695-770 amino acid, type-1 transmembrane protein with an extracellular amino terminus and an intracellular carboxyl terminus (167, 168). APP is produced in large amounts in neurons and quickly metabolized (169) through multiple different pathways of proteolysis by α , β and γ -secretase enzymes (170) at various subcellular locations (171). Initially, APP is sorted in the endoplasmic reticulum (ER) and the Golgi apparatus, where it is subject to post-translational modification such as N- and O-linked glycosylation, tyrosine sulfation and ectodomain and cytoplasmic phosphorylation (172-175). APP is transported to the axon and dendrites in post-Golgi transport vesicles (176) where it undergoes fast axonal transport to synaptic terminals (177) and is either trafficked directly to the cell surface or to endosomal compartments through clathrin-associated vesicles. At the cell surface, APP is internalized into clathrin-coated pits mediated by the interaction of the intracellular YENPTY domain of APP (178) with multiple binding partners. This requires the presence of a phosphotyrosine

binding domain on the interacting protein, with the two best studied proteins being X11 and Fe65. Mutation of the YENPTY domain alters APP endocytosis (179) and diminishes A β production (180). Following internalization, APP is transported to endosomal compartments, where a small portion of endocytosed APP is recycled back to the cell surface, while a considerable amount of APP is degraded in lysosomes (165). Finally, APP retrograde trafficking occurs between endosomes and the trans-Golgi network (TGN), which is mediated by retromer complexes. Sorting protein-related receptor (sorLA) is an adaptor protein that affixes cargo to the retromer complex and binds APP (181).

1.8 APP metabolism

APP undergoes proteolytic processing through one of two pathways: non-amyloidogenic processing of APP, which leads to the generation of non-pathogenic peptide fragments and prevents A β production, or amyloidogenic processing leading to the generation of A β (Figure 1-4). The amyloidogenic processing of APP occurs when the β -secretase, β -site APP cleaving enzyme-1 (BACE1), mediates the initial and rate-limiting step in the processing of APP (182). BACE1 cleaves APP at a position located 99 amino acids from the carboxyl terminus, resulting in release of the soluble amino-terminal ectodomain of APP (sAPP β) and a 99 amino acid membrane-bound intracellular carboxyl-terminal fragment (C99 or β CTF). The carboxyl-terminal fragment is then processed within the membrane by the γ -secretase multi-protein complex, which is composed of presenilin 1 (PS-1), presenilin 2 (PS-2), nicastrin, Aph-1 and Pen-2 (183). The γ -secretase complex cleaves the β CTF at one of several sites between amino acids 38 and 34 to generate A β and the APP intracellular domain (AICD). AICD is released into the cytosol and A β is thought to accumulate intra-neuronally (184) or to be released into extracellular fluids, such as plasma or cerebrospinal fluid through the recycling of endosomal compartments to the cell surface. The γ -secretase cleavage produces A β that is 40 amino acids in length

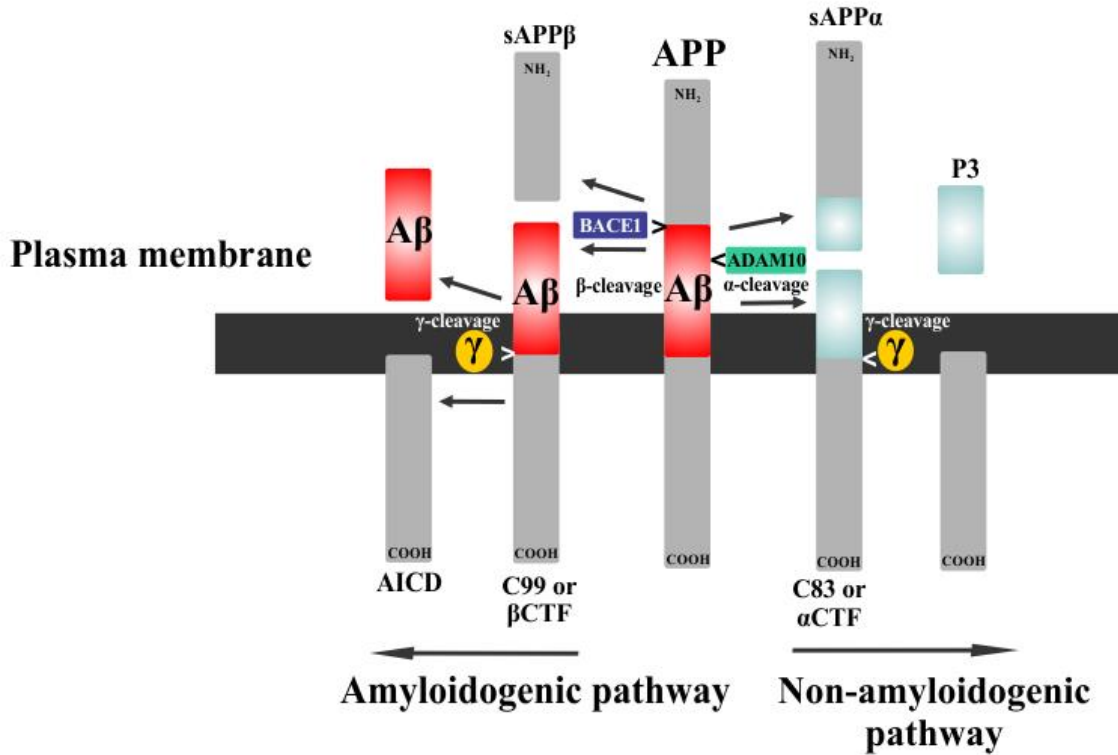


Figure 1-4 APP metabolism through the amyloidogenic and non-amyloidogenic pathway.

Cleavage of APP in the amyloidogenic pathway involves processing by both β -secretase (BACE1) and the γ -secretase complex that releases the soluble amino-terminal ectodomain of APP (sAPP β), the APP intracellular domain (AICD) and an A β peptide that can be of varying length, with the 40 and 42 amino acid A β peptides being the most abundant. Alternatively, APP processing can occur through the non-amyloidogenic pathway where it is first cleaved by the α -secretase (ADAM10) then by the γ -secretase complex, thereby preventing the generation of toxic A β peptides and leading to the production of the soluble amino-terminal ectodomain of APP (sAPP α), the AICD and p3, a truncated peptide that is pathologically irrelevant.

(A β 1-40), and the more toxic A β that is 42 amino acids in length (A β 1-42) at a ratio of 10:1. The A β 1-42 isoform is more hydrophobic, more prone to form fibrils, more resistant to degradation and is the isoform most commonly found within cerebral amyloid plaques (185). The non-amyloidogenic processing of APP is the more prevalent pathway, and occurs when APP is cleaved within the A β domain at a position 83 amino acids away from the carboxyl terminal domain. APP is cleaved by 3 enzymes with α -secretase activity belonging to the ADAM family of proteases: ADAM9, ADAM10 and ADAM17 (186). This generates a truncated membrane-bound intracellular carboxyl-terminal fragment (C83 or α CTF), lacking the amino-terminal portion of the A β domain. The α CTF is then cleaved within the membrane by the γ -secretase protein complex to generate AICD and p3, a truncated A β peptide, which is pathologically irrelevant (187).

Autosomal dominant forms of AD, which typically manifest with early-onset pathogenesis (188), are often caused by mutations in the genes encoding APP, PS-1 and PS-2, and cause changes in the stability and processing of A β . While most mutations in APP are found close to the γ -secretase cleavage site, the Swedish mutation, which is the most well-studied APP mutation, causes a double amino acid change next to the BACE1 cleavage site. This enhances cleavage of the mutant APP by BACE1 leading to increased production of both A β 1-40 and A β 1-42 in the plasma of individuals carrying this mutation (189). Mutations in PS-1 and PS-2 alter the amino acids within their nine TMD and typically increase the production of the more toxic A β 1-42 (190). Other mutations, such as the Arctic mutation, increase the aggregation of A β (191). Increased number of the *APP* gene locus (192) is also known to cause AD, an example of which is seen in Down syndrome, in which trisomy of chromosome 21 occurs and causes early accumulation of A β (193). In total there are 32 *APP*, 179 *PSEN1* and 14 *PSEN2* gene mutations, most of which result in an increase in the production of the more toxic A β 1-42 as compared to A β 1-40 (194).

1.9 Intracellular sites of A β production

The precise subcellular location of APP processing and subsequent A β generation is controversial. A β generation can occur wherever β and γ - secretase enzymes are located,

and thus it is possible that this can occur in various subcellular compartments. Accumulation of A β has been observed in the ER, the TGN, post-TGN secretory vesicles, mitochondria, endosomes, lysosomes, multivesicular bodies, autophagic vacuoles and the cytosol (195-204). While a consensus has not yet been reached, the identities of organelles involved in APP processing and A β generation have been researched extensively. Based on the results of biochemical and genetic studies, the importance of APP endocytic trafficking in A β production is generally agreed upon. *In vivo* experiments demonstrate that endocytosis is required for synaptic activity-dependent release of approximately 70% of A β in neurons (205). According to the most accepted model, APP that reaches the cell surface is predominantly processed by α -secretases (206); however, some unprocessed APP is internalized into early endosomes, where the initial cleavage of APP by BACE1 to form the β CTF occurs. This is supported by the observations that early endosomes have the optimal pH for BACE1 activity, and fluorescence energy resonance transfer analysis showing APP and BACE1 interact predominantly in these compartments (207). The β CTF that is produced in this reaction is then processed further within early endosomes by the γ -secretase complex resulting in the generation of A β , which is subsequently released into the extracellular environment by the recycling of endosomes to the cell surface. Alternatively, the β CTF could potentially be trafficked to other downstream post-endocytic locations such as late endosomes, the multivesicular body or the lysosome for processing. APP that is not cleaved by BACE1 in early endosomes can be recycled back to the cell surface or back to the TGN by the SorLA/retromer protein complex, which is thought to retain APP within the Golgi and prevent its processing to A β . While the standard model indicates that very little A β is generated outside of the endosomal pathways, several groups have identified the ER and TGN as a major site for A β production (208-210), which is consistent with the localization of β - and γ - secretases to this pathway (211, 212). Furthermore, some α -secretase activity has also been observed in the TGN (212).

1.10 Assembly state of A β

A β is produced as a monomer, but can exist in several different assembly states including monomers, dimers, trimers, tetramers, dodecamers, higher-order oligomers, protofibrils and insoluble mature fibrils, which form microscopically visible amyloid plaques that define AD pathology (213). Fibril formation of A β is a complex, nucleation dependent, process of protein aggregation involving the misfolding of A β peptides into soluble and insoluble fibrillar assemblies (214). Kinetic studies have shown that the misfolding of A β monomers precedes the formation of oligomers, which then act as seeds for the formation and elongation of A β fibrils (215). The mechanisms driving this process in the AD brain are not fully understood. For many years, the insoluble fibrillar form of A β was thought to be responsible for the neurodegeneration and cognitive decline associated with AD (216). However, studies showed that accumulation of insoluble fibrillar forms of A β in transgenic mice overexpressing APP was accompanied by minimal neuron loss (217), and that the correlation between fibrillar forms of A β and cognitive impairment was weak (218). Similarly, in humans, a weak correlation between fibrillar A β plaque level in the brain and dementia was found, and cognitively intact individuals have been found to have high levels of fibrillar A β in their brains (219, 220). These observations indicate that a species other than the fibrillar A β could be responsible for the cognitive deficits in the early stages of AD. The toxicity of the various molecular species of A β has been confirmed by different experimental approaches, including using synthetic or endogenous A β peptides, cell culture systems overexpressing APP and APP transgenic mice. A β monomers may play a neuroprotective role by promoting neuronal survival through the activation of the phosphoinositide-3-kinase (PI3K) pathway (221, 222) and *in vitro* and *in vivo* studies have established that oligomeric and protofibril forms of A β are potent neurotoxins (223-225). Oligomeric species of A β are more potent than fibrils and plaques in eliciting synaptic dysfunction and inhibiting long-term potentiation, a form of synaptic plasticity (226, 227). Most importantly, synapse loss and cognitive impairment correlate more with brain levels of soluble oligomeric A β levels than with the density of fibrillar A β plaques (228-230) suggesting that oligomers are the primary toxic species in AD.

1.11 Physiological roles of APP

While the mechanisms involving the production of A β have been well studied, the physiological function of APP, and whether a loss of these functions plays a role in AD, remains unknown. The analysis of APP function *in vivo* is complicated by two major factors. First, APP belongs to an evolutionarily conserved protein family that includes the amyloid precursor-like proteins (APLP1 and APLP2) in mammals, and functional redundancy between these proteins may compensate for APP loss of function in animal models of targeted gene inactivation. Second, the proteolytic processing of APP leads to various extracellular and intracellular APP fragments with different functions.

The combined deletion of APP together with its homologs leads to early postnatal death (231,232), while APP, APLP1 and APLP2 single knockout mice are viable and fertile. However, many studies have shown that animal models of targeted *APP* inactivation have several defects and abnormalities (233,234). In transfected cell lines and cultured neurons, APP has been shown to modulate cell growth, neurite outgrowth (235), neuronal survival (236), cell adhesion (237) and cell motility (238). These functions can be reproduced by the soluble ectodomain of APP, which has also been implicated in cellular processes including neuroprotection, memory enhancing functions, regulation of gene expression and regulation of neuronal excitability and synaptic plasticity (239,240). The AICD is also known to have a functional role by acting as a transcription factor controlling a wide variety of cell functions (241), including apoptosis (242), cell signaling, calcium homeostasis (243) controlling neuronal networks (244), cellular trafficking and cytoskeletal dynamics (245). During neuronal differentiation and maturation APP expression is up-regulated (246), and its expression is also induced during traumatic brain injury (247). APP is targeted to synaptic sites through rapid anterograde transport and the level of APP is correlated to synaptogenesis (248). Taken together, the results from studies using different *in vivo* transgene overexpression or targeted allele animal models and cultured cells indicate that APP plays a key neurotrophic role in early developmental events, including neuronal migration,

synaptogenesis and cell adhesion, with the processing of APP leading to various peptide fragments with several cellular functions.

1.12 Cholesterol as a risk factor for AD

A number of cardiovascular risk factors, such as hypertension, hypercholesterolemia and diabetes mellitus, have been shown in observational and epidemiologic studies to be associated with AD and dementia (249, 250). Studies show that cardiovascular disease (CVD) and AD occur together more often than would be expected by chance (251) and neuritic plaques have been observed in patients with myocardial infarctions without having previously diagnosed dementia (252). Furthermore, vascular injury may lower the threshold for cognitive manifestations of clinical dementia (253). These observations have led to the hypothesis that AD and CVD may share a common risk factor. Data from human epidemiological studies show that hypercholesterolemia, in particular elevated low-density lipoprotein cholesterol (LDL-C), is one of the major risk factors for both AD and CVD (254).

Mean cholesterol levels in individuals with AD are not higher than in those without; however, the results of large epidemiologic studies and prospective population studies suggest that an elevation in plasma cholesterol level in midlife increases the risk of developing AD in older age (255). One study found that individuals with familial hypercholesterolemia were more likely to develop MCI than those without (256), and similarly, another found that a high cholesterol level at midlife was associated with an increased risk of developing dementia later in life (257). In patients with AD, high levels of total cholesterol or LDL-C contributes to faster cognitive decline (258), and in patients without AD or dementia, a separate study reported that high levels of total cholesterol, or LDL-C, were related to lower scores on the Modified Mini-Mental State Exam (259).

1.13 The role of cholesterol in the brain

The brain is the most cholesterol-rich organ in the body, containing approximately 20% of the total body cholesterol, but accounting for only approximately 2% of the body mass

(260). Cholesterol is tightly regulated between the major brain cells, neurons and glia, and is required for normal brain development. Cholesterol forms an essential component of cell membranes and plays a crucial role in development and maintenance of neuronal plasticity and function (261), with depletion of cholesterol resulting in synaptic and dendritic spine degeneration, failed neurotransmission, and decreased synaptic plasticity (262). Cholesterol is synthesized through the isoprenoid biosynthetic pathway from acetyl coenzyme-A by a complex series of reactions catalysed by over 20 enzymes; 3-hydroxy-3-methylglutaryl-coenzyme A (HMG-CoA) reductase catalyses the rate-limiting step of this process and is the target of statin pharmacotherapy (263). Enzymes involved in cholesterol production, such as HMG-CoA, are expressed at high levels in cortical, hippocampal and cholinergic neurons (264) and the expression of enzymes, cholesterol transport proteins and lipoprotein receptors varies between brain regions (265), as does cholesterol content (266). Cholesterol synthesis in the developing central nervous system (CNS) is much higher than that in the adult state. In the mature CNS, most of the cholesterol is found concentrated within the specialized membranes of myelin (267) where it is immobilized due to its slow rate of turnover, with the rest of brain cholesterol being found in the plasma membranes of neurons and glial cells, as well as extracellular lipoproteins. The turnover rate of cholesterol in individual neurons and astrocytes is likely higher than that of myelin bound cholesterol, and is thought to reach an estimated 20% turnover per day depending on the brain area and neuronal cell type (268).

1.14 Cholesterol metabolism in the brain

The majority of cholesterol in the brain is free, unesterified cholesterol and its homeostasis is tightly regulated through a series of processes that include synthesis, storage, transport, and removal. In the periphery, cholesterol homeostasis is mediated by a lipoprotein transport system between the liver, intestine and other organs through blood circulation. Cholesterol levels in the brain do not respond to the homeostatic control mechanisms regulating peripheral plasma cholesterol levels, indicating that there is a distinct metabolism of cholesterol in the CNS. While some studies have demonstrated that a small amount of cholesterol from the periphery can be transported into the CNS in

humans and in mice (269, 270), the majority of experimental evidence indicates that the CNS is isolated from the complex peripheral cholesterol transport system by the blood-brain barrier (271). The endothelial cells that comprise the blood-brain barrier express mRNA for the low-density lipoprotein receptor (LDLR), scavenger receptor class B type I (SR-BI) and members of the ATP binding cassette (ABC) family of transporters and, under *in vitro* conditions, are able to transport cholesterol across the endothelial cells, indicating that these transporters may be involved in mediating cholesterol influx across the blood brain barrier (272). However, *in vivo* studies show that only small amounts of apolipoprotein B, the main apolipoprotein associated with LDL particles in the peripheral cholesterol transport system, are found in the human brain, suggesting that full size particles do not pass by the blood-brain barrier and very little clearance of ¹²⁵I-labeled homologous LDL into the CNS was observed in mice, rabbit and sheep (273-275). Furthermore, in mice fed a high-cholesterol diet, plasma total cholesterol levels were increased 7-fold, while no changes in cholesterol concentration or rate of synthesis were demonstrated in any region of the CNS (276). Thus, it is commonly assumed that the majority of CNS cholesterol (>95%) originates from *de novo* synthesis.

Neurons and glial cells, including astrocytes, microglia and oligodendrocytes, can synthesize cholesterol. *In vitro* cell culture experiments show that the pathway of cholesterol synthesis differs in the sequence of enzymatic steps and resulting precursors between neurons and astrocytes (277). Astrocytes synthesize cholesterol at a higher rate than do neurons, and oligodendrocytes, the cells that are responsible for myelination, have a higher capacity for cholesterol production than do astrocytes (278). In addition to *de novo* synthesis, cholesterol can also be taken up from extracellular sources, and a significant amount of cholesterol is transported between neurons and glial cells by cholesterol-containing lipoproteins, which are mainly secreted by astrocytes (279, 280, 281). A subset of the apolipoproteins found in the plasma are present in the CNS, including apolipoprotein E (APOE), apolipoprotein J/clusterin (APOJ/CLU), and apolipoprotein D (APOD), and have been shown to be up-regulated in various different types of injury and disease (282-284). One of the 3 isoforms of APOE, APOE4, is a well-known risk factor for late-onset AD. Lipoproteins secreted by astrocytes differ in

their chemical and physical properties from those present in plasma (285, 286) having densities similar to those of high-density lipoproteins and containing only either APOE and APOJ/CLU. The mechanisms involved in lipoprotein assembly and secretion by astrocytes are not well understood. After secretion, the nascent lipoproteins may acquire cholesterol in a process similar to high-density lipoproteins, or they could be taken up directly by neurons (287, 288). A specific subtype of the ABC family of transporters, ABCA1, mediates the lipidation of nascent particles and in adult rodents is mainly expressed by neurons and expressed at low levels by glial cells (289). The uptake of lipoproteins in the brain is thought to be mediated by the binding of APO proteins to two specific receptors, the prototypic LDLR, which is expressed by neurons and glial cells (290, 291), and the LDL-related protein 1 (LRP1), which is predominantly expressed by neurons (292). It has been suggested that in the mature state, neurons rely on the delivery of cholesterol-containing, astrocyte-derived lipoproteins and few studies have addressed lipoprotein uptake by astrocytes as they are thought to export rather than import lipids (268). Cholesterol acquired from lipoproteins transits through the endosomal and lysosomal pathway and is mainly stored within subcellular recycling compartments and internal vesicles of multi-vesicular bodies in the endocytic pathway (293). Excess cholesterol is stored intracellularly in lipid droplets after esterification by the enzyme acyl-coenzyme A: cholesterol acyltransferase 1 (ACAT) (294), which has been shown to be present in neurons, but not glial cells (295). Finally, some cholesterol must be exported into the circulation to maintain homeostasis in the brain. There are two methods by which this is accomplished. The first is the excretion of small amounts of APOE-bound cholesterol into the CSF, where 1-2 mg of cholesterol is eliminated daily (296). The second, and the more quantitative method, is the elimination of cholesterol by its conversion to 24S-hydroxycholesterol (24OHC) (297). The hydroxylation of cholesterol at carbon 24 is mediated by the cytochrome P-450 species CYP46A1, and allows its translocation between lipophilic compartments and facilitates its movement through the blood brain barrier (298). Interestingly, CYP46A1 is found localized to neurons, indicating that cholesterol elimination in the brain begins in neurons and not in glial cells (296).

1.15 Statins in AD

There is an established link between elevated plasma cholesterol levels and the risk of developing AD. Statins inhibit cholesterol synthesis, thereby reducing plasma cholesterol levels, and are the first line pharmacological therapy for the treatment of hypercholesterolemia (299). Taken together, these observations have led to the idea that statins could be useful in treating or preventing AD. There are many ways that high cholesterol could affect the progression of AD pathology. Cell culture studies show that cholesterol can increase the activity of the β - and γ -secretases (300-302) and reduce the movement of APP through the non-amyloidogenic pathway (303-306). Following the generation of A β , cholesterol has been shown to influence its aggregation state, with high cholesterol promoting its accumulation following secretion whereas low cholesterol levels allow more internalization and degradation of A β (307, 308). Finally, cholesterol may also affect different non-amyloid factors, such as inflammation, oxidative stress or tau metabolism (309). Preclinical and human studies regarding the relevance of statins as a potential treatment or preventative for AD have shown conflicting results, with preclinical studies suggesting beneficial effects of statins, while human trials have provided more inconsistent results.

The results of various preclinical cell culture experiments have shown that statins can reduce the generation of A β (310, 311) and several *in vivo* studies in animal models of AD have confirmed this finding (312, 313). Statins can also inhibit the production of O₂⁻ by endothelial cells (314) and increase the expression of eNOS either through the inhibition of Rho isoprenylation (315), or directly through activation of the PI3K/Akt pathway (316). Furthermore, statins are protective against A β -induced oxidative stress in mouse models of AD (317, 318). These preclinical observations indicate that statins could provide benefits as a potential treatment or preventative for AD, but it is unclear whether this is due to lower cholesterol levels or to statin pleiotropy (319). Barone et al. (320) found that atorvastatin reduced lipid peroxidation, protein nitration and protein oxidation in the parietal cortex of elderly dogs in an A β and cholesterol-independent manner. The neuroprotective effect observed in this study was suggested to be mediated

through the activation of the cell stress response, as expression of effectors of the adaptive cell response increased and correlated with the reduction of oxidative and nitrosative stress biomarkers in the parietal cortex of these animals (321, 322).

While the consensus from preclinical evidence regarding the neuroprotective effects of statins is encouraging, human clinical trials have shown much more inconsistent results. Several observational studies in humans support the hypothesis that statins may be a potential treatment for dementia or AD or may act to decrease the risk of developing of it (323-330). However, these findings have been challenged by other observational studies. In one study, statins did not improve cognitive performance in non-demented elderly individuals (331) and similar results were observed in a separate large cohort study that assessed more than 2 million individuals, with approximately 11 percent taking statins (332). Furthermore, Zandi et al. (333) found no correlation between statin use and dementia or AD in elderly individuals assessed from 1995 to 1997, and again in 1998-2000. A separate study found that statin treatment did not alter the risk of developing dementia or AD in individuals 65 years and older, which was not affected by the lipophilicity of the statin used (334). The results of randomized control trials (RCT) have yielded similar contradictory results. One large double blind RCT study demonstrated that pravastatin treatment had no protective effect on cognitive function over a follow-up period of 3 years (335), and another showed that atorvastatin treatment for 72 weeks had no significant effect in delaying cognitive decline in patients with mild to moderate AD (336). Similarly, Sano et al. (2011) found simvastatin treatment had no effect in individuals with mild to moderate AD. In contrast to this, administering lovastatin to non-demented individuals reduced serum A β levels in a dose-dependent manner (338). In another study, atorvastatin treatment for 1 year had a positive effect on cognitive performance after 6 month of treatment, but this was restricted to individuals who met specific criteria (339). Other groups have also assessed the effect of statin use in patients diagnosed with AD. Li et al. (2007) examined neuropathological changes of AD and found that statin users had lower Braak stages (a measure of neurofibrillary tangle involvement), but not lower scores on a quantitative scale of amyloid plaque pathology, than non-users. A meta-analysis of all statin RCT results suggests that there is insufficient

evidence to recommend statins as a treatment or preventative for AD (341). This is likely due to major differences in study design and data analysis, as well as the different lipophilicity and chemical structure of different statins which influences their ability to cross the BBB.

1.16 Hypotheses for my thesis research

1.16.1 Working hypothesis

My working hypothesis was that pathological conditions associated with Alzheimer's disease alter CHT function by changing the subcellular trafficking of the transporter in a manner that reduces choline uptake activity and cholinergic neurotransmission. Specifically, my research investigated the effect of peroxynitrite (Chapter 2) and cholesterol manipulation (Chapter 3) on CHT activity and trafficking, and whether CHT is differentially regulated by its interaction with either wild-type APP or APP containing the Swedish mutation (Chapter 4).

1.16.2 Hypothesis for Chapter 2

Experiments in Chapter 2 were designed to determine the effect of the peroxynitrite donor SIN-1 on CHT activity and trafficking. **The hypothesis of this study was that inhibition of CHT by SIN-1 is mediated via alterations in transporter trafficking, as opposed to oxidative or nitrosative modification of CHT protein.**

1.16.3 Hypothesis for Chapter 3

The experiments presented in Chapter 3 were carried out to assess how CHT activity and trafficking is regulated by plasma membrane cholesterol and its association with cholesterol-rich lipid rafts. **For this study, my hypothesis was that CHT is localized to lipid rafts and disruption of rafts alters CHT activity and trafficking, and causes a decrease in choline uptake activity and cholinergic neurotransmission.**

1.16.4 Hypothesis for Chapter 4

The experiments presented in Chapter 4 were designed to assess whether CHT is differentially regulated by its interaction with either the wild-type or Swedish mutant APP. **My hypothesis for this study was that the interaction of CHT with either wild-type APP or APP containing the Swedish mutation alters CHT function through different mechanisms that alter CHT trafficking and choline uptake activity.**

1.17 References

1. Schliebs, R., and Arendt, T. (2006) *J Neural Transm* **11**, 1625-1644
2. Bigl, M., Apelt, J., Lushekina, E. A., Lange-Dohna, C., Robner, S., and Schliebs, R. (2000) *Neurosci Lett* **292**, 107-110
3. Härtig, W., Bauer, K., Brauer, J., Gosche, T., Hortobagyi, P., and Penke, P. (2002) *Rev Neurosci* **13**, 95-165
4. Schliebs, R., and Arendt, T. (2010) *Behav Brain Res* **2**, 555-563
5. Woolf, N. J., and Butcher, L. L. (2011) *Behav Brain Res* **221**, 488-498
6. Dutar, P., Bassant, M., Senut, M., and Lamour, Y. (1995) *Physiol Rev* **75**, 393-427
7. Frotscher, M., and Leranth, C. (1985) *J Comp Neurol* **239**, 237-246
8. Leranth, C., and Frotscher, M. (1987) *J Comp Neurol* **261**, 33-47
9. Vizi, E. S., and Kiss, J. P. (1998) *Hippocampus* **8**, 566-607
10. Nathanson, N. M. (2008) *Pharmacol Ther* **119**, 33-43
11. Gotti, C., Clementi, F., Fornari, A., Gaimarri, A., Guiducci, S., Manfredi, I., Moretti, M., Pedrazzi, P., Pucci, L., and Zoli, M. (2009) *Biochem Pharmacol* **78**, 703-711
12. Yakel, M. (2013) *Eur J Physiol* **465**, 441-450
13. Chang, K. T., and Berg, D. K. (2001) *Neuron* **32**, 855-865
14. Sharma, G., and Vijayaraghavan, S. (2001) *Proc Natl Acad Sci U S A* **98**, 4148-4158
15. Sharma, G., and Vijayaraghavan, S. (2003) *Neuron* **38**, 929-939

16. Wess, J. (2006) *Crit Rev Neurobiol* **10**, 66-99
17. Caulfield, M. P., and Birdsall, N. J. M. (1998) *Pharmacol Rev* **50**, 279-290
18. Wess, J., Eglen, R. M., and Guatam, D. (2007) *Nat Rev Drug Discov* **6**, 721-733
19. Haga, T. (1971) *J Neurochem* **18**, 781-798
20. Kuhar, M.J., and Murrin, L.C. (1978) *J Neurochem* **30**, 15-21
21. Ferguson, S. M., Bazalakova, M., Savchenko, V., Tapia, J. C., Wright, J., and Blakely, R. D. (2004) *Proc Natl Acad Sci U S A* **101**, 8762-8767
22. Yamamura, H. I., and Snyder, S. H. (1972) *J Neurochem* **21**, 1355-1374
23. Haga, T., and Noda, H. (1973) *Biochem Biophys Acta* **291**, 564-575
24. Kuhar, M. J. (1973) *Life Sci* **13**, 1623-1634
25. Okuda, T., Haga, T., Kanai, Y., Endou, H., Ishihara, T., and Katsura, I. (2000) *Nat Neurosci* **3**, 120-125
26. Apparsundaram, S., Ferguson, S.M., and Blakely, R.D. (2001) *Biochem Soc Trans* **29**, 711-716
27. Apparsundaram, S., Ferguson, S.M., George, A.L. jr., and Blakely, R.D. (2000) *Biochem Biophys Res Commun* **276**, 862-867
28. Okuda, T., and Haga, T. (2000) *FEBS Lett* **484**, 92-97
29. Wright, E.M., and Turk, E. (2004) *Pflugers Arch* **447**, 510-518
30. Ribeiro, F.M., Black, S.A., Cregan, S.P., Prado, V.F., Prado, M.A., Rylett, R.J., and Ferguson, S.S. (2005) *J Neurochem* **94**, 86-96

31. Ferguson, S.M., Savchenko, V., Apparsundaram, S., Zwick, M., Wright, J., Heilman, C.J., Yi, H., Levey, A.I., and Blakely, R.D. (2003) *J Neurosci* **23**, 9697-9709
32. Okuda, T., Osawa, C., Yamada, H., Hayashi, K., Nishikawa, S., Ushio, T., Kubo, Y., Satou, M., Ogawa, H., and Haga, T. (2012) *J Biol Chem* **287**, 42826-42834
33. Sitte, H.H., Farhan, H., and Javitch, J.A. (2004) *Mol Interv* **4**, 38-47
34. Cuddy, L.K., Winick-Ng, W., and Rylett, R.J. (2014) *J Neurochem* **128**, 725-740
35. Berse, B., Szczecinska, W., Lopez-Coviella, I., Madziar, B., Zemelko, V., Kaminski, R., Kozar, K., Lips, K.S., Pfeil, U., and Blusztajn, J.K. (2005) *Dev Brain Res* **157**, 132-140
36. Nakata, K., Okuda, T., and Misawa, H. (2004) *Synapse* **53**, 53-56
37. Haerberger, R.V., Pfeil, U., Lips, K.S., and Kummer, W. (2002) *J Invest Dermatol* **119**, 943-948
38. Lips, K.S., Pfeil, U., Haberberger, R.V., and Kummer, W. (2002) *Cell Tissue Res* **307**, 275-280
39. Lips, K.S., Pfeil, U., Reiners, K., Rimasch, C., Kuchelmeister, K., Braun-Dullaeus, R.C., Haberberger, R.V., Schmidt, R., and Kummer, W. (2003) *J Histochem Cytochem* **51**, 1645-1654
40. Pfeil, U., Haberberger, R.V., Lips, K.S., Eberling, L., Grau, V., and Kummer, W. (2003a) *Life Sci* **72**, 2087-2090
41. Pfeil, U., Lips, K.S., Eberling, L., Grau, V., Haberberger, R.V., Kummer, W. (2003b) *Am J Respir Cell Mol Biol* **28**, 473-477
42. Brock, M., Nickel, A.C., Madziar, B., Blusztajn, J.K., and Berse, B. (2007) *Brain Res* **1145**, 1-10

43. Madziar, B., Shah, S., Brock, M., Burke, R., Lopez-Coviella, I., Nickel, A.C., Cakal, E.B., Blusztajn, J.K., and Berse, B. (2008) *J Neurochem* **107**, 1284-1293
44. Krishnaswamy, A., and Cooper, E. (2009) *Neuron* **61**, 272-286
45. Schnitzler, A.C., Lopez-Coviella, I., and Blusztajn, J.K. (2008) *Brain Res* **1246**, 19-28
46. Schnitzler, A.C., Mellot, T.J., Lopez-Coviella, I., Tallini, Y.N., Kotlikoff, M.I., Follettie, M.T., and Blusztajn, J.K. (2010) *J Neurosci* **30**, 8221-8228
47. Ribeiro, F.M., Alves-Silva, J., Volkandt, W., Martins-Silva, C., Mahmud, H., Wilhelm, A., Gomez, M.V., Rylett, R.J., Ferguson, S.S., Prado, V.F., and Prado, M.A. (2003) *J Neurochem* **87**, 136-146
48. Collier, B., and Katz, H.S. (1974) *J Physiol* **238**, 639-655
49. Simon, J.R., and Kuhar, M.G. (1975) *Nature* **255**, 162-163
50. O'Regan, S., and Collier, B. (1981) *Neurosci* **6**, 511-520
51. Saltarelli, M.D., Lowenstein, P.R., and Coyle, J.T. (1987) *Eur J Pharmacol* **135**, 35-40
52. Ivy, M.T., Newkirk, R.F., Karim, M.R., Mtshali, C.M., and Townsel, J.G. (2001) *Neuroscience* **102**, 969-978
53. Ribeiro, F.M., Black, S.A., Prado, V.F., Rylett, R.J., Ferguson, S.S., and Prado, M.A. (2006) *J Neurochem* **97**, 1-12
54. Apparsundaram, S., Martinez, V., Parikh, V., Kozak, R., and Sarter, M. (2005) *J Neurosci* **25**, 3851-3856
55. Faundez, V., Horng, J.T., and Kelly, R.B. (1998) *Cell* **93**, 423-432
56. Misawa, H., Fujigaya, H., Nishimura, T., Moriwaki, Y., Okuda, T., Kawashima,

- K., Nakata, K., Ruggiero, A.M., Blakely, R.D., Nakatsu, F., and Ohno, H. (2008) *Eur J Neurosci* **27**, 3109-3117
57. Ivy, M.T., Newkirk, R.F., Wang, Y., and Townsel, J.G. (2010) *J Neurochem* **112**, 1295-1304
 58. Ford, M.G., Pearse, B.M., Higgins, M.K., Vallis, Y., Owen, D.J., Gibson, A., Hopkins, C.R., Evans, P.R. and McMahon, H.T. (2001) *Science* **291**, 1051-1055
 59. Nichols, B.J., and Lippincott-Schwartz, J. (2001) *Trends Cell Biol* **11**, 406-412
 60. Prado, M.A.M., Alves-Silva, J., Magalhaes, A.C., Prado, V.F., Linden, R., Martins, V.R., and Brentani, R.R. (2004) *J Neurochem* **88**, 769-781
 61. Ribeiro, F.M., Pinthong, M., Black, S.A., Gordon, A.C., Prado, V.F., Prado, M.A., Rylett, R.J., and Ferguson, S.S. (2007a) *Eur J Neurosci* **26**, 3437-3448
 62. Cuddy, L.K., Gordon, A.C., Black, S.A.G., Jaworski, E., Ferguson, S.S.G., and Rylett, R.J. (2012) *J Neurosci* **32**, 5573-5584
 63. Cancela, J.M., Bertrand, N., and Beley, A. (1995) *Biochem Biophys Res Commun* **213**, 944-949
 64. Issa, A.M., Gauthier, S., and Collier, B. (1996) *J Neurochem* **66**, 1924-1932
 65. Cooke, L.J., and Rylett, R.J. (1997) *Brain Res* **751**, 232-238
 66. Vogelsberg, V., Neff, N.H., and Hadjiconstantinou, M. (1997) *J Neurochem* **68**, 1062-1070
 67. Gates, J. jr., Ferguson, S.M., and Blakely, R.D. (2004) *J Pharmacol Exp Ther* **310**, 536-545
 68. Black, S.A.G., Ribeiro, F.M., Ferguson, S.S.G., and Rylett, R.J. (2010) *Neuroscience* **167**, 765-773

69. Meyer, E. M., West, C. M., and Chau, V. (1986) *J Biol Chem* **261**, 14365-14368
70. Meyer, E.M., West, C.M., Stevens, B.R., Chau, V., Nguyen, M., and Judkins, J.H. (1987) *J Neurochem* **49**, 1815-1819
71. Yamada, H., Imajoh-Ohmi, S., and Haga, T. (2012) *Biomed Res* **33**, 1-8
72. Xie, J., and Guo, Q. (2004) *J Biol Chem* **279**, 28266-28275
73. Ribeiro, F.M., Ferreira, L.T., Marion, S., Fontes, S., Gomez, M., Ferguson, S.S., Prado, M.A., and Prado, V.F. (2007b) *Neurochem Int* **50**, 356-364
74. Wang, B., Yang, L., Wang, Z., and Zheng, H. (2007) *Proc Natl Acad Sci U S A* **104**, 14140-14145
75. Bales, K.R., Tzavara, E.T., Wu, S., Wade, M.R., Bymaster, F.P., Paul, S.M., and Nomikos, G.G. (2006) *J Clin Invest* **116**, 825-832
76. Geula, C., and Mesulam, M.M. (1994) *Alzheimer Disease. Raven Press, New York*, pp. 263–291
77. Bartus, R.T. (2000) *Exp Neurol* **163**, 495-529
78. Sarter, M., Bruno, J.P., and Givens, B. (2003) *Neurobiol Learn Mem* **80**, 245-56
79. Woolf, N.J. (1998) *Prog Neurobiol* **55**, 59-77
80. Davies, P., and Maloney, A.J. (1976) *Lancet* **2**, 1403
81. Bowen, D.M., Smith, C.B., and White, P. (1976) *Brain* **99**, 459-496
82. Perry, E.K., Gibson, P.H., and Blessed, G. (1977) *J Neurol Sci* **34**, 247-265
83. Whitehouse, P.H., Price, D.L., and Strubel, R.G. (1982) *Science* **215**, 1237-1239
84. Nilsson, L., Nordberg, A., and Hardy, J.A. (1986) *J Neural Transm* **67**, 275-285
85. Bierer, L.M., Haroutunian, V., Gabriel, S., Knott, P.J., Carlin, L.S., Purohit, D.P.,

- Perl, D.P., Schmeidler, J., Kanof, P., and Davis, K.L. (1995) *J Neurochem* **64**, 749-760
86. Gsell, W., Jungkunz, G., and Riederer, P. (2004) *Curr Pharmacol Design* **10**, 265-293
87. Nordberg, A. (2002) *Cerebrovasc Brain Met Rev* **4**, 303-328
88. Contestabile, A., Ciani, E., and Contestabile, A. (2008) *Neurochem Res* **33**, 318-327
89. Mufson, E.J., Counts, S.E., Perez, S.E., and Ginsberg, S.D. (2008) *Expert Rev Neurother* **8**, 1703-1718
90. Rinne, T., de Kloet, E.R., and Wouters, L. (2002) *Biol Psychiatry* **52**, 1102-1112
91. Shinotoh, H., Namba, H., Fukushi, K., Nagatsuka, S., Tanaka, N., Aotsuka, A., Ota, T., Tanada, S., and Irie, T. (2000) *Ann Neurol* **48**, 194-200
92. Davies, K.L., Mohs, R.C., Marin, D., Purohit, D.P., Perl, D.P., Lantz, M., Austin, G., and Haroutunian, V. (1999) *JAMA* **281**, 1401-1406
93. Tiraboschi, P., Hansen, L.A., Alford, B., Sabbagh, M.N., Schoos, B., Masliah, E., Thal, L.J., and Corey-Bloom, J. (2000) *Neurology* **54**, 407
94. DeKosky, S.T., Ikonomic, M.D., Styren, S.D., Beckett, L., Wisniewski, S., Bennett, D.A., Cochran, E.J., Kordower, J.H., and Mufson, E.J. (2002) *Ann Neurol* **51**, 145-155
95. Mufson, E.J., Ma, S.Y., Dills, J., Cochran, E.J., Leurgans, S., Wu, J., Bennett, D.A., Jaffar, S., Gilmor, M.L., Levey, A.I., Kordower, J.H. (2002) *J Comp Neurol* **443**, 136-153
96. Chu, Y., Cochran, E.J., Bennett, D.A., Mufson, E.J., and Kordower, J.H. (2001) *J Comp Neurol* **437**, 296-307

97. Sofroniew, M.V., Pearson, R.C.A., Eckenstein, F., Cuello, A.C., and Powell, T.P.S. (1983) *Brain Res* **289**, 370-374
98. Pearson, R.C.A., Sofroniew, M.V., Cuello, A.C., Powell, T.P.S., Eckenstein, F., Esiri, M.M., and Wilcock, G.K. (1983) *Brain Res* **289**, 375-379
99. Rinne, J.O., Paljarvi, L., and Rinne, U.K. (1987) *J Neurol Sci* **79**, 67-76
100. Slotkin, T.A., Seidler, F.J., Crain, B., Bell, J.M., Bissette, G., and Nemeroff, C.B. (1990) *Proc Natl Acad Sci* **87**, 2452-2455
101. Pascual, J., Fontan, A., Zarranz, J.J., Berciano, J., Florez, J., and Pazos, A. (1991) *Brain Research* **552**, 179-174
102. Rodriguez-Puertas, R., Pazos, A., Zarranz, J.J., and Pasual J. (1994) *J Neural Transm Park Dis Dement Sect* **8**, 161-169
103. Rylett, R.J., Goddard, S., Schmidt, B.M., and Williams, L.R. (1993) *J Neurosci* **13**, 3956-3963
104. Slotkin, T.A., Nemeroff, C.B., Bissette, G., and Seidler, F.J. (1994) *J Clin Invest* **94**, 696-702
105. Lovell, M.A., and Markesbery, W.R. (2007) *J Neurosci Res* **85**, 3036-3040
106. Nunomura, A., Perry, G., Aliev, G., Hirai, K., Takeda, A., Balraj, E.K., Jones, P.K., Wataya, T., Shimohama, S., Chiba, S., Atwood, C.S., Petersen, R.B., and Smith, M.A. (2001) *J Neuropathol Exp Neurol* **60**, 759-767
107. Halliwell, B. (1992) *Free Radicals in the Brain* pp 21-40
108. Gilgun-Sherki, Y., Melamed, E., and Offen, D. (2001) *Neuropharmacology* **40**, 959-975

109. Esterbauer, H., Schaur, R.J., and Zollner, H. (1991). *Free Radic Biol Med* **11**, 81-128
110. Markesbery, W.R., and Lovell, M.A. (1998) *Neurobiol Aging* **19**, 33-36
111. Selley, M. L., Close, D.R., and Stern, S.E. (2002) *Neurobiol Aging* **23**, 383–388
112. Arlt, S., Beisiegel, U., and Kontush, A. (2002) *Curr Opin Lipidol* **13**, 289-294
113. Montine, T.J., Markesbery, W.R., Morrow, J.D., and Roberts, L.J 2nd. (1998) *Ann Neurol* **44**, 410-430
114. Praticò D., Lee, V.M-Y., Trojanowski, J.Q., Rokach, J., and FitzGerald, G.A. (1998) *FASEB J* **12**, 1777-1783
115. Gabbita, S. P., Lovell, M. A., and Markesbery, W. R. (1998) *J Neurochem* **71**, 2034-2040
116. Hensley, K., Hall, N., Subramaniam, R., Cole, P., Harris, M., Aksenov, M., Aksenova, M., Gabbita, S.P., Wu, J.F., Carney, J.M., Lovell, M., Markesbery, W.R. and Butterfield, D.A. (1995) *J Neurochem* **65**, 2146-2156
117. Good, P.F., Werner, P., Hsu, A., Olanow, C.W., and Perl, D.P. (1996) *Am J Pathol* **149**, 21-28
118. Butterfield, D.A., Reed, T., Newman, S.F., and Sultana, R. (2007) *Free Radical Bio Med* **43**, 658-677
119. Pappolla, M.A., Omar, R.A., Kim, K.S., and Robakis, N.K. (1992) *Am J Pathol* **140**, 621-628
120. Zemlan, F.P., Thienhaus, O.J., and Bosmann, H.B. (1989) *Brain Res* **476**, 160-162
121. Lewen, A., Matz, P. and Chan, P.H. (2000) *J Neurotrauma* **17**, 871-890

122. Suzuki, Y.J., Forman, H.J. and Sevanian, A. (1997) *Free Radic Biol Med* **22**, 269-285
123. Neill, S., Desikan, R., and Hancock, J. (2002) *Curr Opin Plant Biol* **5**, 388-395
124. Andreyev, A.Y., Kushnareva, Y.E., and Starkov, A.A. (2005) *Biochemistry* **70**, 200-214
125. Bush, A.I. (2000) *Curr Opin Chem Biol* **4**, 184-191
126. Deibel, M.A., Ehmann, W.D., and Markesbery, W.R. (1996) *J Neurol Sci* **143**, 137-142
127. Danscher, G., Jensen, K.B., Frederickson, C.J., Kemp, K., Andreasen, A., Juhl, S., Stoltenberg, M., and Ravid, R. (1997) *J Neurosci* **76**, 53-59
128. Donnelly, P.S., Xiao, Z., and Wedd, A.G. (2007) *Curr Opin Chem Biol* **11**, 128-133
129. Butterfield, D.A., and Stadtman, E.R. (1997) *Advantage of Cell Aging Gerontology* **2**, 161-191
130. Multhaup, G., Schlicksupp, A., Hesse, L., Beher, D. Ruppert, T., Masters, C.L., and Beyreuther, K. (1996) *Science* **271**, 1406-1409
131. Bush, A.I., Multhaup, G., Moir, R.D., Williamson, T.G., Small, D.H., Rumble, B., Pollwein, P., Beyreuther, K., and Masters, C.L. (1993) *J Biol Chem* **268**, 16109-16112
132. Huang, X., Atwood, C.S., Hartshorn, M.A., Multhaup, G., Goldstein, L.E., Scarpa, R.C., Cuajungco, M.P., Gray, D.N., Lim, J., Moir, R.D., Tanzi, R.E., and Bush, A.I. (1999a) *Biochemistry* **38**, 7609-7616
133. Huang, X., Cuajungco, M.P., Atwood, C.S., Hartshorn, M.A., Tyndall, J.D., Hanson, G.R., Stokes, K.C., Leopold, M., Multhaup, G., Goldstein, L.E., Scarpa,

- R.C., Saunders, A.J., Lim, J., Moir, R.D., Glabe, C., Bowden, E.F., Masters, C.L., Fairlie, D.P., Tanzi, R.E., and Bush, A.I. (1999b) *J Biol Chem* **274**, 37111-37116
134. Opazo, C., Ruiz, F.H., and Inestrosa, N.C. (2000) *Biol Res* **33**, 125-131
 135. Opazo, C., Huang, X., Cherny, R.A., Moir, R.D., Roher, A.E., White, A.R., Cappai, R., Masters, C.L., Tanzi, R.E., Inestrosa, N.C., and Bush, A.I. (2002) *J Biol Chem* **277**, 40302-40308
 136. Bush, A.I., Pettingell, W.H., Multhaup, G., de Paradis, M., Vonsattel, J.P., Gusella, J.F., Beyreuther, K., Masters, C.L., and Tanzi, R.E. (1994) *Science* **265**, 1464-1467
 137. Atwood, C.S., Moir, R.D., Huang, X., Scarpa, R.C., Bacarra, N.M., Romano, D.M., Hartshorn, M.A., Tanzi, R.E., and Bush, A.I. (1998) *J Biol Chem* **273**, 12817-12826
 138. Huang, X., Atwood, C.S., Moir, R.D., Hartshorn, M.A., Vonsattel, J.P., Tanzi, R.E., and Bush, A.I. (1997) *J Biol Chem* **272**, 26464-26470
 139. Cherny, R.A., Legg, J.T., McLean, C.A., Fairlie, D.P., Huang, X., Atwood, C.S., Beyreuther, K., Tanzi, R.E., Masters, C.L., and Bush, A.I. (1999) *J Biol Chem* **274**, 23223-23228
 140. Tabner, B.J., El-Agnaf, O.M.A., and Turnbull, S. (2005) *J Biol Chem* **280**, 35789–35792
 141. Tabner, B.J., Mayes, J., and Allsop, D. (2010) *Int J Alzheimers Dis* **2011**, 546380-546386
 142. Mayes, J., Tinker-Mill, C., Kolosov, O., Zhang, H., Tabner, B.J., and Allsop, D. (2014) *J Biol Chem* **289**, 12052-12062
 143. Pike, C.J., and Cotman, C.W. (1993) *Neuroscience* **56**, 269-274
 144. Pereira, C., Santos, M.S., and Oliveira, C. (1999) *Neurobiol Dis* **6**, 209-219

145. Blass, J.P., and Gibson, G.E. (1991) *Revue Neurologique* **147**, 513-525
146. Casley, C.S., Canevari, L., Land, J.M., Clark, J.B., Sharpe, M.A. (2002) *J Neurochem* **80**, 91-100
147. Canevari, L., Clark, J.B., and Bates, T.E. (1999) *FEBS Lett* **457**, 131-134
148. Parks, J.K., Smith, T.S., Trimmer, P.A., Bennett, J.P., and Parker, W.D. (2001) *J Neurochem* **76**, 1050-1056
149. Bernardi, P. (1992) *J Biol Chem* **267**, 8834-8839
150. Petronilli, V., Costantini, P., Scorrano, R., Passamonti, S., and Bernardi, P. (1994) *J Biol Chem* **269**, 16638-16642
151. Sheehan, J.P., Swerdlow, R.H., Miller, S.W., Davis, R.E., Parks, J.K., Parker, D., and Tuttle, J.B. (1997) *J Neurosci* **17**, 4612-4622
152. Yankner, B.A., Duffy, L.K., and Kirschner, D.A. (1990) *Science* **250**, 279-282
153. Pike, C.J., Walencewicz, A.J., Glabe, C.G., and Cotman, C.W. (1991) *Eur J Pharmacol* **207**, 367-368
154. Combs, C.K., Johnson, D.E., Cannady, S.B., Lehman, T.M., and Landreth, G. (1999) *J Neurosci* **19**, 929-938
155. Meda, L., Cassatella, M.A., Szendrei, G.I., Otvos, Jr. L., Baron, P., Villalba, M., Ferrari, D., and Rossi, F. (1995) *Nature* **374**, 647-650
156. Tanaka, M., Sotomatsu, A., Yoshida, T., Hirai, S., and Nishida, A. (1994) *J Neurochem* **63**, 266-270
157. Smith, M.A., Richey, Harris, P.L., Sayre, L.M., Beckman, J.S., and Perry, G. (1997) *J Neurosci* **17**, 2653-2657

158. Xie, Z., Wei, M., Morgan, T.E., Fabrizio, P., Han, D., Finch, C.E., and Longo, V.D. (2002) *J Neurosci* **22**, 3484-3492
159. Mark, R.J., Hensley, K., Butterfield, D.A., and Mattson, M.P. (1995) *J Neurosci* **15**, 6239-6249
160. Blanc, E. M., Keller, J. N., Fernandez, S., and Mattson, M. P. (1998) *Glia* **22**, 149-160
161. Mark, R.J., Lovell, M.A., Markesbery, W.R., Uchida, K., and Mattson, M.P. (1997) *J Neurochem* **68**, 255-264
162. Tamagno, E., Robino, G., Obbili, A., Bardini, P., Aragno, M., Parola, M., and Danni, O. (2003) *Exp Neurol* **180**, 144-15
163. Yamamoto, K., Ishikawa, T., Sakabe, T., Taguchi, T., Kawai, S., and Marsala, M. (1998) *Neuroreport* **9**, 1655-1659
164. Mattson, M.P, and Chan, S.L. (2003) *Cell Calcium* **34**, 385-397
165. Haass, C., Schlossmacher, M.G., Hung, A.Y., Vigo-Pelfrey, C., Mellon, A., Ostaszewski, B.L., Lieberburg, I., Koo, E.H., Schenk, D., Teplow, D.B., and Selkoe, D.J. (1992) *Nature* **359**, 322-325
166. Seubert, P., Oltersdorf, T., Lee, M.G., Barbour, R., Blomquist, C., Davis, D.L., Bryant, K., Fritz, L.C., Galasko, D., Thal, L.J., Lieberburg I., and Schenk, D.B. (1993) *Nature* **361**, 260-263
167. Kang, J., Lemaire, H.G., Unterbeck, A., Salbaum, J.M., Masters, C.L., Grzeschik, K.H., Multhaup, G., Beyreuther, K., and Muller-Hill, B. (1987) *Nature* **325**, 733-736
168. Dyrks, T., Weidemann, A., Multhaup, G., Salbaum, J.M., Lemaire, H.G., Kang, J., Muller-Hill, B., Masters, C.L., and Beyreuther, K. (1988) *EMBO J* **7**, 949-957

169. Lee, J., Retamal, C., Cuitino, L., Caruano-Yzermans, A., and Shin, J.E. (2008) *J Biol Chem* **283**, 11501-11508
170. Haass, C. (2004) *EMBO J* **23**, 483-488
171. Weidemann, A., Konig, G., Bunke, D., Fischer, P., Salbaum, J.M., Masters, C.L., and Beyreuther, K. (1989) *Cell* **57**, 115-126
172. Pahlsson, P., Shakin-Eshleman, S.H., and Spitalnik, S.L. (1992) *Biochem Biophys Res Commun* **189**, 1667-1673
173. Knops, J., Gandy, S., Greengard, P., Lieberburg, .I, and Sinha, S. (1993) *Biochem Biophys Res Commun* **197**,380-385
174. Hung, A.Y., and Selkoe, D.J. (1994) *EMBO J* **13**, 534-542
175. Graebert, K.S., Popp, G.M., Kehle, T., and Herzog, V. (1995) *Eur J Cell Biol* **66**, 39-46
176. Kins, S., Lauther, N., Szodorai, A., and Beyreuther, K. (2006) *Neurodegener Dis* **3**, 218-226
177. Koo, E.H., Sisodia, S.S., Archer, D.R., Martin, L.J., Weidemann, A., Beyreuther, K., Fischer, P., Masters, C.L., and Price, D.L. (1990) *Proc Natl Acad Sci* **87**, 1561-1565
178. Chen, W.J., Goldstein, J.L., and Brown, M.S. (1990) *J Biol Chem* **265**, 3116-3123
179. Perez, R.G., Soriano, S., Hayes, J.D., Ostaszewski, B., Xia, W., Selkoe, D.J., Chen, X., Stokin, G.B., and Koo, E.H. (1999) *J Biol Chem* **274**, 18851-18856
180. Ring, S., Weyer, S.W., Kilian, S.B., Waldron, E., Pietrzik, C.U., Filippov, M.A., Herms, J., Buchholz, C., Eckman, C.B., Korte, M., Wolfer, D.P., and Muller, U.C. (2007) *J Neurosci* **27**, 7817-7826

181. Andersen, O.M., Reiche, J., Schmidt, V., Gotthardt, M., Spoelgen, R., Behlke, J., von Arnim, C.A., Breiderhoff, T., Jansen, P., Wu, X., Bales, K.R., Cappai, R., Masters, C.L., Gliemann, J., Mufson, E.J., Hyman, B.T., Paul, S.M., Nykjaer, A., and Willnow, T.E. (2005) *Proc Natl Acad Sci* **102**, 13461-13466
182. Vassar, R., Bennett, B. D., Babu-Kahn, S., Mendiaz, E. A., Denis, P., Teplow, D. B., Ross, S., Amarante, P., Loeloff, R., Luo, Y., Fisher, S., Fuller, J., Edenson, S., Lile, J., Jarosinski, M. A., Biere, A. L., Curran, E., Burgess, T., and Louis, J. C. (1999) *Science* **286**, 735-741
183. Bergmans, B.A., and De Strooper, B. (2010) *Lancet Neurol* **9**, 215-226
184. Gouras, G.K., Tsai, J., Naslund, J., Vincent, B., Edgar, M., Checler, F., Greenfield, J.P., Haroutunian, V., Buxbaum, J.D., Xu, H., Greengard, P., and Relkin, N.R. (2000) *Am J Pathol* **156**, 15-20
185. Younkin, S.G., Eckman, C.B., Ertekin Taner, N., Kawarabayashi, T., Yager, D., Baker, M., Perez-tur, J., Houlden, H., Hutton, M., Younkin, L.H, and Graff-Radford, N.R. (1998) *Soc Neurosci Abstr* **24**, 263
186. Asai, M., Hattori, C., Szabo, B., Sasagawa, N., Maruyama, K., Tanuma, S., and Ishiura, S. (2003) *Biochem Biophys Res Commun* **301**, 231-235
187. Haass, C., Hung, A.Y., Schlossmacher, M.G., Teplow, D.B., and Selkoe, D.J. (1993) *J Biol Chem* **268**, 3021-3024
188. St. George-Hyslop, P.H., and Petit, A. (2005) *C R Biol* **328**, 119-130
189. Citron, M. (2004) *Trends Pharmacol Sci* **25**, 92-97
190. Guo, Q., Fu, W., Sopher, B.L., Miller, M.W., Ware, C.B., Martin, G.M and Mattson, M.P. (1999) *Nat Med* **5**, 101-106

191. Nilsberth, C., Westlind-Danielsson, A., Eckman, C.B., Condron, M.M., Axelman, K., Forsell, C., Stenh, C., Luthman, J., Teplow, D.B., Younkin, S.G., Naslund, J., and Lannfelt, L. (2001) *Nat Neurosci* **4**, 887-893
192. Rovelet-Lecrux, A., Hannequin, D., Raux, G., La Meur, N., Laquerriere, A., Vital, A., Dumanchin, C., Feuillette, S., Brice, A., Vercelletto, M., Dubas, F., Frebourg, T., and Campion D. (2006) *Nat Genet* **38**, 24-26
193. Gyure, K.A., Durham, R., Stewart, W.F., Smialek, J.E., and Troncoso, J.C. (2001) *Arch Pathol Lab Med* **125**, 489-492
194. Shen, J., and Kelleher, R.J. 3rd. (2007) *Proc Natl Acad Sci U S A* **104**, 403-409
195. Busciglio, J., Gabuzda, D.H., and Yankner, B.A. (1993) *Proc Natl Acad Sci* **90**, 2092-2096
196. Cook, D.G., Forman, M.S., Sung, J.C., Leight, S., Kolson, D.L., Iwatsubo, T., Lee, V. M.-Y., and Doms, R.W. (1997) *Nat Med* **3**, 1021-1023
197. Manczak, M., Anekonda, T.S., Henson, E., Park, B.S., Quinn, J., and Reddy, P.H. (2006) *Hum Mol Genet* **15**, 1437-1449
198. Greenfield, J.P., Tsai, J., Gouras, G.K., Hai, B., Thinakaran, G., Checler, F., Sisodia, S.S., Greengard, P., and Xu, H. (1999) *Proc Natl Acad U S A* **96**, 742-747
199. Cataldo, A.M., Petanceska, S., Terio, N.B., Peterhoff, C.M., Durham, R., Mercken, M., Mehta, P.D., Buxbaum, J., Haroutunian, V., and Nixon, R.A. (2004) *Neurobiol Aging* **25**, 1263-1272
200. Petersen, C.A., Alikhani, N., Behbahani, H., Wiehager, B., Pavlov, P.F., Alafuzoff, I., Leinonen, V., Ito, V., Winblad, B., Glaser, E., and Ankarcrona, M. (2008) *Proc Natl Acad U S A* **105**, 13145-13150

201. Pasternak, S.H., Callahan, J.W., and Mahuran, D.J. (2004) *J Alzheimers D* **6**, 53-65
202. Takashi, R.H., Milner, T.A., Li, F., Nam, E.E., Edgar, M.A., Yamaguchi, H., Beal, M.F., Xu, H., Greengard, P., and Gouras, G.K. (2002) *Am J Pathol* **161**, 1869-1879
203. Buckig, A., Tikkanen, R., Herzog, V. and Schmitz, A. (2002) *Histochem Cell Biol* **118**, 353-360
204. Yu, W.H., Cuervo, A.M., Kumar, A., Peterhoff, C.M., Schmidt, S.D., Lee, J-H., Mohan, P.S., Mercken, M., Farmery, M.R., Tjernberg, L.O., Jiang, Y., Duff, K., Uchiyama, Y., Naslund, J., Mathews, P.M., Cataldo, A.M., and Nixon, R.A. (2005) *J Cell Biol* **171**, 87-98
205. Cirrito, J.R., Kang, J.E., Lee, J., Stewart, F.R., Verges, D.K., Silverio, L.M., Bu, G., Mennerick, S., and Holtzman, D.M. (2008) *Neuron* **58**, 42-51
206. Kojro, E., and Fahrenholz, F. (2005) *38*, 105-127
207. Kinoshita, A., Fukumoto, H., Shah, T., Whelan, C.M., Irizarry, M.C., and Hyman, B.T. (2003) *J Cell Sci* **116**, 3339-3346
208. Xu, H., Sweeney, D., Wang, R., Thinakaran, G., Lo, A.C., Sisodia, S.S., Greengard, P., and Gandy, S. (1997) *Proc Natl Acad Sci U S A* **94**, 3748-3752
209. Siman, R., and Velji, J. (2003) *J Neurochem* **84**, 1143-1153
210. Burgos, P.V., Mardones, G.A., Rojas, A.L., DaSilva, L.L., Prabhu, Y., Hurley, J.H., Bonifacino, J.S. (2010) *Dev Cell* **18**, 425-436
211. Baulac, S., LaVoie, M.J., Kimberly, T., Strahle, J., Wolfe, M.S., Selkoe, D.J., and Xia, W. (2003) *Neurobiol Dis* **14**, 194-204
212. Skovronsky, D.M., Moore, D.B., Milla, M.E., Doms, R.W., Lee, V.M. (2000) *J Biol Chem* **275**, 2568-2575

213. Glabe, C.G. (2008) *J Biol Chem* **283**, 29639-29643
214. Yoshiike, Y., Minai, R., Matsuo, Y., Chen, Y-R., Kimura, T., and Takashima, A. (2008) *PLoS ONE* **3**, 3235
215. Ni, C.L., Shi, H.P., Yu, H.M., Chang, Y.C., and Chen, Y.R. (2011) *FASEB J* **25**, 1390-1401
216. Lorenzo, A., and Yankner, B.A. (1994) *Proc Natl Acad Sci U S A* **91**, 12243-12247
217. Irizarry, M.C., Soriano, F., McNamara, M., Page, K.J., Schenk, D., Games, D., and Hyman, B.T. (1997) *J Neurosci* **17**, 7053-7059
218. Westerman, M.A., Cooper-Blacketer, D., Mariash, A., Kotilinek, L., Kawarabayashi, T., Younkin, L.H., Carlson, G.A., Younkin, S.G., and Ashe, K.H. (2002) *J Neurosci* **22**, 1858-1867
219. Terry, R.D., Masliah, E., Salmon, D.P., Butters, N., DeTeresa, R., Hill, R., Hansen, L.A., and Katzman, R. (1991) *Ann Neurol* **30**, 572-580
220. Dickson, D.W., Crystal, H.A., Bevona, C., Honer, W., Vincent, I., and Davies, P. (1995) *Neurobiol Aging* **16**, 285-298
221. Giuffrida, M.L., Caraci, F., Pignataro, B., Cataldo, S., De Bona, P., Bruno, V., Molinaro, G., Pappalardo, G., Messina, A., Palmigiano, A., Garozzo, D., Nicoletti, F., Rizzarelli, E., and Copani, A. (2009) *J Neurosci* **29**, 10582-10587
222. Shoji, M. (2002) *Front Biosci* **7**, 997-1006
223. Lambert, M.P., Barlow, A.K., Chromy, B.A., Edwards, C., Freed, R., Liosatos, M., Morgan, T.E., Rozovsky, I., Trommer, B., Viola, K.L., Wals, P., Zhang, C., Finch, C.E., Krafft, G.A., and Klein, W.L. (1998) *Proc Natl Acad Sci U S A* **95**, 6448-6453

224. Townsend, M., Shankar, G.M., Mehta, T., Walsh, D.M., and Selkoe, D.J. (2006) *J Physiol* **572**, 477-492
225. Klein, W.L., Krafft, G.A., and Finch, C.E. (2001) *Trends Neurosci* **24**, 219-224
226. Shankar, G.M., Li, S., Mehta, T.H., Garcia-Munoz, A., Shepardson, N.E., Smith, I., Brett, F.M., Farrell, M.A., Rowan, M.J., Lemere, C.A., Regan, C.M., Walsh, D.M., Sabatini, B.L., and Selkoe, D.J. (2008) *Nat Med* **14**, 837-842
227. Selkoe, D.J. (2008) *Behav Brain Res* **192**, 106-113
228. Lue, L.F., Kuo, Y.M., Roher, A.E., Brachova, L., Shen, Y., Sue, L., Beach, T., Kurth, J.H., Rydel, R.E., and Rogers J. (1999) *Am J Pathol* **155**, 853-862
229. Naslund, J., Haroutunian, V., Mohs, R., Davis, K.L., Davies, P., Greengard, P., and Buxbaum, J.D. (2000) *JAMA* **283**, 1571-1577
230. Lacor, P.N., Buniel, M.C., Furlow, P.W., Clemente, A.S., Velasco, P.T., Wood, M., Viola, K.L., and Klein, W.L. (2007) *J Neurosci* **27**, 796-807
231. Ivon Koch, C.S., Zheng, H., Chen, H., Trumbauer, M., Thinakaran, G., van der Ploeg, L.H.T., Price, D.L., and Sisodia, S.S. (1997) *Neurobiol Aging* **18**, 661-669
232. Heber, S., Herms, J., Gajic, V., Hainfellner, J., Aguzzi, A., Rulicke, T., Kretschmar, H., von Koch, C., Sisodia, S., Tremml, P., Lipp, H-P., Wolfer, D.P., and Müller, U. (2000) *J Neurosci* **20**, 7951-7963
233. Müller, U., Cristina, N., Li, Z.W., Wolfer, D.P., Lipp, H.P., Rulicke, T., Brandner, S., Aguzzi, A., and Weissmann, C. (1994) *Cell* **79**, 755-765
234. Zheng, H., Jiang, M., Trumbauer, M.E., Sirinathsinghji D.J., Hopkins, R., Smith, D.W., Heavens, R.P., Dawson, G.R., Boyce, S., Conner, M.W., Stevens, K.A., Slunt, H.H., Sisodia, S.S., Chen, H.Y., and Van der Ploeg, L.H. (1995) *Cell* **81**, 525-531

235. Qiu, W.Q., Ferreira, A., Miller, C., Koo, E.H., and Selkoe, D.J. (1995) *J Neurosci* **15**, 2157-2167
236. Perez, R.G., Zheng, H., Van der Ploeg, L.H., and Koo, E.H. (1997) *J Neurosci* **17**, 9407-9414
237. Soba, P., Eggert, S., Wagner, K., Zentgraf, H., Siehl, K., Kreger, S., Lower, A., Langer, A., Merdes, G., Paro R, Masters, C.L., Müller, U., Kin, S., and Beyreuther, K. (2005) *EMBO J* **24**, 3624-3634
238. Chen, M., and Yankner, B.A. (1991) *Neurosci Lett* **125**, 223-226
239. Li, H., Wang, B., Wang, Z., Guo, Q., Tabuchi, K., Hammer, R.E., Südhof, T.C., Wang, R., and Zheng, H. (2010) *Proc Natl Acad Sci* **107**, 17362–17367
240. Zheng, H., and Koo, E.H. (2006) *Mol Neurodegener* **1**, 5
241. Müller, T., Concannon, C.G., Ward, M.W., Walsh, C.M., Tirniceriu, A.L., Tribl, F., Kogel, D., Prehn, J.H., and Egensperger, R. (2007) *Mol Biol Cell* **18**, 201-210
242. Nakayama, K., Ohkawara, T., Hiratochi, M., Koh, C.S., Nagase, H. (2008) *Neurosci Lett* **444**, 127-131
243. Hamid, R., Kilger, E., Willem, M., Vassallo, N., Kostka, M., Bornho, C., Reichert, A.S., Kretzschmar, H.A., Haass, C., and Herms, J. (2007) *J Neurochem* **102**, 1264-1275
244. Vogt, D.L., Thomas, D., Galvan, V., Bredesen, D.E., Lamb, B.T., and Pimplikar, S.W. (2011) *Neurobiol. Aging* **32**, 1725-1729
245. Ghosal, K., Vogt, D.L., Liang, M., Shen, Y., Lamb, B.T., and Pimplikar, S.W. (2009) *Proc Natl Acad Sci* **43**, 18367-18377
246. Bibel, M., Richter, J., Schrenk, K., Tucker, K.L., Staiger, V., Korte, M., Goetz, M., and Barde, Y.A. (2004) *Nat Neurosci* **7**, 1003-1009

247. Murakami, N., Yamaki, T., Iwamoto, Y., Sakakibara, T., Kobori, N., Fushiki, S., and Ueda, S. (1998) *J Neurotrauma* **15**, 993-1003
248. Moya, K.L., Benowitz, L.I., Schneider, E., and Allinquant, B. (1994) *Dev Biol* **161**, 597-603
249. Ravona-Springer, R., Davidson, M., and Noy, S. (2003) *CNS Spectr* **8**, 824-833
250. Samuels, S.C., and Grossman, H. (2003) *CNS Spectr* **8**, 834-845
251. Skoog, I., Nilsson, B., Palmertz, L.A., Andreasson, A., and Svanborg, A. (1993) *N Engl J Med* **328**, 153-158
252. Sparks, D.L., Gross, D.R., and Hunsaker, J.C. (2000) *Neurobiol Aging* **21**, 363-372
253. Sadowski, M., Pankiewicz, J., and Scholtzova, H. (2004) *Neurochem Res* **29**, 1257-1266
254. De Backer, G., Ambrosioni, E., and Borch-Johnsen, K. (2003) *Eur Heart J* **24**, 1601-1610
255. Panza, F., D'Introno, A., Colacicco, A.M., Capurso, C., Pichichero, G., Capurso, S.A., Capurso, A., and Solfrizzi, V. (2006) *Brain Res Rev* **51**, 275-292
256. Zambón, D., Quintana, M., Mata, P., Alonso, R., Benavent, J., Cruz-Sánchez, F., Gich, J., Pocoví, M., Civeira, F., Capurro, S., Bachman, D., Sambamurti, K., Nicholas, J., and Pappolla, M.A. (2010) *Am J Med* **123**, 267-274
257. Whitmer, R.A., Sidney, S., Selby, J., Johnston, S.C., and Yaffe, K. (2005) *Neurology* **62**, 277-281
258. Helzner, E.P., Luchsinger, J.A., Scarmeas, N., Cosentino, S., Brickman, A.M., Glymour, M.M., and Stern, Y. (2009) *Arch Neurol* **66**, 343-348

259. Yaffe, K., Barrett-Connor, E., Lin, F., and Grady, D. (2002) *Arch Neurol* **59**, 378-384
260. Dietschy, J.M., and Turley, S.D. (2001) *Curr Opin Lipidol* **12**, 105-112
261. Pfrieger, F.W. (2003) *Cell Mol Life Sci* **60**, 1158-1171
262. Koudinov, A.R., and Koudinova, N.V. (2005) *J Neurol Sci* **229-230**, 233-240
263. Gaylor, J.L. (2002) *Biochem Biophys Res Commun* **292**, 1139-1146
264. Korade, Z., Mi, Z., Portugal, C., and Schor, N.F. (2007) *Neurobiol Aging* **28**, 1522-1531
265. Ong, W.Y., Kim, J.H., He, X., Chen, P., Farooqui, A.A., and Jenner, A.M. (2010) *Mol Neurobiol* **41**, 299-313
266. Zhang, Y., Appelkvist, E.L., Kristensson, K., and Dallner, G. (1996) *Neurobiol Aging* **17**, 869-875
267. Snipes, G.J., and Suter, U. (1997) *Sub-Cell Biochem* **28**, 173-204
268. Dietschy, J.M., and Turley, S.D. (2004) *J Lipid Res* **45**, 1375-1397
269. Meaney, S., Lütjohann, D., Diczfalussy, U., and Björkhem, I. (2000) *Biochim Biophys* **1486**, 293-298
270. Accad, M., Smith, S.J., Newland, D.L., Sanan, D.A., King, L.E.Jr., Linton, M.F., Fazio, S., and Farese, R.V.Jr. (2000) *J Clin Invest* **105**, 711-719
271. Linton, M.F., Gish, R., Hubl, S.T., Butler, E., Esquivel, C., Bry, W.I., Boyles, J.K., Wardell, M.R., and Young, S.G. (1991) *J Clin Invest* **88**, 270-281
272. Dehouck, B., Dehouck, M.P., Fruchart, J.C., and Cecchelli, R. (1994) *J Cell Biol* **126**, 465-473

273. Turley, S.D., Burns, D.K., Rosenfeld, C.R., and Dietschy, J.M (1996) *J Lipid Res* **37**, 1953-1961
274. Spady, D.K., Huettinger, M., Bilheimer, D.W., and Dietschy, J.M. (1987) *J Lipid Res* **28**, 32-41
275. Osono, Y., Woollett, L.A., Herz, J., and Dietschy, J.M. (1995) *J Clin Invest* **95**, 1124-1132
276. Quan, G., Xie, C., Dietschy, J.M., and Turley, S.D. (2003) *Dev Brain Res* **146**, 87-98
277. Suzuki, S., Kiyosue, K., Hazama, S., Ogura, A., Kashihara, M., Hara, T., Koshimizu, H., and Kojima, M. (2007) *J Neurosci* **27**, 6417-6427
278. Nieweg, K., Schaller, H., and Pfrieder, F.W. (2009) *J Neurochem* **109**, 125-134
279. Boyles, J.K., Notterpek, L.M., Wardell, M.R., and Rall, Jr. S.C. (1990) *J Lipid Res* **31**, 2243-56
280. May, P.C., Lampert-Etchells, M., Johnson, S.A., Poirier, J., Masters, J.N., and Finch, C.E. (1990) *Neuron* **5**, 831-839
281. Lorent, K., Overbergh, L., Moechars, D., De Strooper, B., van Leuven, F., Van den Berghe, H. (1995) *Neuroscience* **65**, 1009-1025
282. Ong, W.Y., Lau, C.P., Leong, S.K., Kumar, U., Suresh, S., and Patel, S.C. (1999) *Neuroscience* **90**, 913-922
283. Thomas, E.A., Dean, B., Pavey, G., and Sutcliffe, J.G. (2001) *Proc Natl Acad Sci USA* **98**, 4066-4071
284. Iwata, A., Browne, K.D., Chen, X.H., Yuguchi, T., and Smith, D.H. (2005) *J Neurosci Res* **82**, 103-14

285. LaDu, M.J., Gilligan, S.M., Lukens, S.R., Cabana, V.G., Reardon, C.A., Van Eldik, L.J., and Holtzman, D.M. (1998) *J Neurochem* **70**, 2070-2081
286. Gong, J.S., Kobayashi, M., Hayashi, H., Zou, K., Sawamura, N., Fujita, S.C., Yanagisawa, K., and Michikawa, M. (2002) *J Biol Chem* **277**, 29919-29926
287. Pfrieger, F.W., and Ungerer, N. (2011) *Prog Lipid Res* **50**, 357-371
288. Krimbou, L., Marcil, M., and Genest, J. (2006) *Curr Opin Lipidol* **17**, 258-267
289. Fukumoto, H., Deng, A., Irizarry, M.C., Fitzgerald, M.L., and Rebeck, G.W. (2002) *J Biol Chem* **277**, 48508-48513
290. Pitas, R.E., Boyles, J.K., Lee, S.H., Foss, D., and Mahley, R.W. (1987) *Biophys Acta* **917**, 148-161
291. Swanson, L.W., Simmons, D.M., Hoffmann, S.L., Goldstein, J.L., and Brown, M.S. (1988) *Proc Natl Acad Sci USA* **85**, 9821-9825
292. Moestrup, S.K., Gliemann, J., and Pallensen, G. (1992) *Cell Tissue Res* **269**, 375-382
293. Möbius, W., Van Donselaar, E., Ohno-Iwashita, Y., Shimada, Y., Heijnen, H.F.G., Slot, J.W., and Geuze, H.J. (2003) *Traffic* **4**, 222-231
294. Chang, T-Y., Bo-Liang, L., Chang, C.C.Y., and Urano, Y. (2009) *Am J Physiol Endocrinol Metab* **297**, 1-9
295. Sakashita, N., Miyazaki, M., Takeya, M., Horiuchi, S., Chang, C.C.Y., Chang, T.Y., and Takahashi, K. (2000) *Am J Pathol* **156**, 227-236
296. Björkhem, I., and Meaney, S. (2004) *Arterioscler Thromb Vasc Biol* **24**, 806-881
297. Russell, D.W., Halford, R.W., Ramirez, D.M., Shah, R., and Kotti, T. (2009) *Annu Rev Biochem* **78**, 1017-1040

298. Meaney, S., Bodin, K., Diczfalusy, U., and Björkhem, I. (2002) *J Lipid Res* **43**, 2130-2135
299. Grundy, S.M., Hansen, B., Smith, S.C. Jr., Cleeman, J.I., and Kahn, R.A. (2004) *Circulation* **109**, 551-556
300. Simons, M., Keller, P., De Strooper, B., Beyreuther, K., Dotti, C.G., and Simons, K. (1998) *Proc Natl Acad Sci U S A* **95**, 6460-6464
301. Frears, E.R., Stephens, D.J., Walters, C.E., Davies, H., and Austen, B.M. (1999) *Neuroreport* **10**, 1699-1705
302. Wahrle, S., Das, P., Nyborg, A.C., McLendon, C., Shoji, M., Kawarabayashi, T., Younkin, L.H., Younkin, S.G., and Golde, T.E. (2002) *Neurobiol Dis* **9**, 11-23
303. Refolo, L.M., Malester, B., LaFrancois, J., Bryant-Thomas, T., Wang, R., Tint, G.S., Duff, K., and Pappolla, M.A. (2000) *Neurobiol Dis* **7**, 321-331
304. Bodovitz, S., and Klein, W.L. (1996) *J Biol Chem* **271**, 4436-4440
305. Kojro, E., Gimpl, G., Lammich, S., Marz, W., and Fahrenholz, F. (2001) *Proc Natl Acad Sci U S A* **98**, 5815-5820
306. Racchi, M., Baetta, R., Salvietti, N., Ianna, P., Franceschini, G., Paoletti, R., Fumagalli, R., Govoni, S., Trabucchi, M., and Soma, M. (1997) *Biochem J* **322**, 893-898
307. Yip, C.M., Elton, E.A., Darabie, A.A., Morrison, M.R., and McLaurin, J. (2001) *J Mol Bio* **311**, 723-734
308. Mizuno, T., Nakata, M., Naiki, H., Michikawa, M., Wang, R., Haass, C., and Yanagisawa, K. (1999) *J Biol Chem* **274**, 15110-15114
309. Shepardson, N.E., Shankar, G.M., and Selkoe, D.J. (2011) *Arch Neurol* **68**, 1239-1244

310. Buxbaum, J.D., Geoghagen, N.S., and Friedhoff, L.T. (2001) *J Alzheimers Dis* **3**, 221-229
311. Paris, D., Townsend, K.P., Humphrey, J., Obregon, D.R., Yokota, K., and Mullan, M. (2002) *Atherosclerosis* **161**, 293-299
312. Chauhan, N.B., Siegel, G.J., and Feinstein, D.L. (2004) *Neurochem Res* **29**, 1897-1911
313. Li, L., Cao, D., Kim, H., Lester, R., and Fukuchi, K.I. (2006) *Ann Neurol* **60**, 729-739
314. Wallerath, T., Deckert, G., Ternes, T., Anderson, H., Li, H., Witte, K., and Förstermann, U. (2002) *Circulation* **106**, 1652-1658
315. Laufs, U., La Fata, V., Plutzky, J., and Liao, J.K. (1998) *Circulation* **97**, 1129-1135
316. Kureishi, Y., Lou, Z., Shiojima, I., Bialik, A., Fulton, D., Lefer, D.J., Sessa, W.C., and Walsh, K. (2001) *Nat Med* **6**, 1004-1010
317. Kurinami, H., Sato, N., Shinohara, M., Takeuchi, D., Takeda, S., Shimamura, M., Ogihara, T., and Morishita, R. (2008) *Int J Mol Med* **21**, 531-537
318. Tong, X.K., Nicolakakis, N., Fernandes, P., Ongali, B., Brouillette, J., Quirion, R., and Hamel, E. (2009) *Neurobiol Dis* **35**, 406-414
319. Mancuso, C., Head, E., Barone, E., Perluigi, M., Preziosi, P., and Butterfield, D.A. (2014) *Handbook of Neurotoxicity* 2339-2354
320. Barone, E., Cenini, G., Di Domenico, F., Martin, S., Sultana, R., Mancuso, C., Murphy, M.P., Head, E., and Butterfield, D.A. (2011) *Pharmacol Res* **63**, 172-180
321. Butterfield, D.A., Barone, E., Di Domenico, F., Cenini, G., Sultana, R., Murphy, M.P., and Head, E. (2012) *Int J Neuropsychopharmacol* **15**, 981-987

322. Mancuso, C., and Barone, E. (2009) *Curr Drug Metab* **10**, 579-594
323. Beydoun, M.A., Beason-Held, L.L., Kitner-Triolo, M.H., Beydoun, H.A., Ferrucci, L., Resnick, S.M., and Zonderman, A.B. (2011) *J Epidemiol Community Health* **65**, 949-957
324. Haag, M.D., Hofman, A., Koudstaal, P.J., Stricker, B.H., and Breteler, M.M. (2009) *J Neurol Neurosurg Psychiatry* **80**, 13-17
325. Li, G., Shofer, J.B., Rhew, I.C., Kukull, W.A., Peskind, E.R., McCormick, W., Bowen, J.D., Schellenberg, G.D., Crane, P.K., Breitner, J.C., and Larson, E.B. (2010) *J Am Geriatr Soc* **58**, 1311-1317
326. Rosenberg, H., and Allard, D. (2008) *Scand Cardiovasc J* **42**, 268-273
327. Sparks, D.L., Kryscio, R.J., Sabbagh, M.N., Connor, D.J., Sparks, L.M., and Liebsack, C. (2008) *Curr Alzheimer Res* **5**, 416-421
328. Cramer, C., Haan, M.N., Galea, S., Langa, K.M., and Kalbfleisch, J.D. (2008) *Neurology* **71**, 344-350
329. Jick, H., Zornberg, G.L., Jick, S.S., Seshadri, S., and Drachman, D.A. (2000) *Lancet* **356**, 1627-1631
330. Yaffe, J., Barrett-Connor, E., Lin, F., and Grady, D. (2002) *Arch Neurol* **59**, 378-384
331. Benito-León, J., Louis, E.D., Vega, S., and Bermejo-Pareja, F. (2010) *J Alzheimer's Dis* **21**, 95-102
332. Hippisley-Cox, J., and Coupland, C. (2010) *BMJ* **340**, c2197
333. Zandi, P.P., Sparks, D.L., Khachaturian, A.S., Tschanz, J., Norton, M., Steinberg, M., Welsh-Bohmer, K.A., Breitner, J.C., and Cache County Study investigators. (2005) *Arch Gen Psychiatry* **62**, 217-224

334. Rea, T.D., Breitner, J.C., Psaty, B.M., Fitzpatrick, A.L., Lopez, O.L., Newman, A.B., Hazzard, W.R., Zandi, P.P., Burke, G.L., Lyketsos, C.G., Bernick, C., and Kuller, L.H. (2005) *Arch Neurol* **62**, 1047-1051
335. Trompet, S., van Vliet, P., de Craen, A.J., Jolles, J., Buckley, B.M., Murphy, M.B., Ford, I., Macfarlane, P.W., Sattar, N., Packard, C.J., Stott, D.J., Shepherd, J., Bollen, E.L., Blauw, G.J., Jukema, J.W., and Westendorp, R.G. (2010) *J Neurol* **257**, 85-90
336. Feldman, H.H., Doody, R.S., Kivipelto, M., Sparks, D.L., Waters, D.D., Jones, R.W., Schwam, E., Schindler, R., Hey-Hadavi, J., DeMicco, D.A., Breazna, A., and LEADe Investigators. (2010) *Neurology* **74**, 956-964
337. Sano, M., Bell, K.L., Galasko, D., Galvin, J.E., Thomas, R.G., van Dyck, C.H., and Aisen, P.S. (2011) *Neurology* **77**, 556-563
338. Friedhoff, L.T., Cullen, E.I., Geoghagen, N.S.M., and Buxbaum, J.D. (2001) *Int J Neuropsychopharmacol* **4**, 127-130
339. Sparks, D.L., Sabbagh, M.N., Connor, D.J., Lopez, J., Launer, L.J., Browne, P., Wasser, D., Johnson-Traver, S., Lochhead, J., and Ziolkowski, C. (2005) *Arch Neurol* **62**, 753-757
340. Li, G., Larson, E.B., Sonnen, J.A., Shofer, J.B., Petrie, E.C., Schantz, A., Peskind, E.R., Raskind, M.A., Breitner, J.C., and Montine, T.J. (2007) *Neurology* **69**, 878-885
341. McGuinness, B., O'Hare, J., Craig, D., Bullock, R., Malouf, R., and Passmore, P. (2010) *Cochrane Database Syst Rev* CD007514

Chapter 2

2 Peroxynitrite donor SIN-1 modifies high-affinity choline transporter activity by altering its intracellular trafficking¹

¹ A version of this work has been published in the following manuscript:

- Cuddy LK, Gordon AC, Black SA, Jaworski E, Ferguson SSG, Rylett RJ. Peroxynitrite donor SIN-1 modifies high-affinity choline transporter activity by modifying its intracellular trafficking. *J Neurosci* 18 April 2012 32 (16):5573-5584

2.1 Introduction

CHT is an integral component of cholinergic neurons that moves choline from the synaptic cleft into cholinergic nerve endings where it is used as substrate for ACh synthesis. This choline uptake is HC-3 sensitive and can be the rate-limiting step for ACh synthesis (1, 2). Importantly, CHT is sensitive to oxidative stress (3,4), and a critical target for disruption of neuronal communication.

Increasing evidence suggests a role for reactive oxygen and nitrogen moieties in progression of neurodegenerative disorders such as Alzheimer's disease (5). ONOO⁻ forms by combination of O₂⁻ and NO, with these reactive species occurring in response to tissue injury (6-9). ONOO⁻ has multiple fates within cells, including contributing to membrane lipid peroxidation and protein oxidation and nitration. ONOO⁻ inhibits the function of some neurotransmitter transporters, including the dopamine (10) and 5-hydroxytryptamine transporters (11). Also, ONOO⁻ decreases CHT activity in synaptosomes from *T. marmorata* (3). Our laboratory found that SIN-1, which generates ONOO⁻ and other reactive oxidants, causes rapid, dose-dependent inhibition of CHT and this is attenuated by ONOO⁻ scavengers (4). Importantly, oxidants such as H₂O₂ did not alter CHT activity (3, 4).

CHT proteins internalize constitutively by clathrin-mediated endocytosis, residing predominantly in intracellular organelles including synaptic vesicles rather than at the cell surface (12-17). Recruitment of CHT to the plasma membrane is a critical mechanism regulating solute transport (12, 15, 17, 18). CHT interaction with the endocytic machinery is mediated by a dileucine-like motif located in its intracellular carboxyl-terminus, and we showed that mutation of a single leucine in this motif (L531A) substantially reduces constitutive trafficking of CHT with L531A-CHT proteins retained at the cell surface (14).

Here, I found that inhibition of choline uptake in SIN-1 treated cells is due to decreased cell surface CHT levels rather than altered solute binding affinity, and that SIN-1 modulates CHT activity by increasing its internalization and this correlates with

decreased plasma membrane CHT (4). However, the mechanisms by which SIN-1 modulates CHT trafficking between plasma membrane and subcellular organelles are unknown. Thus, the aim of this study was to characterize mechanisms by which SIN-1 modulates CHT function. The endocytosis-defective mutant L531A-CHT was used to test my prediction that it would be resistant to SIN-1 inhibition if the mechanism by which SIN-1 decreases CHT activity involves enhancing CHT internalization. I tracked CHT movement in endosomal-lysosomal compartments and found that acute SIN-1 treatment does not alter these events, but importantly, blocking proteasome, but not lysosome, function attenuated SIN-1-mediated inhibition of CHT.

2.2 Materials and methods

2.2.1 Materials

SIN-1 [3-morpholiniosydnonimine] was from Biomol Research Labs (Plymouth Meeting, PA), lactacystin and MG-132 were from Calbiochem, chloroquine was from Sigma-Aldrich (St. Louis, MO), bafilomycin A1 was from Santa Cruz Biotechnology (Santa Cruz, CA), and [methyl-³H]choline chloride (128 Ci/mmol) and [methyl-³H]hemicholinium-3 diacetate ([³H]HC-3) (144.5 Ci/mmol) were from Perkin-Elmer Life Sciences (Boston, MA). Other chemicals were purchased from Sigma-Aldrich at the highest purity available. SH-SY5Y human neuroblastoma cells were from the American Type Culture Collection (Manassus, VA), and Invitrogen (Burlington, ON, Canada) supplied HEK 293 Flp-In cells, fetal bovine serum (FBS), and culture media and reagents. Zenon-Alexa Fluor 488 and 555 mouse IgG labelling kits were from Molecular Probes (Eugene, OR). Enhanced ChemiLuminescence immunoblot reagent (ECL) was from GE Healthcare Life Sciences (Baie d'Urfé, QC, Canada) and Biodegradable Scintillant was from Amersham Canada Ltd. (Oakville, ON, Canada). Polyclonal CHT antibody was raised in rabbits to the antigenic peptide DVDSSPEGSGTEDNLQ that is conserved at the carboxyl-terminus of human and rat CHT (Genemed Synthesis, San Antonio, TX); this peptide was conjugated to KLH carrier protein by an amino-terminal cysteine residue. CHT-specific IgG was affinity-purified in our laboratory from the crude anti-serum on NHS-Sepharose (Amersham) to which antigenic peptide had been coupled

as the binding element. The specificity of this antibody for detection of CHT was described previously (4). Peroxidase-conjugated goat anti-rabbit IgG was from Jackson ImmunoResearch Laboratories (West Grove PA).

2.2.2 Stable transfection and selection of cell lines

Full-length rat CHT cDNA ligated to pSPORT was a gift from Dr. T. Okuda (19); a FLAG epitope tag (DYKDDDDK) was added to the amino-terminus by PCR and the resulting cDNA ligated to pcDNA3.1 or pcDNA5 (4). Mutant L531A-CHT was produced by site-directed mutagenesis using a QuikChange kit (Stratagene). SH-SY5Y cells were transfected with plasmids [FLAG-CHT or FLAG-L531A-CHT cDNA ligated to pcDNA3.1] by Lipofectamine 2000. Stable transformants (SY5Y-CHT and SY5Y-L531A-CHT, respectively) were selected using 500 µg/ml geneticin (G418) for 4 weeks, then grown in Dulbecco's modified Eagle medium (DMEM), 10% fetal bovine serum (FBS), 100 U/ml penicillin, 100 µg/ml each of streptomycin and G418. SH-SY5Y cell differentiation was induced by addition of 10 µM all-trans-retinoic acid (RA) for 3 days. HEK 293 cell lines stably-expressing either FLAG-CHT were created by introducing plasmids in pcDNA5 into the Flp Recombinase Target site in HEK-Flp-In cells by Lipofectamine 2000 transfection (HEK-CHT cells). Stable transformants were selected and expanded in DMEM containing 10% FBS, 10 µg/ml gentamicin and 50 µg/ml hygromycin-B.

To inhibit clathrin-mediated constitutive trafficking of CHT proteins, we used AP180C, a DN protein of the carboxyl-terminal portion of adaptin AP180, which can bind to and sequester clathrin to effectively interfere with clathrin-mediated endocytosis (20). Interruption of dynamin-mediated protein trafficking was achieved using Dyn-K44A as a DN dynamin protein which has a point mutation that ablates dynamin GTPase activity that is required for membrane scission (21).

2.2.3 SIN-1 treatment

The use of ONOO⁻ donors such as SIN-1 allows continuous production of a low level of ONOO⁻ by a substance that is relatively stable over a longer period of time (22). As the

half-life of ONOO^- radical is less than 1 sec, bolus administration of this agent does not produce either consistent or sustained concentrations of ONOO^- under experimental conditions. The donor efficiency of SIN-1 may be altered by changes in pH and buffer composition; previous studies that used a Krebs buffer similar to that employed in the present study estimated that 1 μmol ONOO^- is formed per min in a solution of 1 mM SIN-1. This suggests that the SIN-1 treatments used here could generate ONOO^- levels representative of those seen in brain under some conditions (23). The estimated half-life for SIN-1 in these buffer conditions is 14-26 min, suggesting that donor activity would be sustained throughout the treatment periods used in our study. Total ONOO^- production capacity under these buffer conditions has been estimated to be 30 μM , although the ONOO^- concentration in solution at a given time will be lower than this due to its much shorter half-life.

2.2.4 Confocal cell imaging

Digital images of live and fixed cells were acquired with a Zeiss LSM510-Meta laser scanning confocal microscope using a 63X magnification oil-immersion objective. Fluorescent labelling of FLAG-tagged CHT proteins in live cells was accomplished using rabbit anti-FLAG antibody complexed to either Zenon-555 dye (for Rab5a-GFP, Rab7-GFP and Rab9-YFP) or Zenon-488 dye (for Lamp-1 staining or when no co-stain was used). This fluorescently-tagged antibody was added to the medium bathing cells where it could bind to the FLAG-epitope on the extracellularly-oriented amino-terminus of CHT proteins inserted at the plasma membrane. Imaging of live cells allowed real-time tracking of internalization of CHT into cells and movement of these proteins between subcellular organelles. In some experiments, cells were transfected with fluorescently-labelled subcellular compartment markers including Rab5a-GFP (early endosomes), Rab7-GFP (early to late endosomes) or Rab9-YFP (late endosomes). Also in some experiments, cells were formaldehyde-fixed after allowing the internalization of Zenon-labelled CHT proteins as this facilitated imaging and was required for counter-staining cells to visualize lysosomes using an anti-human antibody directed to LAMP-1. Formalin-fixation of GFP or YFP-fusion protein expressing cells did not alter the image

quality of these fluorophores compared to images that were captured from live cells expressing these fusion proteins.

Colocalization analysis was performed on confocal images using Imaris 7.0 with the Imaris Colocalization module (bit-plane) to examine the colocalization of the brightest 2% of pixels in each channel. Graphing and statistical analysis was performed using Prism GraphPad using one-way ANOVA with Tukey's post-hoc test.

2.2.5 [³H]Choline uptake assay

Monolayers of cells were washed, then incubated at 37°C in Krebs-Ringer HEPES solution (KRH) [mM: NaCl, 124; KCl, 5; MgSO₄, 1.3; CaCl₂, 1.5; glucose, 10; HEPES-NaOH, 20, pH 7.4]. Either vehicle or SIN-1 was added to cells for specified times, followed by incubation for 5 min with 0.5 μM [³H]-choline (0.5 μCi/ml) in the absence or presence of 1 μM HC-3. Cells were placed on ice and washed with cold KRH, then lysed in 0.1 M NaOH. After 30 min incubation, aliquots of samples were analyzed for tritium by liquid scintillation spectrometry and protein concentration using Biorad protein dye. Each independent experiment consisted of triplicate plates of cells per treatment group, with results normalized to sample protein content and averaged. Specific choline uptake was calculated as the difference between total choline uptake and non-specific uptake in the presence of HC-3, with the resulting [³H]choline uptake data expressed as pmol / mg protein per 5 min ± SEM.

2.2.6 [³H]HC-3 binding assay

Monolayers of cells were washed and incubated in KRH at 37°C with the addition of either vehicle or 1 mM SIN-1 for specified times, then washed with ice-cold KRH and kept on ice for 10 min to stop protein trafficking activity. Cells were then incubated with [³H]HC-3 (10 nM; 0.23 Ci/mmol) in the presence or absence of 1 μM unlabelled HC-3 for 1 h on ice. For kinetic analysis, HC-3 binding was measured over the range of 0.5 - 10 nM HC-3 with the specific activity of [³H]HC-3 held constant at 0.23 Ci/mmol. Following incubation, cells were washed rapidly with cold KRH to remove unbound HC-3 and then lysed using 0.1 M NaOH for 30 min. Aliquots of cell lysates were used for

quantification of tritium and protein content. Each independent experiment had triplicate determinations with HC-3 binding normalized to sample protein content and then averaged. Specific HC-3 binding was calculated as the difference between total and non-specific HC-3 binding, and values were expressed as fmol / mg protein \pm SEM.

2.2.7 Cell surface protein biotinylation assay

Cells plated on 60 mm dishes were washed with HEPES-buffered saline solution (HBSS), then treated at 37°C with either vehicle (HBSS) or HBSS containing 1 mM SIN-1 for the times indicated. After treatment, cells were placed on ice under cold HBSS to stop protein trafficking. Plasma membrane proteins were biotinylated on ice by incubating with 1 mg/ml sulfo-NHS-SS-biotin in HBSS for 1 h (4, 24). Unbound biotin was quenched by washing and incubating cells in cold 100 mM glycine in HBSS. After two further washes with HBSS, cells were lysed on ice for 30 min in Triton X-100 lysis buffer [1% w/v Triton-X-100, 150 mM NaCl, 50 mM Tris-HCl pH 7.5, 1 mM AEBSF, 10 μ g/ml each of leupeptin and aprotinin, and 25 μ g/ml pepstatin A, 700 U/ml DNase]. Neutravidin beads were incubated with cell lysates for 1 h at 4°C with gentle mixing to bind biotin-labelled proteins to allow separation from the non-biotinylated proteins. Beads were then washed with lysis buffer three times, PBS twice, and bound proteins were eluted by incubation for 10 min at 55°C with Laemmli sample buffer [2% SDS, 10% glycerol, 62.5 mM Tris-HCl pH 6.8, 2.5% β -mercaptoethanol and 0.001% bromophenol blue]. Aliquots of biotinylated proteins and total cell lysates were separated on a 7.5% SDS-PAGE gel and transferred to polyvinylidene difluoride (PVDF) membrane. Membranes were blocked in 8% non-fat dry milk in wash buffer (PBS, 0.1% Tween-20) for 1 h, then incubated for 2 h with rabbit anti-CHT antibody (1:1,000) in wash buffer with 8% milk. After washing, membranes were incubated for 1 h with peroxidase-conjugated goat anti-rabbit IgG secondary antibody (1:10,000) in wash buffer containing 8% milk, and again washed. Immunoreactive proteins on membranes were detected by chemiluminescence using the enhanced chemiluminescence (ECL) kit (GE Healthcare). Immunopositive bands (at approximately 50-kDa for CHT protein) were quantified by densitometry using Scion Image software (NIH). Bands for cell surface CHT were

normalized by comparison to vehicle-treated control cells in each experiment which represented basal cell surface CHT levels.

2.2.8 Data analysis

Data are presented as the mean \pm SEM with n values representing the number of independent experiments performed on separate populations of cells; each n value was obtained from the average of multiple sample replicates in each experiment. GraphPad Prism 5 and InStat software were used for data analysis. Sigmoid and Michaelis-Menten equations were used to calculate kinetic parameters (B_{\max} and K_D) of HC-3 binding. Statistical significance was assessed by paired Student's t -test, or between groups using one-way ANOVA with either Dunnett's or Tukey's post-hoc multiple comparison test, as appropriate (asterisks denote $p \leq 0.05$).

Replicate experiments were performed on cells cultured in successive passages as much as possible to minimize inter-experiment variability; intra-experiment variability between replicate samples was minimal thus facilitating comparisons of treatment effects.

2.3 Results

2.3.1 SIN-1 decreases activity of wild-type CHT, but not mutant L531A-CHT

Initial experiments in this chapter characterized SIN-1 effects on choline uptake in SH-SY5Y cells stably expressing wild-type CHT or the endocytosis-deficient mutant L531A-CHT. My lab showed previously that SIN-1 treatment of cells decreases choline uptake activity and reduces cell surface CHT levels due to accelerated endocytosis (4). Also, CHT undergoes clathrin-mediated endocytosis and L531A-CHT, which lacks the dileucine trafficking motif, is defective in this internalization (14). Thus, I predicted that if SIN-1 reduces cell surface levels of CHT by increasing its clathrin-mediated endocytosis, then L531A-CHT activity would be resistant to this SIN-1 mediated effect.

Laser scanning confocal images of live cells confirmed that a large proportion of CHT is located in subcellular organelles, whereas L531A-CHT resides at the cell surface (data not shown) (14). Also, consistent with the increased levels of plasma membrane CHT, choline uptake activity in SY5Y-L531A-CHT cells is significantly greater than in SY5Y-CHT cells (1673 ± 151 and 816 ± 106 pmol/mg protein/5 min, respectively). A critical observation made in this study in support of my prediction is that acute SIN-1 exposure caused a dose-dependent decrease in choline uptake by wild-type CHT, but did not alter activity of SY5Y-L531A-CHT. Consistent with our previous findings (4), choline uptake was $49 \pm 14\%$ of control in SY5Y-CHT cells treated with 1 mM SIN-1, but L531A-CHT was resistant to inhibition by 1 mM SIN-1, retaining $95 \pm 11\%$ of control uptake activity. Figure 2-1 illustrates dose-response relationships for choline uptake in SIN-1-treated retinoic acid-differentiated SY5Y-CHT and SY5Y-L531A-CHT cells. A statistically significant difference was seen between SY5Y-CHT and SY5Y-L531A-CHT dose-response curves at 1 mM SIN-1. It is important to note that as 1 mM SIN-1 did not alter activity of L531A-CHT, it is unlikely that inhibition of CHT is due to oxidative or nitrosative modification of CHT proteins.

At higher doses of SIN-1 (5 mM), inhibition of the two transporters did not differ significantly (49% and 33% of control uptake for L531A-CHT and CHT) (data not shown), but this is likely due to non-specific effects of SIN-1 such as the collapse of ionic gradients required for active uptake of choline or compromised membrane integrity, rather than to an effect of the drug on CHT. We showed previously that the decrease in CHT activity mediated by acute exposure of cells to 1 mM SIN-1 is not due to damage to cell integrity or toxicity monitored by LDH release and the MTT assay (4). Also, the SIN-1-mediated inhibition of choline uptake occurs rapidly; choline uptake activity assayed at 5 min of SIN-1 exposure reveals a significant decrease in CHT activity (data not shown).

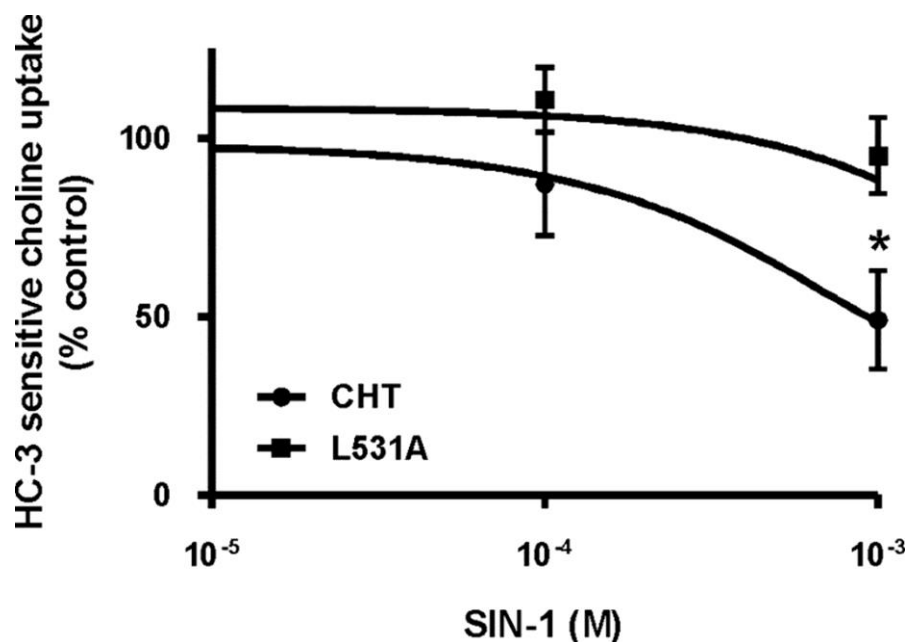


Figure 2-1 SIN-1 inhibits choline uptake activity of wild-type CHT but not L531A-CHT in SH-SY5Y cells.

Retinoic acid-differentiated SH-SY5Y cells stably expressing either wild-type CHT or L531A-CHT were treated for 30 min with either vehicle or varying concentrations of SIN-1, and then HC-3-sensitive choline uptake activity was measured. Baseline uptake was found to be 816 ± 106 and 1673 ± 151 pmol of choline per milligram of protein over 5 min for CHT and L531A-CHT, respectively. Data (percentage of control uptake in the absence of SIN-1) are expressed as mean \pm SEM of four or five independent experiments, each with triplicate measurements. Statistical analysis was performed on the data before it being normalized to vehicle-treated control uptake for each group; asterisks denote statistically significant differences at $p \leq 0.05$.

2.3.2 SIN-1 decreases cell surface levels of wild-type CHT, but not L531A-CHT

Two approaches, equilibrium binding of the CHT antagonist [^3H]HC-3 and plasma membrane protein biotinylation, were used to measure the SIN-1 effects on the amount of CHT protein at the cell surface. Plasma membrane levels of wild-type and L531A-CHT were assayed in SH-SY5Y cells after 15 min incubation with either vehicle or 1 mM SIN-1. Consistent with the data shown in Figure 2-1 on the effects of SIN-1 on choline uptake activity, CHT and L531A-CHT responded differentially to exposure to this ONOO⁻ donor. In the first approach, specific binding of [^3H]HC-3 was significantly decreased in SIN-1-treated SY5Y-CHT cells to $69.0 \pm 3.7\%$ of vehicle-treated cells ($n = 3$ independent experiments; $p = 0.004$). By comparison, there were no differences in specific binding of [^3H]HC-3 between vehicle- and SIN-1-treated SY5Y-L531A-CHT cells ($111.4 \pm 15.6\%$ of vehicle-treated cells; $n = 4$ independent experiments; $p = 0.64$). With the second approach, immunoblots of biotinylated cell surface proteins were used to assess the plasma membrane levels of CHT in vehicle- and SIN-1-treated SY5Y-CHT and SY5Y-L531A-CHT cells. Cell surface levels of wild-type CHT are significantly reduced in SIN-1-treated SY5Y-CHT cells to $61.5 \pm 13.7\%$ when compared with vehicle-treated cells ($n = 4$ independent experiments; $p = 0.005$). By comparison, cell surface levels of mutant L531A-CHT do not differ between control and SIN-1 treatment groups in SY5Y-L531A-CHT cells ($108.5 \pm 14.9\%$ of vehicle-treated cells; $n = 4$ independent experiments; $p = 0.42$). Statistical analysis was by paired Student's *t* test. Thus, based on both [^3H]HC-3 binding and protein biotinylation data, cell surface levels of CHT were significantly decreased by SIN-1. Neither method revealed a significant change in the plasma membrane levels of L531A-CHT protein in SIN-1-treated SH-SY5Y cells when compared with controls.

For kinetic analysis of the effects of SIN-1 on [^3H]HC-3 binding to wild-type CHT protein, HEK-CHT cells were used as they express higher levels of CHT, thereby facilitating quantification of ligand binding. Analysis of [^3H]HC-3 (0.5–10 nM) binding to CHT was performed following treatment with or without 1 mM SIN-1 (Figure 2-2) to

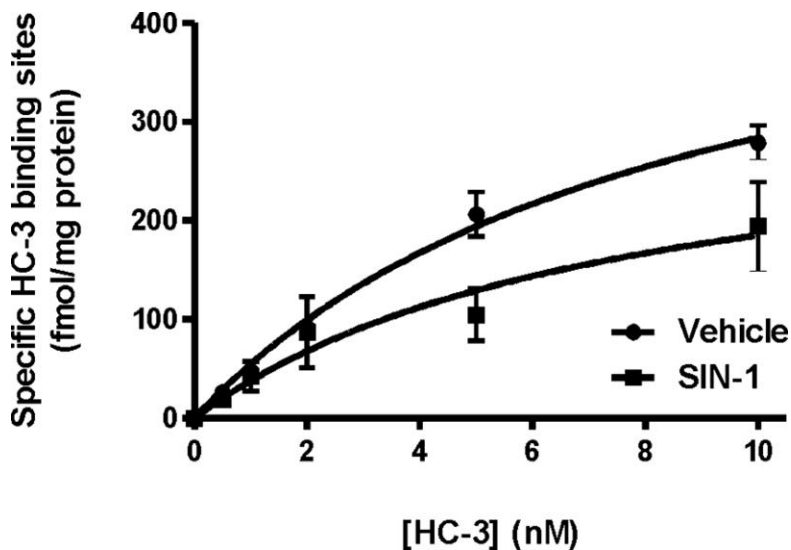


Figure 2-2 SIN-1 decreases CHT activity by changing the number of transporter proteins at the cell surface, but not altering binding of solute to transporters.

Kinetic parameters for cell surface [^3H]HC-3 binding in HEK-CHT cells were estimated using between 0.5 and 10 nM HC-3. Data were calculated as femtomoles of HC-3 bound per milligram of protein, and expressed as mean \pm SEM ($n = 4$). Data were fit by Michaelis-Menten nonlinear regression analysis of individual experiments, and differences between vehicle and SIN-1 treatments were examined by comparison of the apparent binding affinity for ligand (K_D) and the number of CHT sites (B_{\max}) values of the two curves. While the apparent K_D for HC-3 binding to CHT did not differ between vehicle- and SIN-1-treated cells, the B_{\max} for [^3H]HC-3 binding decreased to ~50% of the control value in cells treated with 1mM SIN-1 ($p < 0.05$, Student's t test).

establish whether the observed decrease in cell surface binding of HC-3 was due to a change in binding affinity (K_D) of HC-3 for its target on CHT or only to a change in the plasma membrane level of CHT (B_{max}). The apparent K_D for HC-3 binding to CHT did not differ between vehicle- and SIN-1-treated cells (4 ± 0.9 and 4 ± 0.7 nM, respectively). However, SIN-1 did reduce the cell surface CHT levels with the B_{max} for [3 H]HC-3 binding decreased by ~50% from 473 ± 82 in control cells to 226 ± 71 fmol of [3 H]HC-3 bound/mg protein by SIN-1 ($p < 0.05$; Student's t test).

2.3.3 Blockade of clathrin-mediated endocytosis attenuates inhibition of CHT by SIN-1

Major endocytic pathways for cell surface proteins can be selectively down-regulated by expression in the cells of DN proteins that block the function of critical proteins. In these experiments, I inhibited clathrin-mediated endocytosis with AP180C (20) and used Dyn-K44A as a blocker of both dynamin- and clathrin-dependent endocytosis (21) to examine routes by which CHT internalizes from the plasma membrane during acute SIN-1 exposure. SY5Y-CHT cells were transiently-transfected with plasmids encoding either GFP as a negative control protein or DN proteins, then choline uptake activity was assayed in the absence and presence of SIN-1.

Figure 2-3A reveals that the expression of AP180C blocked the SIN-1 effect indicating that clathrin-mediated endocytosis is involved in the response of CHT to SIN-1 in these cells. Dyn-K44A also attenuated ONOO⁻-mediated inhibition of CHT. To verify that these DN proteins functioned to block CHT internalization, we imaged cells co-expressing CHT and either AP180C or Dyn-K44A; control cells were transfected with empty vector pcDNA3.1. Figure 2-4B illustrates that cells that were transfected to express either of these DN proteins displayed increased CHT localization at the plasma membrane and had substantially reduced subcellular levels of the transporter protein when compared to cells not expressing either of the DN proteins (denoted by arrows) or that were transfected with empty vector.

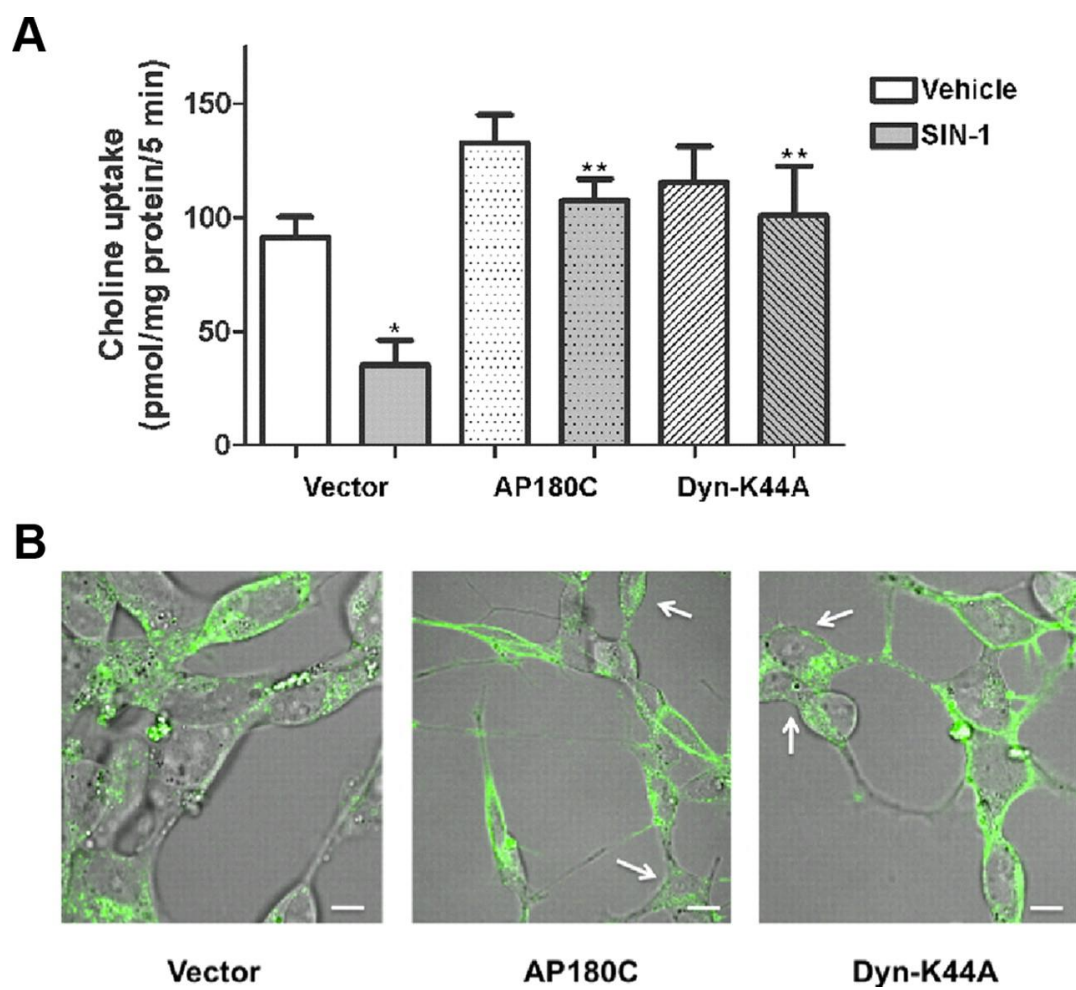


Figure 2-3

Figure 2-3 Inhibition of CHT activity by SIN-1 is attenuated by AP180C and Dyn-K44A.

Selected endocytic pathways were inhibited in SY5Y-CHT cells using DN proteins. **A**, SY5Y-CHT cells were transiently transfected to express either empty vector pcDNA3.1 as a control, AP180C to block the clathrin-dependent pathway, or Dyn-K44A to block dynamin-dependent pathways. HC-3-sensitive choline uptake was assayed in transfected cells after 20 min of either vehicle or 1 mM SIN-1 treatment; HC-3-sensitive choline uptake was determined as the difference between uptake in the absence and presence of 1 μ M HC-3, and expressed as picomoles/milligrams of protein per 5 min. Data were analyzed using a repeated-measures one-way ANOVA with Tukey's *post hoc* multiple-comparisons test. Data are expressed as the mean \pm SEM of five independent experiments. A single asterisk (*) denotes when SIN-1 treatment is significantly different from vehicle treatment ($p \leq 0.05$), and a double asterisk (**) indicates when SIN-1-treated groups are significantly different from each other ($p \leq 0.05$). **B**, Live cells transfected with plasmids encoding either AP180C or Dyn-K44A had visible accumulation of Zenon 488-labeled CHT at the cell surface, whereas cells that were either transfected with the empty vector pcDNA3.1 as the control or that did not become transfected in the DN-transfected plates had substantial internalization of fluorescently labeled CHT into subcellular compartments (these latter cells are identified by white arrows in the AP180C and Dyn-K44A samples). Scale bars: Vector and Dyn-K44A, 5 μ m; AP180C, 10 μ m.

2.3.4 CHT internalizes into Rab5a-positive organelles in control and SIN-1 treated cells

We found previously that acute exposure of cells to the ONOO⁻-donor SIN-1 alters choline uptake activity by increasing the rate at which CHT proteins undergo endocytosis, potentially accounting for the reduction of CHT at the plasma membrane (4). The mechanism by which this occurs is not known, but it could be due to modified interaction of CHT with other proteins and/or internalization machinery such as endocytic and trafficking adaptor or Rab proteins. To address this, I assessed the distribution of CHT internalized from the cell surface to subcellular organelles in live vehicle- and SIN-1-treated SY5Y-CHT and SY5Y-L531A-CHT cells that coexpress GFP-tagged Rab5a as a marker of early endosomes. As shown in Figure 2-4 Panels A-C, wild-type CHT entered Rab5a-positive vesicles in vehicle-treated cells, showing a high level of colocalization with this marker in punctate structures. Acute exposure of SY5Y-CHT cells to SIN-1 did not appear to substantially change the level of internalized CHT colocalizing with Rab5a (Panels D-F). It is interesting to note that the Rab5a-positive vesicles appeared to be larger in SIN-1-treated cells. By comparison, there was negligible internalization of mutant CHT to Rab5a-positive endosomes in either vehicle- or SIN-1-treated SY5Y-L531A-CHT cells during the experimental observation period (Panels G-L).

2.3.5 CHT is present in the late endosome/lysosome system under both vehicle and SIN-1 treatment

Confocal imaging of live cells in which CHT trafficking was followed was used to further address the movement of CHT into late endosomes and lysosomes and to assess if this was altered by SIN-1 treatment. Co-localization was seen between CHT and Rab7-GFP (Figure 2-5), Rab9-YFP (Figure 2-6) and endogenous Lamp-1 (Figure 2-7) in both vehicle-treated control cells and cells that were acutely exposed to 1 mM SIN-1.

As illustrated in Figure 2-5, CHT co-localizes with the late endosomal marker Rab7, but the amount of this co-localization was not substantially altered by SIN-1 treatment. To

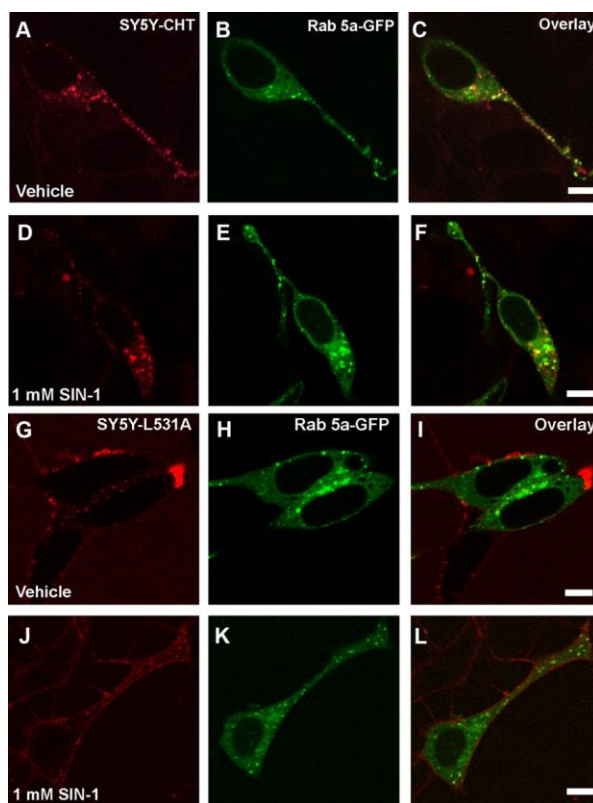


Figure 2-4 Wild-type CHT but not L531A-CHT traffics to Rab5a-positive subcellular compartments in live cells.

Confocal images showing Zenon 555-labeled CHT (red) and GFP-tagged Rab5a (green) distribution in vehicle-treated cells and cells treated with 1 mM SIN-1 for 15 min. Colocalized CHT and Rab5a appear as yellow. Zenon 555 dye conjugated with rabbit anti-FLAG antibody was added to the medium bathing the cells for 10 min at 37°C where it could bind to the extracellular FLAG epitope on CHT, and then the movement of fluorescently labeled proteins into cells was tracked at 10 min after the addition of treatment. Similar levels of colocalization of CHT with Rab5a-GFP were observed in both vehicle (**Panels A–C**)- and SIN-1 (**Panels D–F**)-treated cells expressing wild-type CHT. Interestingly, the subcellular organelles containing CHT-Rab5a in SIN-1-treated cells were larger than those observed in the vehicle-treated cells. In support of my hypothesis, L531A-CHT does not appear to internalize in either vehicle (**Panels G–I**)- or SIN-1 (**Panels J–L**)-treated cells, and the accumulation of Zenon-labeled L531A-CHT can be observed at the cell surface. Scale bars, 5 μ m.

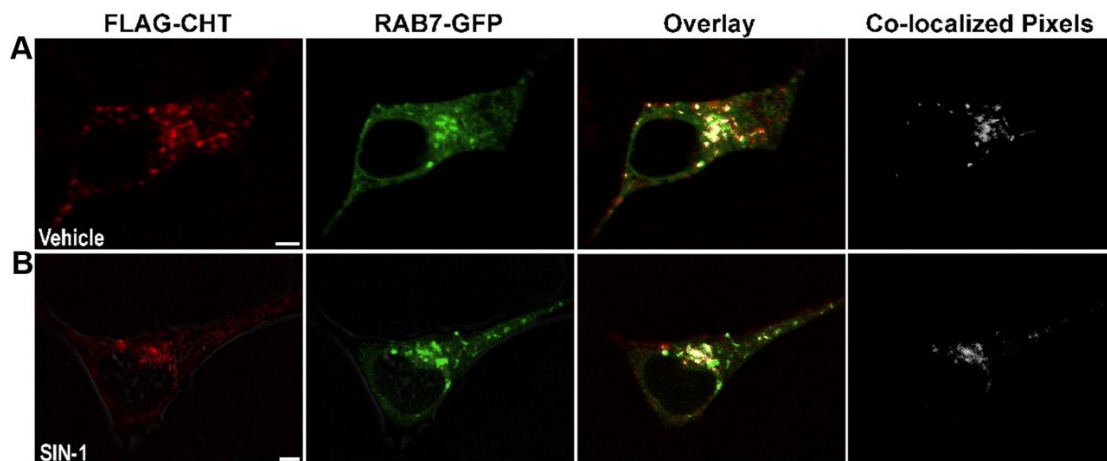


Figure 2-5 CHT colocalization with Rab7-GFP is seen in vehicle-treated (A) and SIN-1-treated (B) SY5Y-CHT cells.

Confocal images show Zenon 555-labeled CHT (red) and GFP-tagged Rab7 (green) distribution in vehicle- and 1 mM SIN-1-treated SY5Y-CHT cells. Colocalized CHT and Rab7 appear as yellow. Zenon 555 dye conjugated to rabbit anti-FLAG antibody was added to the medium bathing the cells for 10 min at 37°C where it could bind to the FLAG epitope on the N terminus of CHT located at the cell surface. This facilitated tracking of the internalization and distribution of CHT proteins in cells after 15 min of either vehicle or SIN-1 treatment. Scale bar, 3 μ m.

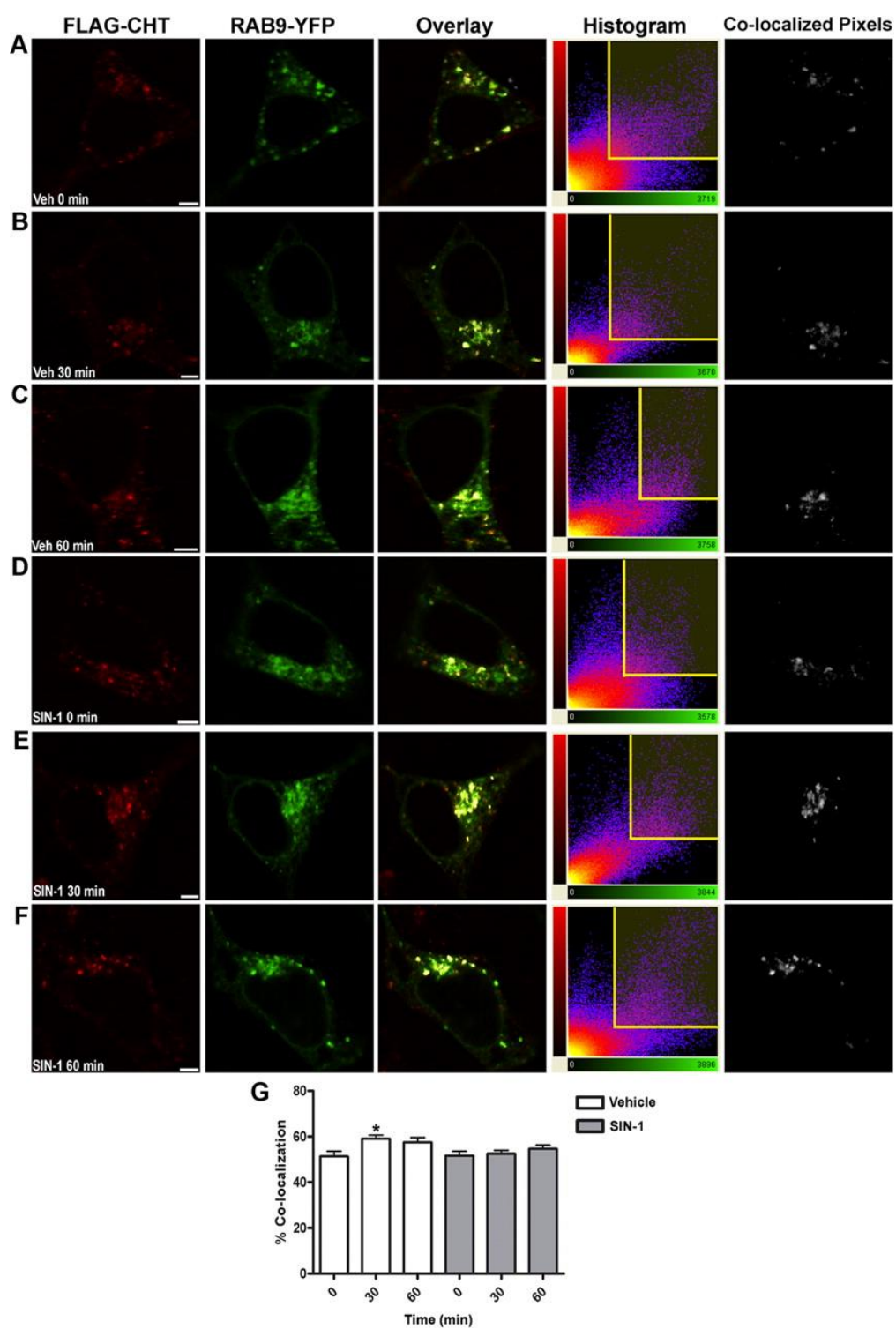


Figure 2-6

Figure 2-6 CHT colocalization with Rab9-YFP in SY5Y-CHT cells is not changed by SIN-1 treatment.

Confocal images show Zenon 555-labeled CHT (red) and YFP-tagged Rab9 (green) distribution in vehicle- and 1 mM SIN-1-treated SY5Y-CHT cells. Zenon 555 dye conjugated to rabbit anti-FLAG antibody was added to the medium bathing the cells for 15 min where it could bind to the FLAG epitope of the extracellular N terminus of CHT proteins that were located at the cell surface. This facilitated tracking of the internalization and distribution of CHT proteins in cells at 0, 30, and 60 min under either vehicle (**Panels A–C**) or SIN-1 (**Panels D–F**) treatment. Colocalized CHT and Rab9-YFP appear as yellow in the Overlay images, and the histograms resulting from analysis of these images are shown (**G**). CHT and Rab9-YFP pixels that were determined to be colocalized in the colocalization channel are shown as white in the Colocalized Pixels images. To quantify colocalization, the brightest 2% of the red pixels (to the right of the vertical yellow line on the histograms) and green pixels (above the horizontal yellow line on the histograms) were selected. Imaris software was used to quantify the colocalization of CHT with Rab9-YFP. Data were analyzed by one-way ANOVA followed by Tukey's posttest and are expressed as mean \pm SEM for a minimum of 40 cells per treatment group from four independent experiments (a single asterisk denotes $p \leq 0.01$). Scale bar, 3 μ m.

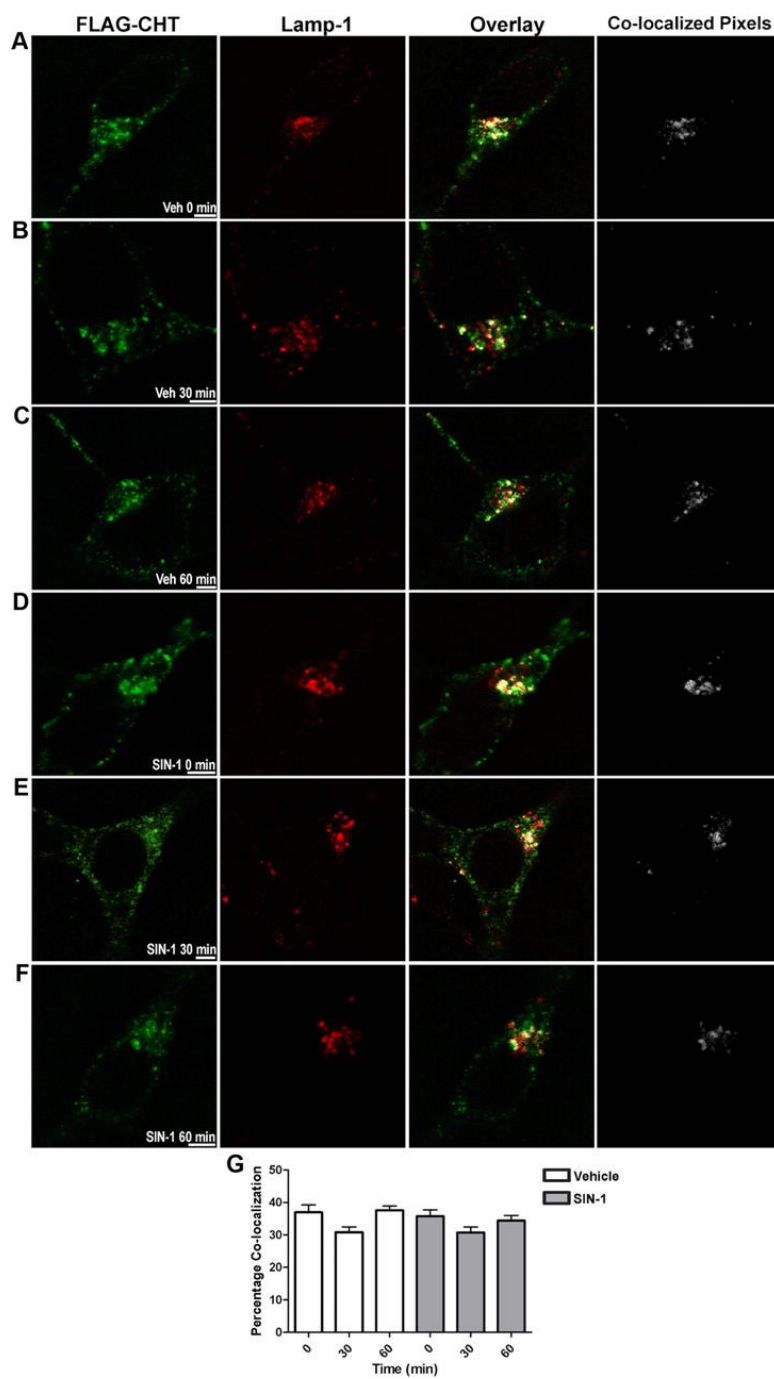


Figure 2-7

Figure 2-7 CHT colocalization with Lamp-1 is seen in vehicle- and SIN-1-treated SY5Y-CHT cells.

Confocal images show Zenon 488-labeled CHT (green) and Alexa Fluor 555-labeled Lamp-1 (red) distribution in vehicle-treated and 1 mM SIN-1-treated SY5Y-CHT cells. Zenon 488 dye conjugated to rabbit anti-FLAG antibody was added to the medium bathing the cells for 15 min where it could bind to the FLAG epitope of the N terminus of CHT located at the cell surface. This facilitated tracking of the internalization and distribution of CHT proteins in cells at 0, 30, and 60 min of either vehicle (**Panels A–C**) or SIN-1 (**Panels D–F**) treatment. The colocalization of CHT and LAMP-1 can be seen as yellow in the Overlay panels. Images were analyzed as described in Figure 2-6 and in Materials and Methods. CHT and Lamp-1 that were determined to be colocalized in the colocalization channel are shown as white in the Colocalized Pixels images. Quantification of colocalized CHT and LAMP-1 is shown (**G**). Data were analyzed with a one-way ANOVA followed by Tukey's posttest and are expressed as the mean \pm SEM for a minimum of 40 cells per treatment from four independent experiments. Scale bar, 3 μ m.

assess the amount of CHT in late endosomes and lysosomes further under SIN-1 and vehicle treatment, I used a quantitative approach to determine the relative amount of CHT co-localization with Rab9-YFP or endogenous Lamp-1 using a method described previously by Lorenzen et al (2010). An example of this analysis is shown in Figure 2-6 for CHT and Rab7-YFP. The brightest 2% of pixels of CHT (red), indicated to the right of the vertical yellow line on the histogram, that fall within the brightest 2% of pixels of Rab9-YFP (green), indicated above the horizontal line on the histogram, was selected as the threshold intensity. The percentage of pixels that were both red and green were then determined as the percent of the two proteins that are colocalized. In these experiments, I found that CHT is extensively colocalized with both the late endosomal marker Rab9 and the lysosomal marker Lamp-1 under both vehicle and SIN-1 treatments. Further analysis to quantify these images revealed that in vehicle treated cells at 0, 30 and 60 min colocalization of CHT with Lamp-1 was 39.9 ± 2.3 , 30.9 ± 1.6 and 37.6 ± 1.3 , respectively, and under SIN-1 conditions at 0, 30, 60 min was 35.7 ± 1.9 , 30.7 ± 1.7 and 35.5 ± 1.6 , respectively. The high levels of colocalization of CHT with both Rab9-YFP and Lamp-1 suggests that CHT transits through the late endosomal/lysosomal pathway. Moreover, this data also suggests that SIN-1 does not alter the trafficking of CHT in this protein degradative pathway.

2.3.6 Inhibition of the proteasome, but not the lysosome, blocks the SIN-1 effect on choline uptake

To further determine if SIN-1 alters CHT trafficking through the late endosome/lysosome pathway and to investigate if SIN-1 targets CHT into an alternate route for degradation by the proteasome, the proteolytic activities of the lysosome and proteasome were blocked using a pharmacological approach. In this experiment, separate sets of cells were treated with either the lysosome inhibitors chloroquine or bafilomycin A1 or the proteasome inhibitors lactacystin or MG132, then choline uptake activity was assayed in the absence and presence of 1 mM SIN-1. Figure 2-8 (A and B) showed that neither chloroquine nor bafilomycin A1 modified the inhibition of CHT activity by SIN-1. This is a further indication that the movement of CHT to the lysosome for degradation is not

altered by SIN-1 treatment. An interesting observation in this experiment is that that chloroquine caused a significant increase in choline uptake activity compared to control in vehicle-treated cells (Figure 2-8A). This is consistent with the idea that CHT is normally trafficked to and degraded by the lysosome, and suggests that inhibition of this degradative process allows more CHT to be available for recycling back to the cell surface. Importantly, both of the proteasome inhibitors lactacystin and MG132 attenuated the SIN-1 mediated inhibition of CHT (Figure 2-8C and 2-8D) indicating that the proteasome may play a role in the inhibition of choline uptake activity observed in SIN-1 treated cells.

2.3.7 Ubiquitination of CHT is enhanced in SIN-1 treated cells

Finally, I investigated whether CHT is ubiquitinated and whether this is modified by acute SIN-1 treatment of SH-SY5Y-CHT cells. Ubiquitination is a reversible posttranslational modification of cellular proteins that can alter their subcellular trafficking or may target them to either lysosomes or proteasomes for degradation. In these experiments, I used either SH-SY5Y cells stably expressing the empty vector pcDNA3.1 and not CHT to serve as a negative control or SY5Y-CHT stably expressing FLAG-tagged CHT protein. Cells were treated with vehicle or 1 mM SIN-1 for 20 min, and FLAG-CHT was recovered from lysates using anti-FLAG affinity resin. Figure 2-9 (bottom two panels) shows a representative immunoblot that was probed for ubiquitin using anti-ubiquitin antibody, stripped, and reprobed for FLAG-CHT using anti-CHT antibody. The anti-ubiquitin immunoblot reveals faint protein bands positive for ubiquitin in both the vehicle- and SIN-1-treated cells. The most robust ubiquitin-positive band appears in the SIN-1-treated cells at an apparent molecular mass of ~80 kDa; a corresponding band is evident in the anti-CHT blot (denoted by the arrows). No ubiquitinated or CHT-positive bands were detected in negative control “vector” cells. Despite CHT having a molecular weight of ~62 kDa, this protein generally appears on SDS-PAGE as a diffuse band with an apparent molecular mass of ~50 kDa. Based on a shift in the mass of FLAG-CHT of ~30 kDa, this suggests that SIN-1 treatment may lead

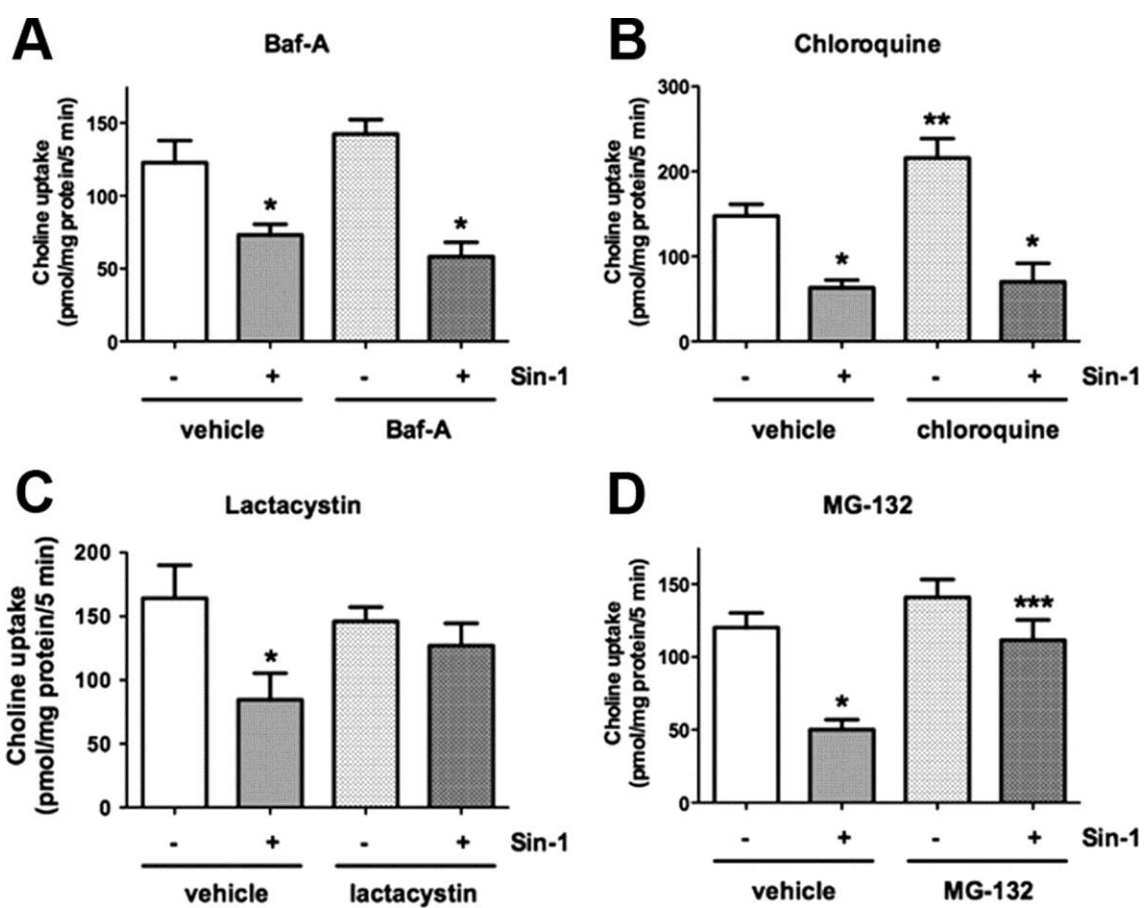


Figure 2-8

Figure 2-8 Inhibition of CHT activity by SIN-1 is attenuated by proteasome inhibitors lactacystin and MG-132, but not by lysosome inhibitors chloroquine and Baf-A.

Proteolytic activity of the lysosome and proteasome were blocked using a pharmacological approach. **A**, Cells were treated with either DMSO or 20 nM Baf-A dissolved in complete medium for 24 h at 37°C. HC-3-sensitive choline uptake was assayed in cells after 20 min of either vehicle or 1 mM SIN-1 treatment. HC-3-sensitive choline uptake was determined as the difference between uptake in the absence and presence of 1 μ M HC-3, and expressed as picomoles/milligram of protein per 5 min. Data are expressed as mean \pm SEM of five independent experiments. **B**, Cells were treated with either double-distilled H₂O or 50 μ M chloroquine dissolved in complete medium for 2 h at 37°C. HC-3-sensitive choline uptake was assayed in cells after 20 min of either vehicle or 1 mM SIN-1 treatment. Data are expressed as mean \pm SEM of five independent experiments. **C**, Cells were treated with either double-distilled H₂O or 0.5 μ M lactacystin dissolved in complete medium for 1 h at 37°C. HC-3-sensitive choline uptake was assayed in cells after 20 min of either vehicle or 1 mM SIN-1 treatment. Data are expressed as mean \pm SEM of five independent experiments. **D**, Cells were treated with either DMSO or 5 μ M MG-132 in complete medium for 30 min at 37°C. Data were analyzed using a repeated-measures one-way ANOVA with Tukey's *post hoc* multiple-comparisons test. Data are expressed as mean \pm SEM of four independent experiments. *SIN-1 treatment is significantly different from vehicle treatment ($p < 0.05$). **Drug treatment is significantly different from vehicle treatment ($p < 0.05$). ***SIN-1-treated groups are significantly different from each other ($p < 0.05$).

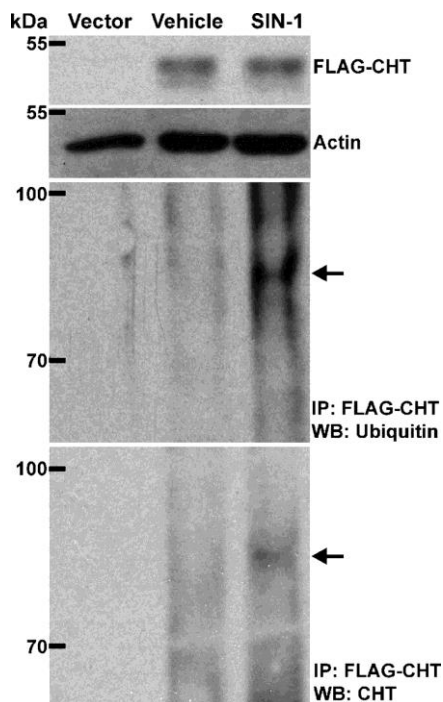


Figure 2-9 SIN-1 treatment causes CHT ubiquitination in SY5Y-CHT cells.

FLAG-CHT was recovered from lysates prepared from SY5Y-CHT cells that were treated with either vehicle or 1 mM SIN-1 for 20 min using anti-FLAG M2 affinity resin. Proteins were resolved by SDS-PAGE, transferred to PVDF membranes, and probed with either anti-ubiquitin or anti-CHT antibodies. Lysates prepared from SH-SY5Y cells that stably express the empty vector pcDNA3.1, and not CHT protein, were used as a negative control (“Vector” lane). Representative immunoblots show total FLAG-CHT and actin proteins in total cell lysates (top two panels). The bottom two panels illustrate FLAG-CHT proteins recovered on anti-FLAG affinity resin probed first with anti-ubiquitin antibody (1:5000), and then with anti-CHT antibody (1:10,000) following stripping. The arrows show ubiquitin and CHT-positive bands that appear at ~80 kDa. The immunoblots shown are representative of data obtained in three independent experiments.

to the addition of approximately four ubiquitin molecules to CHT, indicating that this could be due to multiple mono-ubiquitin or di-ubiquitin molecules or a short polyubiquitin chain.

2.4 Discussion

The mechanisms by which SIN-1 could alter CHT activity include structural modification of the protein by nitration of tyrosine residues or *S*-nitrosylation or oxidation of cysteine residues, changes in cell surface levels of CHT proteins due to altered subcellular trafficking or localization or degradation, dissipation of transmembrane electrochemical gradients, or loss of cell viability. I made novel findings in the present study that support my prediction that CHT inhibition by SIN-1 is mediated by changes to protein trafficking events, since the activity of a CHT mutant that does not undergo clathrin-mediated endocytosis is not affected by SIN-1. I also found that with SIN-1 treatment CHT internalizes from the cell surface by a clathrin- and dynamin-mediated process, since DN proteins that block either clathrin or dynamin function attenuate SIN-1-mediated inhibition of CHT. Moreover, I show for the first time that CHT proteins move through the endosomal–lysosomal pathway colocalizing with compartment markers, but that SIN-1 does not alter this trafficking. Our studies reveal that CHT normally undergoes lysosomal degradation, since lysosome inhibitors enhance choline uptake activity likely by increasing CHT availability for recycling to the cell surface. Importantly, however, proteasome, but not lysosome, inhibitors attenuate SIN-1-mediated inhibition of choline uptake, indicating that proteasomal degradation has a role in CHT protein disposition in cells exposed to SIN-1. Finally, I demonstrate for the first time that CHT protein undergoes ubiquitination, and this is enhanced by SIN-1 treatment.

I made the critical observation that mutant L531A-CHT is resistant to the SIN-1-mediated inhibition that is seen with wild-type CHT. Thus, inactivation of CHT function by SIN-1 is not likely due to oxidative or nitrosative modification of essential amino acids, thereby highlighting the importance of changes in intracellular trafficking of CHT proteins in its response to SIN-1. These findings for CHT inhibition differ from mechanisms by which hDAT activity is decreased in ONOO[−]-treated cells or hSERT is

inhibited in cells exposed to NO and related compounds, including peroxynitrite. With hDAT, inhibition by ONOO^- is caused by modification of a cysteine residue that is critical for transporter function (10). It is interesting, however, that ONOO^- does not block hDAT directly, as it was shown that inhibition is caused by a highly reactive dopamine-quinone moiety formed by reaction of ONOO^- with intracellular dopamine (25). Similarly, hSERT inhibition may involve *S*-nitrosylation of cysteine residues since inhibition was attenuated by addition of L-cysteine to the incubation buffer (11); L-cysteine acts as a “sink” by providing excess thiol groups to interact with reactive compounds (26). CHT is relatively cysteine poor, having only five cysteine residues in human CHT (17) compared with 13 in hDAT (27) and 18 in hSERT (28), but it is not known whether any of these cysteines are critical for CHT function. With regard to nitration of tyrosine residues in CHT, we did not detect this in SIN-1-treated cells by immunoblot using nitrotyrosine antibodies (4).

We reported that SIN-1 enhances CHT endocytosis from plasma membrane, thereby decreasing its cell surface levels and reducing choline uptake capacity (4). Now, my data shows that CHT proteins internalize by clathrin- and dynamin-dependent mechanisms to Rab5a-positive early endosomes in both control and SIN-1-treated cells. Moreover, CHT levels in this compartment are not altered by SIN-1, suggesting that transporters are not retained there and move to other endosomal compartments. In relation to the mechanism underlying changes in CHT endocytosis, dynamin, which carries out endocytic budding of vesicles and membrane scission (29, 30), undergoes *S*-nitrosylation at a critical cysteine residue in NO-treated cells. Importantly, this modification of dynamin causes accelerated endocytosis of plasma membrane proteins (30, 31). There are no data on the effects of ONOO^- on dynamin function, but since NO can be rapidly converted to ONOO^- and both of these highly reactive molecules can *S*-nitrosylate reactive cysteines, enhanced endocytosis associated with dynamin modification might also be mediated by ONOO^- .

In addition to CHT proteins recycling back to the cell surface following endocytosis (32, 15), other potential destinations for CHT in the neuron include being directed into the late endosomal pathway and/or lysosomes for degradation. This would effectively remove

CHT proteins from the recycling pool that is important for supplying CHT to the cell surface and regulating choline uptake activity. I now show that some CHT proteins in both vehicle- and SIN-1-treated cells move to colocalize with late endosome pathway small GTPases Rab7 and Rab9 and LAMP-1-positive lysosomes. The amount of CHT colocalized with these markers did not differ between vehicle- and SIN-1-treated cells; thus, SIN-1 does not promote CHT accumulation in these compartments. My data also shows for the first time that the normal site for CHT degradation is the lysosome, since the lysosome inhibitor chloroquine enhances choline uptake activity.

An unexpected finding is that the decreased CHT activity observed in SIN-1-treated cells was attenuated by proteasome blockers, suggesting that proteasomal protein degradation is involved in SIN-1-mediated loss of CHT function. Trafficking patterns for plasma membrane proteins to lysosomes or proteasomes may be altered under diverse conditions, including oxidative stress [glucose transporter GLUT1 (33)], single point mutations [low-density lipoprotein receptor (34)], and loss of intramolecular disulfide bonding [ATP-binding cassette transporter ABCG2 (35)]. While the mechanisms mediating these changes likely differ, there are similarities between our observations with CHT and effects of oxidative stress on GLUT1. Cell surface GLUT1 levels decrease during oxidative stress due to enhanced internalization and altered subcellular trafficking, with this linked to ubiquitination of GLUT1 and proteasome-dependent changes in protein kinase B (Akt) activation. Under these conditions, GLUT1 also undergoes mono-ubiquitination or di-ubiquitination (33).

Trafficking of solute transporters is also regulated by phosphorylation, and this is modulated by oxidative stress. Like CHT, GLUT4 glucose transporters are located mostly in intracellular vesicles under basal conditions and its plasma membrane levels are increased when solute is needed by the cell; insulin, ischemia, and hypoxia increase GLUT4 translocation (36). Acute exposure of cardiomyocytes to H₂O₂ enhances plasma membrane GLUT4 levels by a mechanism involving activation of AMP-activated protein kinase and PI3-kinase/Akt (37). However, GLUT4 is not the substrate for these kinases, with regulatory proteins including Rab GAP AS160 being phosphorylated and then modulating GLUT4 disposition (38). CHT in neurons is phosphorylated, and PKC

regulates its activity and cell surface levels (39, 40), although the underlying mechanisms are unknown. Multiple kinases are altered by ONOO^- , including activation of p38 kinase and Src kinase (41, 43, 44), but there are no data on the effects of kinases that are modulated by ONOO^- on CHT disposition.

CHT interacts with amyloid precursor protein (APP) through its C-terminal tail, and APP has a role in regulating CHT subcellular trafficking in cholinergic neurons (44); APP serves as substrate for generation of β -amyloid, a critical feature in Alzheimer's disease pathogenesis, which is involved in production of oxidative stress in brain. APP is internalized from plasma membrane by endocytosis and moves through the endosomal pathway to lysosomes where it is cleaved by secretases. However, APP can also enter a novel, rapid transport pathway to move directly from the cell surface to lysosomes (45). It is not known whether this trafficking is altered by oxidative–nitrosative stress or what effect this could have on the function of its binding partner CHT, but this raises important questions about the regulation of cholinergic presynaptic function by APP disposition and trafficking in neuropathology.

In summary, plasma membrane CHT levels are determined by the balance between cell surface recruitment of CHT-containing vesicles and retrieval of CHT proteins to subcellular organelles. Events that alter the dynamics of either this constitutive or the depolarization-regulated recycling of CHT will control the amount of choline that is available for ACh synthesis and the ability of cholinergic neurons to communicate with their target cells. It is not known whether the enhanced endocytosis and loss of cell surface CHT proteins in SIN-1-treated cells is a mechanism to remove damaged proteins from the neuron or a protective measure to prevent protein damage, but our previous work examining transferrin receptor disposition in SIN-1-treated cells shows changes to that receptor that parallel effects on CHT (4), suggesting that this is a more generalized mechanism for the response of some cell surface proteins to cellular stress.

2.5 References

1. Yamamura, H. I., and Snyder, S. H. (1972) *J Neurochem* **21**, 1355-1374
2. Haga, T., and Noda, H. (1973) *Biochem Biophys Acta* **291**, 564-575
3. Guermónprez, L., Ducrocq, C., and Gaudry-Talarmain, Y.M. (2001) *Mol Pharmacol* **60**, 838-846
4. Pinthong, M., Black, S.A., Ribeiro, F.M., Pholpramool, C., Ferguson, S.S., and Rylett, R.J. (2008) *Mol Pharmacol* **73**, 801-812
5. Wang, X., and Michaelis, E.K. (2010) *Front Aging Neurosci* **2**,12
6. Smith, M.A., Richey Harris, P.G., Sayre, L.M., Beckman, J.S., and Perry, G. (1997) *J Neurosci* **17**, 2653-2657
7. Beckman, J.S. (1991) *J Dev Physiol* **15**, 53-59
8. Alkam, T., Nitta, A., Mizoguchi, H., Itoh, A., and Nabeshima, T. (2007) *Behav Brain Res* **180**, 139-145
9. Xu, J., Kim, G.M., Chen, S., Yan, P., Ahmed, S.H., Ku, G., Beckman, J.S., Xu, X.M., and Hsu, C.Y. (2001) *J Neurotrauma* **18**, 523-532
10. Park, S.U., Ferrer, J.V., Javitch, J.A., and Kuhn, D.M. (2002) *J Neurosci* **2**, 4399-4405
11. Bryan-Lluka, L.J., Papacostas, M.H., Paczkowski, F.A., and Wanstall, J.C. (2004) *Br J Pharmacol* **143**, 63-70
12. Ferguson, S.M., Savchenko, V., Apparsundaram, S., Zwick, M., Wright, J., Heilman, C.J., Yi, H., Levey, A.I., and Blakely, R.D. (2003) *J Neurosci* **23**, 9697-9709

13. Ribeiro, F.M., Alves-Silva, J., Volknaendt, W., Martins-Silva, C., Mahmud, H., Wilhelm, A., Gomez, M.V., Rylett, R.J., Ferguson, S.S., Prado, V.F., and Prado, M.A. (2003) *J Neurochem* **87**, 136-146
14. Ribeiro, F.M., Black, S.A., Cregan, S.P., Prado, V.F., Prado, M.A., Rylett, R.J., and Ferguson, S.S. (2005) *J Neurochem* **94**, 86-96
15. Ribeiro, F.M., Black, S.A., Prado, V.F., Rylett, R.J., Ferguson, S.S., and Prado, M.A. (2006) *J Neurochem* **97**, 1-12
16. Ribeiro, F.M., Pinthong, M., Black, S.A., Gordon, A.C., Prado, V.F., Prado, M.A., Rylett, R.J., and Ferguson, S.S. (2007a) *Eur J Neurosci* **26**, 3437-3448
17. Apparsundaram, S., Ferguson, S.M., George, A.L. jr., and Blakely, R.D. (2000) *Biochem Biophys Res Commun* **276**, 862-867
18. Okuda, T., and Haga, T. (2000) *FEBS Lett* **484**, 92-97
19. Okuda, T., Haga, T., Kanai, Y., Endou, H., Ishihara, T., and Katsura, I. (2000) *Nat Neurosci* **3**, 120-125
20. Ford, M.G., Pearse, B.M., Higgins, M.K., Vallis, Y., Owen, D.J., Gibson, A., Hopkins, C.R., Evans, P.R. and McMahon, H.T. (2001) *Science* **291**, 1051-1055
21. Damke, H., Binns, D.D., Ueda, H., Schmid, S.L., and Baba, T. (2001) *Mol Biol Cell* **12**, 2578-2589
22. Pacher, P., Beckman, J.S., and Liaudet, L. (2007) *Physiol Rev* **87**, 315-424
23. Ashki, N., Hayes, K.C., and Bao, F. (2008) *Neurosci* **156**, 107-117
24. Dale, L.B., Seachrist, J.L., Babwah, A.V., and Ferguson, S.S. (2004) *J Biol Chem* **279**, 13110-13118
25. Whitehead, R.E., Ferrer, J.V., Javitch, J.A., and Justice, B. (2001) *J Neurochem* **76**, 1242-1251

26. Kaye, D.M., Wiviott, S.D., Kobzik, L., Kelly, R.A., and Smith, T.W. (1997) *Am J Physiol* **272**, 875-888
27. Giros, B., el Mestikawy, S., Bertrand, L., and Caron, M.G. (1991) *FEBS Lett* **295**, 149-154
28. Ramamoorthy, S., Bauman, A.L., Moore, K.R., Han, H., Yang-Feng, T., Chang, A.S., Ganapathy, V., and Blakely, R.D. (1993) *Proc Natl Acad Sci U S A* **90**, 2542-2546
29. Conner, S.D., and Schmid, S.L. (2003) *Nature* **422**, 37-44
30. Dessy, C., Kelly, R.A., Balligand, J-L., and Feron, O. (2000) *EMBO J* **19**, 4272-4280
31. Wang, G., Moniri, K., Ozawa, K., Stamler, J.S., and Daaka, Y. (2006) *Proc Nat Acad Sci U S A* **103**, 1295-1300
32. Ferguson, S.M., and Blakely, R.D. (2004) *Mol Interv* **4**, 22-37
33. Fernandes, R., Hosoya, K., and Pereira, P. (2011) *Am J Physiol Cell Physiol* **300**, 927-936
34. Martín de Llano, J.J., Fuertes, G., Andreu, E.J., Puig, O., Chaves, F.J., Soutar, A.K., Armengod, M.E., and Knecht, E. (2006) *Int J Biochem Cell Biol* **38**, 1340-1351
35. Wakabayashi, K., Nakagawa, H., Tamura, A., Koshiba, S., Hoshijima, K., Komada, M., and Ishikawa, T. (2007) *J Biol Chem* **282**, 27841-27846
36. Fischer, Y., Thomas, J., Sevilla, L., Munoz, P., Becker, C., Holman, G., Kozka, I.J., Palacin, M., Testar, X., Kammermeier, H., and Zorzano, A. (1997) *J Biol Chem* **272**, 7085-7092
37. Horie, T., Ono, K., Nagao, K., Nishi, H., Kinoshita, M., Kawamura, T., Wada, H., Shimatsu, A., Kita, T., and Hasegawa, K. (2008) *J Cell Physiol* **215**, 733-742

38. Chavez, J.A., Roach, W.G., Keller, S.R., Lane, W.S., and Lienhard, G.E. (2008) *J Biol Chem* **283**, 9187-9195
39. Gates, J., Ferguson, S.M., Blakely, R.D., and Apparsundaram, S. (2004) *J Pharmacol Exp Ther* **310**, 536-545
40. Black, S.A.G., Ribeiro, F.M., Ferguson, S.S.G., and Rylett, R.J. (2010) *Neuroscience* **167**, 765-773
41. Li, X., De Sarno, P., Song, L., Beckman, J.S., and Jope, R.S. (1998) *Biochem J* **331**, 599-606
42. Di Stasi, A.M., Mallozzi, C., Macchia, G., Petrucci, T.C., and Minetti, M. (1999) *J Neurochem* **73**, 727-735
43. Oh-Hashi, K., Maruyama, W., and Isobe, K. (2001) *Free Radic Biol Med* **30**, 213-221
44. Wang, B., Yang, L., Wang, A., and Zheng, H. (2007) *Proc Nat Acad Sci U S A* **104**, 14140-14145
45. Lorenzen, A., Samosh, J., Vandewark, K., Anborgh, P.H., Seah, C., Magalhaes, A.C., Cregan, S.P., Ferguson, S.S.G., and Pasternak, S.H. (2010) *Molecular Brain* **3**, 11

Chapter 3

3 Regulation of the high-affinity choline transporter activity and trafficking by its association with cholesterol-rich lipid rafts²

² A version of this work has been published in the following manuscript:

Cuddy LK, Winick-Ng W, Rylett RJ. Regulation of the high-affinity choline transporter activity and trafficking by its association with cholesterol-rich lipid rafts J Neurochem 4 November 2013 128 (5):725-740

3.1 Introduction

The activity and trafficking of membrane proteins can be regulated by the plasma membrane lipid environment. Proteins can be segregated into cholesterol and sphingolipid-rich microdomains in membranes termed lipid rafts (1, 2) that are involved in cellular events, including membrane organization, protein–protein interactions, and signal transduction (3, 4). Lipid rafts also have a role in trafficking of membrane proteins by facilitating their endocytosis in clathrin-independent caveolae (5, 6). Cholesterol can play a critical role in organization of membrane proteins, and influence their function or activity either indirectly through changes in membrane fluidity or directly by cholesterol–protein interactions (7, 8). The disruption of lipid rafts by removal of cholesterol can significantly affect either the structure or function of some membrane proteins (9). In relation to this study, several neurotransmitter transporters are localized to lipid rafts. One mechanism by which this can regulate their solute uptake activity is by altering their endocytosis and trafficking, thereby affecting the amount of cell surface transporter protein (10-13). However, specific cholesterol–transporter interactions have also been identified that are independent of association of the protein with lipid rafts. For example, reconstitution of 5-HT transporter and GABA transporter activity is not observed when cholesterol is replaced by other sterols that have similar effects on membrane fluidity (14, 15), and depletion of membrane cholesterol can decrease 5-HT transporter affinity for its substrate (14).

CHT is active at the plasma membrane, but experimental evidence indicates that the majority of CHT proteins form a subcellular reserve pool within endocytic and synaptic vesicles (16, 17). Only a small proportion of total cellular CHT proteins are at the cell surface, with a constitutive cycle of endocytosis by a clathrin/dynamin-dependent mechanism and recycling back to the plasma membrane serving as a critical regulatory mechanism that controls cell surface CHT density (16, 17). Plasma membrane CHT levels are enhanced by depolarization-induced exocytosis of synaptic vesicles that deliver additional CHT proteins to the cell surface during excitation of cholinergic nerve terminals, thereby increasing the amount of choline transported into cholinergic nerve

terminals to drive ACh synthesis (18). CHT trafficking is also regulated by phosphorylation (19), extracellular ligand concentration (21), and by interaction with other proteins, such as amyloid precursor protein (22).

To-date, there have been only limited, and conflicting, reports regarding the influence of cholesterol or cholesterol-rich lipid rafts on high-affinity choline uptake; one study shows that cholesterol reduction in isolated nerve endings (synaptosomes) decreased choline uptake (23), whereas another study reports that depletion of membrane cholesterol in synaptosomes did not significantly influence choline uptake (24). A recent study suggests that depleting membrane cholesterol by treating synaptosomes with high concentrations of methyl- β -cyclodextrin (M β C) reduced high-affinity choline uptake (25). Although these observations suggest that cholesterol has a role in regulation of CHT, the underlying mechanisms were not investigated and there has been no assessment of whether CHT proteins are partitioned in membrane lipid rafts. Thus, the goal of this study was to address these points and provide data on cholesterol-related changes to CHT activity. I used pharmacological approaches to modulate membrane cholesterol levels in neural cells, and found that treatments that reduced cholesterol caused a reduction in CHT activity and addition of cholesterol to cells resulted in enhanced CHT activity. I showed for the first time that CHT proteins are enriched in lipid rafts, and that disruption of lipid rafts reduces cell surface CHT. These results suggest that membrane cholesterol and lipid rafts serve as an important regulator of CHT trafficking and activity by retaining functional CHT at the cell surface.

3.2 Materials and methods

3.2.1 Materials

Filipin, M β C, cholesterol-M β C complex (M β C-Chol), and cholesterol oxidase were from Sigma-Aldrich (St. Louis, MO, USA) and [methyl- 3 H]choline chloride (128 Ci/mmol) and [methyl- 3 H]hemicholinium-3 diacetate ([3 H]HC-3) (169 Ci/mmol) were from Perkin-Elmer Life Sciences (Boston, MA, USA). Other chemicals were from Sigma-Aldrich at the highest purity available. SH-SY5Y human neuroblastoma cells

were from American Type Culture Collection (Manassus, VA, USA), and Invitrogen (Burlington, ON, Canada) supplied AlexaFluor 647 cholera toxin subunit B conjugate (CTB), Zenon AlexaFluor 555 rabbit IgG and Zenon AlexaFluor 488 mouse IgG labeling kits, Amplex Red Cholesterol Assay kit, and culture media and reagents. Enhanced ChemiLuminescence immunoblot reagent was from GE Healthcare Life Sciences (Baie d'Urfé, QC, Canada) and Biodegradable Scintillant was from Amersham Canada Ltd. (Oakville, ON, Canada). Purified mouse anti-EEA1 antibody was from BD Biosciences (Mississauga, ON, Canada) and rabbit polyclonal flotillin-1 antibody from Santa Cruz Biotechnology, Santa Cruz, CA, USA. Polyclonal CHT antibody was raised in rabbits to the antigenic peptide DVDSSPEGSGTEDNLQ that is conserved at the carboxyl terminus of human and rat CHT (Genemed Synthesis, San Antonio, TX, USA); this peptide was conjugated to keyhole limpet hemocyanin carrier protein by an amino-terminal cysteine. CHT-specific IgG was affinity purified in our laboratory from crude anti-serum on NHS-Sepharose (Amersham) to which antigenic peptide was coupled as the binding element. Specificity of this antibody for detection of CHT was described previously (26).

3.2.2 Selection of cell line and cell culture

Full-length rat CHT cDNA ligated to pSPORT was a gift from Dr T. Okuda (21); a FLAG epitope tag was added to the amino terminus by PCR and the resulting cDNA ligated to pcDNA3.1 (26). SH-SY5Y cells were transfected with this FLAG-CHT plasmid by Lipofectamine 2000. Stable transformants were selected using 500 µg/mL G418 for 4 weeks, then grown in DMEM, 10% FBS U/mL penicillin, and 100 µg/mL each of streptomycin and G418. SH-SY5Y cell differentiation was induced by addition of 10 µM RA for 3 days; substantial morphological and biochemical differentiation of cells occurred during this time (data not shown).

3.2.3 [³H]Choline uptake assay

Monolayers of cells were washed, then incubated at 37°C in KRH. Vehicle or drug was added to cells for specified times, followed by incubation for 5 min with 0.5 µM [³H]choline (0.5 µCi/mL) in the absence or presence of 1 µM HC-3. Following this

incubation, cells were placed on ice and washed with cold KRH, then lysed in 0.1 M NaOH. After 30 min lysis, aliquots of samples were analyzed for tritium content by liquid scintillation spectrometry and protein concentration using Bio-Rad protein dye (Bio-Rad Laboratories, Hercules, CA, USA). Each independent experiment consisted of triplicate plates of cells per treatment group, with results normalized to sample protein content and averaged. Specific choline uptake was the difference between total choline uptake and non-specific uptake in the presence of HC-3, with the resulting [^3H]choline uptake data expressed as pmol/mg protein per 5 min \pm SEM.

3.2.4 [^3H]HC-3 binding assay

Monolayers of cells were washed and incubated in KRH at 37°C with addition of vehicle or drug for specified times, then washed with ice-cold KRH, and kept on ice for 10 min to stop protein trafficking activity. Cells were incubated with [^3H]HC-3 (10 nM; 1 Ci/mmol) in the presence or absence of 1 μM unlabeled HC-3 for 1 h on ice. For kinetic analysis, HC-3 binding was measured over the range of 0.5–10 nM HC-3 with the specific activity of [^3H]HC-3 held constant at 1 Ci/mmol. Following incubation, cells were washed rapidly with cold KRH to remove unbound HC-3 and lysed in 0.1 M NaOH for 30 min. Aliquots of lysates were used for quantification of tritium and protein content. Each independent experiment had triplicate determinations with HC-3 binding normalized to sample protein content, then averaged. Specific HC-3 binding was calculated as the difference between total and non-specific HC-3 binding, and values were expressed as fmol/mg protein \pm SEM.

3.2.5 Lipid raft preparation and sucrose flotation gradients

SH-SY5Y cells stably expressing CHT were grown to confluence on 100-mm dishes prior to the preparation of membrane fractions. Cells were placed on ice and washed twice with HBSS, then lysed for 30 min in sodium carbonate lysis buffer (0.5 M Na_2CO_3 with 1 mM AEBSF, 10 $\mu\text{g/mL}$ each of leupeptin and aprotinin, and 25 $\mu\text{g/mL}$ pepstatin A) or Triton X-100 lysis buffer (0.5% Triton X-100 with 1 mM AEBSF, 10 $\mu\text{g/mL}$ each of leupeptin and aprotinin, and 25 $\mu\text{g/mL}$ pepstatin A). Cell lysates were

collected and homogenized three times for 10 s each using a Polytron tissue grinder. Homogenates were next sonicated three times for 20 s using a Sonic Dismembrator. Homogenates were adjusted to 40% sucrose, then added to ultracentrifuge tubes and overlaid with 30% sucrose and 5% sucrose solutions. Samples were centrifuged at 120 000 g for 16 h at 4°C using a Beckman SW 41 (Beckman Coulter Canada LP, Mississauga, ON, Canada) Ti rotor. Twelve or ten (for cells lysed in sodium carbonate or Triton X-100, respectively) 1 mL fractions were collected from the top to bottom of each sucrose gradient. Protein aliquots from each fraction were incubated for 10 min at 55°C with Laemmli buffer (2% sodium dodecyl sulfate, 10% glycerol, 62.5 mM Tris-HCl, pH 6.8, 2.5% β -mercaptoethanol, and 0.001% bromophenol blue), then separated on 7.5% SDS-PAGE gels and transferred to PVDF membranes. Membranes were blocked in 8% non-fat dry milk in wash buffer (phosphate-buffered saline, 0.15% Triton X-100) and incubated with either anti-CHT antibody, anti-EEA1 antibody or anti-flotillin antibody overnight at 4°C. After washing, membranes were incubated for 1 h with species-matched secondary antibodies in wash buffer containing 8% milk, and washed again. Immunoreactive proteins on membranes were detected by chemiluminescence using the ECL kit. Immunopositive bands were quantified by densitometry using Scion Image software (NIH).

3.2.6 Synaptosome preparation

Purified nerve terminals [synaptosomes] were isolated from mouse forebrain using established methods (27). Young adult (3–4 months of age) C57B6 mice of either sex bred locally were used in these experiments in compliance with the Canadian Council on Animal Care (CCAC) and the ARRIVE (www.nc3rs.org.uk/ARRIVE) guidelines, and a protocol approved by the Animal Use Subcommittee at the University of Western Ontario. Briefly, tissues were homogenized in 0.32 M sucrose buffered with 5 mM HEPES, pH 7.4. Following differential centrifugation at 1000 g for 10 min and 12 000 g for 20 min to recover the crude P2 fraction, pellets were resuspended in buffered 0.32 M sucrose and layered onto discontinuous gradients comprised of 8.5, 13, and 20% Ficoll in buffered 0.32 M sucrose. Following centrifugation at 27 000 g for 45 min, fractions at the 8.5–13% and 13–20% interfaces were recovered as they

contained purified synaptosomes; these were diluted 5-fold with 0.32 M sucrose, then centrifuged at 12 000 x g for 30 min. Purified synaptosome pellets were lysed in sodium carbonate lysis buffer and the resulting homogenates used directly to isolate lipid rafts, as described above.

3.2.7 Cellular imaging

Digital images of fixed cells were acquired with a Zeiss LSM510-Meta laser-scanning confocal microscope (Carl Zeiss Canada Ltd., Toronto, ON, Canada) using a 63X oil-immersion objective and magnified three times, unless specified otherwise. FLAG-tagged CHT proteins were fluorescently labeled in live cells using rabbit anti-FLAG antibody complexed to either Zenon 555 dye (for EEA1 staining) or Zenon 488 dye (for flotillin staining). The fluorescently tagged antibody was added to medium bathing the cells where it could bind to the FLAG epitope located on the extracellularly oriented amino terminus of CHT proteins at the plasma membrane. After allowing internalization of Zenon-labeled CHT proteins, cells were formaldehyde fixed then counter-stained with AlexaFluor 647 CTB (0.2 ng/ μ L) and either anti-flotillin (1: 200) or anti-EEA1 (1: 100) antibodies. Following immunostaining, images were acquired using 488-nm excitation and 505- to 530-nm emission wavelengths for flotillin; 543-nm excitation and 560- to 615-nm emission for EEA1; and 647-nm excitation and 650-nm emission using a long-pass filter for CTB. FLAG-CHT was visualized using 488-nm excitation and 505- to 530-nm emission (for EEA1-labeled cells) or using 543-nm excitation and 560- to 615-nm emission (for flotillin-labeled cells). Images were processed and colocalization was analyzed in Imaris (version 7.0.0; Bitplane Scientific Software, South Windsor, CT, USA), then formatted in Adobe Illustrator and Photoshop (Adobe Systems Inc, San Jose, CA, USA).

3.2.8 Cholesterol quantification

SH-SY5Y cells expressing FLAG-tagged CHT were grown to confluence on 100-mm dishes, then lysed in sodium carbonate lysis buffer and lipid rafts were isolated on sucrose gradients, as described above. Total cholesterol levels were measured in pooled

raft fractions (#4–6) and non-raft fractions (#9–12) using the Amplex Red Cholesterol Assay, according to manufacturer's instructions. Briefly, 50 μ L of cholesterol standards (0–20 μ M per well) or sample replicates was added to 96-well black plates. Fifty μ L of working solution (300 μ M Amplex Red reagent, 2 unit/mL horseradish peroxidase, 2 unit/mL cholesterol oxidase, and 0.2 unit/mL cholesterol esterase) was added to each well and plates were incubated in the dark for 30 min at 37°C. Fluorescence was measured (excitation 544 nm, emission 590 nm, SpectraMax M5 Molecular Devices, Palo Alto, CA, USA). Relative fluorescence units of samples were converted into μ M cholesterol per μ g sample protein using the standard curve, and data were expressed as a percentage of vehicle-treated controls

3.2.9 Cell surface protein biotinylation assay

Cells plated on 100-mm dishes were washed with HBSS, then treated at 37°C with either vehicle or drug. After treatment, cells were placed on ice under cold HBSS to stop protein trafficking. Plasma membrane proteins were biotinylated at 4°C by incubating with 1 mg/mL sulfo-NHS-SS-biotin in HBSS for 1 h (26, 28) with gentle agitation. Unbound biotin was quenched by washing and incubating cells in cold 100 mM glycine in HBSS. After two further washes with HBSS, cells were lysed on ice for 30 min in sodium carbonate lysis buffer and lipid rafts prepared on sucrose flotation gradients as described above. Twelve 1-mL gradient fractions were collected and pooled as either raft fractions (#4–6) or non-raft fractions (#9–12). Pooled fractions were diluted to 10 mL with lysis buffer (1% w/v Triton X-100, 150 mM NaCl, 50 mM Tris-HCl, and pH 7.5) and pH adjusted to 7.5. Protein concentrations were measured using Bio-Rad dye and aliquots of cell lysates containing 30 μ g protein subjected to SDS–PAGE to determine total CHT, flotillin, and EEA1 levels. Biotinylated proteins in sucrose density gradient fractions were separated from non-biotinylated proteins by Neutravidin bead pull-down from 500 μ g total cellular protein from each sample. Beads were washed three times with lysis buffer to remove non-specifically bound proteins. Proteins were eluted for 10 min at 55°C with Laemmli buffer, then separated on 7.5% SDS–PAGE gels and transferred to PVDF membranes. Immunoblots for CHT, flotillin, and EEA1 were carried out as

described above and analyzed using a Chemidoc Imaging System (Bio-Rad Laboratories).

3.2.10 Internalization cell surface biotinylation assay

Cells plated on 100-mm dishes were washed twice with cold HBSS and placed on ice under cold HBSS to stop protein trafficking. Plasma membrane proteins were biotinylated at 4°C by incubating with 1 mg/mL sulfo-NHS-SS-biotin in HBSS for 1 h with gentle agitation, then unbound biotin was quenched by washing and incubating cells in cold 100 mM glycine in HBSS. Dishes were washed with warm HBSS, then incubated at 37°C with either vehicle or drug to allow constitutive internalization of CHT proteins. CHT internalization was subsequently terminated by transferring dishes of cells to ice and replacing medium with cold HBSS. Residual cell surface biotin was stripped by incubating cells once for 15 min and twice for 30 min with freshly prepared 50 mM mercaptoethanesulfonic acid (MesNa) in TE buffer (150 mM NaCl, 1 mM EDTA, 0.2% bovine serum albumin, 20 mM Tris, and pH 8.6). Stripping efficiency was determined for each experiment on parallel sets of biotinylated cells that were maintained on ice and which did not undergo MesNa stripping to assess the amount of CHT at the plasma membrane. Cells were lysed in lysis buffer (1% w/v Triton X-100, 150 mM NaCl, 50 mM Tris-HCl, pH 7.5, 1 mM AEBSF, 10 µg/mL each of leupeptin and aprotinin, 25 µg/mL pepstatin A, and 700 U/mL DNase) and protein concentration was measured using Bio-Rad dye. Biotinylated proteins were separated from non-biotinylated proteins by Neutravidin bead pull-down from 500 µg protein from each sample. Beads were washed three times with lysis buffer to remove non-specifically bound proteins, then proteins eluted for 10 min at 55°C with Laemmli buffer, separated on 7.5% SDS-PAGE gels, and transferred to PVDF membranes. Immunoblots for CHT were carried out as described above and analyzed using a Chemidoc Imaging System.

3.2.11 Data analysis

Data are presented as mean \pm SEM with *n* values representing the number of independent experiments performed on separate populations of cells. Each *n* value was obtained from

the average of multiple sample replicates in each experiment. Replicate experiments were performed on cells cultured in successive passages as much as possible to minimize interexperiment variability; intraexperiment variability between replicate samples was minimal thus facilitating comparison of treatment effects. GraphPad Prism 5 (GraphPad Software, San Diego, CA, USA), InStat software (GraphPad Software) and Image Lab 4.1 (Bio-Rad Laboratories) were used for data analysis. Sigmoid and Michaelis–Menten equations were used to calculate kinetic parameters (B_{\max} and K_D) of HC-3 binding. Data were assessed for statistically significant differences by unpaired Student's *t*-test, or between groups using repeated measures one-way ANOVA with Tukey's *post hoc* multiple comparison test as appropriate, with statistical significance defined as $p \leq 0.05$.

3.3 Results

3.3.1 Membrane cholesterol manipulation modulates choline uptake activity

The initial experiments were designed to determine the effect of manipulation of membrane cholesterol content on HC-3-sensitive, high-affinity choline uptake activity in SH-SY5Y cells that stably express FLAG-tagged CHT. Three separate pharmacological approaches having different mechanisms of action were used to lower membrane cholesterol levels, and one approach was used to increase the membrane cholesterol level. Cells were treated with either filipin which binds to and sequesters free cholesterol within both lipid raft and non-raft areas of membrane and disrupts lipid rafts (29), M β C which extracts unesterified cholesterol from plasma membrane resulting in the disruption of lipid rafts and direct cholesterol–protein interactions (30), or cholesterol oxidase which converts cholesterol to the inactive sterol cholest-4-en-3-one and does not alter membrane fluidity (31). Neither cell density of cultures nor cell morphology was visibly altered after drug treatments, and the level of total CHT protein was unchanged (data not shown). I predicted that if cholesterol is required for CHT function, then HC-3-sensitive choline uptake activity would be altered by these drugs. Figure 3-1 illustrates dose–response relationships for [3 H]choline uptake in cells treated with filipin, M β C, and

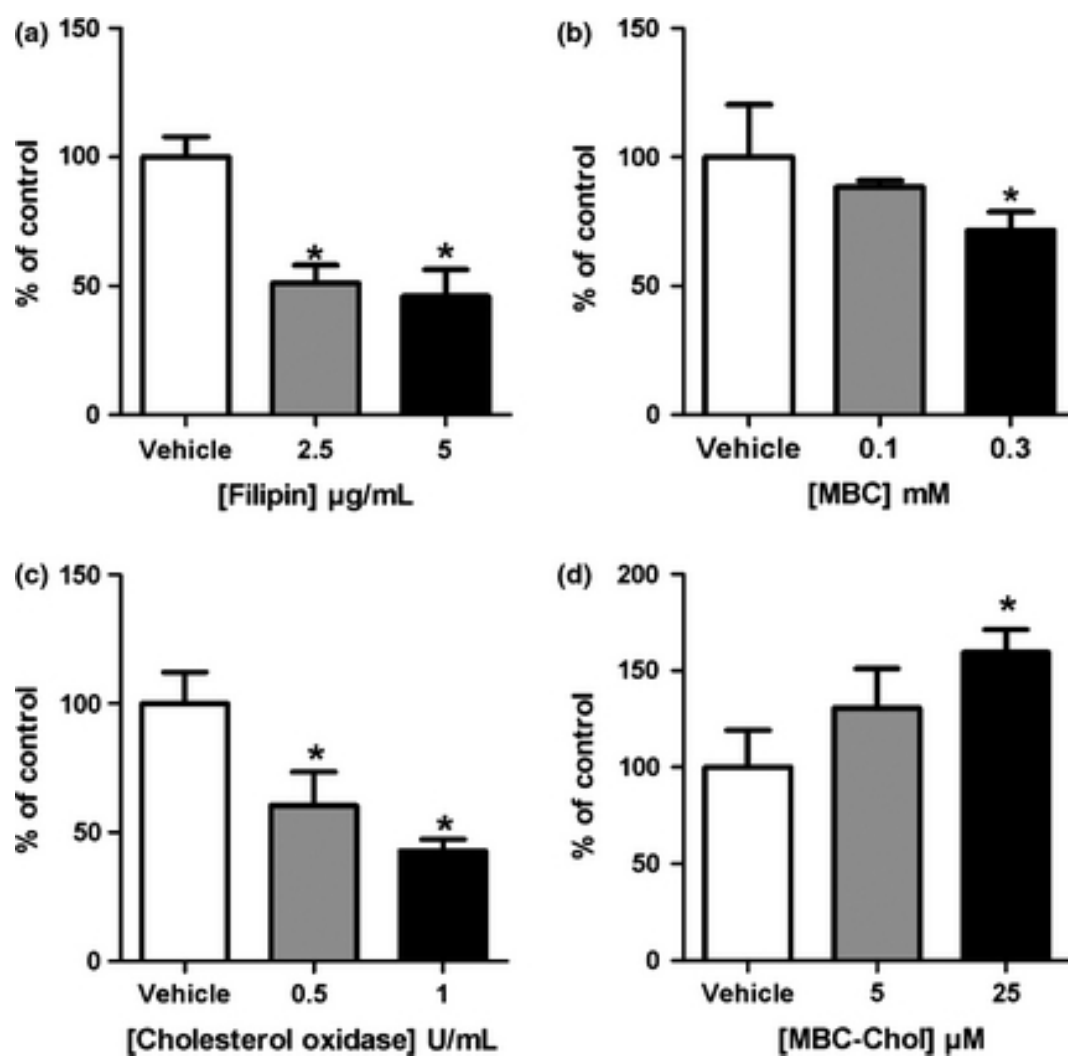


Figure 3-1

Figure 3-1 Manipulation of membrane cholesterol modulates choline uptake in SH-SY5Y cells.

A, Cells were treated with either vehicle (methanol) or 2.5 or 5 $\mu\text{g/mL}$ of filipin for 60 min at 37°C. Hemicholinium-3 (HC-3)-sensitive [^3H]choline uptake activity was assayed in cells during a 5-min incubation at 37°C. **B**, Cells were treated with either vehicle (H_2O) or 0.1 or 0.3 mM methyl- β -cyclodextrin (M β C) for 30 min at 37°C, then [^3H]choline uptake activity was determined. **C**, Cells were treated with either 0, 0.5, or 1 U/mL cholesterol oxidase in a buffer containing 100 mM MES and 3 M NaCl in Krebs-Ringer-HEPES (KRH) solution at 37°C for 30 min, then [^3H]choline uptake was measured. **D**, To assess whether supplementing membranes with additional cholesterol influenced choline uptake, cells were treated with either vehicle (H_2O), 5, or 25 μM cholesterol-methyl- β -cyclodextrin (M β C-Chol), then [^3H]choline uptake was assayed. In all experiments, [^3H]choline uptake activity was determined as the difference between uptake in the absence and presence of 1 μM HC-3, and expressed as pmol/mg of protein per 5 min and transformed to % of the respective control values. Data are expressed as mean \pm SEM of four independent experiments. Non-transformed data were analyzed by one-way anova followed by Tukey's post-test. Asterisks (*) denote when drug treatment groups are significantly different from vehicle groups ($p < 0.05$).

cholesterol oxidase. When cells were pre-treated with vehicle or filipin for 60 min, [3 H]choline uptake was significantly reduced at both doses of filipin (2.5 or 5 μ g/mL) (Figure 3-1A). Similarly, treating cells with M β C for 30 min (0.1 or 0.3 mM) resulted in a statistically significant decrease in [3 H]choline uptake at the higher concentration of the drug (Figure 3-1B). Finally, when cells were treated with cholesterol oxidase for 30 min, a statistically significant reduction in [3 H]choline uptake activity was observed at both concentrations of cholesterol oxidase (0.5 and 1 U/mL) compared to vehicle-treated control cells (Figure 3-1C).

In the next set of experiments, I determined if CHT activity is altered by increasing the level of membrane cholesterol. SH-SY5Y cells were incubated with a cholesterol-saturated form of M β C (M β C-Chol) for 30 min (M β C-Chol complex concentration was 5 or 25 μ M, calculated by weight of cholesterol) or with vehicle, then [3 H]choline uptake was measured. Importantly, when cholesterol was added to cells, a statistically significant increase in choline uptake was observed at 25 μ M M β C-Chol when compared to vehicle-treated cells (Figure 3-1D).

3.3.2 M β C decreases both the B_{\max} and K_D for [3 H]HC-3 binding to CHT

Several studies suggest that membrane cholesterol and lipid rafts regulate neurotransmitter transporter activity by controlling the number of transporters at the cell surface (11, 32, 33). However, cholesterol can also regulate the function of neurotransmitter transporters by modulating their solute binding activity (34, 14, 35). To establish whether the observed decrease in choline uptake following cholesterol depletion was owing to a change in ligand binding affinity (K_D) or to a change in the number of cell surface CHT proteins (B_{\max}), kinetic analysis of binding of the non-transported competitive inhibitor [3 H]HC-3 to CHT was performed following treatment of cells with either vehicle or 0.3 mM M β C (Figure 3-2A). These data revealed that cell surface CHT levels were reduced by approximately 50% by M β C treatment, with B_{\max} for [3 H]HC-3 binding decreased from 470.5 ± 115 to 220.7 ± 77 fmol [3 H]HC-3 bound/mg protein in

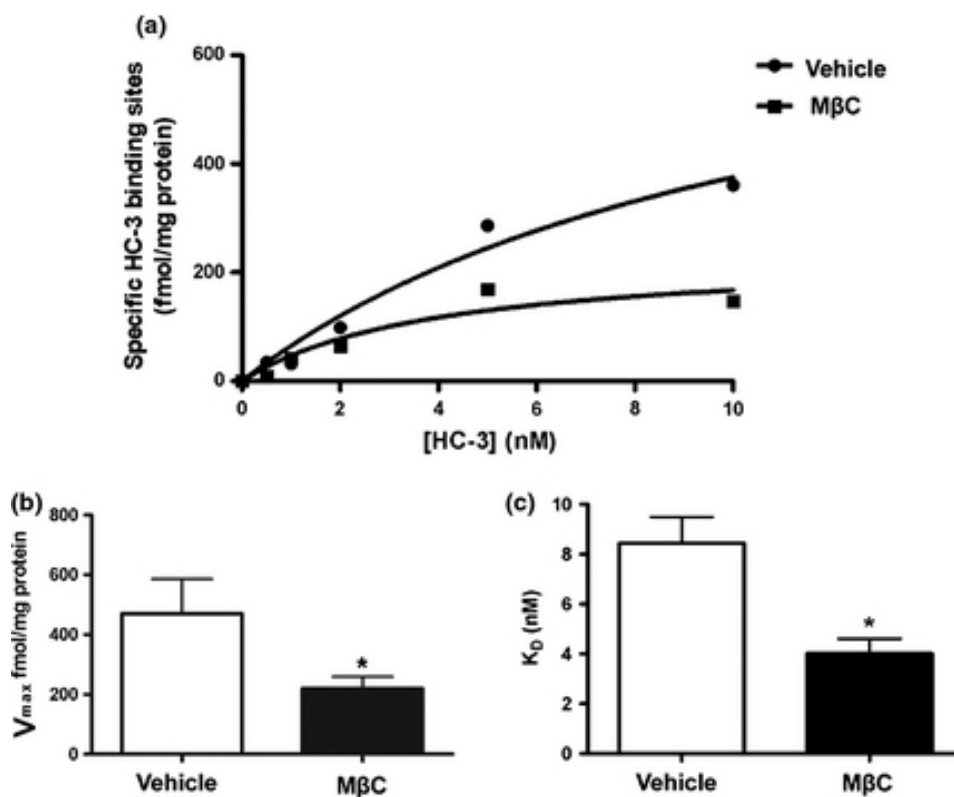


Figure 3-2 MβC modifies the binding kinetics for [³H]HC-3 to high-affinity choline transporters by decreasing B_{\max} and K_D .

Cells were treated with either vehicle (H_2O) or 0.3 mM MβC for 30 min at 37°C, then kinetic parameters for cell surface [³H]HC-3 binding were estimated using 0.5–10 nM hemicholinium-3 (HC-3). Data were calculated as pmol [³H]HC-3 bound/mg protein, and expressed as mean±SEM from five independent experiments. **A**, A representative experiment is shown for equilibrium binding of [³H]HC-3 to SH-SY5Y cells expressing CHT. Data were fit by Michaelis–Menten non-linear regression analysis of individual experiments. Differences between vehicle and MβC treatments were examined by comparison of the number of CHT sites (B_{\max}) **B**, and the apparent binding affinity for ligand (K_D), **C**. When compared to control cells, the K_D for HC-3 binding to CHT was decreased approximately 60% and B_{\max} was reduced by approximately 50% in MβC-treated cells (* $p < 0.05$, unpaired Student's t -test).

control and M β C-treated cells, respectively (Figure 3-2B). This coincides with a small, but significant, M β C-mediated increase in binding affinity with the K_D for [3 H]HC-3 binding reduced from 8.5 ± 1.1 to 4.0 ± 0.6 nM in control and M β C-treated cells, respectively (Figure 3-2C).

3.3.3 CHT proteins are associated with lipid rafts

The observation that choline uptake activity is modulated by changes in membrane cholesterol suggests that CHT proteins may be located in lipid rafts. Technically, lipid rafts are defined as membrane domains that are insoluble in cold non-ionic detergents, such as Triton X-100, and have a specific buoyant density during sucrose gradient centrifugation (36). However, non-ionic detergents can also solubilize proteins that are only weakly associated with lipid rafts, and also lipid and protein composition of rafts can differ between different extraction methods (37-39). Therefore, I used a second approach to isolate lipid rafts and validate our findings using a non-detergent procedure that is based on pH and carbonate resistance of lipid raft domains (40).

Importantly, my data show for the first time that CHT proteins are highly concentrated in lipid rafts prepared from SH-SY5Y cells that stably express the transporter (Figure 3-3). Membrane lipid rafts from cells lysed in either 1 M Na₂CO₃ pH 11 or 0.5% Triton X-100 were isolated using sucrose density gradient ultracentrifugation (41, 42). Solubilized proteins remain in the bottom fractions of the gradient (within 40% sucrose), whereas proteins associated with lipid rafts float to the upper layers (between 5% and 30% sucrose). To confirm isolation of lipid rafts, I also analyzed the distribution of flotillin-1, a lipid raft protein (43), and EEA1, a non-raft protein (41), in gradient fractions. Thus, CHT proteins are found predominantly in lipid raft fractions, and this distribution profile is similar in cells lysed with either Na₂CO₃ (Figure 3-3A and 3-3C) or Triton X-100 (Figure 3-3B and 3-3D). Figure 3-3A and 3-3B show representative immunoblots for CHT protein, with blotting membranes stripped and reprobed with anti-flotillin antibodies and anti-EEA1 antibodies. The histograms displayed in Figure 3-3C and 3-3D illustrate quantification of CHT protein distribution in sucrose density gradients by

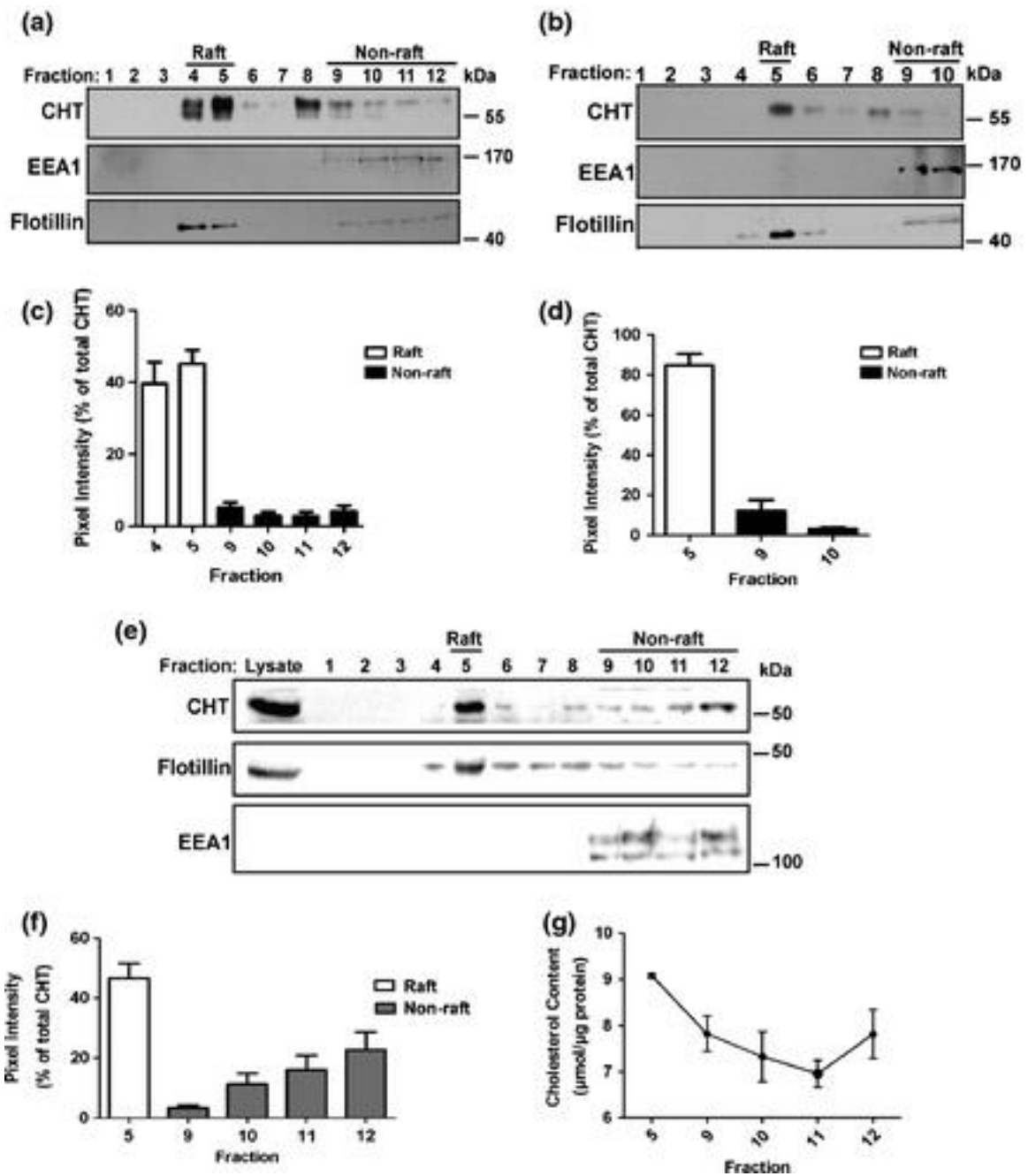


Figure 3-3

Figure 3-3 CHT proteins are distributed between raft and non-raft membrane domains.

Cells were lysed with either 1 M sodium carbonate pH 11 (**A**, **C**) or 0.5% Triton X-100 (**B**, **D**), then lipid rafts were isolated on sucrose gradients based on buoyant density. **A**, Representative immunoblots of gradient fractions 1–12 obtained using the sodium carbonate method showing CHT, non-raft marker EEA1 and raft-resident protein flotillin. **B**, Representative immunoblots of gradient fractions 1–10 obtained using the Triton X-100 method. (**C**, **D**) Densitometric analysis of CHT in raft and non-raft fractions expressed as a percentage of total CHT for cells lysed in either sodium carbonate or Triton X-100, respectively. To determine CHT protein distribution in membrane domains in brain cholinergic neurons, lipid rafts were isolated from mouse forebrain synaptosomes. **E**, Representative immunoblots of gradient fractions 1–12 obtained using the sodium carbonate method, from data obtained in three independent experiments. **F**, Densitometric analysis for CHT in raft and non-raft fractions prepared from synaptosomes expressed as a percentage of total CHT. Data are mean \pm SEM of three independent experiments. **G**, Free cholesterol content was determined in raft (5) and non-raft (9–12) fractions from sucrose density gradients using the Amplex Red Cholesterol Assay Kit (Invitrogen) and normalized to sample protein content. Raft fraction #5 contains the highest cholesterol content when compared to the non-raft fractions #9–12. Data are expressed as the mean \pm SEM of three independent experiments.

densitometry. Enrichment of CHT proteins in lipid rafts is seen with $85 \pm 10\%$ and $85 \pm 6\%$ of total CHT present in pooled flotillin-positive raft fractions, compared to $15 \pm 6\%$ and $15 \pm 5\%$ of total CHT present in EEA1-positive non-raft fractions from cells lysed with Na_2CO_3 and Triton X-100, respectively.

To confirm if CHT proteins are also present in lipid rafts in brain cholinergic nerve terminals, I prepared purified synaptosomes from mouse forebrain. Synaptosomes were lysed in 1 M Na_2CO_3 , then membrane lipid rafts were isolated on sucrose density gradients and immunoblots performed for CHT, EEA1, and flotillin. Figure 3-3E shows a representative immunoblot of the distribution of these proteins in gradient fractions. Importantly, in confirmation of my findings using cultured neural cells, a substantial proportion of CHT protein was found in lipid raft fractions. Densitometric quantification of CHT protein on immunoblots revealed that $47 \pm 5\%$ is present in fraction #5 that also coincides with the greatest density of the lipid raft protein flotillin. This is compared to $53 \pm 15\%$ in EEA1 positive non-raft fractions #9-12 (Figure 3-3F). Interestingly, the maximum CHT protein distribution in fractions #5 and 12 coincide with higher levels of free cholesterol content (Figure 3-3G)

3.3.4 CHT colocalizes with the lipid raft makers flotillin and ganglioside GM1

Confocal imaging experiments where cell surface CHT proteins were fluorescently labeled in live SH-SY5Y cells allowed further assessment of distribution of the transporter in raft and non-raft membrane domains. I assessed the colocalization of CHT with CTB, which binds to ganglioside GM1 and is found concentrated in lipid rafts (44), along with either flotillin (raft marker) or EEA1 (non-raft marker). To identify colocalized proteins, a threshold fluorescence intensity was set that filters for the brightest 2% of pixels of CHT (red channel) that also fall within the brightest 2% of pixels of GM1 (blue channel) and either flotillin (green channel) or EEA1 (green channel); this approach to visualize protein colocalization was validated previously (45). The colocalized pixels are identified in a separate colocalization channel (shown as 'Colocalized pixels' images). I found that CHT colocalizes to a similar extent with both

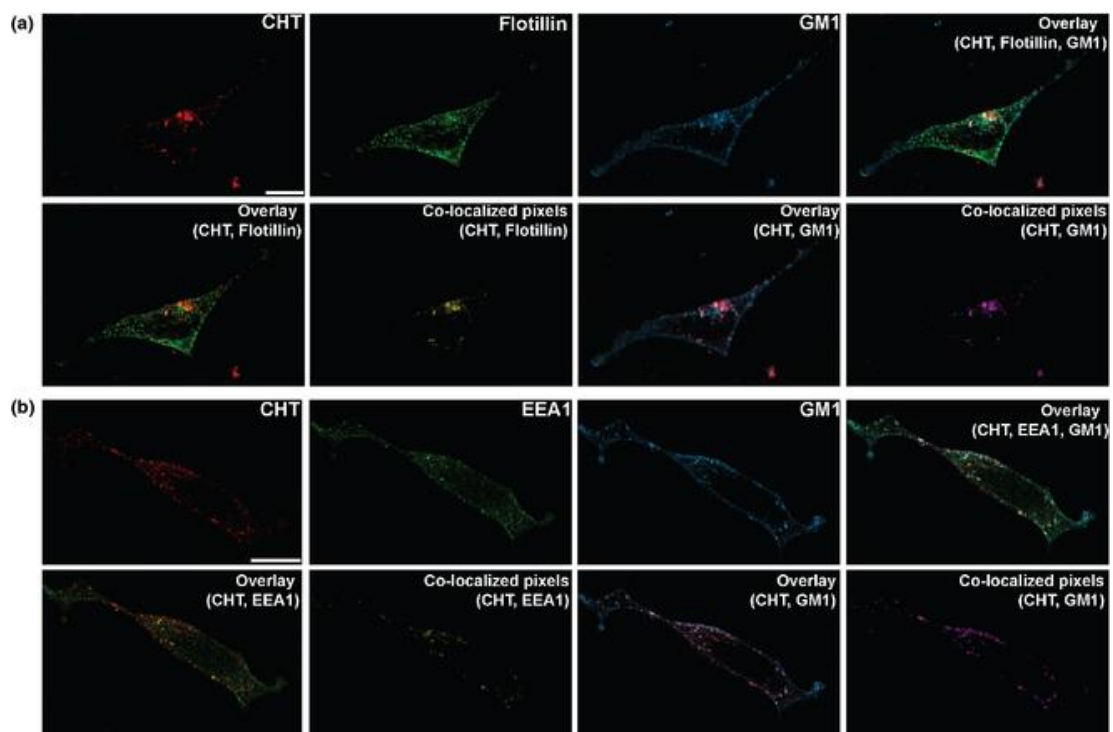


Figure 3-4

Figure 3-4 CHT proteins colocalize with flotillin and cholera toxin-labeled GM1, and to a lesser extent with EEA1.

Panel A, Confocal images show the distribution in SH-SY5Y cells of Zenon 488-labeled CHT (red), AlexaFluor 555-labeled flotillin (green), and AlexaFluor 647-labeled cholera toxin subunit B (CTB) binding to GM1. The Zenon 555 dye conjugated to rabbit anti-FLAG antibody was added to medium bathing live cells for 15 min where it could bind to the FLAG epitope of the amino terminus of CHT located at the cell surface. This facilitated tracking of CHT proteins at the cell surface, and as they are internalized into and traffic within cells. Cells were then formalin fixed and stained for endogenous ganglioside GM1 and flotillin. Colocalization of CHT and flotillin is yellow in Overlay panels and colocalization of CHT and GM1 is white in Overlay panels. Images were analyzed as described in Methods. CHT and flotillin determined to be colocalized in the colocalization channel are shown as yellow in the ‘Colocalized pixels’ image, and CHT and GM1 determined to be colocalized in the colocalization channel are shown as purple in the ‘Colocalized pixels’ image. **Panel B**, Confocal images show Zenon 555-labeled CHT (red), AlexaFluor 488-labeled EEA1 (green), and AlexaFluor 647 CTB-labeled GM1 distribution. Colocalization of CHT and EEA1 is yellow and colocalization of CHT and GM1 is white in the Overlay panels. CHT and EEA1 determined to be colocalized in the colocalization channel are shown as yellow in the ‘Colocalized pixels’ image and CHT and GM1 determined to be colocalized in the colocalization channel are shown as purple in the ‘Colocalized pixels’ image. Data are representative of 10 cells from four independent experiments. Scale bar, 5 μ m.

GM1 (Figure 3-4A, colocalized pixels shown in purple) and flotillin (Figure 3-4A, colocalized pixels shown in yellow), and that all three proteins are found together in a punctate distribution pattern indicative of lipid rafts (triple colocalized pixels panel not shown). In contrast, in cells stained for EEA1 and GM1, I found that CHT appears to be found more in GM1-positive compartments (Figure 3-4B, colocalized pixels shown in purple) than colocalized with EEA1 (Figure 3-4B, colocalized pixels shown in yellow).

3.3.5 Effect of cholesterol manipulating drugs on cholesterol level in SH-SY5Y cell membranes

I analyzed the effect of treatment of SH-SY5Y cells with either M β C or filipin on free and esterified cholesterol content in pooled lipid raft fractions (#4–6) and non-raft fractions (#9–12) obtained from sucrose gradients (Figure 3-5). As expected, total cholesterol levels were higher in lipid raft fractions when compared to non-raft fractions, with about 65% of the cholesterol contained in rafts (data not shown). Filipin, which functionally depletes cholesterol by forming filipin–cholesterol complexes within the membrane, did not significantly alter cholesterol levels. In cells treated with 5 μ g/mL filipin, cholesterol levels were 7.2 ± 0.5 and 3.9 ± 0.5 μ mol/ μ g protein in raft and non-raft fractions, respectively, compared to vehicle-treated controls where cholesterol levels were 7.2 ± 0.4 and 3.9 ± 0.3 μ mol/ μ g protein in lipid raft and non-raft fractions, respectively (Figure 3-5A). In contrast, treatment of cells with 0.3 mM M β C, which extracts cholesterol from membranes, significantly reduced cholesterol content in raft fractions but not in non-raft fractions; in M β C-treated cells, cholesterol levels were 6.8 ± 0.4 and 3.7 ± 0.5 μ mol/ μ g protein in raft fractions and non-raft fractions, respectively, compared to 7.7 ± 0.3 and 3.8 ± 0.4 μ mol/ μ g protein in raft and non-raft fractions, respectively, in vehicle-treated cells (Figure 3-5B). This corresponds to a cholesterol reduction of approximately 10% in lipid raft fractions, which compares with the findings of Foster et al. (2008) (46) who showed that treatment of cells with a much higher concentration of M β C (5 mM) causing a 52% reduction in cholesterol in lipid raft fractions.

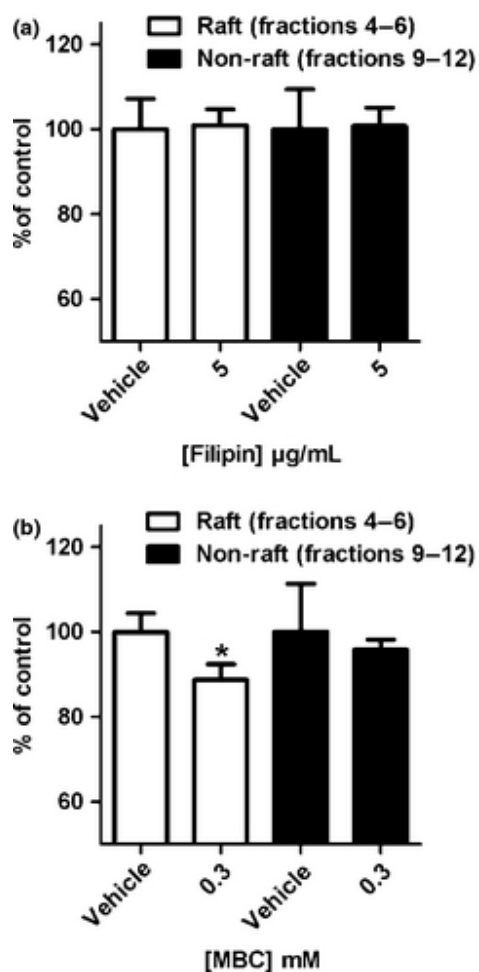


Figure 3-5 The effect of treatments that manipulate membrane cholesterol on cholesterol levels in raft and non-raft fractions from SH-SY5Y cells.

Cholesterol content was determined using the Amplex Red Cholesterol Assay kit and normalized to sample protein content. Methyl-β-cyclodextrin (MβC), but not filipin, significantly decreased cholesterol levels in lipid raft fractions. **A**, No changes in cholesterol content were observed in cells treated with filipin. **B**, MβC caused a significant reduction in cholesterol content in lipid raft fractions, but not non-raft fractions. Samples were measured from pooled raft fractions (#4–6) and non-raft fractions (#9–12) and data are expressed as % of control. Data were analyzed by one-way anova followed by Tukey's post-test and are given as the mean ± SEM of four independent experiments. * $p < 0.05$, paired Student's t -test.

3.3.6 Lipid raft disruption decreases plasma membrane CHT protein levels

Kinetic analysis of [^3H]HC-3 binding to CHT (Figure 3-2) revealed that M β C treatment of cells decreases B_{max} , suggesting that the number of CHT proteins at the plasma membrane is decreased. To confirm this and extend my studies on how lipid raft disruption alters CHT localization at the plasma membrane, we undertook cell surface protein biotinylation experiments. CHT proteins are located predominantly in subcellular endocytic compartments and synaptic vesicles (16) that also contain lipid rafts. Since we wanted to examine the relative distribution of CHT within lipid rafts only at the cell surface, plasma membrane proteins were biotinylated using membrane impermeable sulfo-NHS-biotin at 4°C to ensure that labeled CHT proteins did not undergo endocytosis. Prior to protein biotinylation, cells were treated at 37°C with either 5 $\mu\text{g}/\text{mL}$ filipin, 0.3 mM M β C or vehicle. Na_2CO_3 -insoluble lipid rafts were isolated, then biotinylated proteins were recovered from the pooled raft and non-raft fractions for analysis.

A critical finding is that modification in membrane cholesterol by either filipin or M β C reduced the amount of CHT protein in plasma membrane lipid raft fractions, but not in non-raft fractions (Figure 3-6). Representative immunoblots show the levels of cell surface (biotinylated) CHT protein, and the amount of total CHT protein, flotillin-1, and EEA1 in raft and non-raft fractions from cells treated with either filipin (Figure 3-6A) or M β C (Figure 3-6B). In vehicle-treated cells, plasma membrane CHT proteins are concentrated in lipid rafts with a distribution similar to that seen for total cellular CHT protein. Cell surface CHT levels in raft fractions were significantly reduced by approximately 50% in both filipin- and M β C-treated cells when compared to vehicle-treated cells ($p < 0.05$) (Figure 3-6C and 3-6D). This does not reflect redistribution of CHT to non-raft areas of plasma membrane, as changes were not observed in CHT levels in non-raft fractions between vehicle- and drug-treated cells. Immunoblots for cell surface CHT were reprobed with anti-flotillin and anti-EEA1 antibodies to confirm the

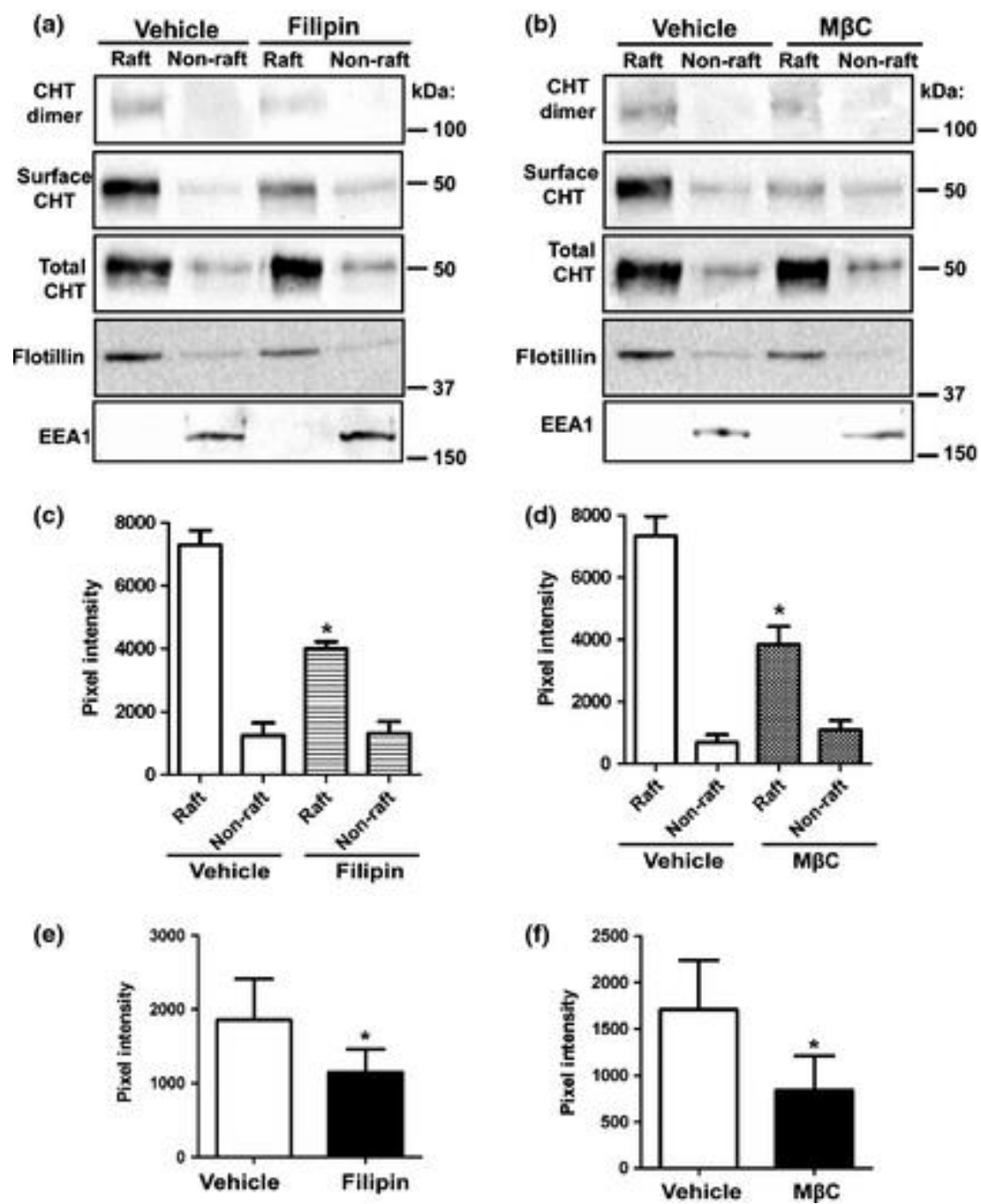


Figure 3-6

Figure 3-6 Filipin and M β C decrease cell surface CHT proteins in lipid rafts.

Cells were treated at 37°C for 60 min with vehicle (methanol) or 5 μ g/mL filipin (**A**, **C**, **E**), or for 30 min with vehicle (H₂O) or 0.3 mM M β C (**B**, **D**, **F**). Cells were washed and placed on ice, then plasma membrane proteins were biotinylated. Sodium carbonate-resistant lipid rafts were prepared and biotinylated proteins were isolated from the pooled raft (#4–6) and non-raft (#9–12) fractions. (**A** and **B**) Representative immunoblots for CHT dimer, cell surface (biotinylated) CHT, total CHT, lipid raft-resident protein flotillin and non-raft marker EEA1. (**C** and **D**) Densitometric analysis of cell surface CHT in raft and non-raft fractions from cells treated with vehicle or drug shows a statistically significant reduction in cell surface CHT in lipid rafts in drug-treated cells compared with control. Data were analyzed by repeated measures one-way ANOVA followed by Tukey's *post hoc* test, and are expressed as mean \pm SEM of four independent experiments $*p < 0.05$. (**E** and **F**) Increased exposures of cell surface CHT immunoblots shown in (**A** and **B**) reveal CHT-immunopositive bands that likely represent CHT dimers in lipid raft fractions. Densitometric analysis of CHT dimers shows a statistically significant reduction in lipid rafts from drug-treated cells compared with control. Data are expressed as mean \pm SEM of four independent experiments. ($*p < 0.05$, paired Student's *t*-test).

isolation of lipid rafts. As predicted, flotillin-1 levels in raft fractions were reduced in drug-treated cells confirming disruption of lipid rafts. No changes in EEA1 levels or distribution were observed between samples from vehicle- and drug-treated cells. Taken together, these results suggest that total cellular and cell surface CHT proteins are partitioned similarly between lipid raft and non-raft membrane domains in SH-SY5Y cells, with lipid raft disruption resulting in reduced cell surface CHT in lipid rafts.

It is important to note the presence of CHT-immunopositive bands with an apparent molecular mass of about 100 kDa in lipid raft fractions at higher exposures of the immunoblots for cell surface CHT proteins (Figure 3-6A and 3-6B). These bands, which are not present in the non-raft fractions, likely represent CHT protein dimers. In both filipin- and M β C-treated cells, levels of the putative CHT dimers at the cell surface are significantly reduced by about 50% ($p < 0.05$) (Figure 3-6E and 3-6F)

3.3.7 Lipid raft disruption does not alter CHT internalization from the cell surface

CHT proteins at the cell surface undergo constitutive internalization by a clathrin-mediated mechanism into early endosomes, and these proteins can recycle back to the cell surface (17). I tested the hypothesis that the decrease in plasma membrane CHT protein in filipin- and M β C-treated cells is because of an increase in internalization of CHT. SH-SY5Y cell plasma membrane proteins were biotinylated on ice, and then cells were incubated at 37°C with either vehicle, 0.3 mM M β C or 5 μ g/mL filipin to allow endocytosis of proteins from the cell surface to subcellular organelles. Only internalized biotinylated proteins were measured as, following drug treatments, cells were returned to ice to terminate endocytosis and residual biotin remaining on cell surface proteins was stripped by membrane-impermeant MesNa. Figure 3-7 illustrates that neither filipin nor M β C significantly alters CHT internalization from the cell surface to subcellular organelles. The amount of internalized biotinylated CHT protein was normalized to total cell surface CHT levels from cells that were incubated on ice in the absence of either filipin or M β C (Figure 3-7A and 3-7C, lane 2). A separate set of cells was incubated on ice throughout the procedure to ensure that MesNa efficiently stripped biotin from cell

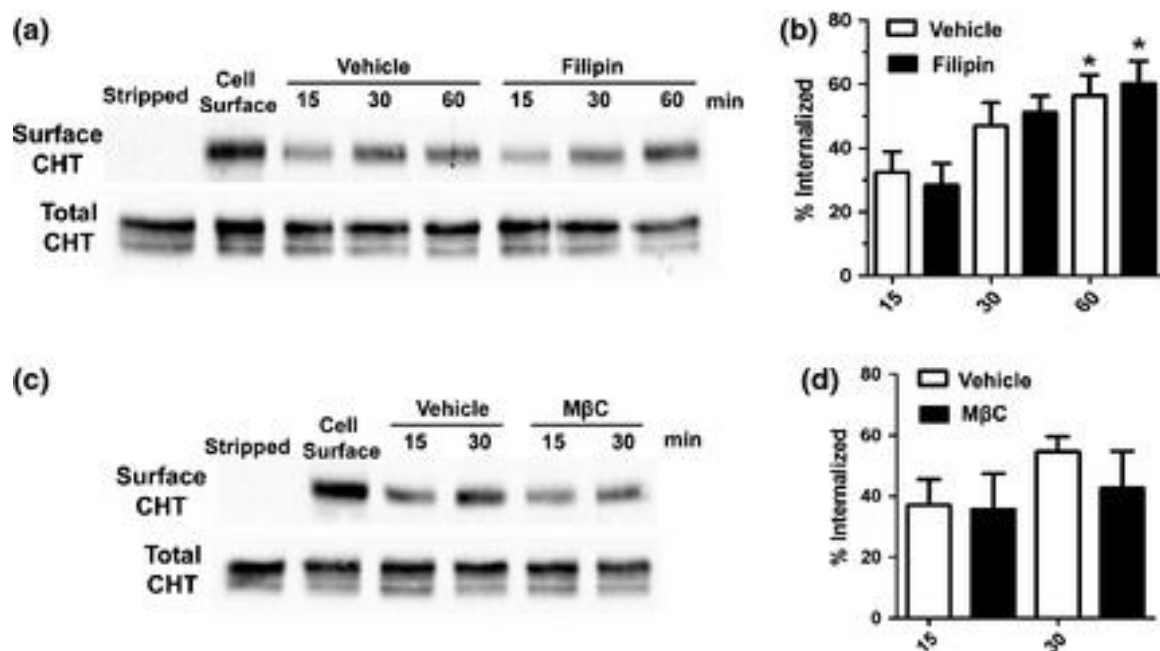


Figure 3-7 Lipid raft disruption does not alter CHT internalization.

Cell surface proteins were biotinylated for 1 h at 4°C, then cells were warmed to 37°C and CHT proteins allowed to internalize in the presence of vehicle or drug. **A**, Representative immunoblots for total and surface CHT showing no change in CHT internalization at 15, 30, and 60 min in cells treated with 5 µg/mL filipin compared with control. **C**, Representative immunoblots for total and surface CHT showing no change in CHT internalization at 15 and 30 min in cells treated with 0.3 mM methyl-β-cyclodextrin (MβC) compared with control. **(B and D)** Histograms show quantification of immunoblots for CHT internalization, with internalized CHT normalized to total cell surface CHT in each experiment. Data were analyzed by repeated measures one-way ANOVA followed by Tukey's *post hoc* test and expressed as mean ± SEM of five independent experiments. (* measurement at 60 min is statistically different from 15 min, $p < 0.05$).

surface proteins (Figure 3-7A and 3-7C, lane 1). Immunoblots of cell lysates (Figure 3-7A and 3-7B, lower panels) show that there were no changes in total CHT levels in cells as a consequence of the treatments. A statistically significant time-related increase in internalized CHT was observed in cells treated with either vehicle or filipin at 60 min when compared to 15 min, but no other statistically significant changes between groups were found (Figure 3-7B and 3-7D).

3.3.8 Identification of putative cholesterol-binding motifs in CHT protein

Transmembrane proteins may bind cholesterol molecules, with the two most common sites for this interaction on the protein being the Cholesterol Recognition/interaction Amino acid Consensus sequence (CRAC domain) and the CARC domain that comprised an inverted CRAC domain sequence (47, 48). The definition of both of these motifs is based on a triad of basic (K or R), aromatic (Y or F), and aliphatic (L or V) residues. The CRAC domain sequence is defined as L/V-(X)₁₋₅-Y-(X)₁₋₅-R/K, where X can be one to five residues of any amino acid. The CARC domain is the reverse sequence and the residue Y may be substituted by F. Analysis of the primary sequence of rat CHT reveals putative cholesterol-binding motifs, with these being conserved between rodent and human proteins. As illustrated in Figure 3-8, candidate sequences for putative CRAC and CARC domains are found in TMD 4, 11, 12, and 13 of CHT. TMD 4 contains the CARC sequence R-X₅-F-X₃-L that could bind cholesterol in the plasma membrane cytoplasmic leaflet. TM 13 contains a CRAC sequence V-X₁-Y-X₂-K, also on the bilayer cytoplasmic side. CRAC-like motifs, bearing close similarity to CRAC sequences, that could potentially bind cholesterol on the cytoplasmic leaflet are in TM 11 and 12 [TM 11, L-X₃-F-X₁-K or L-X₄-F-X₁-K; TM 12, V-X₂-Y-X₆-R]. In addition to cholesterol binding to CRAC and CARC motifs, transmembrane domains containing G-XXX-G motifs may also be engaged in binding cholesterol molecules (48, 49). Importantly, as shown in Figure 3-8, TMD 12 of CHT has a conserved G-XXX-G-XXX-G motif (G-AVA-G-YVS-G) that could potentially serve as both a cholesterol-binding motif and as a

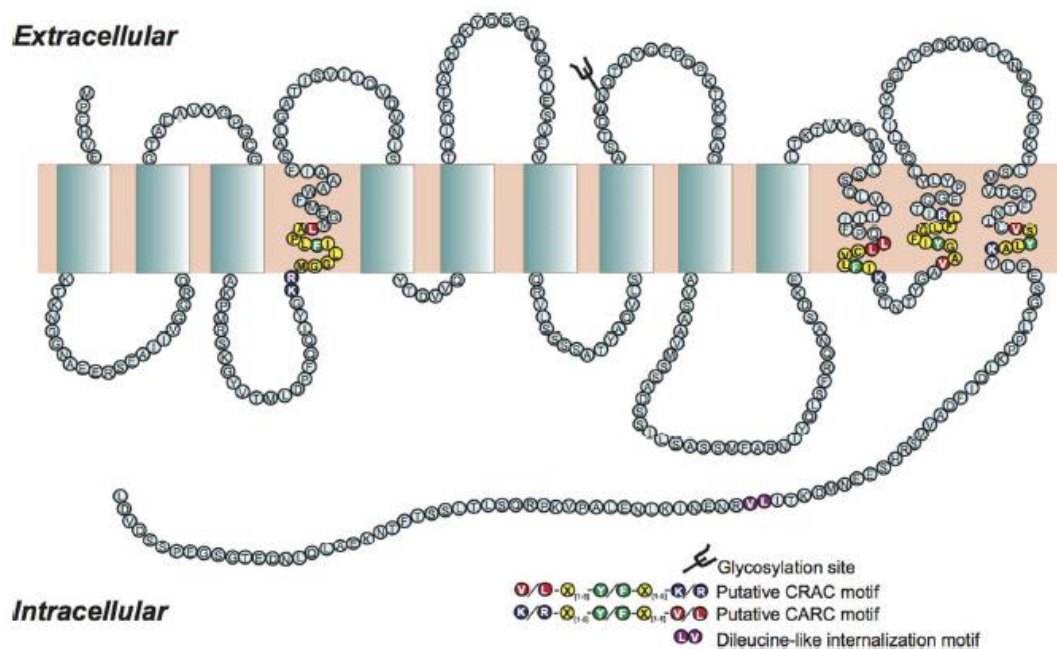


Figure 3-8 Schematic representation of transmembrane topology of rat high-affinity choline transporters showing putative cholesterol-binding motifs.

The positions of putative CRAC-like and CARC sequence motifs are shown in transmembrane domains 4, 11, 12, and 13. The positioning of transmembrane domains shown is based on data for human CHT [Q9GZV3] submitted recently to UniProtKB/Swiss-Prot at <http://www.uniprot.org/uniprot/Q9GZV3> [Last modified July 24, 2013]; rat and human CHT share 93% sequence identity.

dimerization motif. This sequence of the protein also coincides with a CRAC-like domain.

3.4 Discussion

I made several novel findings in this study that indicate that partitioning of CHT proteins into cholesterol-rich lipid rafts, and potentially direct interaction of CHT with cholesterol, may play a critical role in CHT localization at the cell surface and activity. I showed for the first time in both SH-SY5Y cells and mouse brain cholinergic nerve terminals that CHT proteins are partitioned between membrane lipid raft and non-raft microdomains, and tend to be concentrated in lipid rafts. Microscopically, CHT proteins colocalize with the lipid raft-resident protein flotillin and the lipid raft marker ganglioside GM1, and to a lesser extent with the non-raft protein EEA1. Second, I found that choline uptake activity shows a dependence on membrane cholesterol levels. Thus, treatment of neural cells with the cholesterol interfering drugs filipin, cholesterol oxidase, or M β C causes a significant decrease in HC-3-sensitive choline uptake. Moreover, choline uptake is significantly increased by adding exogenous cholesterol to cells. Third, I determined that reducing cell membrane cholesterol levels and disrupting lipid rafts by extracting cholesterol with M β C decreased the number of cell surface CHT proteins when measured by [3 H]HC-3 binding to CHT (decreased B_{\max}) and enhanced ligand binding affinity (decreased K_D). Fourth, I observed that treatment of cells with filipin and M β C results in a decrease in plasma membrane CHT protein levels from lipid rafts, but not non-raft areas, measured by cell surface protein biotinylation. This is not related to an accelerated rate of CHT protein internalization. Finally, I identified putative cholesterol-binding motifs in CHT protein that are conserved between rodent and human.

I used four separate pharmacological approaches that alter membrane cholesterol by different mechanisms to assess how cholesterol may regulate CHT function and activity. Treatment of cells with cholesterol oxidase results in conversion of membrane cholesterol to its functionally inactive analogue steroid 4-cholesten-3-one, but does not alter the physical state of plasma membranes (31). This allowed me to test if the change in choline uptake activity in choline oxidase-treated cells is owing to altered membrane fluidity,

rather than a change in membrane cholesterol levels. Based on my findings, it is unlikely that the decrease in choline uptake observed in these cells is because of an alteration of membrane fluidity. In other experiments, I treated cells with M β C which extracts cellular cholesterol and can disrupt lipid rafts and cholesterol–protein interactions in both raft and non-raft areas (30). Low concentrations of M β C (0.3 mM) significantly decreased cholesterol content measured in membrane lipid raft fractions and resulted in decreased choline uptake activity. However, it is not possible to determine from these experiments if the loss of CHT activity is caused by a direct or indirect effect of lowering cholesterol. Filipin, which binds to and chelates free cholesterol within the membrane resulting in disruption of lipid rafts, was not expected to lower cholesterol levels and our results are in agreement with previous reports with filipin and the polyene antifungal agent nystatin (29, 35). Filipin treatment did, however, reduce choline uptake activity, suggesting that disruption of lipid rafts does impact CHT function. Finally, I incubated cells with M β C–Chol to increase membrane cholesterol levels and this significantly enhanced choline uptake. Based on these experimental manipulations, it appears that CHT function requires the presence of membrane lipid rafts and may also be modulated by changes in cholesterol levels, indicating a potential role for direct interaction between cholesterol and CHT proteins.

Decreased choline uptake in cells treated with agents that reduce membrane cholesterol could be because of a loss of functional transporters at the cell surface, or be the result of conformational changes in CHT protein that alter solute binding affinity or impair solute translocation subsequent to binding. Kinetic analysis of binding of the inhibitor [3 H]HC-3 to CHT in M β C-treated cells and quantification of cell surface protein biotinylation assays in cells treated with either filipin or M β C indicate that there is a reduction in CHT levels at the plasma membrane. Interestingly, the decrease in CHT protein is seen in lipid raft fractions prepared from either filipin- or M β C-treated cells and is not accompanied by an increase in CHT levels in non-raft fractions, indicating that down-regulation of choline uptake activity is not a result of CHT movement between these compartments. Indeed, some proteins display redistribution between these membrane compartments in response to lipid raft disrupting treatments, whereas other proteins do not (36). My results

are in agreement with those found for the dopamine transporter (DAT) by Foster et al. (2008) who showed that while M β C treatment reduced DAT cell surface levels, it did not affect partitioning of DAT proteins between lipid raft and non-raft fractions. My finding of increased binding affinity (K_D) of CHT for HC-3 in M β C-treated SH-SY5Y cells is in agreement with a report of increased HC-3 binding affinity to CHT observed in M β C-treated synaptosomes (25), and is similar to reports of increased ligand binding affinity found for other neurotransmitter transporters, such as DAT in M β C-treated cells (29, 35). The change in binding properties of CHT in M β C-treated cells could indicate that the conformational state of CHT required for solute binding is modulated by either lipid raft association or by cholesterol binding. Previous studies show that CHT proteins may exist in more than one state or conformation and that binding sites in some states may be occluded under some conditions (50, 51). Alternatively, changes to the physical properties of lipid rafts may disrupt cholesterol-sensitive protein–protein interactions involving CHT or affect the ability of CHT to undergo post-translational modifications such as phosphorylation, both of which could affect solute binding or translocation (36, 45).

Membrane cholesterol and/or lipid rafts could have a role in regulating the amount of CHT protein at the cell surface by altering its rate of internalization into endosomes and/or its recycling back to the cell surface. Several reports suggest that proteins can traffic to the plasma membrane and be selectively recruited to lipid raft microdomains (52-54). We showed previously that alterations in CHT internalization critically affect transporter function, while CHT recycling is required to maintain the level of transporter at the cell surface thereby regulating CHT activity to deliver sufficient choline to maintain ACh synthesis. CHT undergoes endocytosis by a clathrin- and dynamin-dependent mechanism, but there is no evidence that CHT internalizes by a clathrin-independent, caveolin-dependent process from lipid raft domains. In this study, we found that CHT protein internalization was not significantly altered by disruption of membrane cholesterol or rafts by either filipin or M β C, suggesting that the decrease in plasma membrane CHT levels was not owing to increased endocytosis; while not measured in my studies, reduced recycling of transporters to the cell surface could result in decreased

cell surface levels of the protein. These experiments also reinforce that CHT proteins do not likely undergo internalization by caveolae since, as lipid rafts were disrupted, an increase in plasma membrane CHT protein would have been predicted. In the current studies, cells were treated with a relatively low concentration of M β C (0.3 mM) since we observed that higher concentrations of the drug (2 or 5 mM) used in other studies led to accumulation of CHT proteins at the cell surface (data not shown). M β C can inhibit clathrin-mediated endocytosis (55) and as CHT undergoes rapid constitutive endocytosis, conditions that disrupt this process can result in substantial accumulation of the protein at the cell surface. Thus, I chose to use an M β C concentration that significantly decreased cholesterol levels in lipid rafts, and was less likely to perturb endocytosis.

Interestingly, we observed a CHT-immunopositive band with an apparent molecular mass of about 100 kDa in lipid raft fractions. These bands could represent homo-oligomers of CHT proteins, with recent work by Okuda et al. (2012) showing that CHT expressed in cultured cells can form homo-oligomers at the cell surface. Here, my studies provide evidence that these homo-dimers are located within lipid rafts, and that these are reduced by lipid raft disrupting treatments. This suggests that oligomerization may result in stabilization of CHT into the raft domain and be required for cell surface localization of CHT. Detection of CHT in cell lysates often reveals multiple protein species and it has been suggested that these represent varying glycosylated forms of CHT (57). CHT may undergo differential post-translational modifications, such as phosphorylation, between raft and non-raft areas of membrane, but it remains to be established if these impact either CHT activity or plasma membrane trafficking. For example, activation of PKC enhances internalization of the noradrenaline transporter through a dynamin- and clathrin-independent lipid raft-mediated process (32). In comparison, PKC-induced internalization of DAT is dynamin and clathrin dependent, and is independent of lipid rafts (46).

Several lines of evidence support a connection between alterations in cholesterol levels and its disposition in aging (58) and AD (59) and the organization of lipid rafts is disrupted in AD brains (60). Here, my studies provide the first evidence that association of CHT proteins with cholesterol-rich lipid rafts is critical for transporter function and localization. These data are important for understanding the normal function of widely

distributed cholinergic neurons, and how they are altered in disorders that involve cognitive dysfunction owing to reduced cholinergic transmission. These studies will allow us to analyze responses to changes in the cholinergic nerve endings and to assess alterations in pathology to aid in the design of new therapies. Therapeutic strategies directed at CHT function may be useful for enhancing cholinergic transmission, for example, early in AD when ACh release is reduced but cholinergic neurons remain viable. Given the projected increases in our aging population and the prevalence of neurodegenerative disorders, these studies are both timely and critical.

3.5 References

1. Allen, J.A., Halverson-Tamboli, R.A., and Rasenick, M.M. (2007) *Nat Rev Neurosci* **8**, 128-140
2. Lingwood, D., and Simons, K. (2010) *Science* **327**, 46-50
3. Simons, K., and Ikonen, E. (1997) *Nature* **387**, 569–572
4. Maekawa, S., Iino, S., and Miyata, S. (2003) *Biochim Biophys Acta* **1610**, 261-270
5. Laude, A.J., and Prior, I.A. (2004) *Mol Membr Biol* **21**,193-205
6. Lajoie, P., and Nabi, I.R. (2007) *J Cell Mol Med* **11**, 644-653
7. McIntosh, T.J., and Simon, S.A. (2006) *Annu Rev Biophys Biomol Struct* **35**, 177-198
8. Hicks, D.A., Nalivaeva, N.N., and Turner A.J. (2012) *Front Physiol* **3**, 189
9. Pike, L.J. (2006) *J Lipid Res* **47**, 1597-1598
10. North, P., and Fleischer, S. (1983) *J Biol Chem* **258**, 1242-1253
11. Butchbach, M.E., Tian, G., Guo, H., and Lin, C.L. (2004) *J Biol Chem* **279**, 34388-34396
12. Helms, J.B., and Zurzolo, C. (2004) *Traffic* **5**, 247-254
13. Magnani, F., Tate, C.G., Wynne, S., Williams, C., and Haase, J. (2004) *J Biol Chem* **279**, 38770-38778
14. Scanlon, S.M., Williams, D.C., and Schloss, P. (2001) *Biochemistry* **40**, 10507-10513
15. Shouffani, A., and Kanner, B.I. (1990) *J Biol Chem* **265**, 6002-6008

16. Ribeiro, F.M., Alves-Silva, J., Volkmandt, W., Martins-Silva, C., Mahmud, H., Wilhelm, A., Gomez, M.V., Rylett, R.J., Ferguson, S.S., Prado, V.F., and Prado, M.A. (2003) *J Neurochem* **87**, 136-146
17. Ribeiro, F.M., Black, S.A., Prado, V.F., Rylett, R.J., Ferguson, S.S., and Prado, M.A. (2006) *J Neurochem* **97**, 1-12
18. Ribeiro, F.M., Pinthong, M., Black, S.A., Gordon, A.C., Prado, V.F., Prado, M.A., Rylett, R.J., and Ferguson, S.S. (2007a) *Eur J Neurosci* **26**, 3437-3448
19. Gates, J., Ferguson, S.M., Blakely, R.D., and Apparsundaram, S. (2004) *J Pharmacol Exp Ther* **310**, 536-545
20. Black, S.A.G., Ribeiro, F.M., Ferguson, S.S.G., and Rylett, R.J. (2010) *Neuroscience* **167**, 765-773
21. Okuda, T., Haga, T., Kanai, Y., Endou, H., Ishihara, T., and Katsura, I. (2000) *Nat Neurosci* **3**, 120-125
22. Wang, B., Yang, L., Wang, A., and Zheng, H. (2007) *Proc Nat Acad Sci U S A* **104**, 14140-14145
23. Waser, P.G., Oxterwalder, M., and Schonenberger, E. (1978) *Naunyn Schmiedebergs Arch Pharmacol* **302**, 173-179
24. North, P., and Fleischer, S. (1983) *J Biol Chem* **258**, 1242-1253
25. Kristofiková, Z., Tejkalová, H., and Klaschka, J. (2001) *Neurochem Res* **26**, 203-212
26. Pinthong, M., Black, S.A., Ribeiro, F.M., Pholpramool, C., Ferguson, S.S., and Rylett, R.J. (2008) *Mol Pharmacol* **73**, 801-812
27. Rylett, R.J., and Walters, S.A. (1990) *Neuroscience* **36**, 483-489
28. Dale, L.B., Seachrist, J.L., Babwah, A.V., and Ferguson, S.S. (2004) *J Biol*

Chem **279**, 13110-13118

29. Cremona, M.L., Matthies, H.J., Pau, K., Bowton, E., Speed, N., Lute, B.J., Anderson, M., Sen, N., Robertson, S.D., Vaughan, R.A., Rothman, J.E., Galli, A. (2011) *Nat Neurosci* **14**, 469-477
30. Zidovetzki, R., and Levitan, I. (2007) *Biochim Biophys Acta* **1768**, 1311-1324
31. Gimpl, G., Burger, K., and Fahrenholz, F. (1997) *Biochemistry* **36**, 10959-10974
32. Jayanthi, L.D., Samuvel, D.J., and Ramamoorthy, S. (2004) *J Biol Chem.* **279**, 19315-19326
33. Samuvel, D.J., Jayanthi, L.D., Bhat, N.R., and Ramamoorthy, S. (2005) *J Neurosci* **25**, 29-41
34. Shouffani, A., and Kanner, B.I. (1990) *J Biol Chem* **265**, 6002-6008
35. Jones, K.T., Zhen, J., and Reith, M.E.A. (2012) *J Neurochem* **123**, 700-71
36. Allen, J.A., Halverson-Tamboli, R.A., and Rasenick, M.M. (2007) *Nat Rev Neurosci* **8**, 128-140
37. Hooper, N.M. (1999) *Mol Membr Biol* **16**, 145-156
38. Janes, P.W., Ley, S.C., Magee, A.I., and Kabouridis, P.S. (2000) *Semin Immunol* **12**, 23-34
39. Waugh, M.G., Lawson, D., and Hsuan, J.J. (1999) *Biochem J* **337**, 591-597
40. Song, K.S., Li, S., Okamoto, T., Quilliam, L.A., Sargiacomo, M., and Lisanti, M.P. (1996) *J Biol Chem* **271**, 9690-9697
41. Di Guglielmo, G.M., Le Roy, C., Goodfellow, A.F., and Wrana, J.L. (2003) *Nat Cell Biol* **5**, 410-421
42. Luga, V., McLean, S., Le Roy, C., O'Connor-McCourt, M., Wrana, J.L., and Di

- Guglielmo G.M. (2009) *Biochem J* **421**, 119-131
43. Lamb, M.E., Zhang, C., Shea, T., Kyle, D.J., and Leeb-Lundberg, L.M. (2002) *Biochemistry* **41**, 14340-14347
 44. Simons, K., and Toomre, D. (2000) *Nat Rev Mol Cell Biol* **1**, 31-39
 45. Lorenzen, A., Samosh, J., Vandewark, K., Anborgh, P.H., Seah, C., Magalhaes, A.C., Cregan, S.P., Ferguson, S.S.G., and Pasternak, S.H. (2010) *Molecular Brain* **3**, 11
 46. Foster, J.D., Adkins, S.D., Lever, J.R., and Vaughan, R.A. (2008) *J. Neurochem* **105**, 1683-1699
 47. Baier, C.J., Fantini, J., and Barrantes, F.J. (2011) *Sci Rep* **1**, 1-7
 48. Fantini, J., and Barrantes, F.J. (2013) *Front Physiol* **4**, 1-9
 49. Barrett, P.J., Song, Y., Van Horn, W.D., Hustedt, E.J., Schafer, J.M., Hadziselimovic, A., Beel, A.J., and Sanders, C.R. (2012) *Science* **336**, 1168-1171
 50. Saltarelli, M.D., Lowenstein, P.R., and Coyle, J.T. (1987) *Eur J Pharmacol* **135**, 35-40
 51. Ferguson, S. M., Bazalakova, M., Savchenko, V., Tapia, J. C., Wright, J., and Blakely, R. D. (2004) *Proc Natl Acad Sci U S A* **101**, 8762-8767
 52. Michaely, P.A., Mineo, C., Ying, Y. and Anderson. R.G.W. (1999) *Biol Chem* **274**, 21430-21436
 53. Lindwasser, O.W. and Resh, M.D. (2001) *J Virol* **75**, 7913-7924
 54. McCabe, J.B., and Berthiaume, L.G. (1999) *Mol Biol Cell* **10**, 3771-3786

55. Subtil, A., Gaidarov, I., Kobylarz, K., Lampson, M.A., Keen, J.H., and McGraw, T.E. (1999) *Proc Natl Acad Sci USA* **96**, 6775-6780
56. Okuda, T., Osawa, C., Yamada, H., Hayashi, K., Nishikawa, S., Ushio, T., Kubo, Y., Satou, M., Ogawa, H., and Haga, T. (2012) *J Biol Chem* **287**, 42826-42834
57. Ferguson, S.M., Savchenko, V., Apparsundaram, S., Zwick, M., Wright, J., Heilman, C.J., Yi, H., Levey, A.I., and Blakely, R.D. (2003) *J Neurosci* **23**, 9697-9709
58. Martin, M., Dotti, C.G., and Ledesma, M.D. (2010) *Biochim Biophys Acta* **1801**, 934-944
59. Simons, M., Keller, P., Dichgans, J., and Schulz J.B. (2001) *Neurology* **57**, 1089-1093
60. Ledesma, M.D., Abad-Rodriguez, J., Galvan, C., Biondi, E., Navarro, P., Delacourte, A., Dingwall, C., and Dotti, C.G. (2003) *EMBO Rep* **4**, 1190-1196

Chapter 4

- 4 Differential regulation of the high-affinity choline transporter CHT by wild-type and Swedish mutant amyloid precursor protein

4.1 Introduction

Pathologically, two major features of AD are the processing of APP to A β , which are the principal component of A β plaques, and the dysfunction and eventual loss of cholinergic neurons. While these two features of AD pathology are well established, the connection between them is not fully understood. APP is a type 1 transmembrane protein that exists in three different isoforms (APP695, APP751 and APP770) as a result of differential splicing of exons 7 and 8 (1), with APP695 being the main isoform expressed in neurons (2). APP_{wt} is trafficked to the cell surface where it undergoes two distinct pathways of proteolytic processing. Amyloidogenic processing of APP_{wt} is thought to occur within the endosomal pathway, where it is cleaved first by BACE1, followed by the γ -secretase complex, resulting in A β production (3). Non-amyloidogenic processing occurs mainly at the cell surface, where APP_{wt} is cleaved by α -secretases within the A β domain (4). Inheritable mutations in the genes encoding APP can alter subcellular trafficking and proteolytic processing of APP. For example, APP695 containing the Swedish mutation (K595N/M596L) (APP_{Swe}), which causes early-onset familial AD by increasing A β production by 6- to 8-fold, undergoes high-efficiency BACE1 cleavage primarily within the TGN and secretory pathway (5, 6), and exhibits differences in its trafficking from the cell surface through the endosomal pathway compared to APP_{wt} (7).

The relationship between APP and cholinergic dysfunction is not well understood. Evidence suggests that cholinergic neurotransmission promotes α -cleavage of APP through ACh stimulation of specific muscarinic AChR subtypes (8), while in turn A β oligomers inhibit ACh synthesis and release (9-11). Importantly, high-affinity choline uptake in rat brain hippocampal synaptosomes is impaired by exposure to picomolar-nanomolar concentrations of A β (11, 12). An important link between APP_{wt} and the cholinergic system identified recently shows a direct physiological role for APP within cholinergic neurons by demonstrating that APP_{wt} interacts with CHT, mediating its presynaptic localization and increasing its rate of internalization from the cell surface (13).

Altering CHT trafficking has a direct impact on choline uptake activity and cholinergic neurotransmission (16). The purpose of this study was to further investigate how APP_{wt} regulates CHT trafficking and activity, and to determine whether this interaction is altered by the Swedish mutation. Here, I observed that CHT protein interacts significantly less with APP_{Swe} than with APP_{wt}. Interestingly however, the expression of either APP_{wt} or APP_{Swe} decreased CHT cell surface levels and CHT activity, and increased CHT colocalization to early endosomes, to the same extent. In these experiments, neural cells expressing APP_{Swe} secreted significantly more A β than did cells expressing APP_{wt}. Importantly, lowering the production of A β through BACE1 inhibition significantly increased CHT cell surface level in cells expressing APP_{Swe}, but not in cells expressing APP_{wt} compared to vehicle-treated control cells. I confirm here that APP_{wt} interacts directly with CHT and make the novel observation that the interaction of CHT with APP is disrupted by the Swedish mutation. Furthermore, I propose that CHT function is inhibited by both APP_{wt} and APP_{Swe}, but the underlying mechanisms by which this occurs differ. My data reveal that APP_{wt} facilitates CHT endocytosis, while APP_{Swe}-mediated inhibition of CHT function could be caused by the susceptibility of the transporter to A β found in the extracellular environment.

4.2 Materials and methods

4.2.1 Materials

BACE1 inhibitor IV was obtained from Calbiochem, anti-FLAG M2 affinity gel, mouse IgG-agarose, Duolink *in situ* orange starter kit mouse/rabbit, protease inhibitor cocktail and polyclonal rabbit anti-APP c-terminal antibody were from Sigma-Aldrich, β -amyloid 1-16 (6E10) mouse monoclonal antibody was from Covance, rabbit polyclonal anti-actin antibody was from Santa Cruz Biotechnology, anti-amyloid precursor protein A4 (clone 22C11) was from Millipore and [*methyl*-³H]choline chloride (88.5 Ci/mmol) was from PerkinElmer Life Sciences. Other chemicals were purchased from Sigma-Aldrich at the highest purity available. SH-SY5Y human neuroblastoma cells were from the American Type Culture Collection, and Invitrogen supplied FBS, Lipofectamine 2000, OptiMEM, and culture media and reagents. AlexaFluor 555 donkey anti-mouse IgG and

AlexaFluor 647 goat anti-rabbit IgG antibodies were from Invitrogen. ECL was from GE Healthcare Life Sciences and Biodegradable Scintillant was from GE Healthcare. Polyclonal CHT antibody was raised in rabbits to the antigenic peptide DVDSSPEGSGTEDNLQ, which is conserved at the carboxyl-terminus of human and rat CHT (Genemed Synthesis); this peptide was conjugated to KLH carrier protein by an N-terminal cysteine residue. CHT-specific IgG was affinity-purified in our laboratory from the crude antiserum on NHS-Sepharose (GE Healthcare) to which antigenic peptide had been coupled as the binding element. Peroxidase-conjugated goat anti-rabbit IgG was from Jackson ImmunoResearch Laboratories.

4.2.2 Cell transfection and selection of cell lines

Full-length rat CHT cDNA ligated to pSPORT was a gift from Dr. T. Okuda (14); a FLAG epitope tag (DYKDDDDK) was added to the amino-terminus by PCR and the resulting cDNA ligated to pcDNA3.1 or pcDNA5. SH-SY5Y cells were transfected with FLAG-CHT cDNA ligated to pcDNA3.1 by Lipofectamine 2000. Stable transformants (SY5Y-CHT) were selected using 500 µg/ml G418 for 4 weeks, and then grown in DMEM containing 10% FBS, 100 U/ml penicillin, and 100 µg/ml each of streptomycin and 100 µg/ml G418. SH-SY5Y cell differentiation was induced by the addition of 10 µM RA for 3 d; substantial morphological and biochemical differentiation of cells occurred during this time frame.

For transient transfection, cells were plated and treated with retinoic acid for 3 d before transfection, and immediately before transfection the culture medium was changed to complete medium that did not contain antibiotics. At the time of transfection, 1 µg of plasmid DNA in 100 µl of OptiMEM was added to 100 µl of OptiMEM containing 2.5 µl of Lipofectamine 2000, and then incubated for 20 min at room temperature. This mixture was added to monolayers of cells in antibiotic-free medium and incubated for 4-6 h. At the end of the incubation with transfection reagents, culture medium was replaced with complete medium containing RA and grown for an additional 24 h.

4.2.3 DNA constructs

Full-length human wild-type APP695 (APP_{wt}) and APP695 containing the Swedish mutation K595N/M596L (APP_{Swe}) cDNA plasmids were generated by Dr. Dennis Selkoe (15) and obtained from Addgene (Addgene plasmid 30137 and Addgene plasmid 30145, respectively). SY5Y-CHT cells were transiently transfected with a ratio of 1 µg APP_{wt} plasmid DNA : 1.5 µg APP_{Swe} plasmid DNA in all experiments to obtain equal levels of expression of these two proteins. Control cells were transiently transfected with the empty vector pcDNA3.1. In some confocal imaging experiments, cells were transiently transfected with plasmids encoding cDNA for either full-length human HA-labeled APP750-YFP (APP_{wt}-YFP) or HA-labeled APP750-YFP containing the Swedish mutation (APP_{Swe}-YFP) to mediate expression of these fusion proteins.

4.2.4 Co-immunoprecipitation of FLAG-CHT and wild-type or Swedish mutant APP

Either SY5Y-CHT cells or SH-SY5Y cells stably-expressing pcDNA3.1 empty vector were plated on 100 mm dishes, then transiently transfected with either 6 µg APP_{wt} plasmid DNA or 9 µg APP_{Swe} plasmid DNA using Lipofectamine 2000, according to manufacturer's instructions. For a control, cells were transfected with 9 µg pcDNA3.1. In experiments where BACE1 activity was to be inhibited, cells were incubated in complete medium containing either vehicle (DMSO) or 25 µM BACE1 inhibitor IV immediately following transfection. Twenty-four hours after transfection, cells were lysed with 1% Triton X-100 lysis buffer (50 mM Tris-HCl, pH 7.5, 150 mM NaCl, 1% Triton X-100, 700 Units/ml DNase I and 10µL/mL protease inhibitor cocktail), then sample protein concentration was measured using a BioRad protein assay reagent. Aliquots of cell lysates containing 500 µg lysate protein were pre-cleared for 60 min with 50 µl mouse IgG-agarose, then incubated overnight with 100 µl of washed anti-FLAG M2 affinity resin. Alternatively, following pre-clearing, lysates were incubated on ice for 30 min with 2µL of anti-APP A4 (22C11) antibody and then incubated overnight with 50 µL of washed Protein-G Sepharose. Anti-FLAG affinity resin with bound proteins and Protein-G Sepharose with bound proteins were collected by centrifugation and washed 3 times

with lysis buffer to remove non-specifically bound proteins. Proteins were eluted by incubation for 10 min at 55°C with Laemmli sample buffer (0.125 M Tris-HCl, pH 6.8, 4% SDS, 20% glycerol, 0.01% bromophenol blue, 5% 2-mercaptoethanol), then separated on 7.5% SDS-PAGE gels and transferred to PVDF membranes. Membranes were blocked in 8% non-fat dry milk in wash buffer (PBS with 0.15% Triton X-100) for 1 h, then incubated overnight at 4°C with anti-CHT (1:1000) antibody or anti-APP - terminal antibody (1:1000). After washing, membranes were incubated for 1 h in wash buffer containing 8% milk and peroxidase-conjugated goat anti-rabbit IgG secondary antibody. Immunoreactive proteins on membranes were detected by chemiluminescence using a Chemidoc Imaging System (BioRad).

4.2.5 Proximity ligation assay

To evaluate the interaction between CHT and either APP_{wt} or APP_{Swe} *in situ*, we used a proximity ligation assay (PLA) method using Duolink technology (Sigma). In these experiments, SY5Y-CHT cells grown on 35 mm confocal dishes were transiently transfected with 1 µg APP_{wt} plasmid DNA or 1.5 µg APP_{Swe} plasmid DNA and allowed to express for 24 h. Cells were then washed twice with warm HBSS, formalin-fixed for 15 min at room temperature and then blocked for 30 min at room temperature in blocking solution (HBSS containing 3% goat serum). Cells were then labeled with primary antibodies against either CHT (anti-CHT 1:500) or APP (anti-APP 6E10 1:100) in blocking solution. Cells were then washed twice in HBSS and incubated with Duolink secondary antibodies (Duolink *in situ* PLA probe anti-rabbit PLUS and Duolink *in situ* PLA probe anti-mouse MINUS). Following binding of probes to target CHT and either APP_{wt} or CHT and APP_{Swe}, protein complexes cells were washed twice in Duolink Wash Buffer A and then incubated in ligation solution (1 U/µL DNA ligase) for 30 min at 37°C. Cells were then washed twice in Duolink Wash Buffer A and the hybridized DNA molecule was amplified by rolling-circle amplification by incubation of the cells in amplification solution (10 U/µL DNA polymerase) containing fluorescently-labeled oligonucleotides for 100 min in the dark at 37°C. Cells were then washed twice with Duolink Wash Buffer B and allowed to dry. Dishes were then mounted with coverslips using Duolink *in situ* mounting media containing DAPI, and images were acquired using

a Zeiss LSM510-Meta laser scanning confocal microscope using a 63X magnification oil-immersion objective. Imaris software version 7.7.0 was used to count the number of spots per cell signifying an interaction between either APP_{wt} and CHT or APP_{Swe} and CHT protein complexes. As a control, background spots per cell were counted in cells that had not been transfected. Statistical analysis was performed using GraphPad Prism using one-way ANOVA with Tukey's post-hoc test.

4.2.6 Cell surface protein biotinylation assay

SY5Y-CHT cells plated on 100 mm dishes were transiently-transfected with either 6 µg APP_{wt} plasmid DNA or 9 µg APP_{Swe} plasmid DNA using Lipofectamine 2000 and allowed to express for 24 h. For a control, cells were transfected with 9 µg empty vector. In experiments where BACE1 activity was to be inhibited, cells were incubated in complete medium containing either vehicle (DMSO) or 25 µM BACE1 inhibitor IV immediately following transfection. Cells were then washed twice with cold HBSS and placed on ice under cold HBSS to stop protein trafficking. Plasma membrane proteins were biotinylated on ice by incubating with 1 mg/ml sulfo-NHS-SS-biotin in HBSS for 1 h. Unbound biotin was quenched by washing and incubating cells in cold 100 mM glycine in HBSS. After two further washes with HBSS, cells were lysed on ice for 30 min in 1% Triton X-100 lysis buffer. Neutravidin beads were incubated with cell lysates for 1 h at 4°C with gentle mixing to bind biotin-labeled proteins to allow their separation from the non-biotinylated proteins. Beads were then washed with lysis buffer 3 times and bound proteins were eluted by incubation for 10 min at 55°C with Laemmli sample buffer. Aliquots of biotinylated proteins and total cell lysates were separated on 7.5% SDS-PAGE gels and transferred to PVDF membranes. Membranes were blocked in 8% nonfat dry milk in wash buffer for 1 h, and then incubated overnight with either anti-CHT antibody (1:1000) or anti-APP c-terminal antibody (1:1000) in wash buffer with 8% non-fat milk. After washing, membranes were incubated for 1 h with peroxidase-conjugated goat anti-rabbit IgG secondary antibody (1:10,000) in wash buffer containing 8% milk, and washed again. Immunoreactive proteins were detected by chemiluminescence using a Chemidoc Imaging System (BioRad). Immunopositive bands (at ~50-kDa for CHT protein and at ~100-kDa for APP) were quantified by

densitometry. Bands for cell surface CHT were compared to vector-transfected control cells in each experiment, which represented the basal cell surface CHT levels.

4.2.7 [³H]Choline uptake assay

Choline uptake activity was evaluated in SY5Y-CHT cells transiently transfected with 1, 2 or 4 µg APP_{wt} plasmid DNA or 1, 2 or 4 µg of APP_{Swe} plasmid DNA. Control cells were transfected with 4 µg pcDNA3.1 DNA. Monolayers of cells were rinsed with warm KRH, then incubated in KRH at 37°C for 15 min. Medium was then aspirated from cells and choline uptake initiated by addition of KRH buffer containing 0.5 µM [³H]choline (0.5 Ci/mmol) either with or without 1 µM HC-3. Uptake was stopped after 5 min by placing cells on ice and washing with ice-cold KRH buffer. Cells were solubilized in 0.1 M NaOH, then aliquots taken for tritium quantification by liquid scintillation counting and protein measurement.

4.2.8 Confocal imaging

Digital images of fixed cells were acquired with a Zeiss LSM510-Meta laser-scanning confocal microscope using a 63x magnification oil-immersion objective and magnified 3 times. SY5Y-CHT cells plated on 35 mm confocal dishes were transfected with either wild-type HA-tagged APP 750-YFP or HA-tagged APP 750-YFP containing the Swedish mutation. Cells were allowed to express for 24 h. Cells were then washed twice in warm HBSS and formaldehyde-fixed. Fixed cells were incubated first with anti-CHT (1:1000) or anti-EEA1 (1:100) primary antibodies, then incubated with secondary antibodies rabbit AlexaFluor 647 (1:1000), to label CHT, and mouse AlexaFluor 555 (1:1000), to label EEA1. Images were then acquired using 488 nm excitation and 505-530 nm emission wavelengths for APP; 543 nm excitation and 560-615 nm emission for EEA1; and 647 nm excitation and 650 nm emission using a long pass filter for CHT. Colocalization analysis was performed on confocal images using Imaris software version 7.7.0 with the Imaris Colocalization module (bit-plane) to examine the colocalization of the brightest 2% of pixels in each channel, as described previously (16). Graphing and statistical

analysis of the data were performed with GraphPad Prism using one-way ANOVA with Tukey's *post-hoc* test.

4.2.9 A β ₁₋₄₂ ELISA assay

SY5Y-CHT cells plated on 100 mm dishes were transiently-transfected with either 6 μ g APP_{wt} or 9 μ g APP_{Swe} plasmid DNA using Lipofectamine 2000 and allowed to express for 24 h. As controls,, cells were transfected with 9 μ g vector DNA. The human A β ₁₋₄₂ released by cells was measured in culture media at 24 h following transfection using the human A β ₁₋₄₂ ELISA kit (Invitrogen), according to the manufacturer's protocols.

4.2.10 Data analysis

Data are presented as the mean \pm SEM with n values representing the number of independent experiments performed on separate populations of cells; each n value was obtained from the average of multiple sample replicates in each experiment. Replicate experiments were performed on cells cultured in successive passages as much as possible to minimize inter-experiment variability, and intra-experiment variability between replicate samples was minimal. GraphPad Prism 5 was used for data analysis. Statistical significance was determined by unpaired Student's *t*-test, or between groups using repeated measures one-way ANOVA with Tukey's *post-hoc* multiple comparison test, as appropriate.

4.3 Results

4.3.1 CHT interacts more with APP_{wt} than with APP_{Swe} in a neural cell line

My initial experiments were designed to confirm the interaction between CHT and APP_{wt} in a neural cell line, and to determine if CHT interacts with APP_{Swe} and how this compares to its interaction with APP_{wt}. I used SY5Y-CHT cells stably-expressing FLAG-tagged CHT protein as a model, with SH-SY5Y cells stably-expressing the empty vector DNA without CHT serving as a negative control. Cells were transiently transfected with

either empty vector or APP_{wt} or APP_{Swe} plasmid DNA and allowed to express for 24 h, then either FLAG-CHT or APP and interacting proteins were recovered from cell lysates using anti-FLAG affinity resin or anti-APP antibody and Protein-G Sepharose, respectively. Figures 4-1A and B show representative immunoblots that were probed for CHT protein using anti-CHT antibody or APP using anti-APP c-terminal antibody. Importantly, the anti-APP immunoblot for APP proteins interacting with FLAG-CHT shown in Figure 4-1A (top panel) reveals strong APP_{wt}-positive protein bands (at ~100-kDa) in SY5Y-CHT cells transfected to express APP_{wt}, but only weak APP_{Swe}-positive protein bands (at ~100-kDa) in SY5Y-CHT cells transfected to express APP_{Swe}. No interacting APP-positive bands were present in co-IPs of lysates from SH-SY5Y cells not expressing FLAG-CHT (vector), suggesting that the interaction is specific to CHT. These data were verified in a reverse protocol using anti-APP antibody to recover APP and interacting proteins. Thus, Figure 4-1B (top panel) shows the anti-CHT immunoblot for CHT proteins interacting with APP revealing strong CHT-positive protein bands (at ~50 kDa) from lysates of SY5Y-CHT cells transfected to express APP_{wt}, but only faint CHT-positive protein bands (at ~50 kDa) from lysates of SY5Y-CHT cells transfected to express APP_{Swe}. Again, no interacting CHT-positive bands were present from lysates of SH-SY5Y cells not expressing FLAG-CHT (vector).

Quantification of the interacting APP and CHT protein bands (Figures 4-1A and B, top panels) by densitometry reveals 3-fold less APP_{Swe}-positive protein interacting with FLAG-CHT in SY5Y-CHT cells expressing APP_{Swe}, when compared to APP_{wt}-positive protein interacting with FLAG-CHT in SY5Y-CHT cells expressing APP_{wt} (Figure 4-1C) ($p \leq 0.05$). The APP-positive protein bands were normalised to the amount of FLAG-CHT recovered on the anti-FLAG affinity resin. In agreement with these findings, significantly less CHT-positive protein was found interacting with APP in SY5Y-CHT cells expressing APP_{Swe}, when compared to CHT-positive proteins interacting with APP in SY5Y-CHT cells expressing APP_{wt} (Figure 4-1D) ($p \leq 0.05$). The CHT-positive protein bands were normalised to the amount of APP recovered on Protein-G Sepharose.

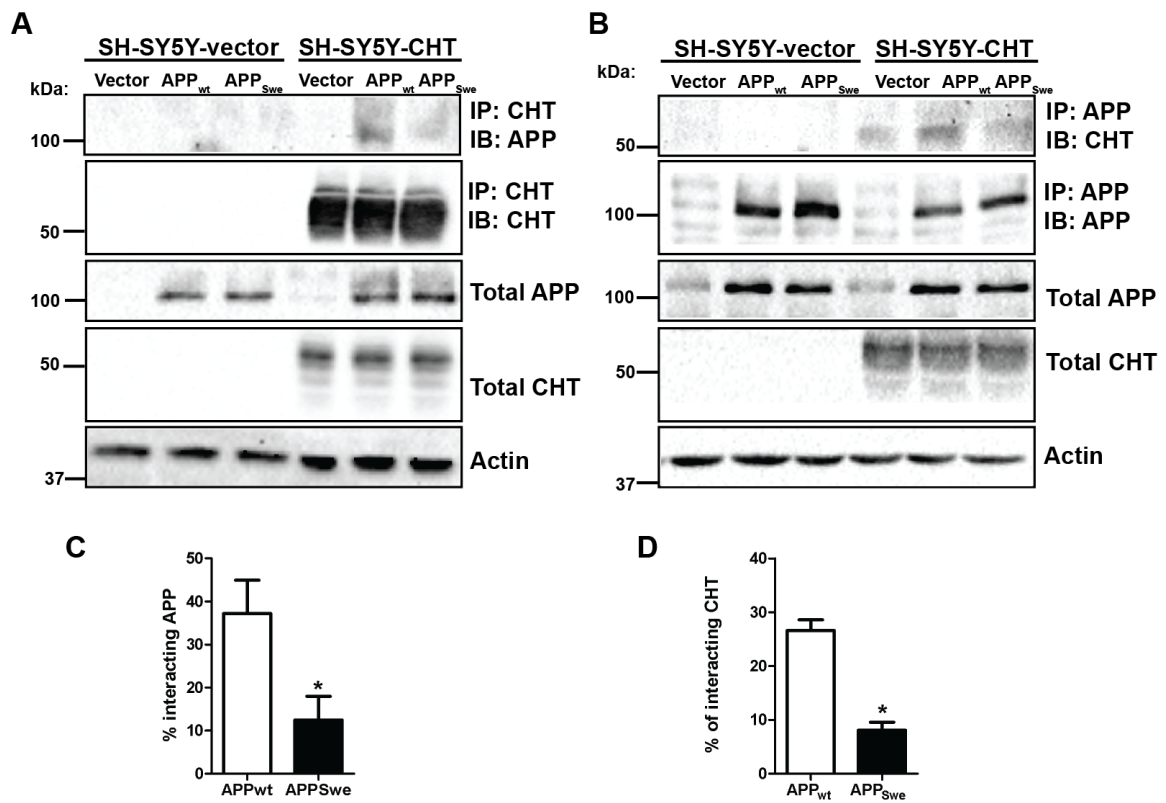


Figure 4-1

Figure 4-1 CHT interacts to a greater extent with APP_{wt} than with APP_{Swe} in SY5Y-CHT cells and cultured cortical neurons.

A, FLAG-tagged CHT was isolated from SY5Y-CHT or SH-SY5Y cells stably expressing empty vector that had been transiently transfected with either the APP_{wt} or APP_{Swe} plasmids using anti-FLAG M2 affinity resin. Proteins were solubilized, separated by SDS-PAGE and transferred to PVDF membranes. Membranes were probed with anti-APP c-terminal and anti-CHT antibodies (top 2 panels). Representative immunoblots show total APP, FLAG-CHT and actin proteins in total cell lysates (bottom 3 panels). Lysates prepared from SH-SY5Y cells not expressing CHT protein (vector) were used as a negative control (left 3 lanes). The immunoblots shown are representative of data obtained from 5 independent experiments. **B**, APP was isolated from SY5Y-CHT or SH-SY5Y cells stably expressing empty vector that had been transiently transfected with either the APP_{wt} or APP_{Swe} plasmids using Protein-G Sepharose. Representative immunoblots show total APP, FLAG-CHT and actin proteins in total cell lysates (bottom 3 panels). The top two panels illustrate APP proteins recovered on protein G Sepharose probed with anti-CHT antibody and anti-APP antibody. The immunoblots shown are representative of data obtained from 3 independent experiments. **C**, Analysis of the interacting APP immunobands in **A** by densitometry revealed that significantly less APP_{Swe} interacts with CHT than does APP_{wt} (* $p \leq 0.05$). Data were analysed by unpaired Student's *t*-test and are expressed as the mean \pm SEM of 5 independent experiments. **D**, Analysis of the interacting CHT immunobands in this Figure **B** by densitometry revealed that significantly less CHT interacts with APP_{Swe} than does APP_{wt} (* $p \leq 0.05$). Data were analysed by unpaired Student's *t*-test and are expressed as the mean \pm SEM of 3 independent experiments.

4.3.2 *In-situ* proximity ligation assay (PLA) detection of the interaction of CHT with APP_{wt} and APP_{Swe}

The FLAG pull-down assay and co-immunoprecipitation experiments shown in Figure 4-1 allowed me to observe stable protein interactions between either CHT and APP_{wt} or CHT and APP_{Swe}, but they do not reveal more transient interactions or the distribution of the interacting proteins within individual cells. To address this, and to confirm my findings above, I used *in situ* PLA to examine protein-protein proximity between either CHT and APP_{wt} or CHT and APP_{Swe} in formalin-fixed SY5Y-CHT cells.

Figure 4-2A shows representative confocal images of SY5Y-CHT cells transiently expressing either APP_{wt} (top panel) or APP_{Swe} (lower panel). The interacting protein complexes are visualized as bright fluorescent red spots and the cell nuclei are visualized in blue. The numbers of discrete spots per cell were quantified and enumerated using Imaris Software version 7.7.0, and are shown in white in Figure 4-2A, far right panels. Interestingly, as shown in Figure 4-2A, I found that interacting CHT and APP_{wt} protein complexes appear to be distributed throughout both the cell body and neuritic projections, whereas CHT and APP_{Swe} appear to interact primarily within the cell body. Furthermore, and consistent with the results of my anti-FLAG affinity pull-down assay and co-immunoprecipitation experiments, quantification of the number of spots per cell revealed a significantly lower number of interacting CHT and APP_{Swe} protein complexes in cells expressing APP_{Swe} (69 ± 5 puncta per cell) compared to interacting CHT and APP_{wt} protein complexes in cells expressing APP_{wt} (108 ± 8 puncta per cell) ($p \leq 0.05$) (Figure 2B). In some images, a small number of interacting endogenous APP and CHT punctate spots were present in surrounding untransfected cells and these were subtracted from the final number of spots counted per image. No bright fluorescent red spots were found to be present in negative control cells where primary antibodies were omitted, and cells labeled with secondary probes alone (data not shown). To confirm that this observation was not related to differences in primary antibody immunostaining due to differences in APP or CHT protein expression, SY5Y-CHT cells transiently-expressing

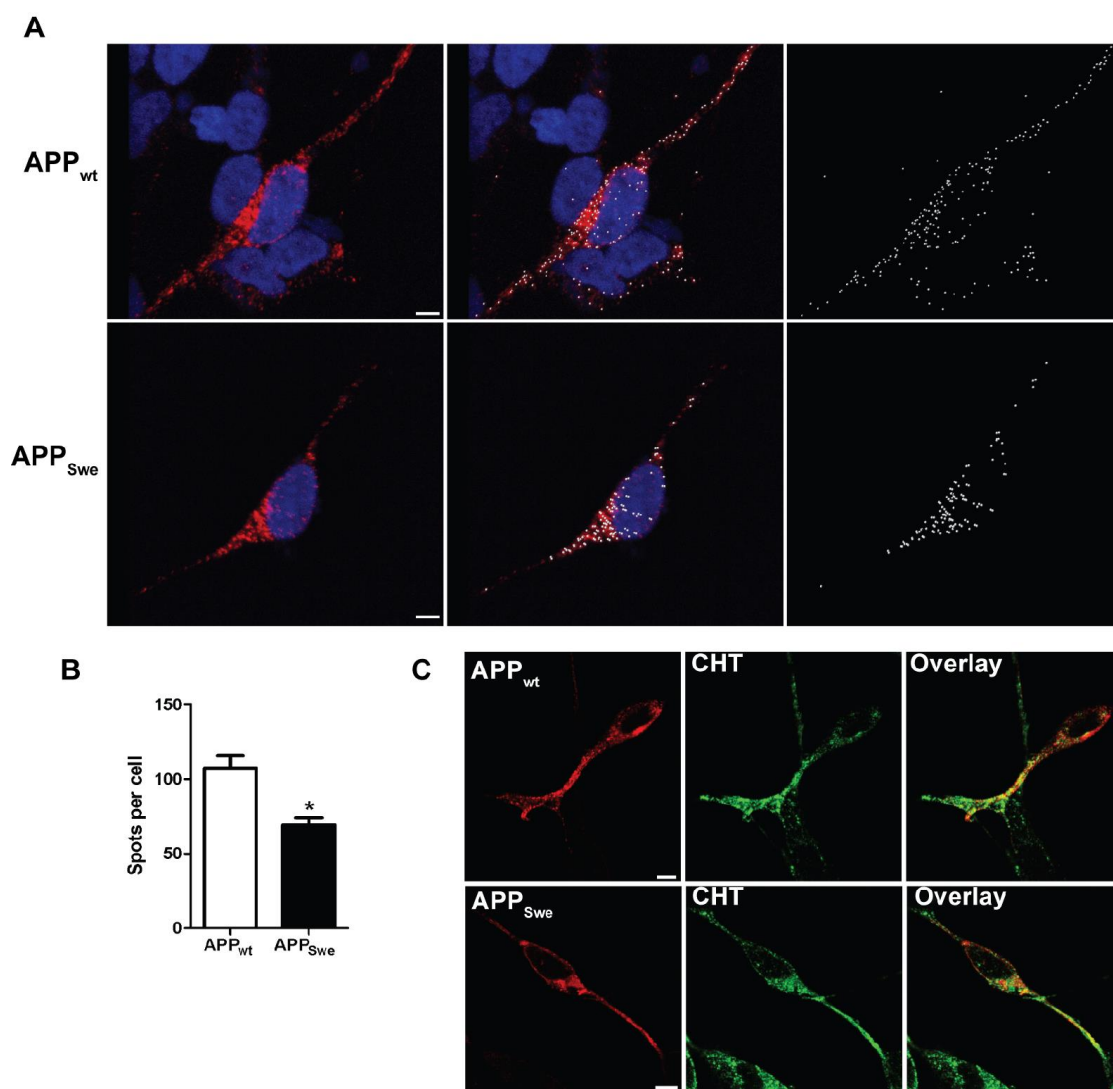


Figure 4-2

Figure 4-2 *In-situ* proximity ligation assay demonstrating the greater interaction of CHT with APP_{wt} than with APP_{Swe}.

A, Confocal microscopy was used to image the interaction of APP_{wt} (top panel) or APP_{Swe} (lower panel) with CHT proteins. SH-SY5Y cells stably expressing CHT were transiently transfected with either APP_{wt} or APP_{Swe}, then labeled with primary antibodies directed against CHT (rabbit anti-CHT) or APP (mouse anti-APP 6E10). The binding of the probes (oligonucleotide-linked secondary antibodies) to CHT and APP proteins in close proximity (~30-40 nm) allowed the hybridization of the DNA strands and ligation into a circular DNA molecule. This DNA circle was then amplified using rolling circle amplification and detected by the hybridization of fluorescently-labeled oligonucleotides. The signal was imaged using confocal microscopy and Imaris Software was used to quantify the number of interacting proteins shown as white spots (far right panels). The interacting protein complexes are visualized as bright fluorescent red spots and the cell nuclei are visualized in blue. Confocal images are representative of 3 independent experiments. **B**, This histogram reports the quantification of the interacting protein complexes (white spots) per cell. Significantly fewer white spots per cell were present in cells expressing APP_{Swe} than in cells expressing APP_{wt}. Data are expressed as the mean \pm SEM for a minimum of 25 cells per transfection group from 3 independent experiments, and were analysed using a repeated-measures one-way ANOVA with Tukey's post hoc multiple comparisons test ($*p \leq 0.05$). **C**, Confocal images show the distribution of AlexaFluor 555-labeled APP (red) and AlexaFluor 488-labeled CHT (green) in SY5Y-CHT cells transiently transfected with either APP_{wt} (top panel) or APP_{Swe} (bottom panel). The colocalization of CHT and APP can be seen as yellow in the Overlay panels.

either APP_{wt} or APP_{Swe} were formalin-fixed and labeled with primary antibodies recognizing either APP or CHT following the PLA experimental protocol, and then incubated with AlexaFluor-labeled secondary antibodies. Representative confocal images of SY5Y-CHT cells show similar immunostaining for APP (red) and CHT (green) between cells expressing either APP_{wt} or APP_{Swe} (Figure 4-2C).

4.3.3 BACE1 inhibition does not alter the preferential interaction between CHT and APP_{wt} versus to APP_{Swe}

The Swedish mutation dramatically accelerates the β -cleavage of APP by BACE1 and thus increases the generation of A β (17, 18). To determine if my observation that CHT interacts less with APP_{Swe} than it does with APP_{wt} is related to differences in the β -cleavage rate of APP_{wt} and APP_{Swe}, I evaluated the interaction of either CHT with APP_{wt}, or CHT with APP_{Swe} in the presence or absence of BACE1 inhibitor IV.

To test this, I used SY5Y-CHT cells stably expressing FLAG-tagged CHT protein. Cells were transiently transfected with either empty vector or APP_{wt} or APP_{Swe} plasmid DNA. Immediately following transfection, cells were treated with vehicle or BACE1 inhibitor IV and allowed to express for 24 h. FLAG-CHT and interacting proteins were recovered from cell lysates using anti-FLAG affinity resin. Figure 4-3A shows a representative immunoblot that was probed for CHT using anti-CHT antibody or for interacting APP proteins using anti-APP C-terminal antibody. These experiments showed that BACE1 inhibition did not alter the relative difference between the interaction of CHT with APP_{wt} compared to that with APP_{Swe}. Thus, quantification of the intensity of the interacting APP protein bands (Figure 4-3A, top panel) by densitometry reveals a greater level of interaction of APP_{wt} with FLAG-CHT when compared to that of APP_{Swe} with FLAG-CHT in SY5Y-CHT cells, regardless of whether the cells were treated with vehicle or BACE1 inhibitor IV (Figure 4-3B). The APP protein bands were normalised to the amount of FLAG-CHT recovered on the anti-FLAG affinity resin. Inhibition of BACE1 activity was confirmed by the observation that the steady-state levels of both total and interacting full-length APP protein were greater, and the level of the β CTF was lower in cells treated with BACE1 inhibitor IV compared to vehicle-treated control cells (Figure

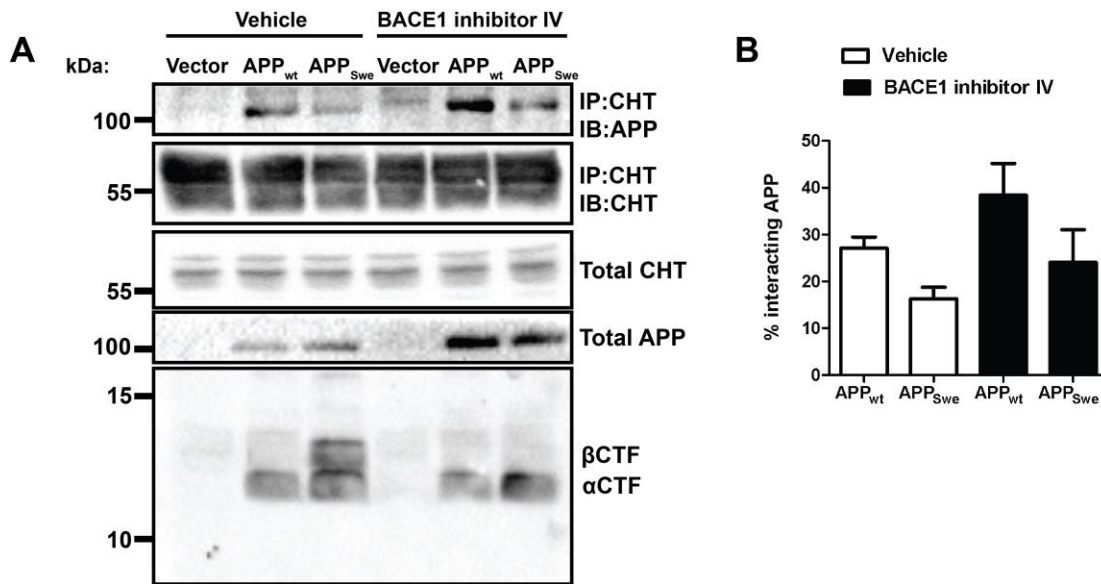


Figure 4-3 The proportion of CHT protein interacting with APP_{wt} versus CHT interacting with APP_{Swe} is the same in cells treated with vehicle or BACE1 inhibitor IV.

A, FLAG-tagged CHT was isolated from SY5Y-CHT or SY5Y cells stably expressing empty vector that had been transiently transfected with either the APP_{wt} or APP_{Swe} plasmids. Cells that were treated with vehicle (DMSO) were used as a negative control (left 3 lanes) for comparison with cells that were treated for 24 h with 25 μ M BACE inhibitor IV (right 3 lanes). Representative immunoblots show total full-length APP, FLAG-CHT and c-terminal APP protein fragments in total cell lysates (bottom 3 panels). The top two panels illustrate FLAG-CHT proteins recovered on anti-FLAG affinity resin probed with anti-APP antibody and anti-CHT antibody. The immunoblots shown are representative of data obtained from 6 independent experiments. **B**, Analysis of the interacting APP immunobands (top panel) by densitometry revealed that less APP_{Swe} interacts with CHT than does APP_{wt}, regardless of whether cells were treated with vehicle or BACE1 inhibitor IV. Data are expressed as the mean \pm SEM of 6 independent experiments, and were analysed using a repeated-measures one-way ANOVA with Tukey's post hoc multiple comparisons test ($*p \leq 0.05$).

4-3A, lower panels). The expression of CHT was comparable in cells treated with either vehicle or BACE1 inhibitor IV.

4.3.4 CHT cell surface levels and choline uptake activity are decreased by expression of APP_{wt} or APP_{Swe}

To compare the effect of the interaction of CHT with either APP_{wt} or APP_{Swe} on CHT function in SY5Y-CHT cells, I assessed high-affinity choline uptake activity and CHT cell surface levels in SY5Y-CHT cells transiently expressing either APP_{wt} or APP_{Swe} by performing ³[H]choline uptake assay and cell surface protein biotinylation experiments, respectively. In the biotinylation experiments, SY5Y-CHT cells were transiently transfected with either vector or the APP_{wt} or APP_{Swe} plasmid and allowed to express for 24 h. Plasma membrane proteins were then biotinylated using membrane impermeable sulfo-NHS-biotin at 4°C to ensure that labeled CHT proteins did not undergo endocytosis. Representative immunoblots in Figure 4-4A show the levels of cell surface (biotinylated) CHT protein and APP protein, and the amount of total CHT and APP protein. Total CHT protein levels are equal between cells expressing either vector, or APP_{wt} or APP_{Swe}, and total APP levels are equal between cells expressing APP_{wt} or APP_{Swe}, and greater than cells expressing vector. Analysis of cell surface (biotinylated) CHT and APP protein immunoblots reveals that CHT cell surface levels were significantly reduced by approximately 30% in SY5Y-CHT cells expressing either APP_{wt} or APP_{Swe} when compared to vector-expressing control cells (Figure 4-4B) ($p \leq 0.05$). Moreover, the APP_{Swe} protein cell surface levels are approximately 50% lower in SY5Y-CHT cells expressing APP_{Swe} when compared to the APP_{wt} protein cell surface levels in cells expressing APP_{wt} (Figure 4-4C) ($p \leq 0.05$).

CHT proteins are active at the cell surface, where they mediate the transport of choline into cholinergic nerve terminals. Since the expression of APP_{wt} or APP_{Swe} significantly reduced the number of CHT proteins at the cell surface, I predicted that the expression of either APP_{wt} or APP_{Swe} would inhibit the high-affinity choline uptake activity of CHT. To test this prediction, we measured ³[H]-choline uptake activity in SY5Y-CHT cells expressing different amounts of either empty vector, or APP_{wt} or APP_{Swe} plasmid DNA.

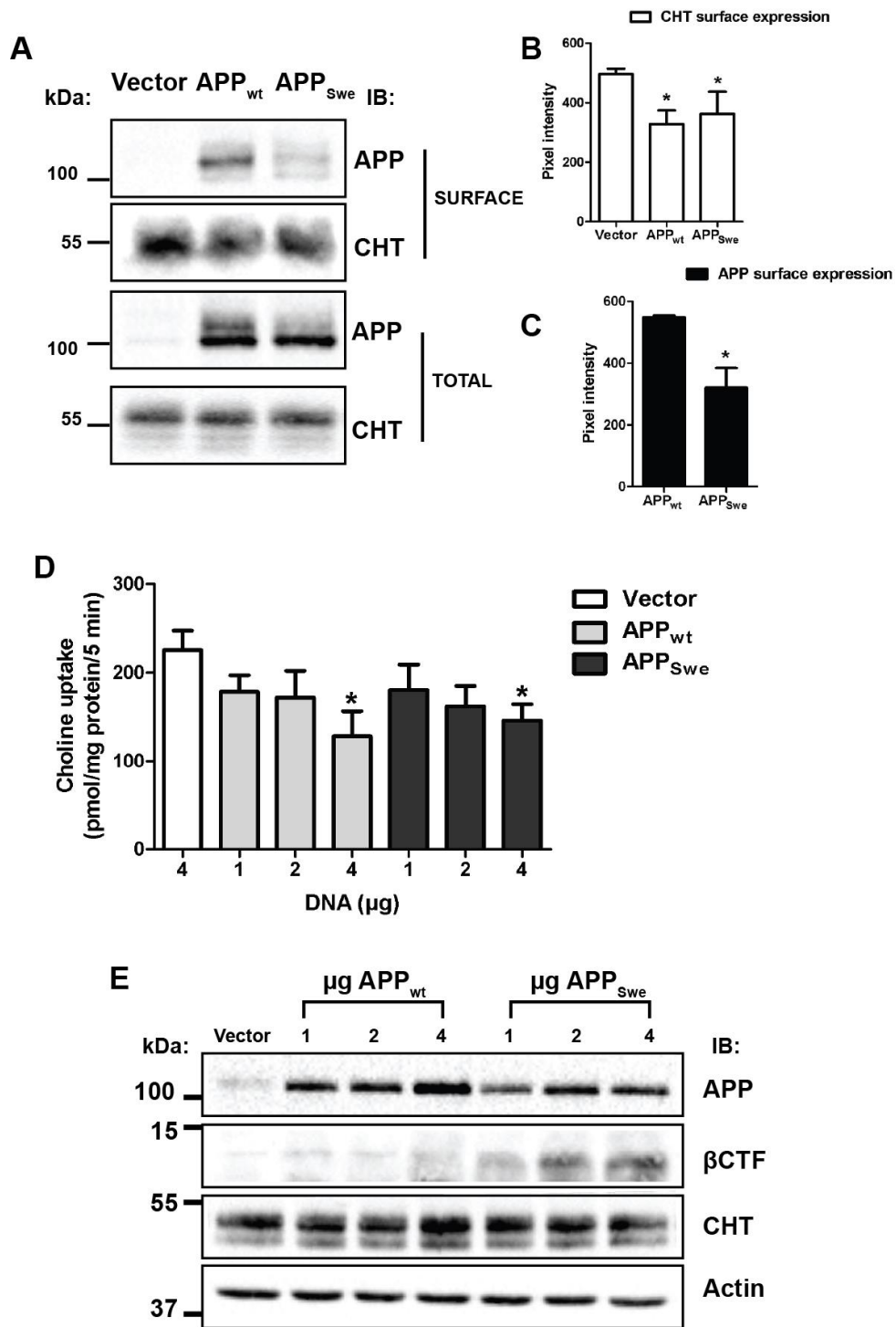


Figure 4-4

Figure 4-4 Both [³H]-choline uptake activity and CHT plasma membrane levels are reduced in SY5Y-CHT cells transfected with either APP_{wt} or APP_{Swe}.

A, Cells were washed and placed on ice, and then plasma membrane proteins were biotinylated. Biotinylated proteins were captured using NeutrAvidin agarose, then proteins were solubilized and separated by SDS-PAGE. PVDF membranes were processed by immunoblotting with antibodies recognizing APP and CHT. Representative immunoblots show steady-state APP and FLAG-CHT protein levels in total cell lysates (2 lower panels). The top two panels illustrate cell surface (biotinylated) FLAG-CHT and APP proteins. The immunoblots shown are representative of data obtained from 4 independent experiments. **B**, Analysis of cell surface CHT protein bands by densitometry reveals that the level of CHT protein at the cell surface is significantly reduced in cells expressing either APP_{wt} or APP_{Swe} when compared to vector-expressing control cells. Data are expressed as the mean \pm SEM of 5 independent experiments, and were analysed using a repeated-measures one-way ANOVA with Tukey's post hoc multiple comparisons test ($*p \leq 0.05$). **C**, Analysis of cell surface APP protein bands by densitometry reveals that the level of APP at the cell surface is significantly less in cells expressing APP_{Swe} when compared to APP_{wt}. Data were analysed using a paired Student's t-test with Tukey's and are expressed as the mean \pm SEM of 5 independent experiments ($*p \leq 0.05$). **D**, Choline uptake was assayed in SY5Y-CHT cells transfected with varying amounts of either vector, or APP_{wt} or APP_{Swe} plasmid DNA. CHT activity was significantly reduced in cells transfected with either 4 μ g of APP_{wt} or 4 μ g of APP_{Swe} plasmid DNA when compared to vector-transfected control cells. Data are expressed as the mean \pm SEM of 5 independent experiments, and were analysed using a repeated-measures one-way ANOVA with Tukey's post hoc multiple comparisons test ($*p \leq 0.05$). **E**, Representative immunoblots show steady-state total APP, β CTF and FLAG-CHT protein levels in total cell lysates from a representative choline uptake experiment.

Figure 4-4D shows that high-affinity choline uptake was significantly reduced in cells expressing higher amounts of either the APP_{wt} plasmid or the APP_{Swe} plasmid, compared to vector-expressing control cells ($p \leq 0.05$). As shown in Figure 4-4E, the steady-state levels of full-length APP_{wt} protein increased, corresponding to the increasing amount of APP_{wt} plasmid DNA transfected. In contrast, the steady-state levels of full-length APP_{Swe} protein did not show a corresponding increase related to the increasing amount of APP_{Swe} plasmid DNA transfected. Importantly, however, in the APP_{Swe} transfected cells, there was an increase in the amount of the β CTF that corresponded to the increasing amount of APP_{Swe} plasmid DNA transfected. The steady-state levels of total CHT protein were equal between all transfection groups. Thus, in cells expressing APP_{wt}, CHT activity appears to be inhibited in a manner that parallels the increase in full-length APP_{wt} protein levels, whereas in cells expressing APP_{Swe}, the inhibition of CHT activity corresponds more to the appearance and levels of β CTF than to the levels of full-length APP_{Swe} protein.

4.3.5 CHT colocalizes with EEA1-positive early endosomes to a similar extent in APP_{wt} or APP_{Swe} expressing cells

Both CHT and APP_{wt} colocalize with early endosome marker Rab5, and co-expression of CHT and APP_{wt} increases the rate at which CHT proteins undergo endocytosis (13). This could potentially account for the observation of a significant reduction of CHT proteins at the plasma membrane in cells expressing either APP_{wt} or APP_{Swe} when compared to vector-expressing control cells (Figure 4-4B). To evaluate whether the interaction of CHT with either APP_{wt}, or APP_{Swe} affects CHT colocalization with early endosomes, I used confocal microscopy to evaluate the subcellular distributions of CHT in conjunction with the early endosome marker EEA1 and either APP_{wt}-YFP or APP_{Swe}-YFP in SY5Y-CHT cells. Images illustrating the distribution of CHT and EEA1 are provided for SY5Y-CHT cells transiently expressing either APP_{wt}-YFP or APP_{Swe}-YFP in Figures 4-5A and 4-5B, respectively. To assess the extent of colocalization between either APP_{wt}-YFP or APP_{Swe}-YFP, and CHT and EEA1, I used a quantitative approach where a threshold fluorescence intensity is set that filters the brightest 2% of pixels of CHT (blue channel)

that also fall within the brightest 2% of pixels of either APP_{wt}-YFP or APP_{Swe}-YFP (green channel) or EEA1 (red channel). In separate analyses, I also evaluated the brightest 2% pixels of either APP_{wt}-YFP or APP_{Swe}-YFP that fall within the brightest 2% of pixels of EEA1, and the brightest 2% of pixels of EEA1 with the colocalized pixels of either APP_{wt}-YFP and CHT or APP_{Swe}-YFP and CHT. The colocalized pixels are identified in a separate colocalization channel and shown as white in the lower overlay panels of Figures 4-5A and 4-5B.

As documented in Figure 4-5C, analysis of the quantified pixels revealed that $45 \pm 1.6\%$ of CHT colocalized with APP_{wt}-YFP and $40 \pm 1.6\%$ of CHT colocalized with APP_{wt}-YFP. The percentage colocalization of APP_{wt}-YFP with EEA1 was significantly greater than the percentage colocalization of APP_{Swe}-YFP with EEA1 ($48 \pm 2.1\%$ and $36 \pm 1.8\%$ colocalization, respectively), which is consistent with the model that rapid cleavage of APP_{Swe}-YFP within the secretory pathway results in a smaller population available at the cell surface for endocytosis to early endosomes. Also in these experiments, the percentage of colocalized pixels of APP_{wt}-YFP and CHT with EEA1 was significantly greater than the percentage colocalization of APP_{Swe}-YFP and CHT with EEA1 ($60 \pm 1.9\%$ and $48 \pm 2.1\%$ colocalization, respectively) (Figure 4-5C) ($p \leq 0.05$). Finally, I determined the effect of transiently expressing either APP_{wt}-YFP or APP_{Swe}-YFP in SY5Y-CHT cells on the localization of CHT to early endosomes. To accomplish this, I compared the colocalization of CHT with EEA1 in cells transiently-expressing either APP_{wt}-YFP or APP_{Swe}-YFP to cells that were untransfected in the same culture dish. Importantly, there were no statistically significant differences in the percentage of colocalization of CHT with EEA1 found in cells expressing either APP_{wt}-YFP or APP_{Swe}-YFP ($34 \pm 1.3\%$ and $33 \pm 1.2\%$ colocalization, respectively). However, both of these values were significantly greater than the percentage colocalization found for CHT with EEA1 in untransfected cells in culture plates that were transfected with either APP_{wt}-YFP or APP_{Swe}-YFP ($24 \pm 1.7\%$ and $24 \pm 1.3\%$ colocalization, respectively) ($p \leq 0.05$) (Figure 4-5D).

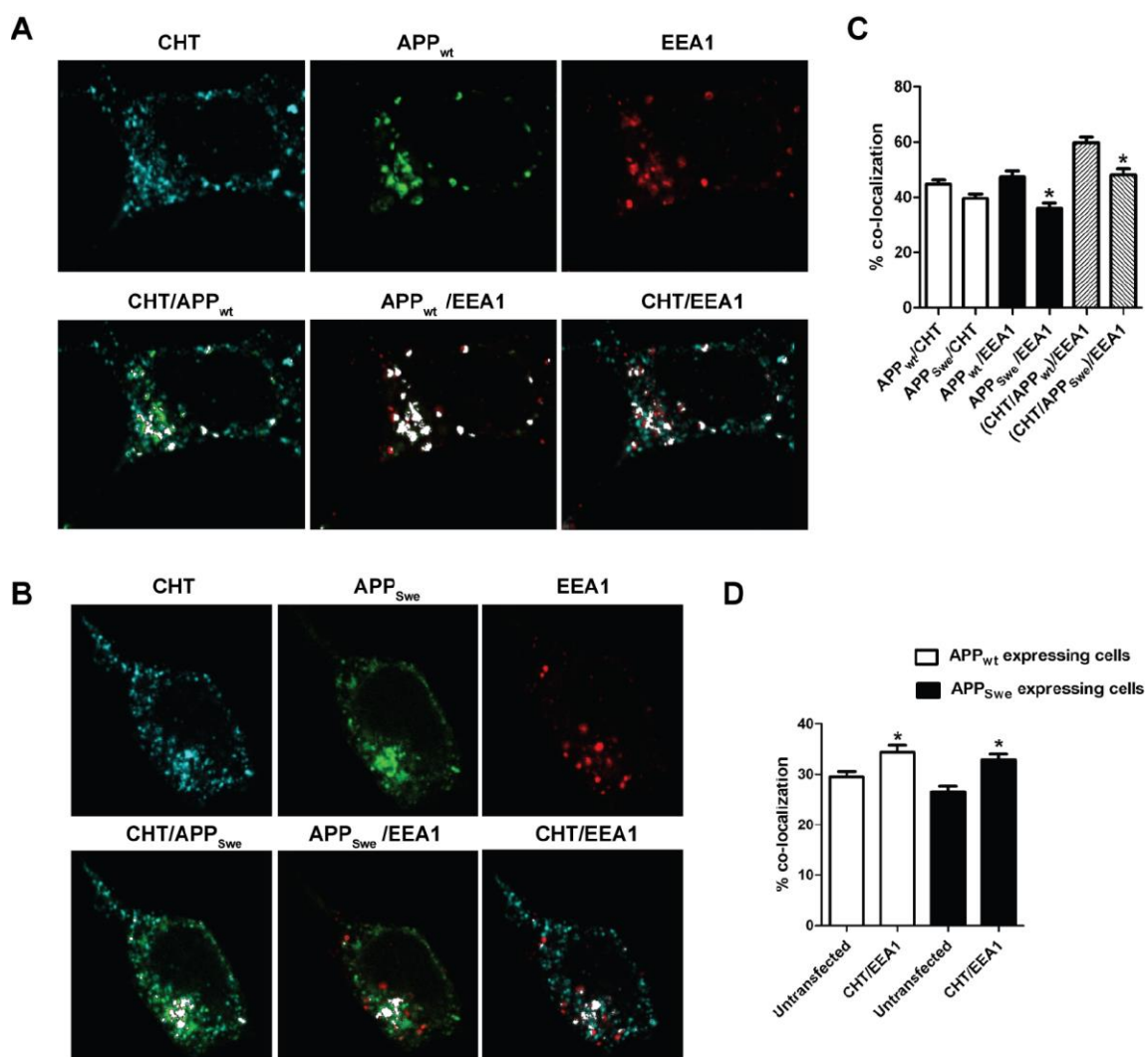


Figure 4-5

Figure 4-5 Colocalization of CHT with EEA1 is increased in SY5Y-CHT cells expressing either APP_{wt} or APP_{Swe}.

Panel A, Confocal images show the distribution of AlexaFluor 647-labeled CHT (blue), AlexaFluor 555-labeled EEA1 (red) and APP_{wt}-YFP (green). Colocalized pixels were identified in the colocalization channel and are shown as white in the lower overlay panels. Scale bar, 5 μ M. **Panel B**. Confocal images show the distribution of AlexaFluor 647-labeled CHT (blue), AlexaFluor 555-labeled EEA1 (red) and APP_{Swe}-YFP (green). Colocalized pixels were identified in the colocalization channel and are shown as white in the lower overlay panels. Scale bar, 5 μ M. **C**, CHT and APP_{wt}-YFP, CHT and APP_{Swe}-YFP, APP_{wt}-YFP and EEA1, and APP_{Swe}-YFP and EEA1 pixels that were determined to be colocalized in the colocalization channel were quantified using Imaris software. Data are expressed as the mean \pm SEM for a minimum of 25 cells per transfection group from 4 independent experiments, and were analysed by one-way ANOVA followed by Tukey's post-test ($*p \leq 0.05$). **D**, CHT and EEA1 pixels that were determined to be colocalized in cells expressing either APP_{wt}-YFP or APP_{Swe}-YFP or in untransfected control cells were quantified using Imaris software. Data are expressed as the mean \pm SEM for a minimum of 25 cells per transfection group from 4 independent experiments, and were analysed by one-way ANOVA followed by Tukey's post-test and ($*p \leq 0.05$).

4.3.6 BACE1 inhibition reduces A β generation and increases CHT protein cell surface levels in SY5Y-CHT cells expressing APP_{Swe}

A critical finding in the present study indicates that CHT proteins interact significantly less with APP_{Swe} than with APP_{wt}. Importantly, however, the expression of either APP_{wt} or APP_{Swe} in SY5Y-CHT cells increases CHT colocalization to early endosomes to a similar extent, and significantly decreases both CHT cell surface levels and CHT activity. Since APP_{Swe} interacts much less with CHT than does APP_{wt}, I next investigated the mechanism by which APP_{Swe} mediates changes to CHT function. Our findings above show that CHT activity is inhibited in a manner that is dependent on the level of full-length APP_{wt} protein, whereas in cells expressing APP_{Swe}, inhibition of CHT activity corresponds more to the processing of APP as shown by the increased production of the β CTF. Thus, I hypothesized that decreases in the activity and cell surface levels of CHT in SY5Y-CHT cells expressing APP_{Swe} are related to the increased generation of β CTF or A β in these cells as a result of enhanced BACE1 processing of APP_{Swe} compared to APP_{wt}.

To test this hypothesis, I measured CHT protein cell surface levels in SY5Y-CHT cells that transiently transfected to express either vector, APP_{wt} or APP_{Swe} and treated with either vehicle or BACE1 inhibitor IV for 24 h. Plasma membrane proteins were then biotinylated using membrane impermeable sulfo-NHS-biotin at 4°C. Representative immunoblots in Figure 4-6A show the levels of cell surface (biotinylated) CHT and APP proteins (top two panels), and the steady-state amount of total CHT, full-length APP, α CTF and β CTF proteins (bottom three panels). Similar to findings above (Figure 4-4A,B), analysis of the cell surface (biotinylated) CHT and APP protein immunoblots reveals that in vehicle-treated cells, CHT cell surface levels are reduced by approximately 30% in SY5Y-CHT cells expressing either APP_{wt} or APP_{Swe} when compared to vector-expressing control cells (Figure 4-6A top panel, 4-6B white bars). Moreover, the cell surface levels of APP_{Swe} are approximately 50% lower when compared to that of APP_{wt} (Figure 4-6A second panel, 4-6C white bars). I next compared the effects of vehicle or

BACE1 inhibitor IV treatment on CHT cell surface levels in groups of cells expressing either vector, APP_{wt} or APP_{Swe}. No significant differences in CHT cell surface expression are found between the vehicle or BACE1 inhibitor IV treated groups of cells expressing either vector or APP_{wt}. Interestingly however, CHT cell surface expression is significantly greater in APP_{Swe}-expressing cells that were treated with BACE1 inhibitor IV when compared to the APP_{Swe}-expressing cells treated with vehicle (Figure 4-6A top panel, Figure 4-6B, $p \leq 0.05$). Moreover, the APP_{Swe} protein cell surface levels are significantly higher in BACE1 inhibitor IV-treated SY5Y-CHT cells expressing APP_{Swe} compared to that observed in vehicle-treated SY5Y-CHT cells expressing APP_{Swe} (Figure 4-6A second panel, Figure 4-6C, $p \leq 0.05$). No significant differences in APP_{wt} cell surface protein expression level are observed between vehicle or BACE1 inhibitor IV-treated SY5Y-CHT cells expressing APP_{wt}. Finally, I measured the amount of A β ₁₋₄₂ secreted into the culture medium by ELISA of SY5Y-CHT cells treated with vehicle or BACE1 inhibitor IV transiently expressing either empty vector, APP_{wt} or APP_{Swe} plasmid DNA for 24 h. As predicted, culture medium collected from vehicle-treated SY5Y-CHT cells expressing APP_{Swe} contains a significantly greater amount of A β ₁₋₄₂ than that collected from vehicle-treated SY5Y-CHT cells expressing either APP_{wt} or empty vector (Figure 4-6D white bars, $p \leq 0.01$). Importantly, BACE1 inhibition significantly lowers the amount of A β ₁₋₄₂ in culture medium collected from cells expressing APP_{Swe} when compared to that collected from vehicle-treated APP_{Swe}-expressing cells ($p \leq 0.01$) (Figure 4-6D).

Also shown in Figure 4-6A (middle panel), the total CHT protein levels are equal between the vehicle and BACE1 inhibitor IV-treated cells expressing either empty vector, APP_{wt} or APP_{Swe}. As anticipated, the steady-state levels of total full-length APP protein are increased and the level of the β CTF is lower in cells treated with BACE1 inhibitor IV when compared to vehicle-treated cells (Figure 4-6A, lower panels).

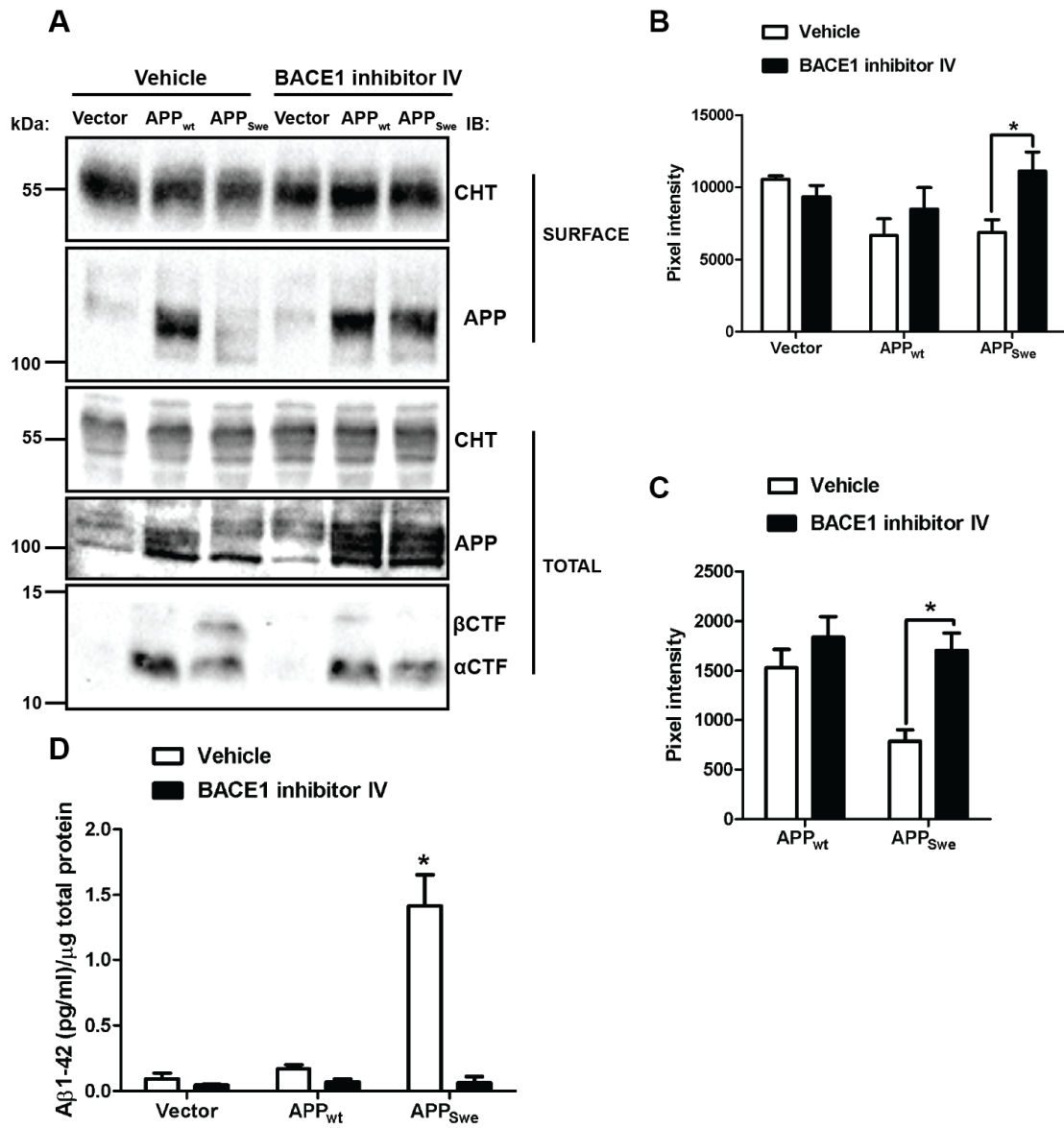


Figure 4-6

Figure 4-6 BACE1 inhibition reduces A β secretion and increases CHT cell surface levels in SY5Y-CHT cells expressing APP_{Swe}.

A, Cells were washed and placed on ice, and then plasma membrane proteins were biotinylated. Biotinylated proteins were captured using NeutrAvidin agarose, then proteins were solubilized and separated by SDS-PAGE. PVDF membranes were processed by immunoblotting with antibodies recognizing APP and CHT. This representative immunoblot shows cell surface (biotinylated) FLAG-CHT and APP proteins (top two panels). Steady-state CHT, APP and β CTF protein levels in total cell lysates are illustrated in the lower 3 panels. The immunoblots shown are representative of data obtained from 6 independent experiments. **B**, Analysis of cell surface CHT protein bands by densitometry reveals that the level of CHT protein at the cell surface is significantly increased in cells expressing APP_{Swe} when compared to vehicle-treated APP_{Swe}-expressing control cells. Data are expressed as the mean \pm SEM of 5 independent experiments, and were analysed using a repeated-measures one-way ANOVA with Tukey's post hoc multiple comparisons test ($*p \leq 0.05$). **C**, Analysis of cell surface APP protein bands by densitometry reveals that the level of APP_{Swe} at the cell surface is significantly greater than that found in vehicle-treated APP_{Swe} expressing control cells. Data were analysed using a two-way ANOVA with Bonferonni's post-test and are expressed as the mean \pm SEM of 5 independent experiments ($*p \leq 0.05$). **D**, Conditioned medium was collected from these cell groups, then the A β_{1-42} levels were measured by ELISA and quantified. Vehicle-treated APP_{Swe}-expressing cells produced significantly higher levels of A β_{1-42} than did BACE1 inhibitor IV –treated APP_{Swe}-expressing cells. Data are expressed as the mean \pm SEM of 5 independent experiments, and were analysed using a repeated measures two-way ANOVA with Bonferonni's post hoc multiple comparisons test ($*p \leq 0.01$)

4.3.7 Choline uptake activity is reduced by conditioned medium from APP_{Swe}-expressing SY5Y-CHT cells

My previous experiment shows that inhibition of BACE1 activity significantly reduces the amount of A β present in the culture medium of APP_{Swe}-expressing cells, and significantly increases CHT cell surface levels in these cells when compared to that found in vehicle-treated APP_{Swe}-expressing SY5Y-CHT cells. Since A β can inhibit high-affinity choline uptake (4), I next examined whether the decrease in CHT activity in SY5Y-CHT cells expressing APP_{Swe} is related to the increased amount A β released into the culture medium of these cells. To accomplish this, I collected culture medium conditioned for 24 h by SY5Y-CHT cells transiently expressing empty vector, APP_{wt} or APP_{Swe} plasmid DNA. Using an A β ₁₋₄₂ ELISA, I found that the amount of A β ₁₋₄₂ secreted into the medium by APP_{Swe}-expressing cells is significantly greater than that from cells expressing either APP_{wt} or empty vector ($p \leq 0.05$) (Figure 4-7A). The conditioned medium was added to SY5Y-CHT cells stably-expressing CHT but not transfected with other plasmids for 30 min, 4 h or 24 h, then [³H]choline uptake activity was measured. As shown in Figure 4-7B, cells treated with conditioned culture medium collected from APP_{Swe}-expressing SY5Y-CHT cells for 24 h have a statistically-significant (32%) decrease in choline uptake activity when compared to cells treated with conditioned culture medium collected from either vector or APP_{wt}-expressing cells. It is interesting to note that this corresponds to the 35% decrease in choline uptake activity that I observed in SY5Y-CHT cells at 24 h after transient transfection with APP_{Swe} (Figure 4-4D).

4.4 Discussion

The subcellular trafficking of CHT maintains a steady level of this solute transporter at the cell surface, thereby regulating choline uptake activity and maintaining cholinergic neurotransmission. Thus, any protein-protein interaction that regulates CHT trafficking will have a direct impact on choline uptake activity and ACh synthesis. Previous studies

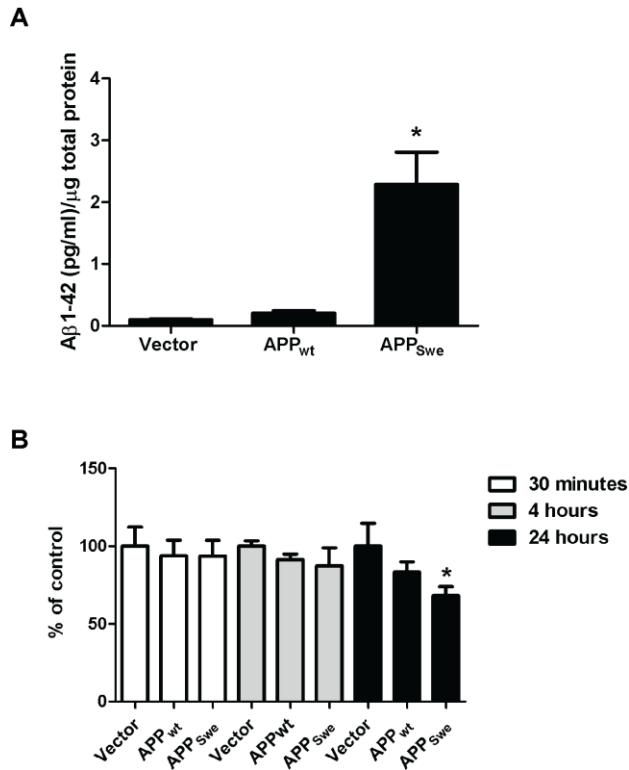


Figure 4-7 Treatment of SY5Y-CHT cells with conditioned medium containing Aβ from cells expressing APP_{Swe} inhibits choline uptake activity.

A, SY5Y-CHT cells were transfected with either vector, or APP_{wt} or APP_{Swe} plasmid DNA and allowed to express for 24 h. APP_{Swe}-expressing cells produced significantly higher levels of Aβ₁₋₄₂ than did either vector or APP_{wt}-expressing cells. Data are expressed as the mean ± SEM of 5 independent experiments, and were analysed using a repeated-measures one-way ANOVA with Tukey's post hoc multiple comparisons test (* $p \leq 0.05$). **B**, SY5Y-CHT cells were treated with conditioned medium collected from SY5Y-CHT cells transiently expressing either empty vector, or APP_{wt} or APP_{Swe}, 24 h, then added to untransfected SY5Y-CHT for either 30 min, 4 h or 24 h prior to [³H]choline uptake assays being performed. CHT activity was significantly reduced only in cells treated for 24 h with conditioned medium collected from SY5Y-CHT cells expressing APP_{Swe}. Data are expressed as the mean ± SEM of 5 independent experiments, and were analysed using a repeated-measures one-way ANOVA with Tukey's post hoc multiple comparisons test (* $p \leq 0.05$).

identified APP as a binding partner for CHT involved in regulating CHT endocytosis and subcellular localization (13). Because APP containing the Swedish mutation is cleaved within the secretory pathway (19, 20) and is trafficked differently from the cell surface through the endosomal pathway as compared to APP_{wt}, (7) the purpose of my study was to investigate further how APP regulates CHT trafficking and activity and whether this is altered by the Swedish mutation.

Through experiments that used co-immunoprecipitation and proximity ligation assays, I made the novel observation that CHT associates significantly less with APP_{Swe} than with APP_{wt} in SY5Y-CHT cells and in cultured mouse brain cortical neurons, and that this was not related to the enhanced BACE1-mediated cleavage of APP_{Swe}. Interestingly, the expression of either APP_{wt} or APP_{Swe} decreased CHT cell surface levels and choline uptake activity to the same extent. Moreover, the proportion of total cellular CHT proteins that colocalize with the early endosomal marker EEA1 was increased to a similar level in cells expressing either APP_{wt}-YFP or APP_{Swe}-YFP when compared to untransfected control cells. In these experiments, SY5Y-CHT cells expressing APP_{Swe} secreted significantly more A β ₁₋₄₂ into the culture medium than did cells expressing APP_{wt}, and lowering the production of A β by BACE1 inhibition significantly increased CHT cell surface level in cells expressing APP_{Swe}, but not in cells expressing either vector or APP_{wt}, when compared to vehicle-treated cells. Finally, I found that treating untransfected SY5Y-CHT cells with the culture medium collected from SY5Y-CHT cells transiently expressing APP_{Swe} significantly inhibited choline uptake activity.

My co-immunoprecipitation data reveal that CHT interacts significantly less with APP_{Swe} than it does with APP_{wt} in both SH-SY5Y cells and cultured cortical neurons from mouse brain. One explanation for this finding is that the subcellular trafficking pathway and processing location of APP_{Swe} (in the TGN), compared to APP_{wt} (in endosomes), substantially reduces the potential for APP_{Swe} to interact with CHT. Differences in the regulation of APP_{wt} and APP_{Swe} as a result of their subcellular processing locations have been observed. For example, the interaction of the cellular prion protein with BACE1 retains BACE1 in the TGN and therefore inhibits its activity towards APP_{wt}, but not towards APP_{Swe}, which is explained by the differential subcellular sites of action of

BACE1 on APP_{wt}, compared with APP_{Swe} (21). Therefore, it is possible that APP_{Swe} and APP_{wt} in turn can regulate other cellular proteins differently as a result of their distinct subcellular processing locations. APP_{wt} is proposed to interact with CHT and facilitate its endocytosis into Rab5-positive early endosomes (13). Retention and processing of APP_{Swe} within the TGN could result in a smaller pool of APP_{Swe} present at the cell surface and in endosomal compartments available to interact with CHT. My PLA experiments provide support for this hypothesis showing that interacting CHT and APP_{wt} protein complexes were distributed throughout both the cell body and neuritic projections, whereas CHT and APP_{Swe} appeared to interact primarily within the cell body. A second explanation for the reduced interaction of CHT with APP_{Swe} compared to APP_{wt} is that the APP and CHT association involves the amino acid residues K595 or M596 that are mutated in APP_{Swe}. While previous studies showed that the carboxyl-terminal domain of APP is sufficient to immunoprecipitate CHT (13), protein-protein interactions depend both on the protein sequence and conformation, so this possibility cannot be completely ruled out. Lastly, the differential interaction between CHT and APP_{Swe} compared to APP_{wt} appears to be unique to CHT, as the Swedish mutation does not appear to alter the ability of APP to mediate protein trafficking in a general manner. For example, APP_{wt} interacts with assembled NMDA receptors and enhances their cell surface trafficking (22, 23) and this is not altered by either the London or Swedish APP mutations (23).

Because CHT associates significantly less with APP_{Swe} than with APP_{wt}, I predicted that APP_{Swe} and APP_{wt} over-expression would have different effects on CHT function and localization. Unexpectedly, CHT cell surface levels were significantly reduced to similar extents in SY5Y-CHT cells expressing either APP_{wt} or APP_{Swe} when compared to vector-expressing control cells, and this corresponds to a significant reduction in high-affinity choline uptake in cells expressing APP_{wt} as well as in cells expressing APP_{Swe}. Consistent with the findings of Yamakawa et al. (2010), I found significantly less APP_{Swe} than APP_{wt} proteins at the cell surface, which could be explained by the greater level of processing of APP_{Swe} within the secretory pathway. Interestingly, in cells expressing APP_{wt}, there was a reciprocal relationship between CHT activity and APP_{wt} levels with

the reduction in CHT activity being greater as the APP_{wt} protein level increased. In contrast, the reduction of CHT activity in cells expressing APP_{Swe} was related more to the increased production and level of β CTF. Finally, CHT localization to early endosomes was significantly increased in cells expressing either APP_{wt}-YFP or APP_{Swe}-YFP when compared to untransfected control cells, suggesting that the internalization rate of CHT is increased similarly in cells expressing either APP_{wt} or APP_{Swe}. The increased movement of CHT from the plasma membrane to early endosomes could represent the mechanism by which CHT activity and cell surface expression was reduced in cells expressing either APP_{wt} or APP_{Swe}. My results indicate that APP_{wt} regulates CHT cell surface expression and activity through a direct interaction with the transporter. Since APP_{Swe} interacts much less with CHT than it does with APP_{wt}, but expression of either APP_{wt} or APP_{Swe} causes a similar inhibition of CHT function, I investigated the hypothesis that the decrease in CHT activity and cell surface expression in SY5Y-CHT cells expressing APP_{Swe} is related to the increased release of A β from these cells. Support for this hypothesis comes from previous observations that A β can interact directly with CHT (26) and impairs high-affinity choline uptake (11), and from my finding that SY5Y-CHT cells expressing APP_{Swe} secrete significantly more A β ₁₋₄₂ into culture media than do cells expressing APP_{wt}. Furthermore, BACE1 inhibition significantly reduced the amount of A β in culture medium of cells expressing APP_{Swe} and significantly increased CHT cell surface level in these cells, but not in cells expressing either vector or APP_{wt}, compared to vehicle-treated cells. Finally, my data show that treating untransfected SY5Y-CHT cells with the culture medium collected from SY5Y-CHT cells transiently expressing APP_{Swe} significantly inhibited choline uptake activity. Therefore, I propose that the inhibition to CHT function observed in APP_{Swe} expressing cells is due to the increased generation of A β in these cells, and not a result of the interaction between CHT and APP_{Swe} itself. In addition to APP itself, APP metabolites including A β , β CTF, sAPP β and AICD also been shown to exert physiological effects. Since BACE1 inhibition not only blocks the production of A β , but also inhibits the generation of sAPP β and β CTF, we cannot rule out the possibility that these fragments may be mediating some of the CHT impairment in APP_{Swe}-expressing SY5Y-CHT cells.

Several previous studies report cognitive impairment beginning in the early stages before A β plaque development in the Tg2576 mouse model over-expressing human APP₆₉₅ with the Swedish mutation compared to non-transgenic controls (27-29). These early studies were not able to determine that the high concentrations of A β were responsible for the memory and learning deficits, and not the over-expression of APP (30); however, this was clarified by a study showing that reduction of A β levels through genetic inactivation of *BACE1* in Tg2576 mice prevented memory deficits and hippocampal neuronal abnormalities (31). My data regarding APP_{Swe} regulation of CHT activity offer a mechanistic explanation for this observation and highlight the importance of future studies comparing mice over-expressing wild-type human APP₆₉₅ with Tg2576 mice. In conclusion, my results support the idea that APP_{wt} plays a physiological role in regulating the trafficking and activity of CHT through a direct protein-protein interaction. The Swedish mutation disrupts this interaction and appears to cause changes to CHT function through increased β -cleavage of APP_{Swe} and subsequent A β production, as opposed to an association between CHT and APP_{Swe} itself.

4.5 References

1. Sandbrick, R., Hartmann, T., Masters, C. L., and Beyreuther, K. (1996) *Mol Psychiatry* **1**, 27-40
2. Gralle, M., and Ferreira, S. T. (2007) *Prog Neurobiology* **82**, 11-32
3. Pasternak, S. H., Callahan, J. W., and Mahuran, D. M. (2004) *J. Alzheimers Dis* **6**, 53-65
4. Lammich, S., Kojro, E., Postina, R., Gilbert, S., Pfeiffer, R., Jasionowski, M., Haass, C., and Fahrenholz, F. (1999) *Proc Natl Acad U S A* **96**, 3922-3927
5. Haass, C., Lemere, C. A., Capell, A., Citron, M., Seubert, P., Schenk, D., Lannfelt, L., and Selkoe, D. J. (1995) *Nature Med* **1**, 1291-1296
6. Thinakaran, G., Teplow, D. B., Siman, R., Greenberg, B., and Sisodia, S. S. (1996) *J. Biol. Chem* **271**, 9390-9397
7. Lorenzen, A., Samosh, J., Vandewark, K., Anborgh, P. H., Seah, C., Magalhaes, A. C., Cregan, S. P., Ferguson, S. S. G., and Pasternak, S. H. (2010) *Molecular Brain* **3**, 11
8. Nitsch, R. M., Slack, B. E., Wurtman, R. J., and Growdon, J. H. (1992) *Science* **258**, 304-307
9. Pedersen, W. A., Kloczewiak, M. A., and Blusztajn, J. K. (1996) *Proc Natl Acad Sci U S A* **93**, 8068-8071
10. Melo, J. B., Agostinho, P., and Oliveira C. R. (2002) *Amyloid* **9**, 221-228
11. Kar, S., Slowikowski, S. P. M., Westaway, D., and Mount, H. T. J. (2004) *J. Psychiatry Neurosci* **29**, 427-441
12. Kristofiková, Z., Kopecký, V. Jr., Hofbauerová, K., Hovorková, P., and Rípová, D. (2008) *Neurochemical Research* **33**, 412-421

13. Wang, B., Yang, L., Wang, Z., and Zheng, H. (2007) *Proc Natl Acad Sci U S A* **104**, 14140–14145
14. Okuda, T., and Haga, T. (2000) *FEBS Lett* **484**, 92–97
15. Young-Pearse, T. L., Bai, J., Chang, R., Zheng, J. B., LoTurco, J. J., and Selkoe, D. J. (2007) *J Neurosci* **27**, 14459-14469
16. Cuddy, L.K., Gordon, A.C., Black, S.A.G., Jaworski, E., Ferguson, S.S.G., and Rylett, R.J. (2012) *J Neurosci* **32**, 5573-5584
17. Cai, X.-D., Golde, T. E., and Younkin, S. G. (1993) *Science* **259**, 514–517
18. Citron, M., Oltersdorf, T., Haass, C., McConlogue, L., Hung, A. Y., Seubert, P., Vigo-Pelfrey, C., Lieberburg, I., and Selkoe, D. J. (1992) *Nature* **360**, 672–674
19. Haass, C., Lemere, C. A., Capell, A., Citron, M., Seubert, P., Schenk, D., Lannfelt, L., and Selkoe, D. J. (1995) *Nat. Med* **1**, 1291–1296
20. Thinakaran, G., Teplow, D. B., Siman, R., Greenberg, B., and Sisodia, S. S. (1996) *J. Biol. Chem* **271**, 9390–9397
21. Griffiths, H. H., Whitehouse, I. J., Baybutts, H., Browns, D., Kellet, K. A. B., Jackson, C. D., Turner, A. J., Piccardos, P., Manson, J. C., and Hooper, N. M. (2011) *J. Biol. Chem* **286**, 33489-33500
22. Cousins, S. L., Hoey, S. A. E., Stephenson, F. A., and Perkinton, M. S. J. (2009) *J. Neurochem* **111**, 1501-1513
23. Hoe, H.-S., Fu, Z., Makarova, A., Lee, J. Y., Lu, C., Feng, L., Pajoohesh-Ganji, A., Matsuoka, Y., Hyman, B. T., Ehlers, M. D., Vicini, S., Pak, D. T. S., and Rebeck, G. W. (2009) *J. Biol. Chem* **284**, 8495-8506
24. Innocent, N., Cousins, S. L., and Stephenson, A. (2011) *Neurosci Lett* **515**, 131-136

25. Yamakawa, H., Yagishita, S., Futai, E., and Ishiura, S. (2009) *J. Biol. Chem* **285**, 1634-1642
26. Bales, K.R., Tzavara, E.T., Wu, S., Wade, M.R., Bymaster, F.P., Paul, S.M., Nomikos, G.G. (2006) *J Clin Invest* **116**, 825-832
27. Westerman, M. A., Cooper-Blacketer, D., Mariash, A., Kotilinek, L., Kawarabayashi, T., Younkin, L. H., Carlson, G. A., Younkin, S. G., and Ashe, K. H. (2002) *J. Neurosci* **22**, 1858-67
28. Apelt, J., Kumar, A., and Schliebs, R. (2002) *Brain Res.* **953**, 17-30
29. Hsiao, K., Chapman, P., Nilsen, S., Eckman, C., Harigaya, Y., Younkin, S., Yang, F., and Cole, G. (1996) *Science* **274**, 99-102
30. Ashe, K. H. (2001) *Learn. Mem.* **8**, 301-308
31. Ohno, M., Sametsky, E. A., Younkin, L. H., Oakley, H., Younkin, S. G., Citron, M., Vassar, R., and Disterhoft, J. F. (2004) *Neuron* **41**, 27-33

Chapter 5

5 Summary of major findings, discussion of results and future directions³

³ Parts of this work have been published and submitted in the following manuscripts:

Cuddy LK, Winick-Ng W, Rylett RJ. Regulation of the high-affinity choline transporter activity and trafficking by its association with cholesterol-rich lipid rafts J Neurochem 4 November 2013 128 (5):725-740

5.1 Summary of major findings

5.1.1 Summary of major findings from experiments regarding the effect of reactive oxygen species ONOO⁻ donor SIN-1 on CHT activity and subcellular trafficking (Chapter 2)

1. The mutant L531A-CHT transporter, but not wild-type CHT, is resistant to SIN-1 effects.
2. Expression of the DN proteins AP180C and dynamin-K44A expression block CHT endocytosis and attenuate CHT inhibition by SIN-1.
3. In both vehicle and SIN-1-treated cells, CHT colocalizes with Rab5-positive early endosomes, Rab7 and Rab9-positive late endosomes and Lamp1-positive lysosomes to a similar extent.
4. Inhibition of the proteasome by lactacystin and MG-132 treatment attenuate SIN-1-mediated inhibition of choline uptake.
5. SIN-1 treatment enhances CHT ubiquitination.

5.1.2 Summary of major findings from experiments regarding the effect of cholesterol and lipid raft association on CHT activity and substrate binding (Chapter 3)

1. CHT is partitioned between lipid raft and non-raft membrane compartments and tends to be concentrated in lipid rafts.
2. CHT colocalizes with flotillin and cholera toxin, and to a lesser extent with EEA1.
3. Choline uptake activity depends on membrane cholesterol levels.

4. Filipin and M β C cause a decrease in plasma membrane CHT protein levels from lipid rafts, but not non-raft areas, which is not related to an accelerated rate of CHT protein internalization.
5. CHT contains putative cholesterol binding motifs in CHT that are conserved between rodent and human.

5.1.3 Summary of major findings from experiments investigating whether CHT differentially interacts with APP_{wt} versus APP_{Swe} and how this affects CHT surface expression and activity (Chapter 4)

1. CHT interacts significantly less with APP_{Swe} than with APP_{wt} in SH-SY5Y cells stably expressing the transporter and in primary cortical neurons.
2. BACE1 inhibition increases the expression levels of both APP_{wt} and APP_{Swe}, and enhances both the interaction between CHT and APP_{wt} and between CHT and APP_{Swe}.
3. APP_{wt} or APP_{Swe} expression significantly reduced both CHT cell surface levels and choline uptake activity.
4. CHT colocalization with EEA1-positive early endosomes is increased in cells expressing either APP_{Swe}-YFP or APP_{wt}-YFP when compared to untransfected control cells.
5. BACE1 inhibition significantly increases CHT cell surface levels in cells expressing APP_{Swe} when compared to vehicle-treated control cells.

5.2 Discussion of results and future studies

A wide range of neuron models were used in the experiments described in this thesis to investigate and validate the mechanisms by which CHT protein function is regulated. The majority of the studies carried out in this thesis were performed in monolayers of intact SH-SY5Y human neuroblastoma cells that stably-express FLAG-tagged rat CHT proteins as an experimental model. These cells were differentiated with all-*trans* retinoic acid to cause neurite outgrowth and enhance the cholinergic and neuronal phenotype of the cells. In several confocal imaging experiments, the FLAG-tagged amino terminus of CHT was labeled using Zenon Alexafluor-conjugated FLAG antibodies, which allowed us to track the internalization of CHT from the plasma membrane. Since cell type-dependent differences in the regulation of CHT trafficking have been observed (1), some studies performed in this thesis were repeated using different experimental models. In the investigations described in Chapter 4, transiently transfected cortical neurons cultured from embryonic mouse brain were used as an experimental model to verify the results from co-immunoprecipitation experiments carried out in the SH-SY5Y neuronal cell line. In the studies performed in Chapter 3, mouse brain synaptosomes were utilized as an experimental model to confirm the plasma membrane distribution of CHT between raft and non-raft membrane. While these models more closely replicate the endogenous environment of CHT proteins, mouse cortical neuron cultures have a low percentage of cholinergic neurons and a low transfection efficiency, which prevented the examination of either the trafficking or activity of the endogenous or transiently transfected CHT proteins. Synaptosomes are re-sealed synaptic nerve terminals that are created during the homogenization of brain tissue and isolated by centrifugation. These likely contain a higher density of CHT proteins than do cultures of primary cortical neurons since CHT proteins are found to be concentrated within axon terminals and neuronal processes (2-7). However, a potential caveat with the use of synaptosomes is that the synaptosomal membranes may not reseal properly during their isolation. Consequently, they may not be an ideal model for some experiments performed in the studies outlined in this thesis, and in this case cultured cells with intact plasma membranes were used in assays to measure the levels and internalization of cell surface proteins by biotinylation.

The experiments in Chapter 2 were designed to characterize the effect of the ONOO⁻ donor SIN-1 on CHT activity and trafficking. The first observation that CHT is sensitive to ONOO⁻ was made by Guermonprez et al. (2001). These authors found that CHT activity was inhibited by ONOO⁻, but not H₂O₂, indicating that CHT displays selective sensitivity to ONOO⁻. Further work by Pinthong et al. (2008) found that ONOO⁻ inhibited choline uptake by reducing the level of cell surface CHT expression. Moreover, these authors found that ONOO⁻ increased the rate of CHT internalization from the plasma membrane, and that CHT inhibition occurred at concentrations of SIN-1 that did not disrupt cell membrane integrity or cause cell death. Taken together, the results of this previous work suggested that inhibition of CHT activity by SIN-1 is due to a change in CHT protein localization, as opposed to a change in the conformation of the protein due to nitration or oxidation. The goal of Chapter 2 of this thesis was to determine the route of CHT subcellular trafficking under SIN-1 treatment. The results of the initial experiments in Chapter 2, which examined [³H]HC-3 binding kinetics of CHT under SIN-1 treatment, and compared high-affinity choline uptake kinetics between cells stably expressing wild-type CHT or L531A-CHT, which is unable to undergo endocytosis, confirmed that SIN-1 inhibition is not due to a direct nitrosative or oxidative modification of CHT protein itself. To assess the route of CHT subcellular trafficking under SIN-1 treatment, I used various different experimental approaches and found that SIN-1 did not alter CHT endocytosis through a clathrin and dynamin-dependent pathway, or the movement of CHT through early and late endosomes to lysosomes. Importantly, exposure of cells to SIN-1 resulted in CHT ubiquitination and blocking the proteasome restored choline uptake activity in SIN-1 treated cells. Figure 5-1 shows a general schematic of the results found in Chapter 2 in regard to CHT trafficking in a cholinergic nerve terminal under ONOO⁻ stress.

The nitration of tyrosine residues is a well-characterized consequence of ONOO⁻ treatment and increased 3-nitrotyrosine (3-NT) immunoreactivity is found in necropsy AD brain (10). Early studies found that inhibitors of protein nitration did not protect CHT activity from ONOO⁻ (8) and experiments carried out in our laboratory found no evidence of nitration of tyrosines in CHT (9). While increased 3-NT levels are the signature

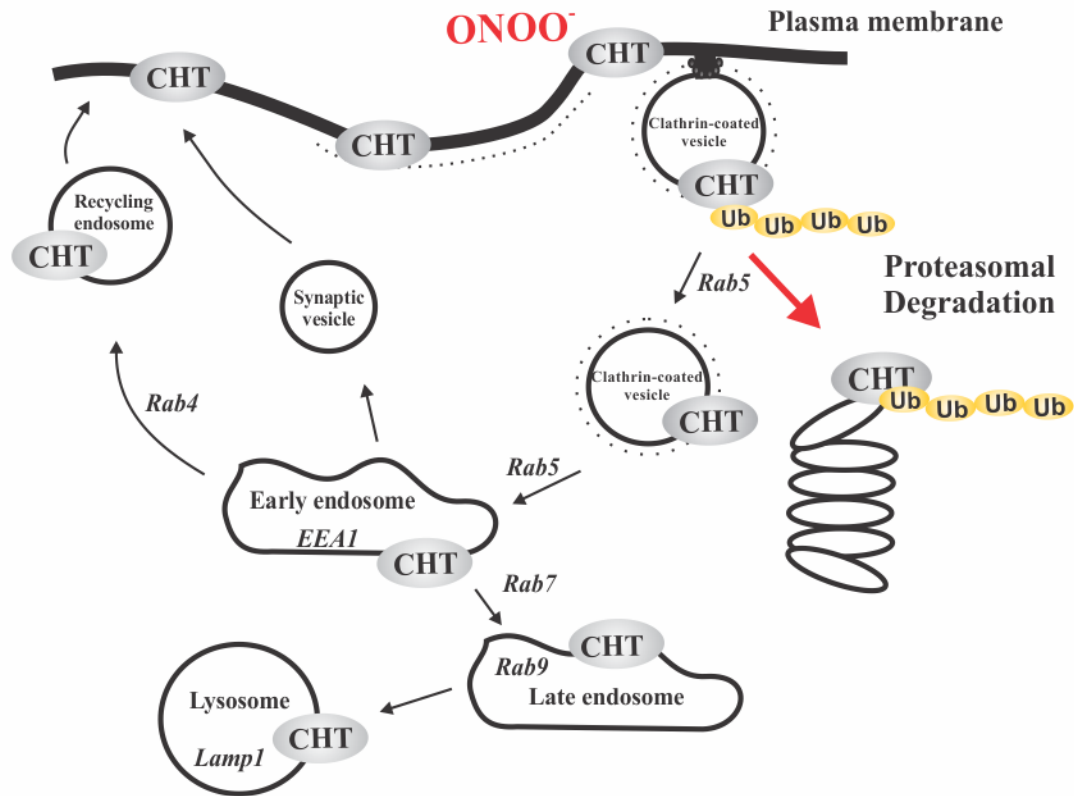


Figure 5-1 Pathways of CHT subcellular trafficking in cells treated with ONOO⁻ donor SIN-1.

In vehicle and SIN-1 treated cells, CHT is internalized from the plasma membrane through a clathrin-dependent mechanism. Once internalized, CHT colocalizes with Rab-5-positive early endosomes, and can be transported through Rab-7 and Rab-9 positive late endosomes to lysosomes for degradation. This subcellular trafficking pathway does not appear to be altered by SIN-1 treatment. My studies suggest that CHT undergoes polyubiquitination following SIN-1 treatment, and that this then can result in the subcellular trafficking of the transporter to the proteasome for degradation.

marker of ONOO⁻-mediated damage in post-mortem AD brain, it can be expected that other direct modifications to proteins, including oxidation, or nitrosylation of amino acids (11), or indirect changes to protein function, for example, through the activation of phosphorylation pathways by ONOO⁻ (12-14) are occurring in the brain under pathological conditions. The production of ONOO⁻ depends on the availability of its precursors, O₂ and NO, which are not normally produced in large quantities in the brain. However, under certain conditions associated with AD, such as tissue injury and inflammation, or a reduced antioxidant capacity, ONOO⁻ becomes a significant pathological risk. The ONOO⁻ treatment used in this study parallels physiological levels of ONOO⁻ produced in the brain under multiple disease conditions including AD, thus the observed alteration in CHT trafficking could occur in the cholinergic nerve terminal microenvironment in the brain.

The results of experiments in Chapter 2 reveal that the loss of CHT activity in cells treated with ONOO⁻ is mediated by proteasomal degradation of the protein. ONOO⁻-treatment also results in enhanced CHT ubiquitination. Although not tested, the internalization of modified or damaged CHT proteins into ONOO⁻-treated cells may result in either polyubiquitination, which promotes protein degradation, or monoubiquitination, which alters protein trafficking, as a measure of quality control within the cell. My results show the addition of approximately four ubiquitin molecules to CHT, which could indicate the presence of a short polyubiquitin chain. A very recent study by Hartnett et al. (2014) confirmed my observation that CHT undergoes polyubiquitination using tandem ubiquitin binding entities technology. These authors also found that CHT interacts with ubiquitin carboxyl-terminal hydrolase L1 (UCHL1), a deubiquitinating enzyme involved in the ubiquitin-proteasome system, and showed that UCHL1 knockdown increases CHT polyubiquitination and decreases CHT protein expression level. Interestingly, UCHL1 activity is altered (16, 17) and down-regulated (18) by its oxidation in the brains of patients with AD. Another recent study found that CHT interacts with the exogenous ubiquitin ligase Nedd4-2 causing a reduction its cell surface levels (19). Nedd4-2 has also been shown to cause the internalization of other membrane proteins, including the neurotransmitter transporter hDAT and the voltage-

gated potassium channel (20, 21). ONOO⁻ inhibits hDAT function (22), suggesting the possibility that during pathological conditions ONOO⁻ regulates the production or activity of Nedd4-2, which in turn mediates the ubiquitination of membrane proteins altering protein degradation or subcellular trafficking. It is clear that the ubiquitin-proteasome system is disrupted in AD based on the observation that hallmark features of AD, for example the deposition of amyloid fibrils and the formation of tau helices, are the product of ubiquitin-mediated protein defects (23). It is not understood how CHT is regulated by the ubiquitin-proteasome system, and how this is altered by pathological conditions associated with AD. Future studies investigating an association between CHT and Nedd4-2 or UCHL1 could provide interesting and novel information regarding the mechanisms involved in CHT regulation during AD, in particular under conditions of oxidative stress.

In addition to oxidative stress, a second important modifiable risk factor for AD is high serum cholesterol level at midlife. Cholinergic neurons rely on cholesterol for synapse formation and membrane integrity, thus changes in cholesterol homeostasis in the brain could potentially lead to changes in the microenvironment of the cholinergic nerve terminal, leading to alterations in the function of CHT. Early reports regarding CHT regulation by cholesterol are limited and contradictory. One report shows that lowering cholesterol in rat brain synaptosomes reduced choline uptake activity (24), whereas another study found that membrane cholesterol depletion did alter choline uptake (25). The experiments proposed in Chapter 3 were focused on defining the mechanistic changes occurring to CHT in response to changes in membrane cholesterol levels. Here, I found that membrane cholesterol and lipid rafts serve as an important regulator of CHT trafficking and activity by retaining functional CHT proteins at the cell surface.

In these experiments, I used a variety of drug treatments to manipulate membrane cholesterol levels with the goal of disrupting lipid rafts and specific cholesterol-protein interactions. While many studies have looked at the effect of statin drugs on the development and pathology of AD, I did not use statins to manipulate membrane cholesterol levels in the experiments performed in Chapter 3 due to their pleiotropic effects. The majority of cholesterol-independent, pleiotropic effects of statins come from

their ability to block the synthesis of critical isoprenoid intermediates. Isoprenylation is an important post-translational modification of the Ras superfamily of G-proteins, including Rab proteins (26). The inhibition of Rab GTPase isoprenylation by statin treatment causes these proteins to lose their normal function and leads to dysfunction in protein trafficking and cellular signalling (27). Importantly, Rab proteins facilitate the movement of CHT through endosomal and lysosomal compartments, and therefore statin treatment could have a compounding influence on CHT function through inhibition of both cholesterol and isoprenoid synthesis. Future studies assessing the individual effects of cholesterol and isoprenoids on CHT trafficking and activity could provide vital information about the underlying mechanisms involved in statin-mediated AD risk reduction.

The results of experiments in Chapter 3 revealed that CHT association with lipid rafts is critical for its function. As depicted in Figure 5-2, lipid rafts could play a role in regulating the amount of CHT at the cell surface by altering its internalization rate and/or its recycling back to the cell surface. In this study, I found that CHT internalization was not altered by raft disruption, suggesting that decreased recycling of transporters to the cell surface could be responsible for the reduction in CHT plasma membrane levels and choline uptake activity following lipid raft disruption. Thus, the mechanism by which CHT is targeted to rafts is of particular importance. My results show that CHT has a conserved motif within TMD12 that could serve both as a cholesterol-binding motif and as a protein dimerization motif these data reveal the presence of a homo-oligomer of CHT protein within lipid raft fractions. However, it cannot be ruled out that other modifications to CHT protein may be responsible for its inclusion into lipid rafts. For example, protein-protein interactions or post-translational modifications of CHT, such as phosphorylation, could be involved in the targeting of CHT to raft areas of the plasma membrane. Previous work done in our lab found treatment of cells with the PKC activator PMA increases choline uptake activity by diminishing CHT endocytosis and increasing CHT recycling to the cell surface (28). A potential mechanism underlying this observation may be that specific residues, when phosphorylated, promote the retention of CHT at the plasma membrane. It is also possible that there is differential phosphorylation

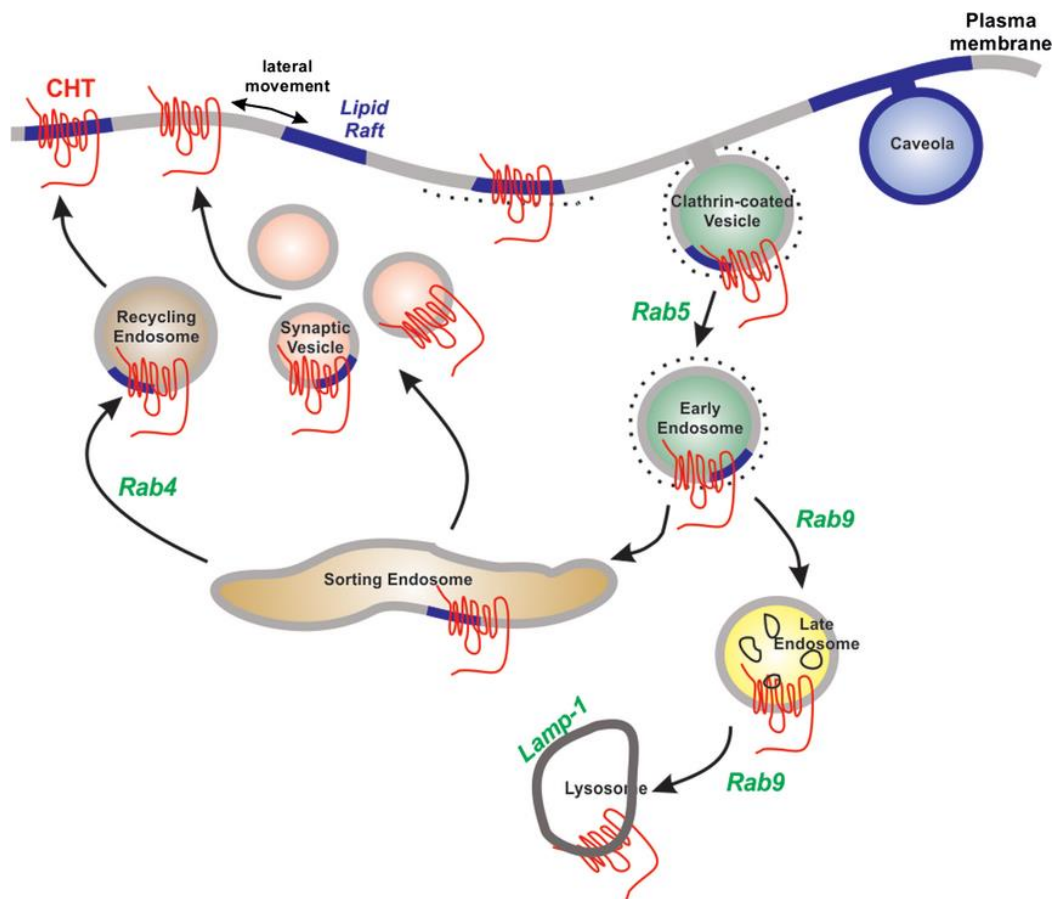


Figure 5-2 CHT trafficking is regulated by its association with lipid rafts.

The results of my experiments in Chapter 3 show that CHT association with lipid rafts is critical for its function. Lipid rafts could play a role in regulating the amount of CHT at the cell surface by altering its lateral movement at the plasma membrane, altering the transporters internalization either through clathrin-mediated endocytosis, or through clathrin-independent caveola. Lipid rafts found in endosomal or synaptic vesicle plasma membrane could alter the subcellular trafficking pathway of CHT. Lipid rafts may also play a role in altering the rate of CHT internalization and/or its recycling back to the cell surface. CHT internalization was not altered by raft disruption, suggesting that decreased recycling of transporters to the cell surface could be responsible for the reduction in CHT plasma membrane levels and choline uptake activity following lipid raft disruption.

of CHT proteins in raft and non-raft areas of the plasma membrane, with this potentially modulating its membrane retention and trafficking. This is the case for PKC-induced internalization of the DAT that, like CHT, is dynamin- and clathrin-dependent, but is independent of lipid rafts. DAT in rafts has a lower constitutive level of phosphorylation, but a higher level of PMA-induced phosphorylation when compared to non-raft DAT, indicating that rafts are preferential sites for PKC-mediated phosphorylation (29).

The movement of CHT to lipid rafts could also be influenced by protein-protein interactions. One protein of interest is APP, which binds to CHT and plays a role in regulating its subcellular trafficking, as demonstrated by the results of experiments described in Chapter 4 of this thesis. APP is found in lipid rafts; however, it is not known whether APP and CHT interact in raft or non-raft membrane and what affect this has on the function of CHT. Amyloidogenic processing of APP by BACE1 occurs in lipid rafts (30), thus modulating the properties of rafts to reduce the association of APP or BACE1 with these microdomains could reduce the production of A β and slow the progression of AD. In contrast to this, my observations suggest that altering raft properties to exclude CHT would reduce choline available for ACh synthesis and diminish cholinergic neurotransmission. Several lines of evidence suggest that the organization of lipid rafts is disrupted in AD brains (31) and a strong link between cholesterol and AD comes from the identification of the ϵ 4 allele of *APOE* as the strongest genetic risk factor for the development of late-onset AD (32). Alterations in cholesterol homeostasis in the brain, as a result of hypercholesterolemia or the *APOE* genotype, could result in reduced membrane cholesterol levels in cholinergic neurons and cause the disruption of lipid rafts. Alternatively, increased cholesterol levels in the brain could result in the formation of lipid rafts, or reduce the fluidity of the plasma membrane, causing raft disruption and/or inhibition of lateral protein movement. It is unknown how altered cholesterol homeostasis, and lipid raft disorganization, affects the plasma membrane distribution and function of raft-associated proteins, such as CHT and APP, in the AD brain. Future studies should investigate whether APP and CHT interact in raft or non-raft membrane, how this is altered by cholesterol manipulation and the impact on CHT function and APP processing.

The goal of the experiments carried out in Chapter 4 was to further investigate how APP regulates CHT trafficking and activity, and to determine whether this interaction is altered by the Swedish mutation. In this study, several experiments were carried out in neural cells treated with either vehicle or a BACE1 inhibitor. BACE1 inhibition represents an important therapeutic strategy for lowering A β generation, and several BACE1 inhibitors are currently being tested in clinical trials for their efficacy and safety for use in individuals with AD. The experiments performed in Chapter 4 provide important mechanistic data regarding CHT and APP that suggest BACE1 inhibition may have beneficial effects that are not directly related to lowering A β generation in patients with AD. First, I found that BACE1 inhibition increased the cell surface levels of both APP_{wt} and APP_{Swe}. This could potentially increase the movement of APP through the non-amyloidogenic pathway and increase production of the sAPP α , which is thought to have neuroprotective properties. Second, I made the critical observation that, unlike the APP_{wt/Swe}-mediated reduction in cell surface CHT levels observed in vehicle-treated cells, treatment of cells expressing either APP_{wt} or APP_{Swe} with a BACE1 inhibitor restores the cell surface levels of CHT protein either to (APP_{wt}) or above (APP_{Swe}) that found in vector-expressing cells. The mechanism underlying this observation was not investigated further in this study. BACE1 inhibition blocks the production of both A β and β CTF. I hypothesized that lowering A β concentration in the culture medium of cells expressing APP_{wt} or APP_{Swe} by BACE1 inhibition could be responsible for the preservation of CHT cell surface levels, particularly in cells expressing APP_{Swe} that produce much more A β . However, it is possible my observations are due to the reduction of β CTF generation by inhibiting BACE1. While my study examined the interaction of CHT with full-length APP, the carboxyl-terminal domain of APP is sufficient to immunoprecipitate CHT (33). It is possible that the interaction of CHT with the β CTF alone, rather than with full-length APP, is required for the internalization of CHT. BACE1 inhibition would result in less β CTF available for interaction with CHT, thus reducing its endocytosis. Therefore, BACE1 inhibition could preserve the levels of CHT at the cell surface, thereby maintaining CHT activity and ACh production, and have a positive effect on cholinergic neurotransmission in patients with AD.

In these studies, I observed important differences in the regulation of CHT by APP_{wt} and APP_{Swe}. I found that CHT interacted significantly less with APP_{Swe} than with APP_{wt}, but caused a similar level of decrease in CHT activity and cell surface expression. The results of my study, and those of the study done by Wang et al. (2007), support the hypothesis that APP_{wt} plays a physiological role in cholinergic neurons by facilitating CHT presynaptic localization and endocytosis through a direct interaction with the transporter, while APP_{Swe}-mediated inhibition of CHT function could be caused by the susceptibility of the transporter to A β that is found in the extracellular environment. This suggests that independent therapeutic strategies for maintaining cholinergic neurotransmission could be designed for AD patients depending on whether they have sporadic AD or familial AD caused by the Swedish mutation. In the case of a patient in the early stages of sporadic AD, a therapeutic strategy targeted towards promoting the interaction between CHT and APP_{wt} could maintain the normal trafficking and activity of CHT in cholinergic neurons. As the disease progresses and A β accumulates, lowering A β generation through BACE1 inhibition may be more relevant to maintain CHT cell surface levels, choline uptake activity and ACh production. In the case of a patient in the early stages of familial AD caused by the Swedish mutation, my results suggest that the normal physiological interaction between CHT and APP is disrupted, with much higher levels of A β produced. Thus, in individuals with AD caused by the Swedish mutation, targeting BACE1 early on in the course of the disease may be the most effective strategy to promote cholinergic neurotransmission.

The Swedish mutation of *APP* is quite rare, found in less than 1 percent of the general population. However, there are more than 50 different mutations in the *APP* gene that can cause early-onset AD and these account for up to 10 percent of all early-onset cases of the disorder (34). It is possible that other mutations of *APP* could also alter the interaction of APP with CHT. The underlying reason for the reduced interaction of CHT with APP_{Swe} compared to APP_{wt} was not investigated in my study. However, I hypothesize that it is likely related to differences in subcellular location and trafficking of APP_{Swe} compared to APP_{wt}. A recent study examining APP trafficking found distinct intracellular trafficking pathways of APP_{Swe}, as well as APP containing the London mutation, when compared to

APP_{wt} (35). If less APP_{Swe} than APP_{wt} interacts with CHT proteins as a result of differences in their subcellular trafficking pathways, and various other *APP* mutations also alter the trafficking of APP, it is reasonable to conclude that other mutations of APP could also alter the interaction of APP with CHT. To test this, the experiments outlined in Chapter 4 could be repeated using different APP constructs expressing various other familial *APP* mutations, such as the London mutation or the Arctic mutation. Despite the fact that the Swedish mutation affects only 1% of the general population, the human mutant APP mouse Tg2576, which overexpresses the Swedish mutant form of APP695, is the most commonly used AD mouse model (36). This is because these mice display an AD phenotype, exhibiting five times the level of endogenous murine APP in the brain and develop plaque-like deposits of A β in the brain at an early age. However, experiments carried out in Chapter 4 reveal important differences in protein regulation, subcellular trafficking and subcellular processing between APP_{wt} and APP_{Swe}. Therefore, depending on the type of study to be performed, a mouse model overexpressing wild-type APP could be a more appropriate choice.

5.2.1 Significance

Several reports have suggested that the cognitive deficits seen in AD are related to the loss and dysfunction of cholinergic neuron signalling. However, the specific changes that occur in the aging brain that result in cholinergic dysfunction, and the extent to which they can be prevented or reversed, is still unclear. Understanding the mechanisms involved in CHT protein trafficking is critical since this regulates CHT activity, thereby sustaining ACh production and maintaining cholinergic neurotransmission. Three important risk factors for AD include high serum cholesterol level at midlife, mutations in genes encoding APP and increased generation of ROS and RNS in the brain. Gaining a greater understanding of the molecular events occurring in the cholinergic presynaptic nerve terminal that could alter CHT activity in these pathological situations is essential for developing new treatment methods for AD and was the overall goal of this thesis.

Within the cholinergic nerve terminal microenvironment, changes in APP processing and A β generation, ONOO⁻ production, or plasma membrane cholesterol levels, could cause a

decrease in CHT activity, thereby reducing high-affinity choline uptake and diminishing ACh production. The binding of ACh to certain mAChR subtypes is thought to promote the non-amyloidogenic cleavage of APP (37), while A β inhibits various steps involved in both ACh synthesis and release (38-41). As a result of a decrease in CHT activity, less ACh would be available to bind to mAChR, which could potentially reduce the movement of APP through the non-amyloidogenic pathway and result in more APP available to undergo amyloidogenic processing and generate A β . The results of experiments reported in Chapter 4 of this thesis, as well as those of other groups, show that A β can inhibit high-affinity choline uptake (42, 43), which could potentially be through a direct interaction with CHT (44). Interestingly, A β can indirectly impair CHT activity by causing the activation of microglia and the production of ONOO⁻ (45). Aggregated forms of A β can also bind to cholesterol and interfere with the plasma membrane lipid bilayer (46), which could cause a disruption of lipid raft organization and a decrease in CHT activity. Since the uptake of choline by CHT is the rate-limiting step to ACh production, a decrease in CHT activity would critically impair ACh synthesis and release, potentially causing more A β to be produced, which could result in a further reduction in CHT activity. This reciprocal relationship is shown schematically in Figure 5-3. Therefore, promoting CHT activity and ACh production may not only be important for supporting cognition and memory, but could also critically affect the progression of AD pathology by preventing the generation of A β . The studies reported in this thesis reveal important mechanistic information regarding the regulation of CHT trafficking and activity under pathological conditions where cholinergic signalling is compromised. This information may aid the design of therapeutic strategies to protect against pathological situations in the cholinergic nerve terminal, which could play an important role early on in the course of the disease by maintaining CHT activity and ACh signalling, which is critical to many diverse biological processes.

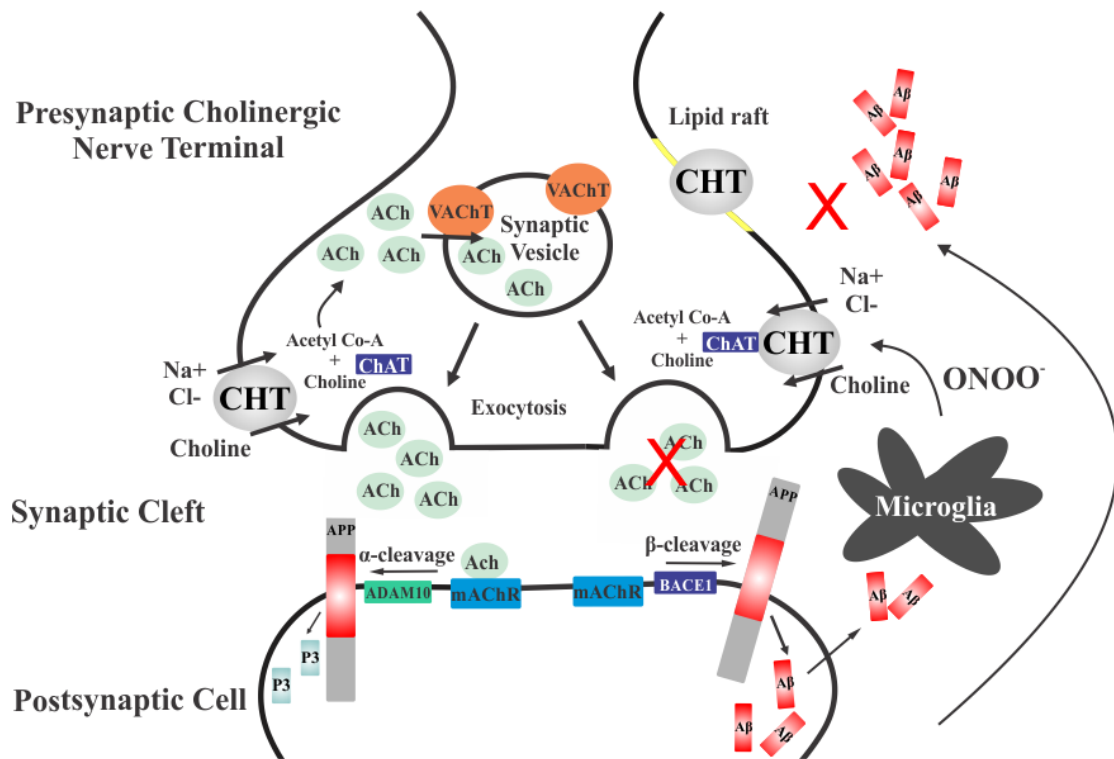


Figure 5-3 The relationship between APP and the cholinergic system.

Following the release of ACh into the synaptic cleft, the binding of ACh to certain post-synaptic mACHR subtypes promotes the non-amyloidogenic cleavage of APP, resulting in the production of non-pathogenic peptides. Alternatively, Aβ, produced as a result of amyloidogenic processing, can inhibit various steps involved in both ACh synthesis and release. Aβ can potentially inhibit ChAT activity directly or indirectly by activating microglia and causing ONOO⁻ production or through effects on lipids at the plasma membrane. Inhibition of ChAT activity would impair ACh synthesis. Less ACh would be available to bind to mACHR, which could potentially reduce the movement of APP through the non-amyloidogenic pathway and result in more APP available to undergo amyloidogenic processing and the generation of toxic Aβ peptides.

5.3 References

1. Ribeiro, F.M., Pinthong, M., Black, S.A., Gordon, A.C., Prado, V.F., Prado, M.A., Rylett, R.J., and Ferguson, S.S. (2007) *Eur J Neurosci* **26**, 3437-3448
2. Misawa, H., Fujigaya, H., Nishimura, T., Moriwaki, Y., Okuda, T., Kawashima, K., Nakata, K., Ruggiero, A.M., Blakely, R.D., Nakatsu, F., and Ohno, H. (2008) *Eur J Neurosci* **27**, 3109
3. Kobayashi Y, Okuda T, Fujioka Y, Matsumura G, Nishimura Y, Haga T (2002) *Neurosci Lett* **317**, 25-28
4. Lips KS, Pfeil U, Haberberger RV, Kummer W (2002) *Cell Tissue Res* **307**, 275-280
5. Ferguson, S.M., Savchenko, V., Apparsundaram, S., Zwick, M., Wright, J., Heilman, C.J., Yi, H., Levey, A.I., and Blakely, R.D. (2003) *J Neurosci* **23**, 9697-9709
6. Kus, L., Borys, E., Ping, Chu, Y., Ferguson, S.M., Blakely, R.D., Emborg, M.E., Kordower, J.H., Levey, A.I., and Mufson, E.J. (2003) *J Comp Neurol* **463**, 341-357
7. Hoover, D.B., Ganote, C.E., Ferguson, S.M., Blakely, R.D., Parsons, R.L. (2004) *Cardiovasc Res* **62**, 112-21
8. Guermonprez, L., Ducrocq, C., and Gaudry-Talarmain, Y.M. (2001) *Mol Pharmacol* **60**, 838-846
9. Pinthong, M., Black, S.A., Ribeiro, F.M., Pholpramool, C., Ferguson, S.S., and Rylett, R.J. (2008) *Mol Pharmacol* **73**, 801-812
10. Smith, M.A., Richey, Harris, P.L., Sayre, L.M., Beckman, J.S., and Perry, G. (1997) *J Neurosci* **17**, 2653-2657

11. Alvarez, B., and Radi, R. (2003) *Amino Acids* **25**, 295-311
12. Oh-Hashi, K., Maruyama, W., and Isobe, K. (2001) *Free Radic Biol Med* **30**, 213-221
13. Oh-Hashi, K., Maruyama, W., Yi, H., Takahashi, T., Naoi, M., and Isobe, K. (1999) *Biochem Biophys Res Commun* **263**, 504-509
14. Tommasini, I., Cerioni, L., Guidarelli, A., and Cantoni, O. (2005) *Biochem Biophys Res Commun* **329**, 1282-1287
15. Hartnett, S., Zhang, F., Abitz, A., and Yifan, L. (2014) *Neurosci Lett* **564**, 115-119
16. Butterfield, D.A., Gnjec, A., Poon, H.F., Castegna, A., Pierce, W.M., Klein, J.B., and Martins, R.N. (2006) *J Alzheimer's Dis* **10**, 391-397
17. Setsuie, R., and Wada, K. (2007) *Neurochem Int* **51**, 105-111
18. Choi, J., Levey, A.I., Weintraub, S.T., Rees, H.D., Gearing, M., Chin, L.S., and Li, L. (2004) *J Biol Chem* **279**, 13256-13264
19. Yamada, H., Imajoh-Ohmi, S., and Haga, T. (2012) *Biomed Res* **33**, 1-8
20. Ekberg, J., Schuetz, F., Boase, N.A., Conroy, S-J., Manning, J., Kumar, S., Poronnik, P., and Adams, D.J. (2007) *J Biol Chem* **282**, 12135-12142
21. Sorkina, T., Miranda, M., Dionne, K.R., Hoover, B.R., Zahniser, N.R., and Sorkin, A. (2006) *J Neurosci* **26**, 8195-8205
22. Park, S.U., Ferrer, J.V., Javitch, J.A., and Kuhn, D.M. (2002) *J Neurosci* **22**, 4399-4405
23. Mori, H., Kondo, J., and Ihara, Y. (1987) *Science* **235**, 1641-1644
24. Waser, P.G., Oxterwalder, M., and Schonenberger, E. (1978) *Naunyn*

25. North, P., and Fleischer, S. (1983) *J Biol Chem* **258**, 1242-1253
26. Zhang, F.L., and Casey, P.J. (1996) *Annu Rev Biochem* **65**, 241-269
27. Cordle, A., Koenigsknecht-Talboo, J., Wilkinson, B., Limpert, A., and Landreth, G. (2005) *J Biol Chem* **280**, 34202-34209
28. Black, S.A.G., Ribeiro, F.M., Ferguson, S.S.G., and Rylett, R.J. (2010) *Neuroscience* **167**, 765-773
29. Sorkina, T., Hoover, B.R., Zahniser, N.R., and Sorkin, A. (2005) *Traffic* **6**, 157-170
30. Hartmann, T., Kuchenbecker, J., and Grimm, M.O. (2007) *J Neurochem* **103**, 159-170
31. Ledesma, M.D., Abad-Rodriguez, J., Galvan, C., Biondi, E., Navarro, P., Delacourte, A., Dingwall, C., and Dotti, C.G. (2003) *EMBO Rep* **4**, 1190-1196
32. Herze, J., and Beffert, U. (2000) *Nat Rev Neurosci* **1**, 51-58
33. Wang, B., Yang, L., Wang, Z., and Zheng, H. (2007) *Proc Natl Acad Sci U S A* **104**, 14140-14145
34. Campion, D., Dumanchin, C., Hannequin, D., Dubois, B., Belliard, S., Puel, M., Thomas-Anterion, C., Michon, A., Martin, C., Charbonnier, F., Raux, G., Camuzat, A., Penet, C., Mesnage, V., Martinez, M., Clerget-Darpoux, F., Brice, A., and Frebourg, T. (1999) *Am J Hum Genet* **65**, 664-70
35. Lorenzen, A., Samosh, J., Vandewark, K., Anborgh, P.H., Seah, C., Magalhaes, A.C., Cregan, S.P., Ferguson, S.S.G., and Pasternak, S.H. (2010) *Molecular Brain* **3**, 11

36. Hsiao, K., Chapman, P., Nilsen, S., Eckman, C., Harigaya, Y., Younkin, S., Yang, F., and Cole, G. (1996) *Science* **274**, 99-102
37. Nitsch, R.M., Slack, B.E., Wurtman, R.J., and Growdon, J.H. (1992) *Science* **258**, 304-307
38. Pedersen, W.A., Kloczewiak, M.A., and Blusztajn, J.K. (1996) *Proc Natl Acad Sci U S A* **93**, 8068-8071
39. Melo, J.B., Agostinho, P., and Oliveira, C.R. (2002) *Amyloid* **9**, 221-228
40. Kar, S., Slowikowski, S.P.M., Westaway, D., and Mount, H.T.J. (2004) *J Psychiatry Neurosci* **29**, 427-441
41. Cleary, J.P., Walsh, D.M., Hofmeister, J.J., Shankar, G.M., Kuskowski, M.A., Selkoe, D.J., and Ashe, K.H. (2005) *Nat Neurosci* **8**, 79-84
42. Kar, S., Issa, A.M., Seto, D., Auld, D.S., Collier, B., and Quirion, R. (1998) *J Neurochem* **70**, 2179-2187
43. Kristofiková, Z., Tejkalová, H., and Klaschka, J. (2001) *Neurochem Res* **26**, 203-212
44. Bales, K.R., Tzavara, E.T., Wu, S., Wade, M.R., Bymaster, F.P., Paul, S.M., Nomikos, G.G. (2006) *J Clin Invest* **116**, 825-832
45. Xie, Z., Wei, M., Morgan, T.E., Fabrizio, P., Han, D., Finch, C.E. and Longo, V.D. (2002) *J Neurosci* **22**, 3484-3492
46. Avdulov, N.A., Chochina, S.V., Igbavboa, U., Warden, C.S., Vassiliev, A.V., Wood, W.G. (1997) *J Neurochem* **69**, 1746-1752

Cirriculum Vitae

Name:

Leah Katherine Cuddy

Post-secondary Education:

Western University
London, Ontario, Canada
PhD Pharmacology and Toxicology
2009-2014

Western University
London, Ontario, Canada
B.M.Sc. Honours Specialization in Medical
Sciences
2004-2009

Honours and Awards:

Alzheimer Society Canada Doctoral
Research Scholarship
2013–2015

Ontario Graduate Scholarship
2013–2014, award declined

Hari and Gudrun Sharma Scholarship
Award 2012

Queen Elizabeth II Graduate Scholarship in
Science and Technology
2012-2013

Schulich Graduate Scholarship
2009-2014

Alzheimer Society London and Middlesex
Studentship
2010-2011

Teaching Experience:

Teaching Assistant
Physiology 4100b
Western University, Canada
2013

Teaching Assistant
Physiology 2130
Western University, Canada
2011-2013

Publications:

Cuddy LK, Winick-Ng W, Rylett RJ.
Regulation of the high-affinity choline
transporter activity and trafficking by its
association with cholesterol-rich lipid rafts
J Neurochem 4 November 2013 128
(5):725-740

Cuddy LK, Gordon AC, Black SA,
Jaworski E, Ferguson SSG, Rylett RJ.
Peroxynitrite donor SIN-1 modifies high-
affinity choline transporter activity by
modifying its intracellular trafficking. J
Neurosci 18 April 2012 32 (16):5573-5584

Work Experience:

Graduate Research Assistant
Robarts Research Institute
London, ON
2009-2014

Summer Student
Robarts Research Institute
London, ON
2009